Millimeter Wave Scattering by Rain

in an Antenna's Near Field

by

Harry Barksdale

Dissertation submitted to the Faculty of the

Virginia Polytechnic Institute and State University

in partial fulfillment of the requirements for the degree of

DOCTOR OF PHILOSOPHY

in

Electrical Engineering

APPROVED:

Charles W. Bostian, Chairman

Warren L. Stutzman

Timothy Pratt

David A. de Wolf

Werner E. Kohler

December, 1987

Blacksburg, Virginia

Millimeter Wave Scattering by Rain

In an Antenna's Near Field

by

Harry Barksdale

Charles W. Bostian, Chairman

Electrical Engineering

(ABSTRACT)

One of the important considerations in radio link analysis is the signal degradation that accompanies rainfall in a link's path. Random scattering by rain can adversely affect a propagating wave in two ways. First, it results in attenuation and depolarization of the coherent field which is associated with the forward propagating wave. In addition to this, random scattering gives rise to an incoherent field component that can further degrade the signal in a manner similar to multipath.

This dissertation presents an analysis of the coherent and incoherent effects of rain scatter at millimeter wave frequencies. Within it, the scattering properties of individual spherical and non-spherical are quantified. Spherical raindrops are treated using the Mie theory and non-spherical ones analyzed with Waterman's Extended Boundary Condition Method. Computed values of forward scattering amplitudes and scattering cross-sections for both spherical and non-spherical raindrops at 30, 45, 70 and 90 GHz are presented; the computer programs used to obtain the scattering data are also provided. Following the analysis of individual raindrops scatterers, the Foldy-Lax Twersky integral equations for coherent field and incoherent intensity are used to derive the coherent and incoherent outputs of a generic radio receiver. In doing so, the effects of scattering in an antenna's far field and radiating near field (Fresnel Region) are analyzed. Through this analysis, it is shown that the expected system outputs are essentially the same in either case.

Using the computed raindrop scattering parameters and msodels developed for the coherent and incoherent system outputs, specific cases are looked at for 30, 45, 70 and 90 GHz operation and theoretical data presented. The data consists of the predicted attenuation and isolation of the coherent signal and the ratio of coherent to incoherent power in the presence of rain. From the latter it is found that during heavy rainfall, the incoherent effects can be appreciable and should be taken into account.

Acknowledgements

I would like to express my deepest appreciation to Dr. Charles Bostian for his advice and unending patience during the course of my doctoral work. Dr. Bostian not only provided me the guidance I needed for conducting my research but advice which will be invaluable to me in my future endeavors as well. For this I am truly grateful.

I am also indebted to Drs. David de Wolf, Werner Kohler, Timothy Pratt and Warren Stutzman. Each provided me with timely suggestions which, along with their continued encouragement, enabled me to persevere through some difficult junctures in my work.

I would also like to thank for her patience, understanding and diligence in typing my dissertation.

Finally, I would like to acknowledge the support of and dedicate this work to my family. Without the encouragement and forbearance of my wife and children I would have never made it this far. :eacknow.

Table of Contents

Chapter 1 Introduction

When designing radio communications systems, engineers must contend with a number of factors which can adversely affect system performance. Of these factors, one of the more important is the signal degradation caused by the presence of hydrometeors in a radio link's path. Not surprisingly then, researchers have put a considerable amount of effort into developing models for predicting how electromagnetic scattering by precipitation affects a propagating wave.

The focus of attention in this treatise will be the analysis of electromagnetic scattering by a particular form of precipitation: rain. The presence of randomly distributed raindrops in a radio link's path poses essentially two problems for a design engineer. On one hand it must be recognized that raindrops are lossy dielectric scatterers. Therefore, as a wave propagates through a rain medium, its fields will undergo attenuation and phase shifting. In addition to this, the random nature of the drops composing a raincell will cause the fields to be random. Therefore the total field in the presence of rain can be viewed as the superposition of an average component and a fluctuating component which, by analogy to the discipline of signal analysis, can be considered as noise.

To appreciate this two part problem in a systems context, consider the block diagrams shown in Figure 1.1. Figure 1.1a depicts the situation encountered during normal, clear weather conditions. In this case, a receiving antenna intercepts the field, ψ_i, which has been transmitted from a distant source. The system's output is characterized by a voltage V which can be analytically modeled as the result of a (presumably) linear operation on ψ_i:

$$V = F(\psi_i) \tag{1.1}$$

with the operator $F(\bullet)$ dependent upon the antenna's gain pattern.

Figure 1.1b is the same system during a rain event. When a raincell is between the source and receiver, the total field illuminating the receiver's antenna is no longer the intended field ψ_i. Rather, it is a random quantity since the fields within the medium are scattered by randomly distributed particles. This random field will give rise to a random output voltage consisting of an average or coherent component $<V>$ which is the output "signal" and a fluctuating or incoherent component V_f which is the output "noise". Thus, the presence of rain in a radio link's path presents both a coherent and an incoherent problem. In the coherent problem the received "signal" is determined and its deviation from the intended system output characterized in terms of attenuation and depolarization. The incoherent problem entails predicting the amount of "noise" power to be expected during a rain event.

The original motivation for the work leading to this dissertation dealt with the effect of scatterer location vis-a-vis the receiving antenna in the canonic problems we have just presented. Specifically, we set out to determine analytically whether a system's output would be significantly altered if a given rain cell falls in an antenna's near field rather than its far field. When analyzing the generic problem illustrated by Figure 1.1b, researchers have customarily modeled the receiving antenna using its far field properties. This presupposes that an antenna's near field will be sufficiently small to render scattering effects in this region

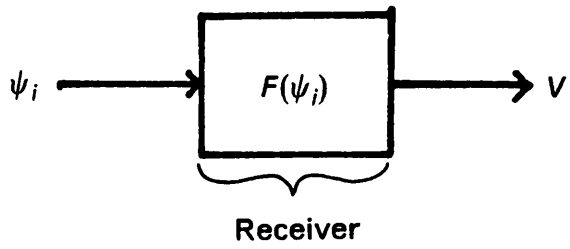

Clear Weather Model
Figure 1.1a

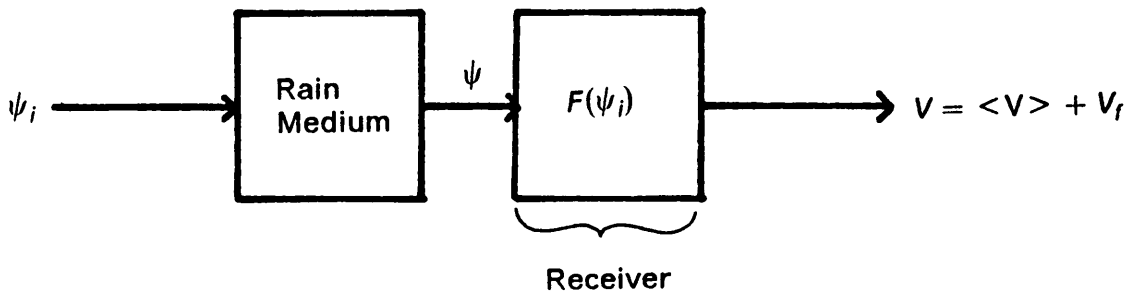

System Model During Rain Event
Figure 1.1b

negligible. However very large antennas can have extended near field regions in which a significant amount of scattering can occur during periods of rain. This has led to questions with regard to the applicability of the results of past analyses to systems employing extremely large antennas. We therefore undertook the task of analyzing the coherent and incoherent properties of a receiver's output when rainscatter occurs in the near field of its antenna. During the course of our investigating the near field rain scatter problem, it became apparent that a related topic warranted our attention. Specifically, we found there to be a lack of theoretical data available on the effects of rain scatter above 35 GHz. So, we expanded the scope of our analysis to include this are of study.

In commencing with our investigation of the rain scatter problem, we found that we could base our analysis on one of two approaches: the multiple scattering theory or the radiative transfer theory. The multiple scattering theory evolved from considering the behavior of fields in the presence of randomly distributed scatterers. The fundamental works in the development of the multiple scattering theory are those of Foldy [14], Lax [33], and Twersky [56] and numerous applications based on their research can be found in the literature (see, for example, references [9], [11], [27], [43], [55], [59], and [62]). In contrast to the multiple scattering theory, the radiative transfer theory deals with the propagation of intensities through a scattering medium and does not take into account field behavior. General discussions of the radiative transfer theory can be found in references [23] and [22] and examples of its use in treating rain scatter in references [24], [25], [28] and [39]. Because it deals with the properties of fields rather than intensities, we found the multiple scattering theory to be better suited for analyzing the near field problem than is the radiative transfer theory. Therefore, we chose it as the basis of our work.

Regardless of whether one employs the multiple scattering theory to study the coherent or the incoherent aspect of the rain scatter problem, there are essentially three steps involved in the analysis. First, the scattering and absorbing characteristics of individual raindrops must

be quantified. Following this, integral equations for coherent and incoherent quantities are derived and approximate solutions to these equations obtained. In the final step, the properties of the receiver are incorporated into the process to determine the coherent and incoherent components of its output. Using this three part approach, we have analyzed the generic problem we have previously discussed; the results of our work are documented in this treatise.

We have organized the analysis put forth in this dissertation into three parts. Chapter 2 deals with scattering by an individual raindrop. Much of the discussion in this chapter is for the purposes of reviewing fundamental concepts and providing definitions pertinent to our study. However, we also give detailed analyses of scattering by raindrops and provide computed values of raindrop scattering parameters at various millimeter wave frequencies. In Chapter 3 we treat the coherent aspect of the rain scatter problem and derive a general equation for the average output of a system. We derive this model by expanding scattered fields into plane wave modes using Fourier transforms so that random scattering in the near field can be considered. This technique has been used to study deterministic scattering in the near field of antennas but, prior to now, does not appear to have been applied to the random case. The subject of Chapter 4 is the incoherent problem. In it we derive expressions for the intensity of the incoherent signal at the output of a receiver for both the far field and near field scattering cases. Using the results of the analysis in this chapter, we look at various practical situations so that we can gain some insight as to the conditions under which the incoherent problem bears consideration. Following Chatpers 2, 3 and 4 we provide a brief conclusion in which the contributions and significant findings of our research are summarized.

Chapter 2 Scattering by an Individual Raindrop

An important goal in analyzing electromagnetic scattering by rain is to predict the effects a distribution of raindrops will have on a system's performance. But before this analysis can be performed the scattering properties of an individual raindrop must be understood. Therefore we begin this treatise with an investigation of how scattering by a single drop is characterized.

This chapter is in four parts. We begin with a general formulation of the individual scatterer problem and discuss some approaches for analyzing it. Following this we define some important scattering parameters and establish their physical significance. The final two sections are devoted to detailed analyses of spherical and oblate spheroidal raindrops.

We should note that raindrop scattering parameters have been computed and published for numerous cases (eg [34], [38] and [53]). However there is very little data available for frequencies above 35 GHz. Therefore, so that we could study the effects of rainscatter in the higher portions of the millimeter wave band, it was necessary for us to derive equations for and compute raindrop scattering parameters.

2.1 Millimeter Wave Scattering by a Single Raindrop-General Discussion

Determining the fields scattered by an individual raindrop is a formidable problem the and is best understood by first examining the general formulation of scattering by a dielectric body. So let us begin by considering an arbitrary dielectric scatterer such as that shown in Figure 2.1. The scattering body is composed of isotropic material having dielectric constant $\varepsilon(\vec{r})$ and is illuminated by a monochromatic plane wave whose electric field and propagation vectors will be denoted $\vec{E}_o$ and $\vec{k}_i$ respectively.

In the presence of the external field, a polarization current will exist within the particle. This current will produce a scattered field $\vec{E}_s(\vec{r})$, and the total field $\vec{E}(\vec{r})$ is the sum of this scattered field and the primary field $\vec{E}_i(\vec{r})$, viz

$$\vec{E}(\vec{r}) = \vec{E}_i(\vec{r}) + \vec{E}_s(\vec{r}) \tag{2.1}$$

The total field can also be expressed as the solution to the intplex integral equation [18].

$$\vec{E}(\vec{r}) = \vec{E}_i(\vec{r}) + \nabla x \nabla x \int [\varepsilon(\vec{r}\,') - 1] g(k_0 R) d\vec{r}\,' \tag{2.2}$$

where the intplex integral is over the volume of the scattering body, $g(k_0R)$ is the free-space scalar Green's function for outgoing waves

$$G(k_0R) = \frac{e^{-jk_0R}}{4\pi R} \tag{2.3a}$$

$$R = |\vec{r} - \vec{r}\,'| \tag{2.3b}$$

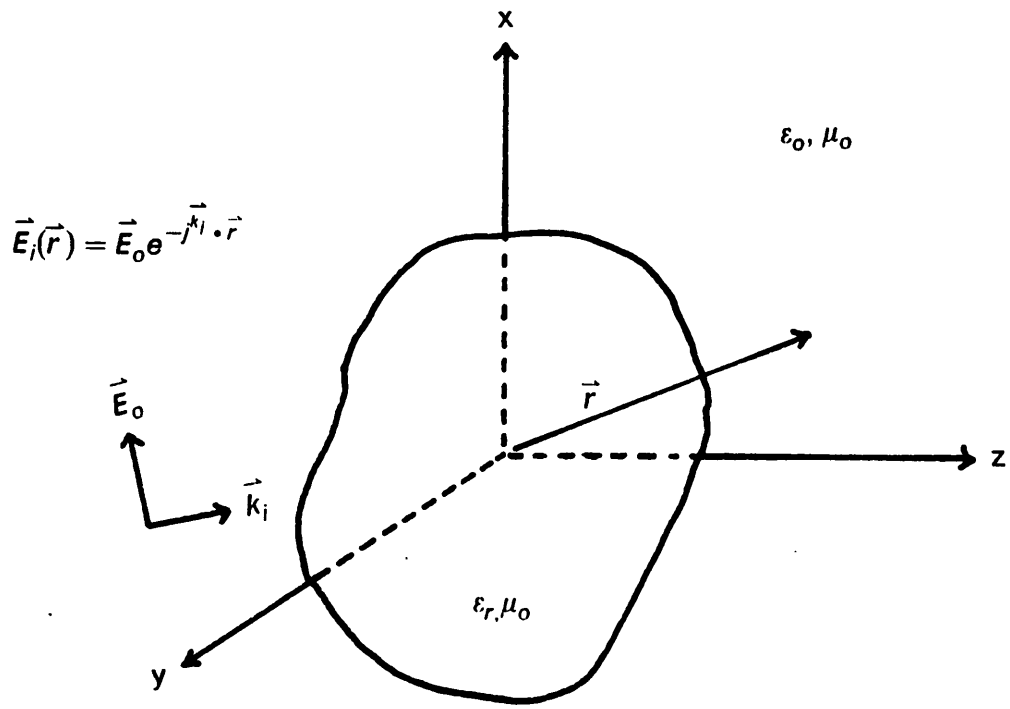

Geometry for Scattering by an Arbitrary Body

Figure 2.1

and

$$\vec{E}_i(\vec{r}) = \vec{E}_o e^{-j\vec{k}_i \cdot \vec{r}} \tag{2.3c}$$

It follows then that the scattered field is given by the radiation integral

$$E_s(\vec{r}) = \nabla x \nabla x \int [\varepsilon(\vec{r}\,') - 1]\vec{E}(\vec{r}\,') g(k_o R) d\vec{r}\,' \tag{2.4}$$

In general the far-zone scattered field is the scattered field of interest. This is obtainable from (2.4) by using the far-field approximation of the scalar Green's function, i.e.

$$g(k_0 R) \simeq g(k_0 r) \exp(jk_0 \hat{r} \cdot \vec{r}\,') \tag{2.5}$$

Using this approximation in (2.4), the far-zone scattered field becomes [23].

$$\vec{E}_s(\vec{r}) = -k_0^2 g(k_0 r) \int [\varepsilon(\vec{r}\,') - 1]\{\hat{r} x [\hat{r} x \vec{E}(\vec{r}\,')]\} \exp(jk_0 \hat{r} \cdot \vec{r}\,' d\vec{r}\,') \tag{2.6}$$

In considering the expression for the scattered field given in (2.4) and (2.6), the major difficulty involved in treating the individual scatterer problem is readily apparent. Note that while these equations provide a formal basis for determining the scattered field, they also show that the field scattered by the particle is dependent upon an internal field which is itself an unknown quantity. In many instances, this difficulty can be overcome by approximating the field within the scatterer so that the intplex integral in (2.6) can be evaluated.

The conditions under which one may reasonably approximate the scatterer's internal field are related to the size and dielectric properties of the scatterer. Specifically, letting D be the maximum linear dimension of the scattering body, the field within the particle can be approximated when any of the following conditions are met [4, 23, 60]:

$$k_0 D << 1 \quad and \quad |k_0 \varepsilon_r D| << 1 \tag{2.7}$$

$$K_0 D |\varepsilon_r - 1| << 1 \tag{2.8}$$

$$|\varepsilon - 1| k_0 D >> 1 \quad and \quad |\varepsilon_r - 1| < 1 \tag{2.9}$$

The constraints specified by (2.7) indicate a scattering body which is very small compared to wavelength. Under these conditions, the Rayleigh approximation is applicable and the field within the scatterer can be taken as that present when the scatterer is embedded in a uniform static field. Scatterers meeting the condition given in (2.8) can be analyzed using the Born approximation. This approximation is also referred to as Rayleigh-Gans scattering and is based on the observation that with $k_0 D |\varepsilon_r - 1| << 1$, the dielectric properties of the scatterer are very near those of free space. Thus, the internal field will be approximately equal to the incident field and can be approximate by $\vec{E}_i(\vec{r})$ in (2.6). When satisfying the conditions specified by (2.9), a scatterer will be very large in comparison to a wavelength and WKB theory can be applied to estimate the internal field. The WKB approximation is an asymptotic method under which the internal field is assumed to be a plane wave propagating in the same direction as $\vec{E}_i$ but having wavenumber $k_0\sqrt{\varepsilon_r}$ rather than k_0 .

The Rayleigh, Born and WKB approximations are applicable to numerous practical cases. However in the millimeter wave region, raindrops are generally "resonance" sized; that is D is on the order of as opposed to much less than or much greater than the wavelength. In addition, the magnitude of the dielectric constant of water is much greater than unity at millimeter wave frequencies. Hence, the aforementioned field approximation techniques are inappropriate for analyzing rain scatter in the millimeter wave band and other, more rigorous techniques have to be employed. These techniques can usually be classified as being either intplex integral equation or boundary condition methods.

The intplex integral equation methods involve a numerical treatment of the intplex integral expressions for the total and scattered fields (ie, equations (2.2) and (2.4)). Among the intplex integral equation techniques we cite the Fredholm intplex integral equation method developed by Holt, Uzonoglu and Evans [21] which is well suited to the analysis of hydrometeor scatterers. The method is implemented by using the Fourier transform of the field within a scatterer to recast the intplex integral expressions for the total field and far-zone scattered field as a pair of coupled intplex integral equations. These equations are then solved by numerical quadrature to determine the scattered field. The chief advantages of this technique are numerical stability and that it can be applied to a wide range of scatterer shapes and sizes.

The boundary condition methods involve expanding the incident and scattered fields and the fields within the scatterer in fundamental modes constructed from eigensolutions to the scalar wave equation (Generally the expansions are made in spherical modes, but spheroidal wave expansions have also been employed, e.g. [38]). The unknown internal and scattered fields are determined by equating tangential fields across the surface of the raindrop to determine their expansion coefficients. Methods which are included in this category are the Mie theory for spherical raindrops and perturbation and point matching techniques for non-spherical drops. The Mie theory provides an exact solution to the problem of scattering by a sphere and we discuss it in detail in Section 2.3. Perturbation analysis is, in a sense, an extension of the Mie theory in that a scatterer is considered a distortion of a sphere [34], [36], [37]. The method was the first used in treating non-spherical raindrops and provides good results for scatterers which are only slightly non-spherical. In terms of raindrop scatterers, perturbation analysis gives excellent results for smaller raindrops, however larger drops should be analyzed using a different method; the reason for this is that as drop size increases a raindrop's deviation from being spherical also increases [40], [51]. Point matching techniques have been used to analyze raindrop scatterers throughout the entire range of

expected drop sizes [34], [37], [53]. In point matching, the tangential fields are equated at discrete points along the surface of the scatterer to determine the expansion coefficients of the unknown fields. The point matching methods are superior to perturbation in that they are applicable to a greater number of cases; however, they are more expensive to implement. It should also be noted that the point matching methods appear to be limited to treating raindrops which scatter at frequencies below about 35 GHz [20]. This limitation is due to the breaking down of the Rayleigh approximation which allows point matching of spherical modes across a non-spherical surface [61].

Another technique for analyzing raindrop scatterers, the extended boundary condition method (EBCM), is a boundary condition method which also employs techniques used with intplex integral equation formulations. The method involves matching tangential fields to determine modal expansion coefficients for surface currents, the scattered fields are then obtained by operating on the surface currents with radiation integrals. We will discuss this method in detail in Section 2.4.

When analyzing individual raindrop scatterers, one of the important parameters that must be considered is drop shape. Smaller raindrops are well modelled as spheres; however, with increasing size, raindrops become significantly non-spherical. In practice it is quite difficult to model the shape of non-spherical raindrops analytically [40]. However, studies of the effects of rain on propagating waves have shown that modeling a rain cell as a mix of spherical and oblate spheroidal raindrops yields results which are in good agreement with experimental data [51]. Generally then scattering data are computed for spherical and oblate spheroidal raindrops. (An oblate spheroid is defined by revolving an ellipse about its minor axis.) In Sections 2.3 and 2.4 we derive scattering coefficients for drops of these shapes using the Mie theory and the extended boundary condition method. Prior to doing so however, let us discuss the scattering characteristics of a dielectric scatterer in terms of its scattering amplitude and cross sections.

2.2 Scattering Amplitude and Cross Sections

In Section 2.1 we discussed several methods for obtaining the fields scattered by an individual raindrop. When analyzing the overall effects of a distribution of scatterers, the field scattered by each particle is generally not computed directly by one of these methods. Rather, the properties of the scattered field are related to those of the incident field using the scattering amplitudes and cross sections of a particle; our intent in this section is to define these parameters.

Let us consider an arbitrary dielectric scatterer which is illuminated by a linearly polarized unit plane wave (see Figure 2.2)

$$\vec{E}_i(\vec{r}) = \hat{u}_0 e^{-j\vec{k}_i \cdot \vec{r}} \tag{2.10a}$$

where $\hat{u}_0$ is a unit vector defining the polarization of the incident field and

$$\vec{k}_i = k_0 \hat{k}_i \tag{2.10b}$$

As evidenced by (2.6) the scattered field in the far-zone of the particle is an outgoing spherical wave. Thus, we can write the scattered field as

$$\vec{E}_s(\vec{r}) = \vec{f}(\hat{k}_i, \hat{k}_s)\frac{e^{-jk_0 r}}{r} \tag{2.11}$$

where $\hat{k}_s$ is a unit vector in the direction of scattering. $\vec{f}(\hat{k}_i, \hat{k}_s)$ is the vector scattering amplitude of the particle and defines the magnitude, phase and polarization of the scattered field in direction $\hat{k}_s$ when the particle is subject to unit plane wave incidence via $\hat{k}_i$. It is clear from (2.6) that

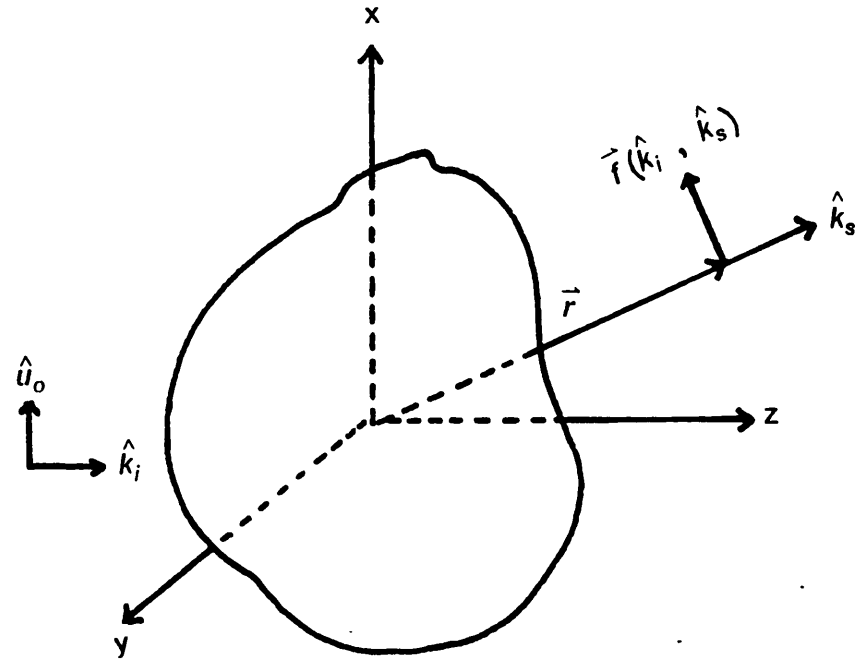

Scattering of a Unit Plane Wave
Figure 2.2

$$\vec{f}(\hat{k}_i, \hat{k}_s) = -\frac{k_0^2}{4\pi}\int[\varepsilon(\vec{r}\,') - 1]\left\{\hat{k}_s x[\hat{k}_s x\vec{E}(\vec{r}\,')]\right\}\exp(jk_0\hat{k}_s \cdot \vec{r}\,')dr)' \tag{2.12}$$

The parametric representation of the scattered field can be generalized to include elliptic, partially polarized, and unpolarized waves by defining a tensor scattering amplitude. To define this parameter, consider a particle which is subject to plane wave incidence via $\hat{k}_i$; the far-zone scattered field in the direction defined by $\hat{k}_s$ is to be observed (see Figure 2.3). The plane of scattering is defined as the plane containing the unit vectors $\hat{k}_i$ and $\hat{k}_s$ and both the incident and scattered field can be resolved into components which are perpendicular and parallel to this plane. We will designate these components as

E_{i1}: Component of incident field perpendicular to scattering plane
E_{i2}: Component of incident field parallel to scattering plane
E_{s1}: Component of scattered field perpendicular to scattering plane
E_{s2}: Component of scattered field parallel scattering plane

E_{s2} and E_{s1} are linearly related to E_{i1} and E_{i2} and can be written in matrix form as [60]

$$\underline{E}_s = \underline{f}(\hat{k}_i, \hat{k}_s)\underline{E}_i\frac{e^{-jk_0r}}{r} \tag{2.13a}$$

where

$$\underline{E}_s = [E_{s1} \;\; E_{s2}]^t \tag{2.13b}$$

$$\underline{E}_i = [E_{i1} \;\; E_{i2}]^t \tag{2.13c}$$

and $\underline{f}(\hat{k}_i, \hat{k}_s)$ is the 2 x 2 tensor scattering amplitude of the particle, viz

$$\underline{\underline{f}}(\hat{k}_i, \hat{k}_s) = \begin{bmatrix} f_{11}(\hat{k}_i, \hat{k}_s) & f_{12}(\hat{k}_i, \hat{k}_s) \\ f_{21}(\hat{k}_i, \hat{k}_s) & f_{22}(\hat{k}_i, \hat{k}_s) \end{bmatrix} \tag{2.13d}$$

In (2.12), $\underline{E}_i$ is evaluated at the origin of the coordinate system. Also, the elements of the tensor scattering amplitude, i.e. f_{11}, f_{12}, f_{21}, and f_{22}, vary only in the longitudinal angle θ .

The expression for the scattered field given by (2.13) is the most convenient for analyzing the effects of a distribution of scatterers on a propagating wave. Hence, the analysis of a signal scatterer generally entails the determination of its tensor scattering amplitude; this is accomplished by using one of the techniques described in Section 2.1.

In addition to the tensor scattering amplitude, the scattering, absorption and total cross sections of a particle are also useful parameters in describing the characteristics of the scattered field [4], [23], [60]. The scattering cross section of a particle, which we will designate C_s, is defined in terms of the total scattered power at all angles surrounding the scatterer. It is a constant of proportionally and is the total amount of power the particle scatters when it is illuminated by a plane wave having unit power per unit area. C_s can be expressed in terms of a scatterer's vector scattering amplitude by

$$C_s = \int_0^{2\pi} \int_0^{\pi} |\vec{f}(\hat{k}_i, \hat{k}_s)|^2 \sin\theta d\theta d\phi \tag{2.14}$$

The absorption cross section of a particle, C_a, is related to the energy it dissipates and is the power it absorbs when illuminated by a plane wave with unit power per unit area. The plex sum of a particle's scattering and absorption cross sections is its total cross section C_t:

$$C_t = C_s + C_a \tag{2.15}$$

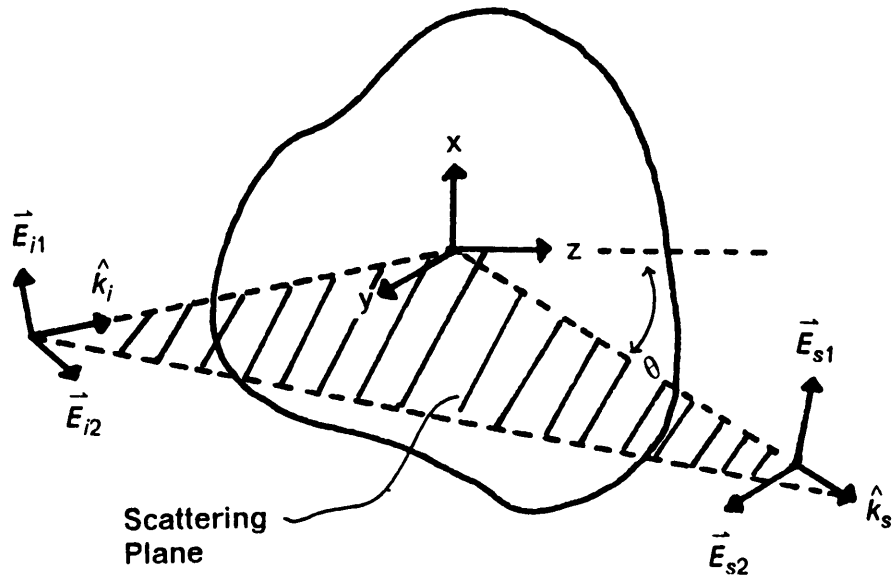

Geometry for Defining the Tensor Scattering Amplitude
Figure 2.3

The total cross section of a scatterer can be related to the elements of its tensor scattering amplitude by the forward scattering theorem [8]. Specifically,

$$C_t = -\frac{4\pi}{k_0} Im[f_{jj}(\hat{k}_i, \hat{k}_s)] \tag{2.16}$$

with j=1 or 2 depending upon the polarization of the incident field.

Having defined the scattering amplitudes and cross sections of a particle let us now turn our attention to computing some of these parameters for specific cases.

2.3 Scattering by a Spherical Raindrop-The Mie Theory

The Mie theory was developed independently by Lorentz in 1890 and Mie in 1908 and, as pointed out in Section 2.1, it provides an exact solution to the problem of scattering by a sphere. In this section we detail the steps involved in the Mie procedure and use the results to compute scattering data for raindrops at millimeter wave frequencies.

2.3.1 Derivation of the Field Scattered by a Sphere

Let us consider a unit plane wave which is incident upon a spherical particle of radius $\bar{a}$ as shown in Figure 2.4 . For convenience we assume the incident field propagates in the z direction and is polarized in the x direction so that

$$\vec{E}_i(\vec{r}) = \hat{x} e^{-jk_0 z} \tag{2.17}$$

In the Mie procedure, the fields scattered by the particle in Figure 2.4 are determined by first expanding the known incident field and unknown scattered and internal fields in spherical modes and then determining the expansion coefficients for the unknown fields by matching tangential fields across the surface of the scatterer. Consider first the expansion of the incident fields.

The primary fields $\vec{E}_i$ and $\vec{H}_i$ can be expanded in vector spherical harmonics constructed from eigensolutions to the scalar wave equation. Specifically, it can be expressed in terms of the $\vec{M}$ and $\vec{N}$ harmonics which are defined by Stratton as [50]

$$\vec{M}_{\substack{e\\o}\ell m}(kr) = \mp z_\ell(kr)\left[\frac{mP_\ell^m(\cos\theta)}{\sin\theta}\right]\begin{matrix}\sin\\\cos\end{matrix}(m\phi)\hat{\theta}$$

$$- z_\ell(kr)\left\{\frac{d}{d\theta}[P_\ell^m(\cos\theta)]\right\}\begin{matrix}\cos\\\sin\end{matrix}(m\phi)\hat{\phi} \qquad (2.18a)$$

$$\vec{N}_{\substack{e\\o}\ell m}(kr) = \ell(\ell+1)\left[\frac{z_\ell(kr)}{kr}\right][p_\ell^m(\cos\theta)]\begin{matrix}\cos\\\sin\end{matrix}(m\phi)\hat{r}$$

$$\mp \left\{\frac{1}{kr}\frac{\partial}{\partial r}[rz_\ell(kr)]\right\}\left\{\frac{d}{d\theta}[p_\ell^m(\cos\theta)]\right\}\begin{matrix}\cos\\\sin\end{matrix}(m\phi)\hat{\theta}$$

$$+ \left\{\frac{1}{kr}\frac{\partial}{\partial r}[rz_\ell(kr)]\right\}\left[\frac{mP_\ell^m(\cos\theta)}{\sin\theta}\right]\begin{matrix}\sin\\\cos\end{matrix}(m\phi)\hat{\phi} \qquad (2.18b)$$

where $P_\ell^m(\cos\theta)$ is the associated Legendre function of degree ℓ and order m and $z_\ell(kr)$ an appropriate spherical Bessel function.

The spherical harmonic expansion for the x polarized electric field given by (2.17) is derived in Appendix A and is

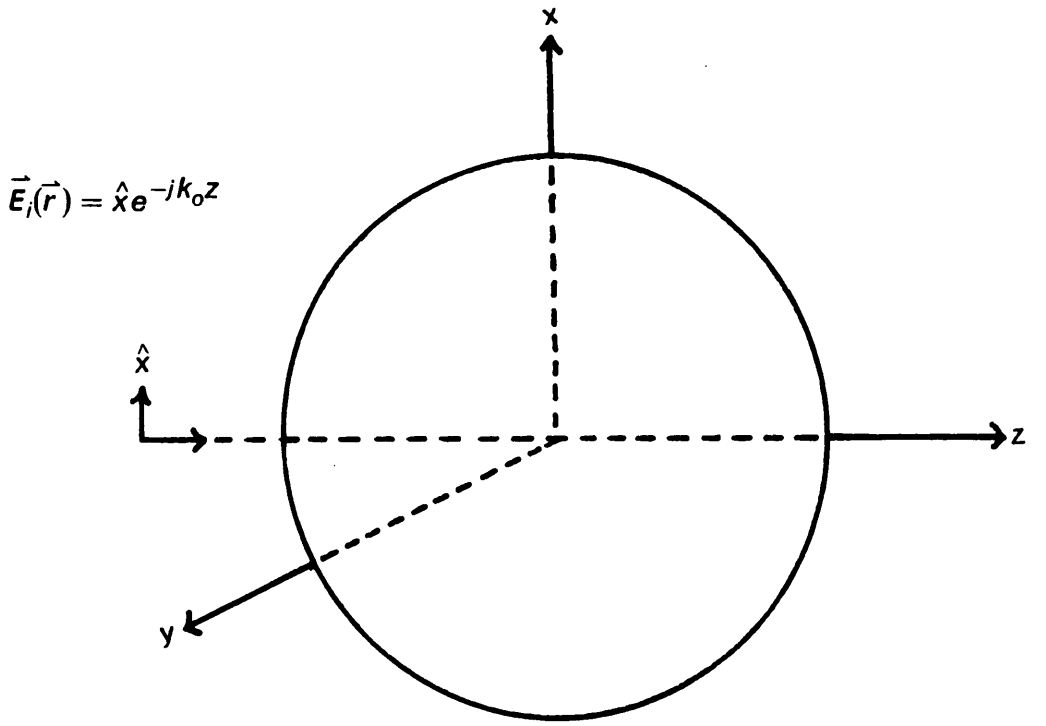

Geometry for Mie Theory Analysis
Figure 2.4

$$\vec{E}_i(\vec{r}) = \sum_{\ell=1}^{\infty} \beta_\ell \left[\vec{M}^{(1)}_{o\ell 1}(k_0 r) + j\vec{N}^{(1)}_{e\ell 1}(k_0 r) \right] \tag{2.19a}$$

where

$$\beta_\ell = j^{-\ell} \frac{2\ell + 1}{\ell(\ell + 1)} \tag{2.19b}$$

and the (1) superscript indicates the spherical Bessel function of the first kind $j_\ell(k_0 r)$ is used in the $\vec{M}$ and $\vec{N}$ vector harmonics.

The modal expansion of the primary magnetic field follows directly from (2.19), the Maxwell curl equation

$$\vec{H}_i = \frac{j}{\omega \varepsilon_0} \nabla x \vec{E}_i \tag{2.20}$$

and the curl equations relating the $\vec{M}$ and $\vec{N}$ vector harmonics which are [50]

$$\vec{M}_{\ell m}(kr) = k \nabla x \vec{N}_{\ell m}(kr) \tag{2.21a}$$

$$\vec{N}_{\ell m}(kr) = k \nabla x \vec{M}_{\ell m}(kr) \tag{2.21b}$$

Specifically,

$$\vec{H}_i(\vec{r}) = -\frac{1}{\eta_0} \sum_{\ell=1}^{\infty} \beta_\ell \left[\vec{M}^{(1)}_{e\ell 1}(k_0 r) - j\vec{N}^{(i)}_{o\ell 1}(k_o r) \right] \tag{2.22}$$

where η_0 is the intrinsic impedance of free space, i.e.

$$\eta = \sqrt{\mu_o / \varepsilon_o} \tag{2.23}$$

and

$$k_0 = \omega\sqrt{\mu_o \varepsilon_0} \tag{2.24}$$

To determine the scattered fields, we assume expansions similar to those in (2.19) and (2.22) for the scattered fields $[\vec{E}_s, \vec{H}_s)$ and the fields within the scatterer $(\vec{E}_t, \vec{H}_t)$, viz

$$\vec{E}_s(\vec{r}) = \sum_{\ell} \beta_\ell \left[a_\ell \vec{M}^{(4)}_{o\ell 1}(k_0 r) + j b_\ell \vec{N}^{(4)}_{e\ell 1}(k_0 r) \right] \tag{2.25a}$$

$$H_s(\vec{r}) = -\frac{1}{\eta_o} \sum_{\ell} \beta_\ell \left[b_\ell \vec{M}^{(4)}_{e\ell 1}(k_o r) + -j a_\ell \vec{N}^{(4)}_{o\ell 1}(k_o r) \right] \tag{2.25b}$$

$$\vec{E}_t(\vec{r}) = \sum_{\ell} \beta_\ell \left[c_\ell \vec{M}^{(1)}_{o\ell 1}(nk_0 r) - j d_\ell \vec{N}^{(1)}_{e\ell 1}(nk_0 r) \right] \tag{2.26a}$$

$$\vec{H}_t(\vec{r}) = -\frac{n}{\eta_o} \sum_{\ell} \beta_\ell \left[d_\ell \vec{M}^{(1)}_{e\ell 1}(nk_o r) - j c_\ell \vec{N}^{(1)}_{o\ell 1}(nk_0 r) \right] \tag{2.26b}$$

where n is the refractive index of the material composing the scatterer and the (4) superscript indicates the spherical Bessel function of the fourth kind $h_\ell^{(2)}(k_0 r)$ is used. The spherical Bessel functions used in (2.25) and (2.26) are chosen to ensure proper behavior of the internal and scattered fields. (Note: in general one would assume a full set of harmonics for unknown field expansions. However, the surface of the scatterer being considered is independent of ϕ. Consequently, the internal and scattered fields will consist only of those modes composing the primary fields.)

The scattered and internal fields are fully specified by determining the unknown expansion coefficients a_ℓ, b_ℓ, c_ℓ, and d_ℓ. This is accomplished by noting the fact that the tangential fields across the surface of the scatterer must be continuous. That is, at $r = \bar{a}$, the following must hold

$$E_{t\theta} - E_{s\theta} = E_{i\theta} \tag{2.27a}$$

$$E_{t\phi} - E_{s\phi} = E_{i\phi} \tag{2.27b}$$

$$H_{t\theta} - H_{s\theta} = H_{i\theta} \tag{2.27c}$$

$$H_{t\phi} - H_{s\phi} = H_{i\phi} \tag{2.27d}$$

After equating the tangential fields as specified by (2.27), the orthogonality of the associated Legendre functions across the surface of the scatterer can be exploited [50]. This leads to a system of equations in each mode for determining the unknown coefficients. Specifically we obtain

$$c_\ell j_\ell(nk_0\bar{a}) - a_\ell h_\ell^{(2)}(k_0\bar{a}) = j_\ell(k_0\bar{a}) \tag{2.28a}$$

$$nc_\ell G_\ell(nk_0\bar{a}) - a_\ell F_\ell(k_0\bar{a}) = G_\ell(k_0\bar{a}) \tag{2.28b}$$

$$nd_\ell j_\ell(nk_0\bar{a}) - b_\ell h_\ell^{(2)}(k_0\bar{a}) = j_\ell(k_0\bar{a}) \tag{2.28c}$$

$$d_\ell G_\ell(nk_0\bar{a}) - b_\ell F_\ell(k_0\bar{a}) = G_\ell(k_0\bar{a}) \tag{2.28d}$$

where we have used the notation

$$F_\ell(kr) \doteq \frac{1}{kr}\frac{\partial}{\partial r}[rh_\ell^{(2)}(kr)] \tag{2.29a}$$

$$G_\ell(kr) \doteq \frac{1}{kr}\frac{\partial}{\partial r}[rj_\ell^{(2)}(kr)] \tag{2.29b}$$

The system of equations in (2.28) is readily solved for a_ℓ, b_ℓ, c_ℓ, and d_ℓ to give

$$a_\ell = \frac{nj_\ell(k_0\bar{a})G_\ell(nk_0\bar{a}) - j_\ell(nk_0\bar{a})G_\ell(k_0\bar{a})}{j_\ell(nk_0\bar{a})F_\ell(nk_0\bar{a}) - nh_\ell^{(2)}(k_0\bar{a})G_\ell(nk_0\bar{a})} \tag{2.30a}$$

$$b_\ell = \frac{nj_\ell(k_0\bar{a})G_\ell(k_0\bar{a}) - j_\ell(nk_0\bar{a})G_\ell(nk_0\bar{a})}{h_\ell^{(2)}(k_0\bar{a})G_\ell(nk_0\bar{a}) - nj_\ell(k_0\bar{a})F_\ell(nk_0\bar{a})} \tag{2.30b}$$

$$c_\ell = \frac{j}{k_0\bar{a})^2}\left[nh_\ell^{(2)}(k_0\bar{a})G_\ell(nk_0\bar{a}) - j_\ell(nk_0\bar{a})F_\ell(k_0\bar{a})\right]^{-1} \tag{2.31a}$$

$$d_\ell = \frac{j}{(k_0\bar{a})^2}\left[h_\ell^{(2)}(k_0\bar{a})G_\ell(nk_0\bar{a}) - nj_\ell(nk_0\bar{a})f_\ell(k_0\bar{a})\right]^{-1} \tag{2.31b}$$

where the Wronskian identity [1]

$$j_\ell(\zeta)\frac{\partial}{\partial\zeta}\left[h_\ell^{(2)}(\zeta)\right] - h_\ell^{(2)}(\zeta)\frac{\partial}{\partial\zeta}\left[h_\ell^{(2)}(\zeta)\right] - h_\ell^{(2)}(\zeta)\frac{\partial}{\partial\zeta}[j_\ell(\zeta)]\frac{-j}{\zeta^2} \tag{2.32}$$

has been used in (2.31)

The series expansions of (2.25) with the coefficients calculated from (2.30) fully specify the scattered fields. We will now use these formulae to compute scattering parameters for spherical raindrops.

2.3.2 Computations of Scattering Coefficients for Spherical Raindrops

Consider the electric field scattered by a sphere as specified by (2.18), (2.19b) and (2.25):

$$\vec{E}_s(\vec{r}) = \sum_{\ell=1}^{\infty} j^{l-\ell}\frac{(2\ell+1)}{\ell(\ell+1)}\left[jb_\ell[\ell(\ell+1)]\left[\frac{h_\ell^{(2)}(k_0r)}{k_0r}\right][P_\ell^1(\cos\theta)]\cos\phi\hat{r}\right.$$

$$+\left\{a_\ell h_\ell^{(2)}(k_0r)\left[\frac{P_\ell^1(\cos\theta)}{\sin\theta}\right] + jb_\ell F_\ell(k_0r)\frac{d}{d\theta}[P_\ell^1(\cos\theta)]\right\}\cos\phi\hat{\theta}$$

$$\left.-\left\{a_\ell h_\ell^{(2)}(k_0r)\frac{d}{d\theta}[P_\ell^1(\cos\theta)] + jb_\ell F_\ell(k_0r)\left[\frac{P_\ell^1(\cos\theta)}{\sin\theta}\right]\right\}\sin\phi\hat{\phi}\right] \tag{2.33}$$

The far-zone scattered field is obtained from (2.33) by using the following asymptotic relationships [18]

$$h_\ell^{(2)}(k_0r) \sim j^{\ell+1}\frac{e^{-jk_0r}}{k_0r} \quad , r\to\infty \tag{2.34a}$$

$$F_\ell(k_0)r \sim j^\ell\frac{e^{-jk_0r}}{k_0r} \quad , r\to\infty \tag{2.34b}$$

Substituting these into (2.33) and discarding the radial term which is asymptotic to $\frac{1}{(k_0r)^2}$, we obtain for $k_0r >> 1$

$$\vec{E}_s(\vec{r}) = \frac{je^{-jk_0r}}{r}\sum_{\ell=1}^{\infty}\frac{2\ell+1}{\ell(\ell+1)}\left\{\left[a_\ell\frac{P_\ell^1(\cos\theta)}{\sin\theta} + b_\ell\frac{d}{d\theta}P_\ell^1(\cos\theta)\right]\cos\phi\hat{\theta}\right.$$

$$- \left[a_\ell \frac{d}{d\theta} P_\ell^1(\cos\theta) + b_\ell \frac{P_\ell^1(\cos\theta)}{\sin\theta} \right] \sin\phi \hat{\phi} \} \tag{2.35}$$

Equation (2.35) expresses the far-zone field scattered by a sphere which is illuminated by an x polarized unit plane wave propagating in the z direction. In comparing this expression with the definition of the vector scattering amplitude given by (2.10), it is readily apparent that $\vec{f}(\hat{z}, \hat{k}_s)$ is given by

$$\vec{f}(\hat{z}, \hat{k}_s) = \frac{j}{k_o} \sum_{\ell=1}^{\infty} \frac{2(\ell+1)}{\ell(\ell+1)} \left\{ \left[a_\ell \frac{P_\ell^1(\cos\theta)}{\sin\theta} + b_\ell \frac{d}{d\theta} P_\ell^1(\cos\theta) \right] \cos\phi \hat{\theta} \right.$$

$$.in10 - \left. \left[a_\ell \frac{d}{d\theta} P_\ell^1(\cos\theta) + b_\ell \frac{P_\ell^1(\cos\theta)}{\sin\theta} \right] \sin\phi \hat{\phi} \right] \tag{2.36}$$

The elements of the more general tensor scattering amplitude can also be deduced from (2.35) and the definition of $\underline{f}(\hat{k}_i, \hat{k}_s)$ put forth in Section 2.2. Specifically, we have

$$f_{11}(\hat{z}, \hat{k}_s) = \frac{j}{k_o} \sum_\ell \frac{2\ell+1}{\ell(\ell+1)} \left[a_\ell \frac{P_\ell^1(\cos\theta)}{\sin\theta} + b_\ell \frac{d}{d\theta} P_\ell^1(\cos\theta) \right] \tag{2.37a}$$

$$f_{12}(\hat{z}, \hat{k}_s) = f_{21}(\hat{z}, \hat{k}_s) = 0 \tag{2.37b}$$

$$f_{22}(\hat{z}, \hat{k}_s) = \frac{j}{k_o} \sum_\ell \frac{z(\ell+1)}{\ell(\ell+1)} \left[a_\ell \frac{d}{d\theta} P_\ell^1(\cos\theta) + b_\ell \frac{P_\ell^1(\cos\theta)}{\sin\theta} \right] \tag{2.37c}$$

Of particular interest is the scattering amplitude in the forward direction, where $\hat{k}_s = \hat{z}$. In this case, the expressions for the diagonal elements of the tensor scattering amplitude can be simplified by noting that [50]

$$\frac{P_\ell^1(\cos\theta)}{\sin\theta}\Big|_{\theta=0} = \frac{d}{d\theta}P_\ell^1(\cos\theta)\Big|_{\theta=0} = \frac{1}{2}\ell(\ell+1) \tag{2.38}$$

The diagonal elements f_{11} and f_{12} are then

$$f_{11}(\hat{z},\hat{z}) = f_{22}(\hat{z},\hat{z}) = \frac{j}{2k_0}\sum_\ell (2\ell+1)(a_\ell + b_\ell) \tag{2.39}$$

Therefore the (scalar) forward scattering amplitude of a sphere, which we will denote by $f_{sph}(0)$ is independent of the polarization and direction of propagation of the incident field and is

$$f_{sph}(0) = \frac{j}{2k_0}\sum_\ell (2\ell+1)(a_\ell + b_\ell) \tag{2.4}$$

As pointed out in Section 2.2, the cross sections of a spherical particle can be obtained from its scattering amplitudes. The scattering cross section can be determined by substituting the expression for the vector scattering amplitude given by (2.36) into (2.14). Doing so and evaluating the resulting integrals gives [60]

$$C_s = \frac{\pi}{k_o^2}\sum_\ell (2\ell+1)(|a_\ell|^2 + |b_\ell|^2) \tag{2.41}$$

The total and absorption cross sections of the scatterer are readily obtained using equations (2.15), (2.16), (2.40) and (2.41).

We have computed scattering parameters for spherical raindrops at 30, 45, 70 and 90 GHz. The values and the code we used to calculate them are presented in Appendix B. In making the calculations, we obtained the refractive index of water at the frequency of interest and a temperature of 20° C using formulae given by Ray [45].

2.4 Scattering by Non-Spherical Raindrops-The Extended Boundary Condition Method (EBCM)

Having considered the problem of scattering by spherical raindrops, we not turn our attention to the more difficult case of non-spherical drops. As pointed out in Section 2.1, several methods have been employed to analyze scattering by non-spherical raindrops. Of these techniques however, only the Fredholm integral equation and extended boundary condition methods are applicaple throughout the millimeter wave band for raindrop scatterers [20].

The EBCM was introduced by Waterman and originally used in the analysis of scattering by conducting bodies [65], [66]; it was later extended to treating dielectric scatterers by several researchers (e.g., [2], [3], [64]). The method is implemented by using Schelknunoff's equivalence principle [48] to replace a scattering body with equivalent magnetic and electric surface currents. These currents are determined by enforcing boundary conditions and used to obtain the scattered fields.

In this section we will use the EBCM to analyze scattering by an oblate spheroidal body and the results of the analysis to compute raindrop scattering parameters. Our treatment of

the problem is based upon the general presentation of the EBCM given by Barber and Yeh [3] but is tailored to the specific case of a spheroidal scatterer.

2.4.1 Analysis of Scattering by an Oblate Spheroidal Body Using the EBCM

The geometry for the problem considered in this analysis is given in Figure 2.5 where an oblate spheroidal body is shown being illuminated by a unit plane wave. The incident field is given by

$$\vec{E}_i(\vec{r}) = \vec{E}_1(\vec{r}) \text{ or } \vec{E}_2(\vec{r}) \tag{2.42}$$

where

$$\vec{E}_1(\vec{r}) = (\hat{x}\cos\alpha - \hat{z}\sin\alpha)\exp[-jk_0(x\sin\alpha + z\cos\alpha)] \tag{2.43a}$$

$$\vec{E}_2(\vec{r}) = \hat{y}\exp[-jk_0(x\sin\alpha + z\cos\alpha)] \tag{2.43b}$$

and α is as shown in Figure 2.5.

The fields external to the scatterer in Figure 2.5 can also be determined by considering the problem shown in Figure 2.6. The situation depicted by Figure 2.6 is constructed from the original problem using the equivalence principle and we will henceforth refer to it as the equivalent problem. In this equivalent problem, the surface S is that which encloses the scattering volume in the original problem and $\vec{J}_i$ and $\vec{M}_i$ are the source currents for the primary fields $\vec{E}_i$ and $\vec{H}_i$. Also, the fields within S are null and the surface currents on S, $\vec{J}_+$ and $\vec{M}_+$, are given by

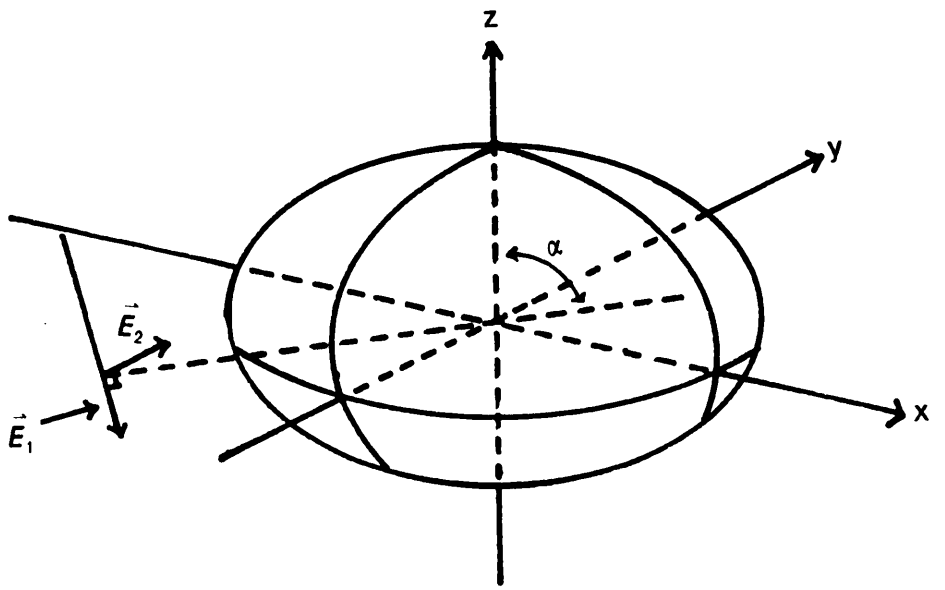

Geometry For Scattering by an Oblate Spheroid

Figure 2.5

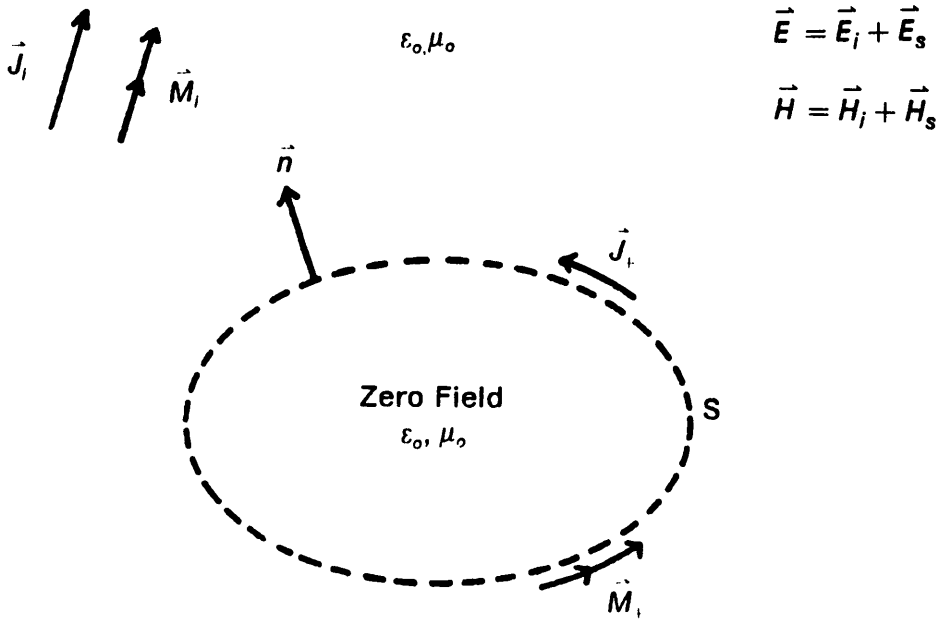

Equivalent Problem for Scattering
by an Oblate Spheroid

Figure 2.6

$$\vec{J}_+ = \hat{n}x(\vec{H}_i + \vec{H}_s) = \hat{n}x\vec{H}_+ \tag{2.44a}$$

$$\vec{M}_+ = (\vec{E}_i + \vec{E}_s)x\hat{n} = \vec{E}_+x\hat{n} \tag{2.44b}$$

with $\hat{n}$ the outward normal unit vector on S and $\vec{E}_s$ and $\vec{H}_s$ the scattered fields.

Since the field within S is zero for the equivalent problem, the scattered field in S must offset the primary field, viz

$$\vec{E}_s(\vec{r}) + \vec{E}_i(\vec{r}) = 0 \quad , \ \vec{r} \ within \ S \tag{2.45}$$

Equation (2.45) can be recast in terms of the surface currents $(\vec{E}_+x\hat{n})$ and $(\hat{n}x\vec{H}_+)$ by expressing the scattered field $\vec{E}_s(\vec{r})$ in terms of radiation integrals involving the surface currents. Specifically we have [18]

$$\vec{E}_s(\vec{r}) = \nabla x\int(\hat{n}x\vec{E}_+)g(k_oR)d\vec{r}\,' - \nabla x\nabla x\int(\hat{n}x\vec{H}_+)g(k_oR)d\vec{r}\,' \tag{2.46a}$$

where the integrals are over the surface of the scatterer and

$$R = |\vec{r} - \vec{r}\,'| \tag{2.46b}$$

So, substituting (2.46) into (2.45) we find that the surface currents will satisfy the integral equation

$$\nabla x\int(\hat{n}x\vec{E}_+)g(k_oR)d\vec{r}\,' - \frac{j}{\omega\varepsilon_o}\nabla x\nabla x\int(\hat{n}x\vec{H}_+)g(k_oR)d\vec{r}\,' = -\vec{E}_i(\vec{r}) \tag{2.47a}$$

with

$$|\vec{r}| < |\vec{r}'| \tag{2.47b}$$

In order to obtain the surface currents $(nx\vec{E}_+)$ and $(\hat{n}x\vec{H}_+)$ the incident field is expanded in Stratton's spherical harmonics (c.f. (2.18)) as follows:

$$\vec{E}_i(\vec{r}) = \sum_{\ell=1}^{\infty}\sum_{m=0}^{\ell} D_{\ell m}[\xi_{\ell m}\vec{M}^{(1)}_{o\ell m}(k_o r) + \eta_{\ell m}\vec{N}^{(1)}_{e\ell m}(k_o r)] \tag{2.48a}$$

where

$$D_{\ell m} = \varepsilon_m \frac{(2\ell+1)(\ell-m)!}{4\ell(\ell+1)(\ell+m)!} \tag{2.48b}$$

$$\varepsilon_m = \begin{cases} 1 \ , & m = 0 \\ 2 \ , & m > 0 \end{cases} \quad (\textit{Neumann's Number}) \tag{2.48c}$$

$$\sigma = \begin{cases} o(odd) \ , & \vec{E}_i = \vec{E}_1 \\ e(even) \ , & \vec{E}_i = \vec{E}_2 \end{cases} \tag{2.48d}$$

$$\tau = \begin{cases} e \ , & \vec{E}_i = \vec{E}_1 \\ o \ , & \vec{E}_i = \vec{E}_2 \end{cases} \tag{2.48e}$$

$$\frac{mP_\ell^m(\cos\alpha)}{\sin\alpha} \quad , \quad \vec{E}_i = \vec{E}_1$$

$$\xi_{\ell m} = 4j^{-\ell} \tag{2.48f}$$

$$-\frac{d}{d\alpha}[P_\ell^m(\cos\alpha)] \quad , \quad \vec{E}_1 = \vec{E}_2$$

$$\frac{d}{d\alpha}[P_\ell^m(\cos\alpha)] \quad , \quad \vec{E}^l = \vec{E}_1$$

$$\eta_{\ell m} = 4j^{-(\ell-1)} \tag{2.48g}$$

$$\frac{mP_\ell^m(\cos\alpha)}{\sin\alpha} \quad , \quad \vec{E}_i = \vec{E}_2$$

(The expansion coefficients and appropriate subscripts, e or o, for the incident field's expansion are derived in Appendix A.)

The integrands of (2.47) are also expanded in spherical modes by noting that

$$\begin{Bmatrix} (\hat{n}\times\vec{E}_+) \\ (\hat{n}\times\vec{H}_+) \end{Bmatrix} g(k_oR) = \begin{Bmatrix} (\hat{n}\times\vec{E}_+) \\ \hat{n}\times\vec{H}_+) \end{Bmatrix} \cdot \underline{1}g(k_oR) \tag{2.49}$$

with $\underline{1}$ the idemfactor or unit dyadic and by using the spherical harmonic expansion of the free space Green's dyadic $\underline{1}g(k_oR)$ [35]:

$$\underline{1}g(k_oR) = \frac{-jk_o}{\pi}\sum_{\ell=1}^{\infty}\sum_{m=0}^{\ell}\sum_{\upsilon} D_{\ell m}\ \vec{M}^{(1)}_{\upsilon\ell m}(k_or')\vec{M}^{1}_{\upsilon\ell m}(k_0r) + \vec{N}^{(1)}_{\upsilon\ell m}(k_or')\vec{N}^{(1)}_{\upsilon\ell m}(k_or)$$

$$+ \vec{N}^{(4)}_{\upsilon\ell m}(k_or')\vec{N}^{(1)}_{\upsilon\ell m}(k_or)$$

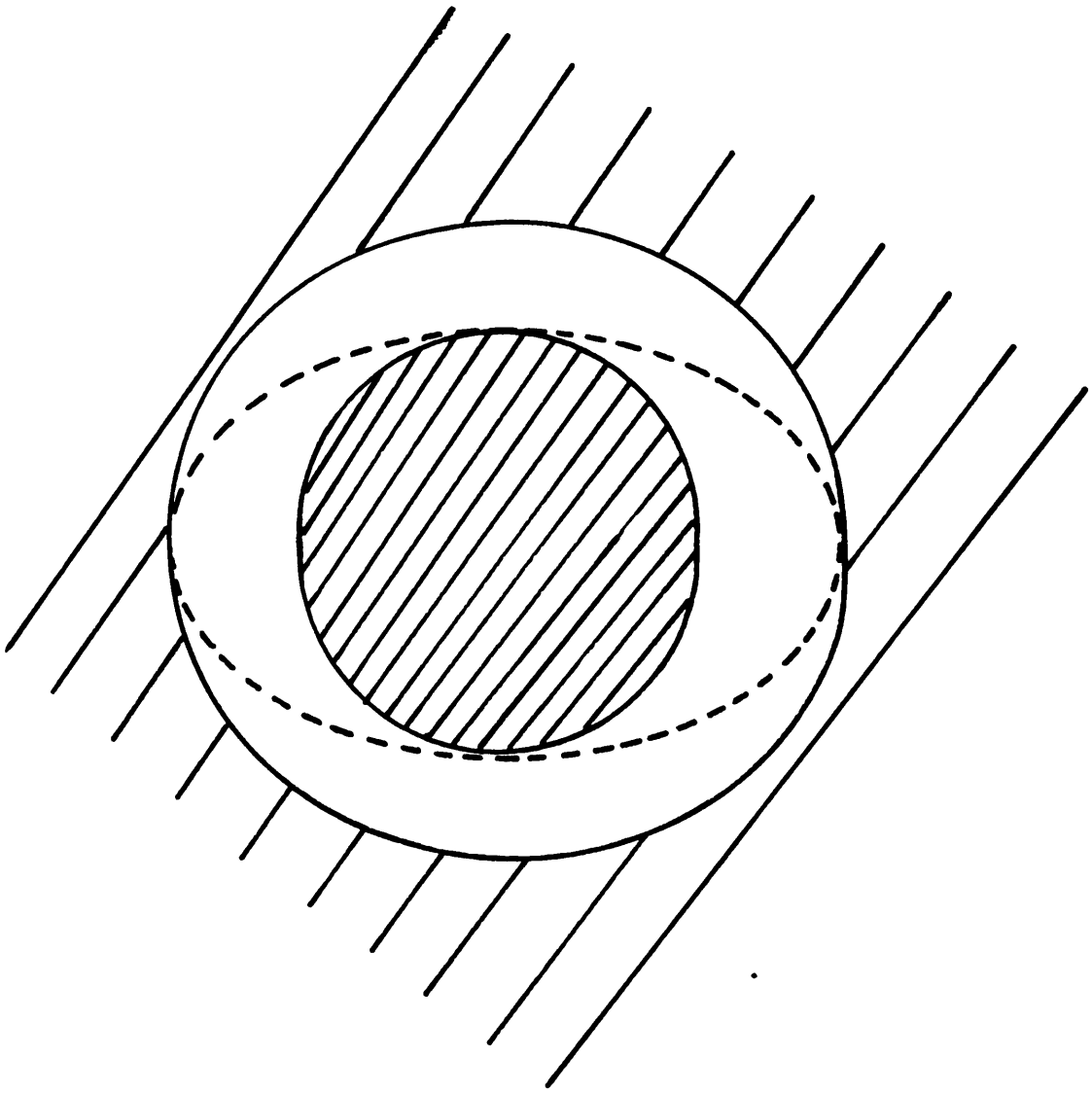

Regions of Convergence for Spherical Harmonic
Expansions of Free Space Green's Dyadic (shaded)
Areas are Regions of Convergence

Figure 2.7

$$+ \textit{ irrotational terms}]$$

$$|\vec{r}| < |\vec{r}'| \tag{2.50}$$

$$1g(k_o R) = -\frac{jk_o}{\pi}\sum_{\ell=1}^{\infty}\sum_{m=0}^{\ell}\sum_{v} D_{\ell m}\Big[\ \vec{N}^{(1)}_{v\ell m}(k_o r')\vec{M}^{(4)}_{v\ell m}(k_o r) + \vec{N}^{1}_{v\ell m}(k_0 r')N^{(4)}_{v\&lit.m}(k_0 r)$$

$$+ \textit{ irrotational terms}\Big[\ ,$$

$$|\vec{r}| > |\vec{r}'| \tag{2.51}$$

In (2.50) and (2.51), v indicates e or 0.

Before continuing, the region of convergence of the expansions given in (2.48), (2.50), and (2.51) should be considered. The series expansion for the incident field given by (2.48) has no singularities in S, however, the free space Green's function $g(k_o R)$ has a singularity at $\vec{r} = \vec{r}'$. Hence, the series expansion given by (2.50) is only valid within a sphere which is inscribed within S and centered at the origin; similarly, the expansion of (2.51) is only valid outside of a sphere circumscribed about S (see Figure 2.7).

Therefore we will assume that $\vec{r}$ in (2.47) is the position vector of a point within the inscribed sphere shown in Figure 2.7. Then, we can correctly substitute the expansions given by (2.48) and (2.50) into (2.57). Doing so and noting that the curl operation eliminates the "irrotational terms" we obtain

$$-\frac{jk_o^2}{\pi}\sum_{\ell,\,m,\,v} D_{\ell m}\int d\vec{r}'\Big[\big[\vec{M}^{(4)}_{v\ell m}(k_o r')\cdot(\hat{n}\times\vec{E}_+) - j\eta_o\vec{N}^{(4)}_{v\ell m}(k_o r')\cdot(\hat{n}\times\vec{H}_+)\big]\vec{N}^{(1)}_{v\ell m}(k_o r)$$

$$+\ \Big[\vec{N}^{(4)}_{v\ell m}(k_o r')\cdot(\hat{n}\times\vec{E}_+) - j\eta_o\vec{M}^{(4)}_{v\ell m}(k_o r')\cdot(\hat{n}\times\vec{H}_+)\Big]\vec{M}^{(1)}_{v\ell m}(k_o r)$$

$$= -\sum_{\ell, m} D_{\ell m}\left[\varepsilon_{\ell m}\vec{M}_{o\ell m}(1)(k_o r) + \eta_{\ell m}\vec{N}^{(1)}_{\tau\ell m}(k_o r)\right] \tag{2.52}$$

By exploiting the orthogonality of the vector spherical harmonics in (2.52) [50], the equation can be recast as the following system of equations:

$$\frac{jk_0^2}{\pi}\int d\vec{r}\,'\left[\vec{N}^{(4)}_{o\ell m}(k_0 r')\cdot(\hat{n}\times\vec{E}_+) - j\eta_o\vec{M}^{(4)}_{o}(k_0 r')\cdot(\hat{n}\times\vec{H}_+)\right] = \varepsilon_{\ell m} \tag{2.53a}$$

$$\frac{jk_0^2}{\pi}\int_S d\vec{r}\,'\left[\vec{M}^{(4)}_{\tau\ell m}(k_0 r')\cdot(\hat{n}\times\vec{E}_+) - j\eta_o\vec{N}^{(4)}_{\tau\ell m}(k_0 r')\cdot(\hat{n}\times\vec{H}_+)\right] = \eta_{\ell m} \tag{2.53b}$$

Surface currents satisfying the system of equations given in (2.53) will guarantee zero field within the inscribed sphere shown in Figure 2.7. However, we require a null field throughout the entire volume enclosed by S. By using analytic continuation arguments, Waterman has shown that the solution to (2.53) does in fact guarantee zero field throughout this volume. Thus, (2.53) partially defines the surface currents in our equivalent problem.

In order to specify completely the surface currents in the equivalent problem, they must also be expressed in terms of the size and dielectric properties of the scatterer under analysis. We accomplish this by expanding the fields internal to the scatterer in spherical modes and equating the tangential fields across the surface of the scatterer. Specifically, we assume the following expansion of the internal electric field:

$$\vec{E}_t(\vec{r}) = \sum_{P=1}^{\infty}\sum_{q=0}^{P}\left[c_{pq}\vec{M}^{(1)}_{\sigma pq}(nk_0 r) + d_{pq}\vec{N}^{(1)}_{\tau pq}(nk_0 r)\right] \tag{2.54}$$

Where c_{pq} and d_{pq} are unknown expansion coefficients and the spherical Bessel function of the first kind is used to ensure the field is finite at the origin.

The modal expansion of the internal magnetic field is obtained directly from (2.54) by using (2.20), (2.21), (2.23) and (2.24), ie

$$\vec{H}_t(\vec{r}) = \frac{jn}{\eta_o}\sum_{P=1}^{\infty}\sum_{q=0}^{P}[c_{pq}\vec{N}^{(1)}_{\sigma pq}(nk_0r) + d_{pq}\vec{M}^{(1)}_{\tau pq}(nk_0r)] \tag{2.55}$$

Note that in the expansions of (2.54) and (2.55) we only include modes which are present in the incident field. This follows from the axial symmetry of the scatterer.

By now equating the tangential fields across the surface of the scatterer, that is by setting

$$\hat{n}x\vec{E}_t(\vec{r}\,') = \hat{n}x\vec{E}_+(\vec{r}\,') \tag{2.56a}$$

$$\hat{n}x\vec{H}_t(\vec{r}\,') = \hat{n}x\vec{H}_+(\vec{r}\,') \tag{2.56b}$$

we obtain the following modal expansions for the surface currents in the equivalent problem:

$$\hat{n}x\vec{E}_+ = \hat{n}x\sum_{p,\,q}[c_{pq}\vec{M}^{(1)}_{\sigma p1}(nk_0r') + d_{pq}\vec{N}^{(1)}_{\tau p1}(nk_0r')] \tag{2.57a}$$

$$\hat{n}x\vec{H}_+ = \frac{jn}{\eta_o}\hat{n}x\sum_{p,\,q}[c_{pq}\vec{N}^{(1)}_{\sigma pq}(nk_0r') + d_{pq}\vec{M}^{(1)}_{\tau pq}(nk_0r') \tag{2.57b}$$

Upon substituting equations (2.57) into (2.53) and using the vector identity $\vec{A}\cdot\vec{B}x\vec{C} = -\vec{B}\cdot\vec{A}x\vec{C}$ [19], the following system of equations is obtained:

$$\sum_{\substack{p=m \\ p\neq 0}}^{\infty} \left\{ c'_{pm}[I^{(4)} + nJ^{(4)}] + d'_{pm}[K^{(4)} + nL^{(4)}] \right\} = \frac{\xi_i}{\ell_m} \tag{2.58a}$$

$$\sum_{\substack{p=m \\ p\neq 0}}^{\infty} \left\{ c'_{pm}[L^{(4)} + nK^{(4)}] + d'_{pm}[J(4) + nI^{(4)}] \right\} = \eta_{\ell m} \tag{2.58b}$$

with

$$c'_{pm} = -\frac{jk_0^2}{\pi} c_{pm} \tag{2.58c}$$

$$d'_{pm} = -\frac{jk_0^2}{\pi} d_{pm} \tag{2.58d}$$

and

$$I^{(i)} = \int_s \left[\hat{n} \cdot \vec{N}^{(i)}_{\sigma\ell m}(k_0 r') x \vec{M}^{(1)}_{\sigma pm}(nk_0 r') \right] d\vec{r}' \tag{2.58e}$$

$$J^{(i)} = \int_s [\hat{n} \cdot \vec{M}^{(i)}_{\sigma\ell m}(k_0 r') x N^{(1)}_{\sigma pm}(nk_0 r')] d\vec{r}' \tag{2.58f}$$

$$K^{(i)} = \int_s [\hat{n} \cdot \vec{N}^{(i)}_{\sigma\ell m}(k_0 r') x \vec{N}^{(1)}_{\tau pm}(nk_0 r')] d\vec{r}' \tag{2.58g}$$

$$L^{(i)} = \int_s [\hat{n} \cdot \vec{M}^{(i)}_{\sigma\ell m}(k_0 r') x \vec{M}^{(1)}_{\tau pm}(nk_0 r')] d\vec{r}' \tag{2.58h}$$

$I^{(0)}$, $J^{(0)}$, $K^{(0)}$ and $L^{(0)}$ are obtained from (2.58 e - h) by replacing σ with τ and τ with σ . Equation's (2.57) and (2.58) fully specify the surface currents $(\hat{n}x\vec{E}_+)$ and $(\hat{n}x\vec{H}_+)$. Thus, the scattered field outside of the circumscribed sphere in Figure 2.7 can now be obtained via the radiation integral of (2.46). Specifically, if we substitute (2.57) into (2.46) and use the modal expansion of the free space Green's dyadic given by (2.51) we obtain

$$E_s(\vec{r}) = \sum_{\ell=1}^{\infty}\sum_{m=0}^{\ell} D_{\ell m}[a_{\ell m}\vec{M}^{(4)}_{\sigma\ell m}(k_0 r) + b_{\ell m}\vec{N}^{(4)}_{\tau\ell m}(k_0 r)] \tag{2.59a}$$

with

$$a_{\ell m} = -\sum_{\substack{p=m \\ p\neq 0}}^{\infty}\left[c'_{pm}[I^{(1)} + nJ^{(1)}] + d'_{pm}[K^{(1)} + nL^{(1)}]\right] \tag{2.59b}$$

$$b_{\ell m} = -\sum_{\substack{p=m \\ P\neq 0}}^{\infty}\left[c'_{pm}[L^{(1)} + nK^{(1)}] + d'_{pm}[J^{(1)} + nI^{(1)}][\right. \tag{2.59c}$$

With (2.58) and (2.59), the scattered field outside of a sphere circumscribed about the scatterer is specified and the EBCM analysis is complete. We note that the solution obtained is exact and theoretically unlimited in its application. There are, however, practical limitations which are dictated by machine capacity.

As we have previously indicated, the forward scattering amplitude and scattering cross section of a particle are of particular interest. Let us consider these parameters for the case at hand beginning with the situation $\vec{E}_i(\vec{r}) = \vec{E}_1(\vec{r})$. Using (2.18) to express the vector harmonics in (2.59) and noting from (2.48) that $\sigma = 0$ and $\tau = e$, we have

$$\vec{E}_s^{(1)}(\vec{r}) = \sum_{\ell}\sum_{m} D_{\ell m}\ b_{\ell m}^{(1)}\left[\ell(\ell+1)\frac{h_\ell^{(2)}(k_0 r)}{k_0 r}P_\ell^m(\cos\theta)\cos(m\phi)\hat{r}\right.$$

$$+\left\{A_{\ell m}^{(1)}h_\ell^{(2)}(k_0 r)\left[\frac{mP_\ell^m(\cos\theta)}{\sin\theta}\right] + b_{\ell m}^{(1)}F_\ell(k_0 r)\frac{d}{d\theta}[P_\ell^m(\cos\theta)\right\}\cos(m\phi)\hat{\theta}$$

$$-\left\{A_{\ell m}^{(1)}h_\ell^{(2)}(k^o r)\frac{d}{d\theta}[P_\ell^m(\cos\theta)] + b_{\ell m}^{(1)}F_\ell(k_0 r)\left[\frac{mP_\ell^m(\cos\theta)}{\sin\theta}[\right\}\sin(m\phi)\hat{\phi} \qquad (2.60)$$

where the (i) superscript indicates values for $\vec{E}_i = \vec{E}_1$.

The far-zone scattered field is obtained by making use of the asymptotic relationships of (2.34) and neglecting the radial term which varies as $1/(k_o r)^2$. The vector scattering amplitude $\vec{f}_1(\hat{k}_i, \hat{k}_s)$ then follows and is

$$\vec{f}_1(\hat{k}_i, \hat{k}_s) = \frac{1}{k_o}\sum_{\ell}\sum_{m} j^\ell D_{\ell m}\left[x\ \textit{lbrac} b_{\ell m}^{(1)}\frac{d}{d\theta}[P_\ell^m(\cos\theta] + ja_{\ell m}^{(1)}\left[mP_\ell^m\frac{(\cos\theta}{\sin\theta}\right]\right\}\cos(m\phi)\hat{\theta}$$

$$-\left\{{}^{(1)}_{\ell m}\left[\frac{mP_\ell^m(\cos\theta)}{\sin\theta}\right] + ja_{\ell m}^{(1)}\frac{d}{d\theta}[P_\ell^m(\cos\theta)]\right\}\sin(m\phi)\hat{\phi} \qquad (2.61)$$

In the forward direction, $\theta = \alpha$ and $\phi = 0$. Thus, the forward scattering amplitude, which we denote $\vec{f}_1(0, \alpha)$, is

$$\vec{f}_1(0, \alpha) = \frac{1}{k_o}\sum_{\ell}\sum_{m} j^\ell D_{\ell m}\left\{b_{\ell m}^{(1)}\frac{d}{d\alpha}[P_\ell^m(\cos\alpha)] + ja_{\ell m}^{(1)}\left[\frac{mP_\ell^m(\cos\alpha)}{\sin\alpha}\right]\right\}\hat{\theta} \qquad (2.62)$$

The scattering cross section of the spheroid for $\vec{E}_i(\vec{r}) = \vec{E}_1(\vec{r})$ is obtained by substituting (2.61) into (2.14). Doing so and evaluating the resulting intplex integral yields

$$C_s^{(1)} = \frac{\pi}{k_0^2}\sum_{\ell}\sum_{m}\varepsilon_m D_{\ell m}\left[|a_{\ell m}|^2 + |b_{\ell m}|\right]2 \tag{2.63}$$

ε_m being Neumann's number, (see (2.48c))

In obtaining (2.63), we have used the identities [34], [50]

$$m\int_o^{\pi}\left\{P_\ell^m(\cos\theta)\frac{d}{d\theta}[P_n^m(\cos\theta)] + P_n^m(\cos\theta\frac{d}{d\theta}[P_\ell^m(\cos\theta)]\right\}d\theta = 0 \tag{2.64}$$

and

$$\int_o^{\pi}\left\{\frac{d}{d\theta}[P_\ell^m(\cos\theta)]\frac{d}{d\theta}[P_n^m(\cos\theta)] + \frac{m^2}{\sin^2\theta}P_\ell^m(\cos\theta)P_n^m(\cos\theta)\right\}\sin\theta d\theta$$

$$= \frac{2\ell(\ell+1)(\ell+m)!}{(2\ell+1)}(\ell-m)!\delta_{\ell m} \tag{2.65}$$

where $\delta_{\ell n}$ is the Kronecker delta, i.e.

$$\delta_{\ell n} = \begin{matrix} 1 & , \ell = n \\ 0 & , otherwise \end{matrix}$$

Similarly, the forward scattering amplitude and scattering cross section for the case $\vec{E}_i = \vec{E}_2$ are found to be

$$\vec{f}_2(0,\alpha) = \frac{1}{k_o}\sum_{\ell}\sum_{m} j^{\ell} D_{\ell m}\left\{ b_{\ell m}^{(2)}\left[\frac{mP_\ell^m(\cos\alpha)}{\sin\alpha}\right] - ja_{\ell m}^{(2)}\frac{d}{d\alpha}[P_\ell^m(\cos\alpha)]\right\}\hat{\phi} \tag{2.66}$$

$$C_s^{(2)}(0,\alpha) = \frac{\pi}{k_0^2}\sum_{\ell}\sum_{m} \varepsilon_m D_{\ell m}[|a_{\ell m}^{(2)}|^2 + |b_{\ell_m}|^{(2)}] \tag{2.67}$$

Let us now consider the steps involved in computing scattering data using the EBCM.

2.4.2 Numerical Implementation of the EBCM for Oblate Spheroidal Scatterers

In order to compute scattering data with the EBCM, it is helpful to express the fundamental equations given in (2.58) and (2.59) in a more compact form. So, consider the series expansion for the scattered field as given by (2.59a). Let us assume that L_{max} radial modes and M_{max} azimuthal modes are required for convergence of the series to a desired tolerance so that

$$\vec{E}_s(\vec{r}) = \sum_{m=0}^{M_{max}} \sum_{\substack{\ell=m \\ \ell\neq 0}}^{L_{max}} D_{\ell m}\left[{}_{\ell m}\vec{M}_{\sigma\ell m}^{(4)}(k_0 r) + b_{\ell m}\vec{N}_{\tau\ell m}^{(4)}(k_0 r)\right] \tag{2.68}$$

Similarly, by truncating (2.58 a & b) and (2.59 b & c) at upper limits of $p = L_{max}$, we obtain the following systems of equations in each azimuthal mode m:

$$\sum_{\substack{p=m \\ P\neq 0}}^{L_{max}} \left\{c'_{pm}[I^{(4)} + nJ^{(4)}] + d'_{pm}[K^{(4)} + nL^{(4)}]\right\} = \xi_{\ell m} \tag{2.69a}$$

$$\sum_{\substack{p=m \\ p\neq 0}}^{L_{max}} \left\{c'_{pm}[L^{(4)} + nK^{(4)}] + d'_{pm}[J^{(4)} + nI^{(4)}]\right\} = \eta_{\ell m} \tag{2.69b}$$

$$A_{\ell m} = -\sum_{\substack{p=m \\ p\neq 0}}^{L_{max}} \left\{c'_{pm}[I^{(1)} + nJ^{(1)}] + d'_{pm}[K^{(1)} + nL^{(1)}]\right\} \tag{2.70a}$$

$$b_{\ell m} = -\sum_{\substack{p=m \\ p\neq 0}}^{L_{max}} \left\{c'_{pm}[L^{(1)} + nK^{(1)}] + d'_{p}m[J^{(1)} + nI^{(1)}]\right\} \tag{2.70b}$$

It is clear that (2.69) and (2.70) can be recast as a pair of coupled matrix equations, i.e.

$$\underline{S}_m^{(4)}\underline{C}_m = \underline{X}_m \tag{2.71a}$$

$$\underline{A}_m = -\underline{S}_m^{(1)}\underline{C}_m \tag{2.71b}$$

where

$S_m^{(i)}$ = $2\,L_{max} - mx1 + 2(L_{max} - m + 1)$ matrix whose elements are determined by the refractive index n and the surface integrals $I^{(i)}$, $J^{(i)}$, etc.

$\underline{C}_m$ = $2\,(L_{max} - m + 1)$ column vector containing the unknown coefficients c'_{pm} and d'_{pm}

$\underline{A}_m$ = $2\,(L_{max} - m + 1)$ column vector containing the unknown coefficients $a_{\ell m}$ and $b_{\ell m}$.

$\underline{X}_m$ = $2\,(L_{max} - m + 1)$ column vector containing the expansion

coefficients $\zeta_{\ell m}$ and η_{ℓ_m}.

Thus, the unknown coefficients for the modal expansion of the scattered field are given by

$$A_m = -S_m^{(1)}[\underline{S}_m^{(4)}]^{-1}\chi_m \tag{2.72}$$

The matrix $-\underline{S}_m^{(1)}[\underline{S}_m^{(4)}]^{-1}$ is often written as $\underline{T}_m$ and referred to as the $T-matrix$, hence the designation T-matrix method which is often used when referring to the EBCM.

For the purposes of computing scattering data, (2.72) is the most convenient form of expressing the ECMS's fundamental equations. With this representation, the computation of scattering parameters can be broken down into the following five steps:

1. Pick L_{max} and M_{max}
2. For each azimuthal mode, fill the matrices $\underline{S}_m^{(1)}$ and $\underline{S}_m^{(4)}$ and compute the T-matrix.
3. Compute the scattered field's expansion coefficients a_{lm} and b_{lm} using (2.72).
4. Compute the scattered field or a desired parameter such as the scattering amplitude or scattering cross section.
5. Check for convergence

If convergence within a prescribed tolerance has not been achieved L_{max} and M_{max} can be increased and the process repeated.

2.4.3 Computed Values of Raindrop Scattering Parameters Obtained Using the EBCM.

In order to compute scattering data using the EBCM, the surface integrals given in (2.58) must be recast in a suitable manner. To accomplish this, we assumed the following linear

relationship between an oblate spheroidal raindrop's equivolumetric radius and its axial ratio [34], [5]:

$$\frac{a}{b} = 1 - \bar{a} \tag{2.73}$$

where a and b are, respectively, the semiminor and semimajor axes of the spheroid and $\bar{a}$ its equivolumetric radius in cm. Using (2.73), the outward normal unit vector on the surface of the scatterer is (see Appendix C)

$$\hat{n} = v_r \hat{r} + v_\theta \hat{\theta} \tag{2.74a}$$

with

$$v_r = \left[1 + \left(\frac{\upsilon \sin\theta \cos\theta}{1 - \upsilon \sin^2\theta}\right)^2\right]^{-1/2} \tag{2.74b}$$

$$v_\theta = -v_r \frac{v \sin\theta \cos\theta}{1 - \sin \upsilon \sin^2\theta} \tag{2.74c}$$

$$\upsilon = \bar{a}(2 - \bar{a}) \tag{2.74d}$$

Using the above, expression which are suitable for computation were obtained for the surface integrals and are given in Appendix C.

We have computed oblate spheroidal raindrop scattering parameters for the following cases:

Frequency = 30, 45, 70, 90 GHz

$\bar{a}$ = .025 through .350 cm (steps of .025 cm)

α = 0 through 90 degrees (steps of 15 degrees)

Polarizations = 1 and 2

The computed data and our EBCM program are in Appendix C. The data we will use to make computations in Chatpers 3 and 4 is that for $\alpha = 90°$. We note that the values of $f(0, \alpha)$ for $\alpha = 0°$ *and* $90°$ at 30 GHz are in excellent agreement with those Thompson obtained using point matching [53].

Chapter 3 Analysis of the Coherent Field in the Presence of Rain

The focus of attention in Chapter 2 was the scattering properties of individual raindrops. In this chapter we extend the raindrop scattering problem and begin looking at the scattering properties of a randomly distributed ensemble of drops.

Our concern here will be the coherent properties of millimeter wave propagation through rain and the chapter is divided into five sections. In Section 1 we present a general discussion of the coherent and incoherent parts of a random field. This section is provided to briefly describe these quantities and establish their physical significance. Section 2 of this chapter is preliminary to the analysis that will be conducted and puts forth the assumptions and definitions that will be used.

In Section 3 of this chapter we derive the vector coherent field within a rain cell using a multiple scattering analysis based on the Twersky procedure [56]-[58]; this section is basically a review of past analyses (for example [54]). The focus of Section 4 is the coherent output of a receiver during a rain event. In this section, we employ a rigorous analysis using Fourier

expansions of the scattered field. By treating the problem in this fashion, the effects of random scattering in the near field of an antenna can be taken into account. Section 5 of this chapter deals with applications. Specifically, the fundamental model derived in Section 4 is used to predict the attenuation and depolarization of the coherent field for various cases.

3.1 Coherence vs. Incoherence

In subsequent portions of this dissertation, we will be concerned with the coherent and incoherent properties of waves propagating through rain. The intent of this section is to provide qualititative descriptions of the coherent and incoherent parts of a propagating wave. Our purpose in providing these descriptions is to establish a physical basis for the mathematical representations we will be using.

Consider a field which propagates in the presence of a medium of randomly distributed particles; for the purposes of this discussion, the field will be assumed scalar and designated $\psi(\vec{r})$. $\psi(\vec{r})$ will be composed of a primary field and the field scattered by particles within the medium. Inasmuch as these particles are randomly distributed, the scattered and, hence, total fields will be random and can be expressed as the sum of an average component, $<\psi(\vec{r})>$, and a fluctuating, zero mean component, $\psi_f(\vec{r})$, viz

$$\psi(\vec{r}) = <\psi(\vec{r})> + \psi_f(\vec{r}) \tag{3.1a}$$

$$<\psi_f(\vec{r})> = 0 \tag{3.1b}$$

The average and fluctuating parts of the field are respectively termed the coherent and incoherent field.

The intensity of the field is defined as the squared modulus of the field and is directly proportional to power. This too will be random and is given in terms of the coherent and incoherent components of the field by

$$|\psi(\vec{r})|^2 = |<\psi(\vec{r})>|^2 + <\psi(\vec{r})>\psi_i(\vec{r}) + <\psi(\vec{r})>\psi_i(\vec{r}) + |\psi_i(\vec{r}|^2 \quad (3.2)$$

where the asterisk denotes complex conjugation. Therefore the average total intensity , or simply total intensity, consists of the coherent intensity and the average intensity of the fluctuating field which is referred to as the incoherent intensity, i.e.

$$<|\psi(\vec{r})|^2> = |<\psi(\vec{r})>|^2 + <|\psi_i(\vec{r})|^2> \quad (3.3)$$

From a system's performance standpoint, the coherent part of the total signal is generally taken as the "usable" signal. On the other hand, the incoherent signal is typically treated as noise because of its random nature [11]. Because it is sometimes appreciable, the incoherent signal one expects to receive during a rain event should be taken into account during system planning.

We will address the problem of predicting the incoherent signal in Chapter 4. In the remainder of this chapter however we will consider the coherent properties of millimeter wave signals in the presence of rain.

3.2 Analysis of the Coherent Field-Statement of the Problem

The problem we will consider in the chapter is illustrated by Figure 3.1 which shows a normally incident plane wave illuminating a rain cell. The rain cell is modeled as a plane-parallel slab of scatterers which is of length d and indefinite extent, and the incident wave has electric field vector

$$\vec{E}^i(\vec{r}) = \vec{E}_o e^{-jk_0 z} \tag{3.4a}$$

$$\vec{E}_o \cdot \hat{z} = 0 \tag{3.4b}$$

Our objective will be to derive expressions for the average signal at the output of the receiver shown in Figure 3.1 so that the attenuation and depolarization caused by the rain can be predicted. To do this some assumptions about the characteristics of the rain must be made and the properties of the receiving system defined.

We will assume the raincell shown in Figure 3.1 is a sparse medium in the sense that each raindrop lies in the far field radiation zone of all others within the slab. Furthermore, the scatterers will be taken to be independently and identically distributed with joint probability density [54], [55].

$$\rho(\vec{\omega}) = \frac{n(\vec{\omega})}{N} \tag{3.5}$$

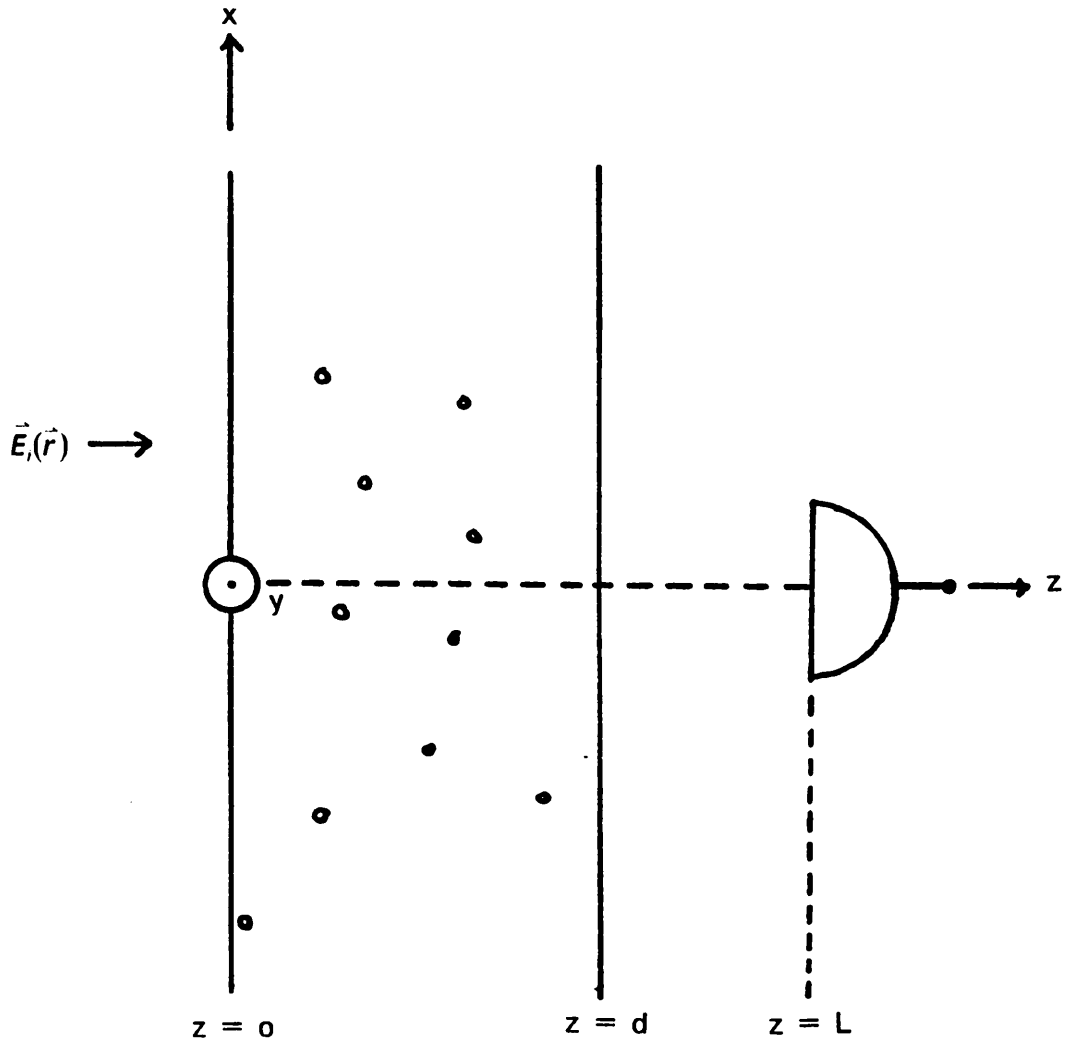

Geometry for Analysis of the Coherent Signal

Figure 3.1

where $\vec{\omega}$ is a random vector describing the statistical properties of a raindrop , $n(\vec{\omega})$ is the number of drops per unit volume whose parameters are given by $\vec{\omega}$ and N is the total number of scatterers in the slab.

The statistical parameters which describe a raindrop scatterer are its position, size, shape and orientation. We will assume the raindrops are uniformly distributed in position and that the size, shape and orientation of a raindrop are statistically independent so that [54]

$$\rho(\vec{\omega}) = n(\bar{a})p(s)p\frac{(\alpha}{N} \tag{3.6}$$

where

$\bar{a}$ = Equivolumetric radius of a raindrop.
$n(\bar{s})$ = Number of raindrops per unit volume having radius $\bar{a}$.
s = Variable indicating drop shape.
α = Raindrop canting angle with respect to the axes transverse to the directions of propagation (see Figure 3.2).
$p(s)$, $p(\alpha)$ = Probability densities which statistically describe drop shape and orientation.

It should be noted that by statistically modeling raindrops in the above fashion, we have made simplifying assumptions regarding the drop size distribution $n(\bar{a})$ and a raindrop's orientation. The assumption we have made in connection with $n(\bar{a})$ is that it is independent of position. However, the drop size distribution of a raincell is dependent upon the rain rate which can vary with z [43], [51]. Consequently, it is more generally correct to write the drop size distribution as $n'(\bar{a}, RR(z))$, RR(z) being the rain rate. For our analysis, we employ the path averaged drop size distribution

$$n(\bar{a}) = \frac{1}{d}\int_o^d n'(\bar{a}, RR(z))dz \tag{3.7}$$

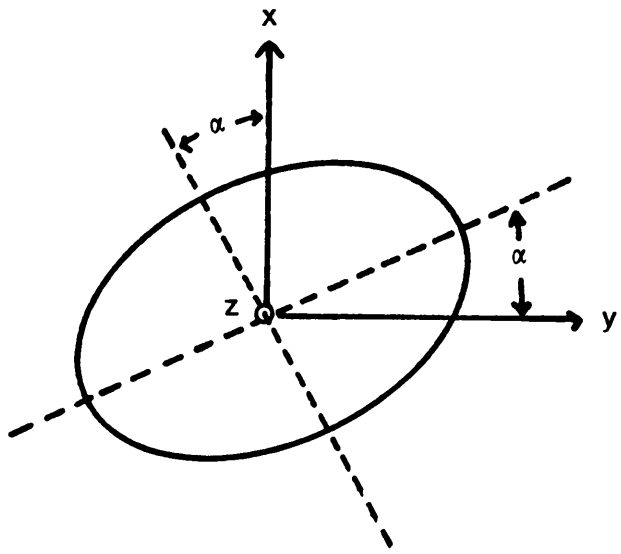

Canting Angle α of an Oblate Spheroidal Raindrop

Figure 3.2

Our assumption concerning raindrop orientation is that there is only rotation about the z axis. An actual raindrop can also be canted about the y axis; however, Oguchi has shown that only that about the z axis need be considered [40].

Now consider the characteristics of the receiver. The receiver's properties can be defined in terms of an effective length $\vec{F}(\theta, \phi)$ where [12]

$$\vec{F}(\theta, \phi) = F_\theta(\theta, \phi)\hat{\theta} + F_\phi(\theta, \phi)\hat{\phi} \tag{3.8}$$

and (θ, ϕ) define the direction cosines of a uniform plane wave which illuminates the receiver's antenna. If we let $\vec{E}$ be the vector amplitude of this plane wave, the voltage at the output of the receiver is given by

$$V = \vec{F}(\theta, \phi) \cdot \vec{E} \tag{3.9}$$

Equation (3.9) expresses the received signal as a function of both the propagation direction and polarization of the wave illuminating the antenna. We can extend this model to include dual polarizations by defining a response matrix $\underline{E}(\theta, \phi)$ and a voltage vector $\vec{V}$, viz

$$\vec{V} = \underline{E}(\theta, \phi) \cdot \vec{E} \tag{3.10a}$$

where

$$\vec{V} = [V_1 \; V_2]^T \tag{3.10b}$$

$$\underline{E}(\theta, \phi) = \begin{bmatrix} \vec{F}_1(\theta, \phi) \\ \vec{F}_2(\theta, \phi) \end{bmatrix} \tag{3.10c}$$

$$V_i = \vec{F}_i(\theta, \phi) \cdot \vec{E} \tag{3.10d}$$

and V_i is the voltage at the receiver's output for polarization state i.

With the properties of the scattering medium and the receiver modeled, we may now conduct our analysis of the coherent field. We begin by considering the average vector field within a raincell.

3.3 The Coherent Field Within A Rain Cell-Multiple Scattering Analysis

Consider the total field at a point $\vec{r}$ within the slab of Figure 3.1. The total field is the plex sum of the primary and scattered fields; therefore, with N scatterers in the slab we have

$$\vec{E}(\vec{r}) = \vec{E}_i(\vec{r}) + \sum_{j=1}^{N} \vec{E}_s(\vec{r}, \vec{r}_j) \tag{3.11}$$

where $\vec{E}(\vec{r}, \vec{r}_j)$ is the field scattered to $\vec{r}$ from the scatterer at $\vec{r}_j$ (see Figure 3.3)

We assume that scattered field can be expressed parametrically by

$$\vec{E}_s(\vec{r}, \vec{r}_j) = \underline{u}(\vec{r}, \vec{r}_j)\vec{E}(\vec{r}_j) \tag{3.12}$$

where $\vec{E}(\vec{r}_j)$ is the total field at $\vec{r}_j$ (i.e. the plex sum of the incident and scattered fields in the absence of a scatterer) and $\underline{u}(\vec{r}, \vec{r}_j)$ a tensor operator.

Equations (3.11) and (3.12) are the fundamental ones used in the Twersky procedure [56]-[58]. By successively substituting one into the other, it can readily be seen that the total field at $\vec{r}$ can be expressed as the infinite series of summations.

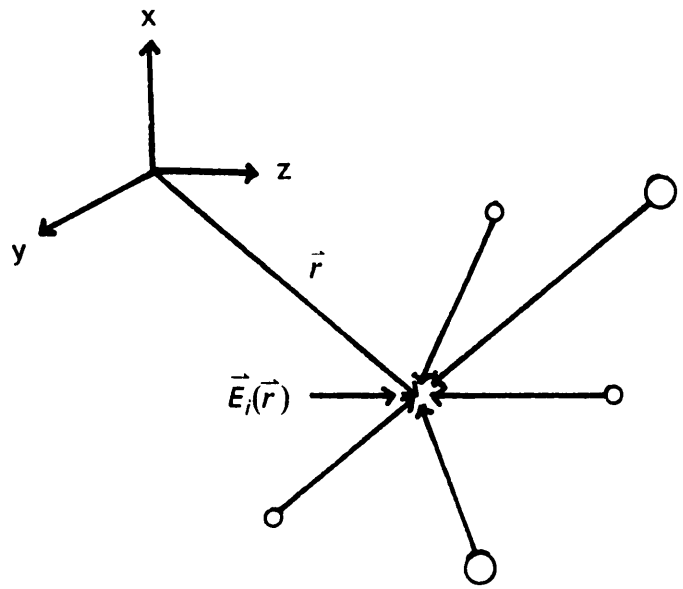

The Total Field at $\vec{r}$ as the Sum of the Primary and Scattered Fields

Figure 3.3

$$\vec{E}(\vec{r}) = \vec{E}_i(\vec{r}) + \sum_{j=1}^{N} u(\vec{r}), \vec{r}_j \vec{E}_i(\vec{r}_j)$$

$$+ \sum_{j=1}^{N} \sum_{k=1(j)}^{N} \underline{u}(\vec{r}, \vec{r}_j)\underline{u}(\vec{r}_j, \vec{r}_k)\vec{E}_i(\vec{r}_k)$$

$$+ \sum_{j=1}^{N} \sum_{k=1(j)}^{N} \sum_{\substack{\ell=1 \\ (k)}}^{N} \underline{u}(\vec{r}, \vec{r}_j)\underline{u}(\vec{r}_j, \vec{r}_k)\underline{u}(\vec{r}_k, \vec{r}_\ell)\vec{E}_i(\vec{r}_\ell)$$

$$+ \ldots \qquad (3.13)$$

with

$$\sum_{\substack{n=1 \\ (m)}}^{N} \textit{implying} \sum_{\substack{n=1 \\ n \neq m}}^{N}$$

The right-hand side of (3.13) describes all possible scattering combinations of the incident field enroute to $\vec{r}$; the process is shown pictorially in Figure 3.4.

Now, the third term on the right hand side of (3.13) can alternately be expressed as

$$\sum_{j=1}^{N} \sum_{k=1(j)}^{N} \sum_{\ell=1(k)}^{N} \underline{u}(\vec{r}, \vec{r}_j)\underline{u}(\vec{r}_j, \vec{r}_k)\underline{u}(\vec{r}_k, \vec{r}_\ell)\vec{E}_i(\vec{r}_\ell)$$

$$= \sum_{j=1}^{N} \sum_{k=1(j)}^{N} \underline{u}(\vec{r}, \vec{r}_j)\underline{u}(\vec{r}_j, \vec{r}_k)\underline{u}(\vec{r}_k, \vec{r}_j)\vec{E}_i(\vec{r}_j)$$

$$+\sum_{j=1}^{N}\sum_{k=1(j)}^{N}\sum_{\substack{\ell=1\\(j,k)}}^{N}\underline{u}(\vec{r},\vec{r}_j)\underline{u}(\vec{r}_j,\vec{r}_k)\underline{u}(\vec{r}_k,\vec{r}_\ell) \tag{3.14}$$

Note that the first term on the right hand side of (3.14) defines N(N-1) scatterings and the second term N(N-1)(N-2) scatterings. Thus, (3.14) indicates $N(N-1)^2$ scatterings and as $N \to \infty$

$$N(N-1) << N(N-1)^2 \tag{3.15a}$$

$$N(N-1)(N-2) \simeq N(N-1)^2 \tag{3.15b}$$

So, if we neglect the double summation term in (3.15), the number of scatterings left out is asymptotically small for large N. We therefore do so and recast (3.13) as

$$\vec{E}(\vec{r}) = \vec{E}_i(\vec{r}) + \sum_{j=1}^{N}\underline{u}(\vec{r},\vec{r}_j)\vec{E}_i(\vec{r}_j)$$

$$+\sum_{j=1}^{N}\sum_{k=1(j)}\underline{u}(\vec{r},\vec{r}_j)\underline{u}(\vec{r}_j,\vec{r}_k)\vec{E}_i(\vec{r}_k)$$

$$+\sum_{j=1)}^{N}\sum_{\substack{k=1\\(j)}}\sum_{\substack{\ell=1\\(j,k)}}\underline{u}(\vec{r},\vec{r}_j)\underline{u}(\vec{r}_j,\vec{r}_k)\underline{u}(\vec{r}_k,\vec{r}_\ell)\vec{E}_i(\vec{r}_\ell)$$

$$+ \ldots. \tag{3.16}$$

In (3.16) the higher order terms have been treated in the same manner as the triple plex sum term so that a particular scatterer appears only once in a scattering "chain".

If we now average (3.16) over the joint probability density of (3.5) we obtain the following series expansion for the vector coherent field at $\vec{r}$:

$$<\vec{E}(\vec{r})> = \vec{E}_i(\vec{r}) + \frac{1}{N}\sum_{j=1}^{N}\int \underline{u}(\vec{r},\vec{r}_j)\vec{E}_i(\vec{r}_i)n(\vec{\omega}_j)d\vec{\omega}_j$$

$$+ \frac{1}{N^2}\sum_{j=1}^{N}\sum_{K=1(j)}^{N}\int\int \underline{u}(\vec{r},\vec{r}_j)\underline{u}(\vec{r}_j,\vec{r}_k)\vec{E}_i(\vec{r}_k)n(\vec{\omega}_j)n(\omega_k)d\vec{\omega}_j d\vec{\omega}_k$$

$$+ \frac{1}{N^3}\sum_{j=1}^{N}\sum_{k=1(j)}^{N}\sum_{\ell=1(j,\,k)}^{N}\int\int\int \underline{u}(\vec{r},\vec{r}_j)\underline{u}(\vec{r}_j,\vec{r}_k)\underline{u}(\vec{r}_k),(\vec{r}_\ell)\vec{E}_i(\vec{r}_\ell)n(\vec{\omega}_j)n(\vec{\omega}_k)n(\vec{\omega}_{\times llt})d\vec{\omega}_j d\vec{\omega}_k d\vec{\omega}_\ell$$

$$+ \ldots \qquad (3.17)$$

Using our assumption that the scatterers are independently and identically distributed, (3.17) can be rewritten as

$$<\vec{E}(\vec{r})> = \vec{E}_i(\vec{r}) + \int \underline{u}(\vec{r},\vec{r}_j)\vec{E}_i(\vec{r}_j)n(\omega_j)d\vec{\omega}_j$$

$$+ N\frac{(N-1)}{N^2}\int \rightarrow,\vec{r}_j)\underline{u}(\vec{r}_j,\vec{r}_k)\vec{E}_i(\vec{r}_k)n(\vec{\omega}_j)n(\vec{\omega}_K)d\vec{\omega}_j s\vec{\omega}_k$$

$$+ \frac{N(n-1)(N-1)}{N^3}\int\int\int \underline{u}(\vec{r},\vec{r}_j)\underline{u}(\vec{r}_j,\vec{r}_k)\underline{u}(\vec{r}_k,\vec{r}_\ell)\vec{E}_i(\vec{r}_\ell)n(\vec{\omega}_j)n(\vec{\omega}sbuk)n(\vec{\omega}_\ell)d\vec{\omega}_j d\vec{\omega}_K d\vec{\omega}sbu\ell$$

$$+ \ldots \tag{3.18}$$

If we now allow the number of particles in the scattering volume to approach infinity so that

$$\frac{N(N-1)\cdots(N-m+1)}{N^m} \simeq 1 \tag{3.19}$$

it can be readily seen that (3.18) then corresponds to the Liouville-Neumann iterative expansion of the intplex integral equation

$$<\vec{E}(\vec{r})> = \vec{E}_i(\vec{r}) + \int \underline{u}(\vec{r},\vec{r}\,')<\vec{E}(\vec{r}\,')> n(\vec{\omega})d\vec{\omega} \tag{3.20}$$

Equation (3.20) is the Foldy-Lax-Twersky intplex integral equation for the vector coherent field. The equation was initially put forth by Foldy [14] but its physical significance was later established by Twersky.

The difficulty in obtaining a solution to (3.20) depends upon the complexity of the operator $\underline{u}(\vec{r},\vec{r}\,')$. For the problem we are considering, symmetry dictates that $<\vec{E}(\vec{r})>$ depend only upon z; also, we are assuming the raincell is a sparse medium. Therefore, we can approximate $\underline{u}(\vec{r},\vec{r}\,')<\vec{E}(\vec{r}\,')>$ in (3.20) by [54]

$$\underline{u}(\vec{r},\vec{r}\,')<\vec{E}(\vec{r}\,')> \simeq \underline{f}(\hat{z},\hat{k}_s,\vec{\omega}_1) \cdot <\vec{E}(z')> \frac{e^{-jk_0R}}{R} \tag{3.21a}$$

where

$$\vec{\omega}_1 = (\bar{a}, s, \alpha) \tag{3.21b}$$

$$R = \sqrt{(x-x')^2 + (y-y')^2 + (z-z')^2} \tag{3.21c}$$

$$\hat{k}_s = \frac{(\vec{r} - \vec{r}')}{R} \tag{3.21d}$$

and $\underline{f}(\hat{z}, \hat{k}_s, \vec{\omega}_1)$ is the tensor scattering amplitude of the particle at $\vec{r}'$; it is a function of the size ($\bar{a}$), shape (s) and orientation (α) of the scatterer. Using this approximation in (3.20) we obtain

$$<\vec{E}>(z) = \vec{E}_i(z)> + \int_0^d dz' \iint dx'dy' \underline{g}(\hat{z}, \hat{k}_s) <\vec{E}(z')> \frac{e^{-jk_0R}}{R} \tag{3.22a}$$

where

$$\underline{g}(\hat{z}, \hat{k}_s) \doteq \int \underline{f}(\hat{z}, \hat{k}_s, \vec{\omega}_1) n(\vec{\omega}_1) d\vec{\omega}_1) \tag{3.22b}$$

We can perform the intplex integral over x′ and y′ in (3.22) by the method of stationary phase [5]. Doing so gives [23]

$$<\vec{E}(z)> = \vec{E}_i(z) - j\underline{k}_1(\hat{z}) \int_0^z <\vec{E}(z')> \exp[-jk_0(z - z')] dz'$$

$$- j\underline{k}_2(\hat{z}) \int_d^z <\vec{E}(z')> \exp[-jk_0(z' - z)] dz' \tag{3.23}$$

where $\underline{k}_1(\hat{z})$ and $\underline{k}_2(\hat{z})$ are defined by

$$\underline{k}_1(\hat{z}) \doteq \frac{2\pi}{k_o} \int \underline{f}(\hat{z}, \hat{z}, \vec{\omega}_1) n(\vec{\omega}_1) d\vec{\omega}_1) \tag{3.24a}$$

$$\underline{k}_2(\hat{z}) \doteq \frac{2\pi}{k_o}\int f(\hat{z}, -\hat{z}, \vec{\omega}_1)n(\vec{\omega}_1)d\vec{\omega}_1 \tag{3.24b}$$

Note that the third term on the right hand side of (3.23) defines backscattered contributions to the coherent field at $\vec{r}$. According to Rogers and Olsen, these contributions should be negligible for a sparse medium [47]. Therefore, let us assume for now that the backscatter term in (3.23) can be ignored so that

$$<\vec{E}(z')> = \vec{E}_i(z) - j\underline{k}_1(\hat{z})\int <\vec{E}(z')> \exp[-jk_0(z-z')]dz' \tag{3.25}$$

An exact solution to (3.25) can be obtained analytically. If we define $\vec{A}(z)$ by

$$\vec{A}(z) \doteq <\vec{E}(z)> e^{jk_o z} \tag{3.26}$$

Then, (3.25) can be rewritten as

$$\vec{A}(z) = \vec{E}_o - j\underline{k}_1(\hat{z})\int_o^z \vec{A}(z')z' \tag{3.27}$$

Equation (3.27) can be recast as an initial value problem by solving it at $z=0$ and taking its derivative with respect to z. Upon doing so, it is found that

$$\frac{d}{dz}\vec{A}(z) + j\underline{k}_1(\hat{z})\vec{A}(z) = 0 \tag{3.28a}$$

$$\vec{A}(0) = \vec{E}_o \tag{3.28b}$$

The initial value problem of (3.28) is readily solved in terms of the matrix exponential [15] to give

$$\vec{A}(z) = e^{-j\underline{k}_1(\hat{z})}\vec{E}_o \tag{3.29}$$

Substituting now (3.29) into (3.26), we obtain as the coherent field within the slab when backscattering is ignored

$$<\vec{E}(z)> = e^{-j\underline{k}(\hat{z})}\vec{E}_o \tag{3.30a}$$

with

$$\underline{k}(\hat{z}) \doteq \underline{k}_0 + \underline{k}_1(\hat{z}) \tag{3.30b}$$

and $\underline{k}_o$ the diagonal matrix

$$\underline{k}_0 = \begin{bmatrix} k_0 & 0 \\ 0 & k_0 \end{bmatrix} \tag{3.30c}$$

Let us now investigate the validity of neglecting the backscatter term in (3.23). Substituting the solution given by (3.30) into (3.23) and evaluating the resulting integrals results in

$$\begin{aligned} <\vec{E}(z)> &= e^{-j\underline{k}_1(\hat{z})}\vec{E}_o \\ &+ \underline{k}_2(\hat{z})[\underline{k}(\hat{z}) + \underline{k}_o]^{-1}e^{-j\underline{k}(\hat{z})z}\vec{E}_o \\ &- \underline{k}_2(\hat{z})[\underline{k}(\hat{z}) + \underline{k}_o]^{-1}e^{-j\underline{k}(\hat{z})d}\vec{E}_o \exp[-jk_0(d-z)] \end{aligned} \tag{3.31}$$

The magnitude of the elements of the matrix $\underline{k}_2(\hat{z})[\underline{k}(\hat{z}) + \underline{k}_o]^{-1}$ will be small enough to render the bracketed term, $\{\bullet\}$, in (3.31) negligible. In dropping this term, one finds that (3.31) reverts to (3.30a). We therefore, conclude that neglecting the backscatter term in (3.23) is justified and that the vector coherent field within the slab is well approximated by (3.30).

3.4 Received Coherent Signal

Our objective in this section will be to derive the average of the voltage vector defined in Section 3.2 (c.f. eq (3.10)) at the output of the receiver shown in Figure 3.1. The usual procedure for obtaining this vector is to first solve for the coherent field at $\vec{r}_o = (0, 0, L)$ (the center of the antenna's aperture) and then operate on the result with the antenna's response matrix $\underline{E}$. In doing this one obtains [33]

$$\langle \vec{V} \rangle = \underline{E}(0, 0) \bullet e^{-j\underline{k}_1(\hat{z})} \vec{E}_i(\vec{r}) \; ; \; \vec{r} = (0, 0, L) \tag{3.32}$$

As we have previously indicated however, questions have arisen as to whether or not the above procedure is correct when the scatterers are in the near field of the receiving aperture. To determine if this controversy is warrented, we will allow the scatterers to lie in any field region of the receiving aperture and incorporate the antenna's characteristics into the analysis. In this analysis we will make the reasonalbe assumption that the receiving aperture is in the far field of all scatterers in the slab.

Consider then the output of the receiver in Figure 3.1. The receiving aperture will be illuminated by the primary field and the field scattered into it by each particle within the slab. So, with N scatterers in the rain cell, the receiver's output vector is

$$\vec{V} = \underline{E}(0,0) \cdot \vec{E}_i(\vec{r}_0) + \sum_{j=1}^{N} \vec{V}_s(\vec{r}_j) \tag{3.33}$$

with $\vec{r}_0 = (0, 0, L)$ and $\vec{V}_s(\vec{r}_j)$ the contribution to $\vec{V}$ made by the field scattered from $\vec{r}_j$.

Averaging (3.33) over the joint probability density of (3.5), we obtain as the average system output

$$\langle \vec{V} \rangle = \underline{E}(0,0) \cdot \vec{E}_i(\vec{r}_0) + \int d\vec{\omega}_1, n(\vec{\omega}_1) \int_0^d dz' \int_{-\infty}^{\infty} \int dx'dy' \vec{V}_s(\vec{r}\,') \tag{3.34}$$

Note that the limits of integration in x′ and y′ have been taken to be $(-\infty, \infty)$ in equation (3.34). This is an approximation that will ultimately simplify the analysis and is justified because of the spatial filtering properties of the antenna. Specifically, appreciable contributions to the system output will only come from scatterers lying in a narrowly defined "active region" which is concentrated about the z-axis [49]; this "active region" is roughly defined by the funnel-shaped region depicted by Figure 3.5. Therefore, by assuming the scattering volume extends over all x′ and y′, little error should be incurred.

Now, to predict the average system output from (3.34), the contribution from the scatterer at $\vec{r}\,'$ must be determined. To derive this, consider the scattered field due to the particle at $\vec{r}\,'$. Recall from (3.12) that the field scattered to $\vec{r}\,'$ is expressible as

$$\vec{E}_s(\vec{r}, \vec{r}\,') = \underline{u}(\vec{r}, \vec{r}\,')\vec{E}(\vec{r}\,') \tag{3.35}$$

The total field at $\vec{r}$ in the absence of the scatterer, $\vec{E}(\vec{r})$, is random and, consists of an average component and a fluctuating component. The incoherent part of the field will ultimately make no contribution to the received coherent signal so we will ignore it and, for

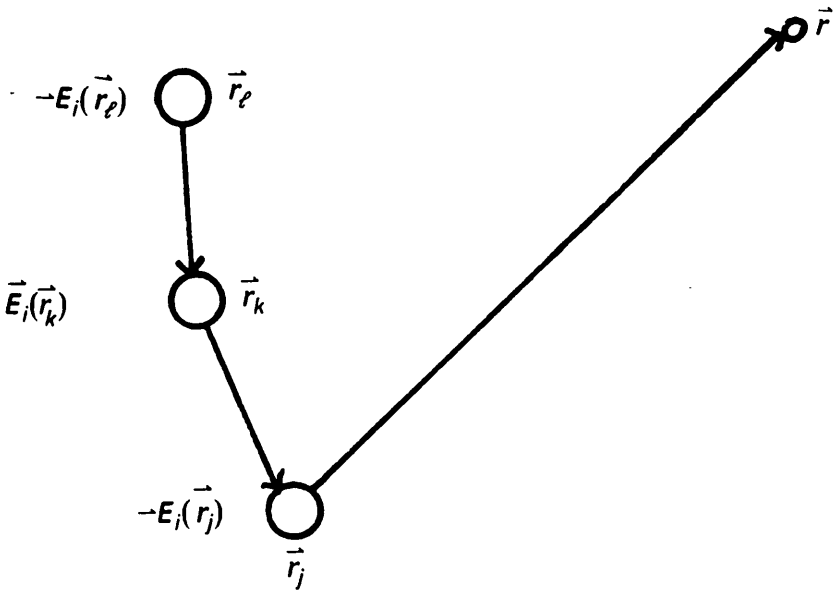

Pictorial Representation of Multiple Scattering Process
(Up to Third Order)

Figure 3.4

the purposes of determining the receiver's average output, express the field scattered by the particle at $\vec{r}'$ as

$$\vec{E}_s(\vec{r}, \vec{r}') = \underline{u}(\vec{r}, \vec{r}') < \vec{E}(\vec{r}') > \tag{3.36}$$

If we now use the far zone representation for $\underline{u}(\vec{r}, \vec{r}')$ and recall from section 3.3 that

$$< \vec{E}(\vec{r}') > = e^{-j\underline{k}(\hat{z})z'} \vec{E}_o \tag{3.37}$$

we can rewrite (3.36) as

$$\vec{E}_s(\vec{r}, \vec{r}') = \underline{f}(\hat{z}, \hat{k}_s, \omega_1) \cdot e^{-j\underline{k}(\hat{z})z'} \vec{E}_o \frac{e^{-jk_0 R}}{R} \tag{3.38a}$$

with

$$R = |\vec{r} - \vec{r}'| \tag{3.38b}$$

and

$$\hat{k}_s = \frac{(\vec{r} - \vec{r}')}{R} \tag{3.38c}$$

Now consider the receiver's response to the field scattered from $\vec{r}'$. If $\vec{r}'$ is in the far field of the receiving aperture, the scatted field can be taken as planar and $\vec{V}_s(\vec{r}')$ expressed simply as

$$\vec{V}_s(\vec{r}') = \underline{E}(\theta, \phi) \cdot \vec{E}_s(\vec{r}, \vec{r}') \tag{3.39}$$

However, we are not discounting the possibility that $\vec{r}'$ may lie in the antenna's Fresnel region. Consequently, it is generally incorrect to assume the field scattered into the

receiver is a single plane wave; rather, it must be considered a spectrum of plane waves each component of which will contribute to $\vec{V}_s(\vec{r}')$. Hence, we will express the scattered field as a linear combination of plane wave modes in the following manner [42]

$$\vec{E}_s(\vec{r}, \vec{r}') = \int_{-\infty}^{\infty} \int \vec{A}(\vec{k}) \exp(-j\vec{k} \cdot \vec{r}) \tag{3.40}$$

where $\vec{A}(\vec{k})$ is the wave number or plane wave spectrum of the scattered field and

$$\vec{K} = (k_x, k_y, k_z) = k_o(\sin\theta\cos\phi, \sin\theta\sin\phi, \cos\theta) \tag{3.41a}$$

$$k_z = [k_o^2 - k_x^2 - k_y^2]^{1/2} \tag{3.41b}$$

$$\vec{k} \cdot \vec{A}(\vec{k}) = 0 \tag{3.41c}$$

$$\vec{A}(\vec{k}) = (A_x(\vec{k}), A_y(\vec{k}), A_z(\vec{k})) \tag{3.41d}$$

It is clear from (3.40) that the wave number spectrum is given by the inverse Fourier transform of the scattered field, ie

$$\vec{A}(\vec{k}) = \frac{e^{jk_z z}}{4\pi^2} \int_{-\infty}^{\times} \times \infty \int \vec{E}_s(\vec{r}, \vec{r}') \exp(jk_x x + jk_y y) dx dy \tag{3.42}$$

In Appendix D, we derive the plane wave spectrum for the scattered field given by (3.38) using the inverse Fourier Transform relationship of (3.42); the resulting expression is

$$\vec{A}(\vec{k}) = \frac{j}{2\pi k_o} \exp(j\vec{k} \cdot \vec{r}) \underline{u}(\vec{k}) \underline{f}(\hat{z}, \hat{k}, \vec{\omega}_1) e^{-jk_1(\hat{z})z'} \vec{E}_o \tag{3.43a}$$

where

$$\hat{k} = \frac{vecto}{k_o} \tag{3.43b}$$

and

$$\underline{u}(\underline{k}) = (k_x^2 + k_y^2)^{-1/2} \begin{bmatrix} k_x & -k_o k_y/k_z \\ k_y & -k_o k_x/k_z \\ (k_x^2 + k_y^2)/k_2 & 0 \end{bmatrix} \tag{3.43c}$$

By expressing the scattered field as a spectrum of plane wave modes, the voltage vector $\vec{V}_s(\vec{r}')$ can be written as the superposition of the responses to each component of the plane wave spectrum [42], viz

$$\vec{V}_s(\vec{r}') = \int_{-\infty}^{\infty}\int \underline{E}(\theta, \phi) \cdot \vec{A}(\vec{k}) \exp(-j\vec{k} \cdot \vec{r}_o) dk_x dk_y \tag{3.44}$$

Thus, using (3.43) and (3.44) we obtain as the total expression for $\vec{V}_s(\vec{r}')$

$$\vec{V}_s(\vec{r}') = -\frac{j}{2\pi k_o}\int_{-\infty}^{\infty}\int \underline{E}(\theta, \phi) \cdot \underline{u}(\vec{k}) \underline{f}(\hat{z}, \hat{k}, \vec{\omega}_1) \exp[j\vec{k} \cdot (\vec{r}' - \vec{r}_o)] dk_x dk_y$$

$$\cdot \qquad x e^{-j\underline{k}(\hat{z})z'} \vec{E}_o \tag{3.45}$$

substituting now (3.45) into (3.34),4we find that the average output of the receiver is given by

$$<\vec{V}> = \underline{E}(0, 0) \cdot \vec{E}_o e^{-jk_o L}$$

$$-\frac{j}{2\pi k_o}\int d\vec{\omega}_1 n(\vec{\omega})\int -\infty\infty\int dz'\int_{-\infty}^{\infty}\int dz'dy'\int_{-\infty}^{\infty} dk_x dk_y$$

$$x\underline{E}(\theta,\phi)\bullet\underline{u}(\vec{k})\underline{f}(\hat{z},\hat{k},\vec{\omega}_1)\exp[jk_x x'+jk_y y'+jk_z(z'-L)]$$

$$x\ e^{-j\underline{k}(\hat{z})z'}\vec{E}_o \tag{3.46}$$

Equation (3.46) is a rather involved expression for the receiver's coherent output; however,it can be simplified considerably. To do so, we integrate first in x′ and y′ and use the Fourier identity [31]

$$\int_{-\infty}^{\infty}\int \exp(jk_x x'+jk_y y')dx'dy' = 4\pi^2\delta(k_x)\delta(k_y) \tag{3.47}$$

where $\delta(k_x)$ is the two dimensional Dirac delta function and defined by

$$\int_{-\infty}^{\infty}\delta(k_x)dk_x = \begin{cases}1 & , \ k_x = 0\\ 0 & , \ otherwise\end{cases} \tag{3.48}$$

Equation (3.46) then reduces to

$$<\vec{V}> = \underline{E}(0,0)\bullet\vec{E}_o e^{-jk_o L}$$

$$-\frac{j2\pi}{k_o}\int d\vec{\omega}_1 n(\vec{\omega})\int_{-\infty}^{\infty} dz'\int_{-\infty}^{d}\int dk_x dk_y$$

$$\underline{E}(\theta,\phi)\bullet\underline{u}(\vec{k})\underline{f}(\hat{z},\hat{k},\vec{\omega}_1)exp[jk_z(z'-L)]\delta(k_x)\delta(k_y)$$

$$x e^{-j\underline{k}(\hat{z})z'} \vec{E}_o \tag{3.49}$$

With the presence of the delta function in (3.48), the integration in k_x and k_y is easily performed by using the identity [31]

$$\int_{-\infty}^{\infty}\int G(k_x, k_y)\delta(k_x)\delta(k_y)dk_x dk_y = G(0, 0) \tag{3.50}$$

for any function $G(k_x, k_y)$.

Making use of (3.49) and noting that

$$\underline{E}(\theta, \phi) \cdot \underline{u}(\vec{k})\underline{f}(\hat{z}, \hat{k}, \vec{\omega}_1) \exp[jk_z(z' - L)]\,|_{k_x = k_y = 0}$$

$$= \underline{E}(0, 0) \cdot \underline{f}(\hat{z}, \hat{z}, \vec{\omega}_1) \exp[jk_o(z' - L)] \tag{3.51}$$

we obtain

$$< \vec{V} > = \underline{E}(0, 0 \cdot \quad 1 - \frac{j2\pi}{k_o}\int \underline{f}(\hat{z}, \hat{z}, \vec{\omega}_1)n(\vec{\omega})d\vec{\omega}_1$$

$$x\int_0^d \exp\{-j[\underline{k})\hat{z}) - \underline{k}_o]z'\}dz' \tag{3.52}$$

The remaining intplex integral in z' is readily evaluated. Doing so and noting from (3.24) and (3.30) that

$$\underline{k}(\hat{z}) - k_o = \frac{2\pi}{k_o}\int f(\hat{z}, \hat{z}, \vec{\omega}_1) n(\vec{\omega}) d\vec{\omega}_1 \tag{3.53}$$

we finally obtain

$$< \vec{V} > = \underline{E}(0, 0) \cdot e^{-j\underline{k}_1(\hat{z})d} \vec{E}_i(\vec{r}_o) \tag{3.54}$$

In deriving the result given by (3.54) we have employed a somewhat rigorous approach so that the effects of scatterer location vis-a-vis the receiving aperture can be assessed. We see however that our result is identical to that given by (3.32). We conclude then that the location of a raincell with respect to the receiving aperture (i.e. near field or far field) plays no role in determining how it affects the coherent signal.

We should note that there is a physical reason for the conclusion we have just reached mathematically. To understand it, let us recall the expression for the coherent field within a raincell which we derived in Section 3.3:

$$< \vec{E}(\vec{r}) > = e^{-j\underline{k}(\hat{z})z} \vec{E}_o \tag{3.55}$$

Observe that within the slab of raindrops, the coherent field propagates as a plane wave and satisfies the vector wave equation

$$[\nabla^2 + \underline{k}^2(\hat{z})] < \vec{E}(\vec{r}) > = 0 \tag{3.56}$$

Therefore the overall effect of the rain cell with respect to the coherent field is the same as that of a continuous medium composed of anisotropic material whose constituent parameters are defined by $\underline{k}(\hat{z})$. It follows then that the coherent field emerging from the rain

cell will likewise be planar and hence, the antenna's response to it independent of the position of the slab of scatterers.

3.5 Attenuation and Depolarization of the Coherent Signal for Dual Polarized Systems

In this final section of Chapter 3, we will undertake the task of applying the result derived in Section 3.4. Specifically, the model given by equation (3.54) will be used to predict the attenuation and depolarization of the coherent signal.. Before delving into the mathematics involved however, let us first address the issue of analytically defining attenuation and depolarization.

Recall from Section 3.3 that the received signal can be expressed in terms of a voltage vector $\vec{V}$. For a dual polarized system, we shall write this vector as

$$\vec{V} = [V_c \;\; V_x]^T \tag{3.57}$$

with V_c the output voltage for the copolarized channel, V_x the output voltage for the cross polarized channel and polarization states c and x are orthogonal.

We will define the attenuation A as the power in the copolarized channel under normal (clear weather) conditions relative to that during a rain event. Analytically the attenuation is given by [11]

$$A = \frac{|V_{co}|^2}{|V_c|^2} \tag{3.58}$$

with V_{co} the output voltage for the coplarized channel in clear weather.

The depolarization caused by a raincell will be expressed in terms of the isolation between the co and cross polarized states. The isolation, which we denote I, is given in terms of the output voltages by [11]

$$I = \frac{|V_{co}|^2}{|V_x|^2} \tag{3.59}$$

Now consider the output voltage vector as given by (3.54):

$$\vec{V} = \underline{E}(0, 0) \cdot e^{-j\underline{k}_1(\hat{z})d}\vec{E}_i(\vec{r}_o) \tag{3.60}$$

The antenna response matrix $\underline{E}(0, 0)$ will be taken as

$$\underline{E}(0, 0) = \underline{E}' e^{jk_o L} \tag{3.61a}$$

$$\underline{E}' = \begin{bmatrix} \cos\gamma_c & \sin\gamma_c e^{-j\delta_c} \\ \cos\gamma_x & \sin\gamma_x e^{-j\delta_x} \end{bmatrix} \tag{3.61b}$$

where (γ_c, δ_c) and (γ_x, δ_x) are polarization parameters for the co and cross polarized states [32]. Then

$$\vec{V} = \underline{E}'(0, 0)e^{-j\underline{k}_1(\hat{z})d}\vec{E}_o \tag{3.62}$$

The matrix exponential $\exp[-j\underline{k}_1(\hat{z})d]$ can be evaluated using the Cayley-Hamilton theorem [10]. Let the matrix $\underline{k}_i(\hat{z})$ be given by

$$\underline{k}_1(\hat{z}) = \begin{bmatrix} k_{11} & k_{12} \\ k_{21} & k_{22} \end{bmatrix} \tag{3.63}$$

Then, $\underline{k}_1(\hat{z})$ has eigenvalues λ_1 and λ_2 given by

$$\lambda_1, \lambda_2 = \frac{1}{2}\{(k_{11} + k_{22}) \pm [(k_{11} - k_{12})^2 + 4k_{12}k_{21}]^{1/2}\} \tag{3.64}$$

By exploiting the Cayley-Hamilton theorem, it is found that the matrix exponential is given by

$$e^{j\underline{k}_1(\hat{z})d} = a_0 1 + a_1 \underline{k}_1(\hat{z}) \tag{3.65}$$

where a_o and a_1 are constants satisfying

$$a_0 + a_1\lambda_1 = e^{-j\lambda_1 d} \tag{3.66a}$$

$$a_0 + a_1\lambda_2 = e^{-j\lambda_2 d} \tag{3.66b}$$

Solving (3.66) for a_0 and a_1 yields

$$a_o = (\lambda_1 - \lambda_2)^{-1}(\lambda_1 e^{-j\lambda_2 d} - \lambda_2 e^{-j\lambda_1 d}) \tag{3.67a}$$

$$a_1 = (\lambda_1 - \lambda_2)^{-1}(e^{-j\lambda_1 d} - e^{-j\lambda_2 d}) \tag{3.67b}$$

Substituting (3.67) into (3.65) we obtain

$$e^{-j\underline{k}_1(\hat{z})d} = (\lambda_1 - \lambda_2)^{-1}\begin{bmatrix} E_{11} & E_{12} \\ E_{21} & E_{22} \end{bmatrix} \tag{3.68a}$$

with

$$E_{11} = (\lambda_1 - k_{11})e^{-j\lambda_2 d} - (\lambda_2 - k_{11})e^{-j\lambda_2 d} \tag{3.68b}$$

$$E_{12} = k_{12}(e^{-j\lambda_1 d} - e^{-j\lambda_2 d}) \tag{3.68c}$$

$$E_{21} = k_{21}(e^{-j\lambda_1 d} - e^{-j\lambda_2 d}) \tag{3.68d}$$

$$E_{22} = (\lambda_1 - k_{22})e^{-j\lambda_2 d} - (\lambda_2 - k_{22})e^{-j\lambda_1 d} \tag{3.68e}$$

The evaluation of the matrix elements k_{ij} remains. From (3.6) and (3.24) we have

$$\underline{k}_1(\hat{z}) = \frac{2\pi}{k_o}\int d\bar{a}n(\bar{a})\int d\alpha p(\alpha)\int ds p(s)\underline{f}(\hat{z}, \hat{z}, \vec{\omega}_1) \tag{3.69}$$

Since raindrops are assumed to be either spherical or oblate spheroidal, the probability density p(s) can be expressed analytically as

$$p(s) = p_o\delta(s_0) + p_1\delta(s_1) \tag{3.70a}$$

where $s_0(s_1)$ indicates a sphere (oblate spheroid), $p_o(p_1)$ is the fraction of the total number of raindrops which are spherical (oblate spheroidal) and

$$p_1 = 1 - p_o \tag{3.70b}$$

With the above model of the drop shape distribution, $\underline{k}_1(\hat{z})$ becomes

$$\underline{k}_1(\hat{z}) + \frac{2\pi}{k_0} p_o \underline{1}\int f_0(0, \bar{a})n(\bar{a})d\bar{a}$$

$$+ p_1\int d\bar{a}n(\bar{a})\int d\alpha p(\alpha)\underline{f}_{os}(o, \bar{a}, \alpha) \tag{3.71}$$

with $f_0(0, \bar{a})$ the forward scattering amplitude of a spherical raindrop having radius $\bar{a}$ and $\underline{f}_{os}(0, \bar{a}, \alpha)$ the tensor forward scattering amplitude of an oblate shperoidal drop with equivolumetric radius $\bar{a}$ and canted at angle α .

Let us define E_{os}, F_0, F_1 and F_2 by

$$E_{os} = \int d\bar{a} n(\bar{a}) \int d\alpha p(\alpha) f_{os}(0, \bar{a}, \alpha) \tag{3.72a}$$

$$F_0 = \int f_0(0, \bar{a}) n(\bar{a}) d\bar{a} \tag{3.72b}$$

$$F_1 = \int f_1(0, \bar{a}) n(\bar{a}) d\bar{a}) \tag{3.72c}$$

$$F_2 = \int f_2(0, \bar{a}) n(\bar{a}) d\bar{a} \tag{3.72d}$$

where $f_1(f_2)$ is the forward scattering amplitude of an aligned oblate spheroidal raindrop for polarization 1 (2) as defined in Section 2.4.

Consider then E_{os} which can be written as [51].

$$E_{os} = \frac{1}{2} \int \begin{bmatrix} F_{11}(\alpha) & F_{12}(\alpha) \\ F_{12}(\alpha) & F_{22}(\alpha) \end{bmatrix} p(\alpha d\alpha) \tag{3.73a}$$

where

$$F_{11}(\alpha) = F_1 + F_2 + (F_1 - F_2) \cos 2\alpha \tag{3.73b}$$

$$F_{12}(\alpha) = (F_2 - F_1) \sin 2\alpha \tag{3.73c}$$

$$F_{22}(\alpha) = F_1 + F_2 + (F_2 - F_1) \cos 2\alpha \tag{3.73d}$$

We will take $p(\alpha)$ to be Gaussian with mean $\bar{\alpha}$ and variance σ_α^2 :

$$p(\alpha) = \frac{1}{\sigma_\alpha \sqrt{2\pi}} \exp[-(\alpha - \bar{\alpha})^2/2\sigma_\alpha^2]\,;\ \alpha \text{ in radians} \tag{3.74}$$

The integrals in (3.73) can then be evaluated by using [17]

$$\int_{-\infty}^{\infty} \exp(q^2x^2) \begin{matrix}\sin\\ \cos\end{matrix} ([p(x+\lambda)]dx = \frac{\sqrt{\pi}}{q} \exp(-p^2/4q^2) \begin{matrix}\sin\\ \cos\end{matrix} (p\lambda) \tag{3.75}$$

to obtain

$$\int_{-\infty}^{\infty} p(\alpha \begin{matrix}\sin\\ \cos\end{matrix} (2\alpha)d\alpha = \exp(-2signam_\alpha^2) \begin{matrix}\sin\\ \cos\end{matrix} (2\alpha) \tag{3.76}$$

Making use then of (3.76) in (3.73) and substituting (3.72) into (3.71), the elements of $\underset{(z)}{k}$ are found to be

$$k_{11} = \frac{\pi}{k_o}\Big\{2p_oF_o + p_1[1 + \exp(-2\sigma_\alpha^2)\cos 2\bar{\alpha}]F_1$$

$$+ p_1[1 - \exp(-2\sigma_\alpha^2)\cos 2\bar{\alpha}]F_2 \tag{3.77}$$

$$k_{12} = k_{21} = \frac{2\pi}{k_0} p_o \exp(-2\sigma_\alpha^2)\sin 2\bar{\alpha}(F_2 - F_1)\} \tag{3.77b}$$

$$k_{22} = \frac{\pi}{k_o}\ 2p_oF_o + p_1[1 + \exp(-2\sigma_\alpha^2)\cos 2\alpha]F_2$$

$$+ p_1[1 - \exp(-2\sigma_\alpha^2)\cos 2\alpha]F_1 \tag{3.77c}$$

Now consider F_i , i = 0, 1, 2:

$$F_i = \int f_i(o, \bar{a}) n(\bar{a}) d\bar{a} \tag{3.78}$$

For the drop size distribution $n(\bar{a})$, we will assume a uniform rain rate and use the Marshall-Palmer model which is [51]

$$n(\bar{a}) = N_o e^{-\beta \bar{a}} \; m^{-3} mm^{-1} \tag{3.79a}$$

with

$$N_o = 16000 \tag{3.79b}$$

$$\beta = 8.2 RR^{-.21} \tag{3.79c}$$

and RR the rain rate in mm/hr. then F_i becomes

$$F_i = N_o \int_0^{3.5} f_i(o, \bar{a}) e^{-\beta \bar{a}} \tag{3.80}$$

with $\bar{a}$ in millimeters and $f_i(0, \bar{a})$ in meters.

The intplex integral in (3.80) will be evaluated numerically using scattering data provided in Appendicies B and C (for $\alpha = 90°$). Recall that we computed forward scattering amplitudes for equivolumetric radii $\bar{a} = .25 through 3.50$ mm in steps of .25 mm. Beyond $\bar{a} = 3.50$ mm, contributions to the intplex integral in (3.80) will be negligible due to the exponential. Therefore, F_i will be approximated as

$$F_i = N_o \int_0^{3.5} f_i(o, \bar{a}) n(\bar{a}) d\bar{a} d\bar{a} \tag{3.81}$$

The integrals in (3.81) will be numerically evaluated using the M+1 point composite Simpson's rule algorithm [30]

$$\int_{x_o}^{x_M} g(x)dx \simeq \frac{h}{3} g(s_o) + g(s_M) + 2j = 1(M-2)/2 g(x_{2j} + 4 \sum_{j=1}^{(m-2)/2} g(x_{2j+1}) \tag{3.82}$$

where M is even and $h = (x_M - x_0)/M$.

Using (3.81) and (3.82) with M=14, we find F_i is given approximately by

$$F_i = \frac{N_o}{12} S_i \tag{3.83a}$$

where

$$S_i = 4f_i(0, .25), .25) \exp(-.25\beta) + f_i(0, 3.5) \exp(-3.5\beta).in.in10:df. + \sum_{j=1}^{6} \{2f_i(0, .5j) \exp(-.5j)$$

$$+ 4f_i(0, .5_j + .25) \exp[-(5j + .25)\beta\} \tag{3.83}$$

Using the formulae presented in this section, we have written a computer program to compute and plot the attenuation and isolation of the coherent signal versus slab length d; the code is listed in Appendix E. We now conclude this chapter by presenting sample computations made using the code in Appendix E. The calculated data are presented in Figures 3.6 through 3.13.

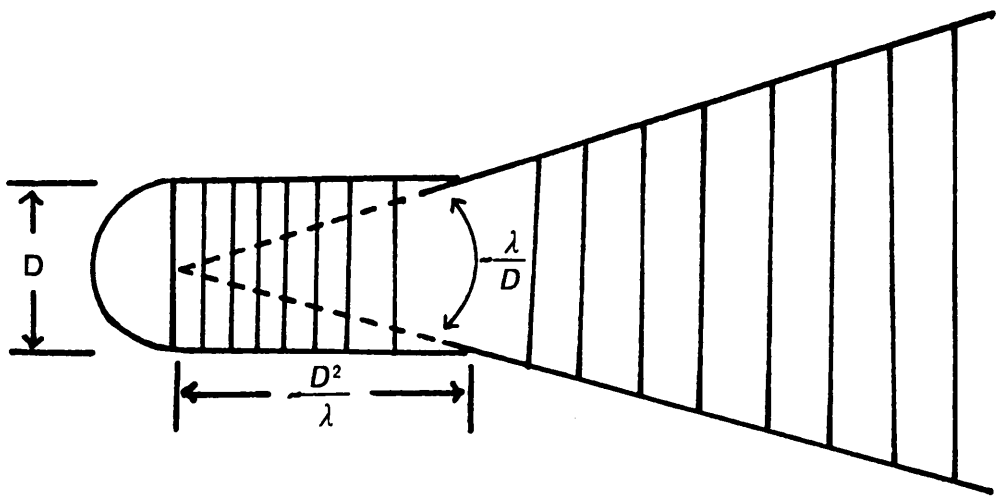

"Active Regions" of a Receiving Aperture (Shaded)

Figure 3.5

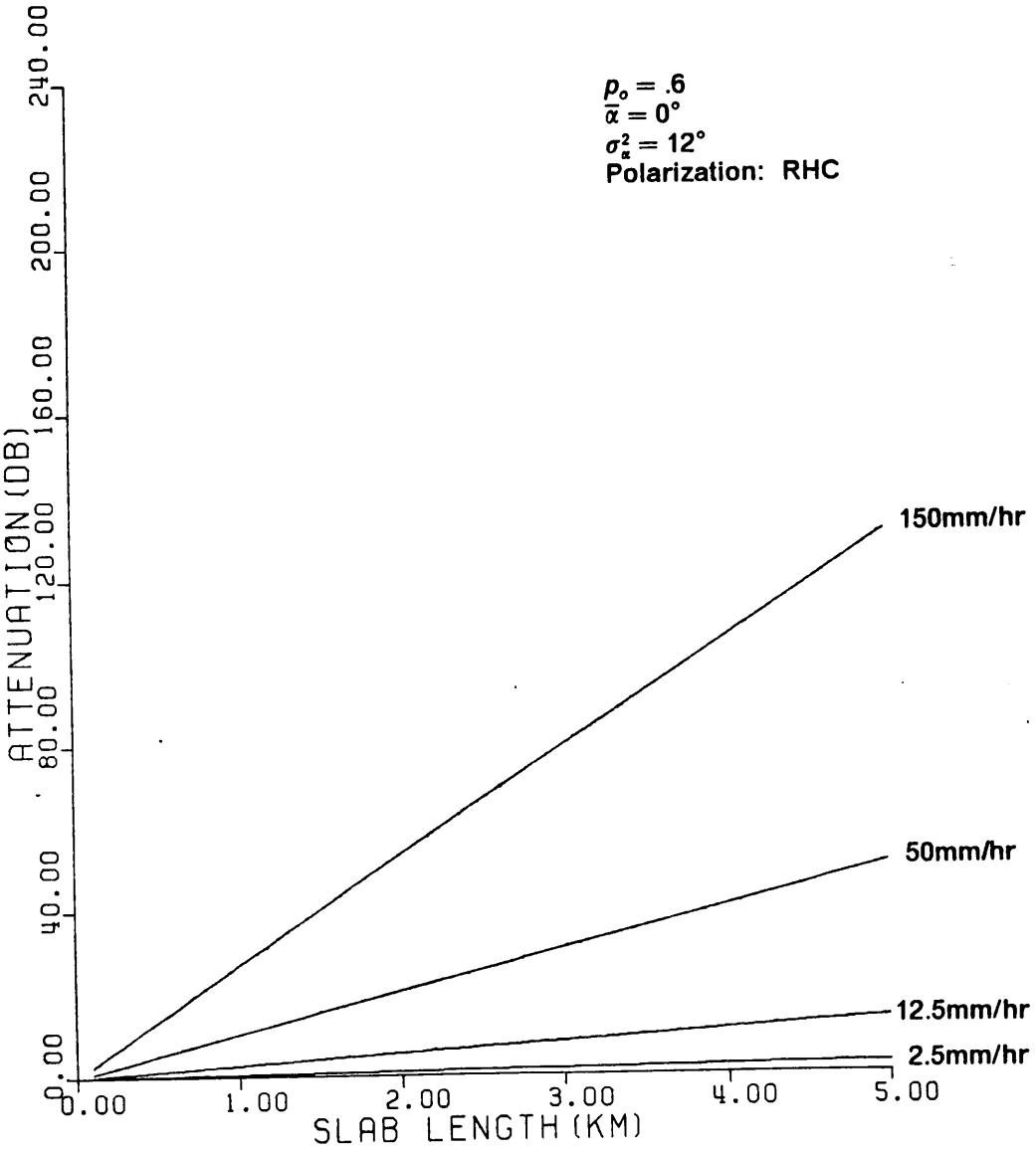

Attenuation vs Slab Length ; 30GHz
Figure 3.6

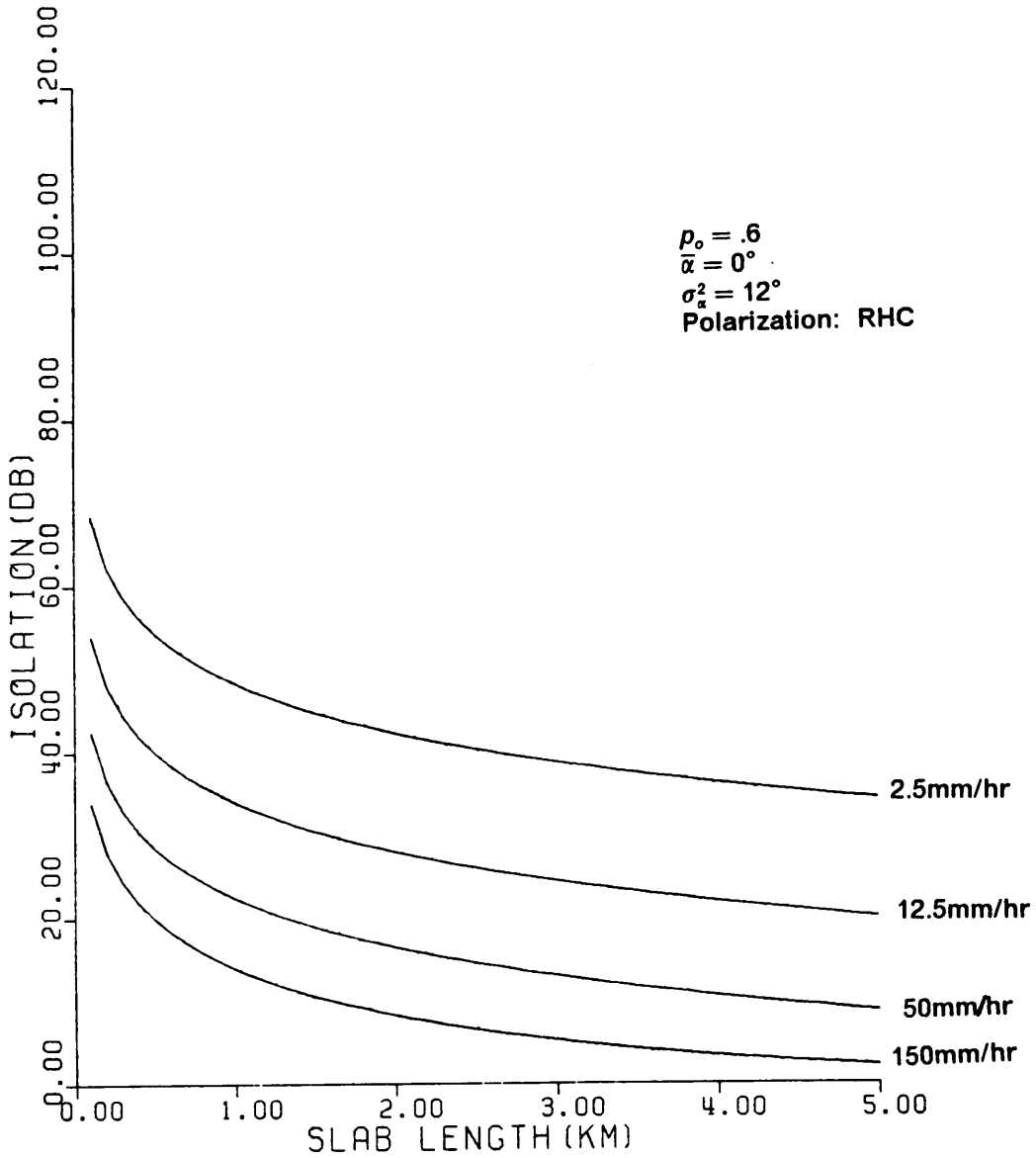

Isolation vs Slab Length ; 30GHz
Figure 3.7

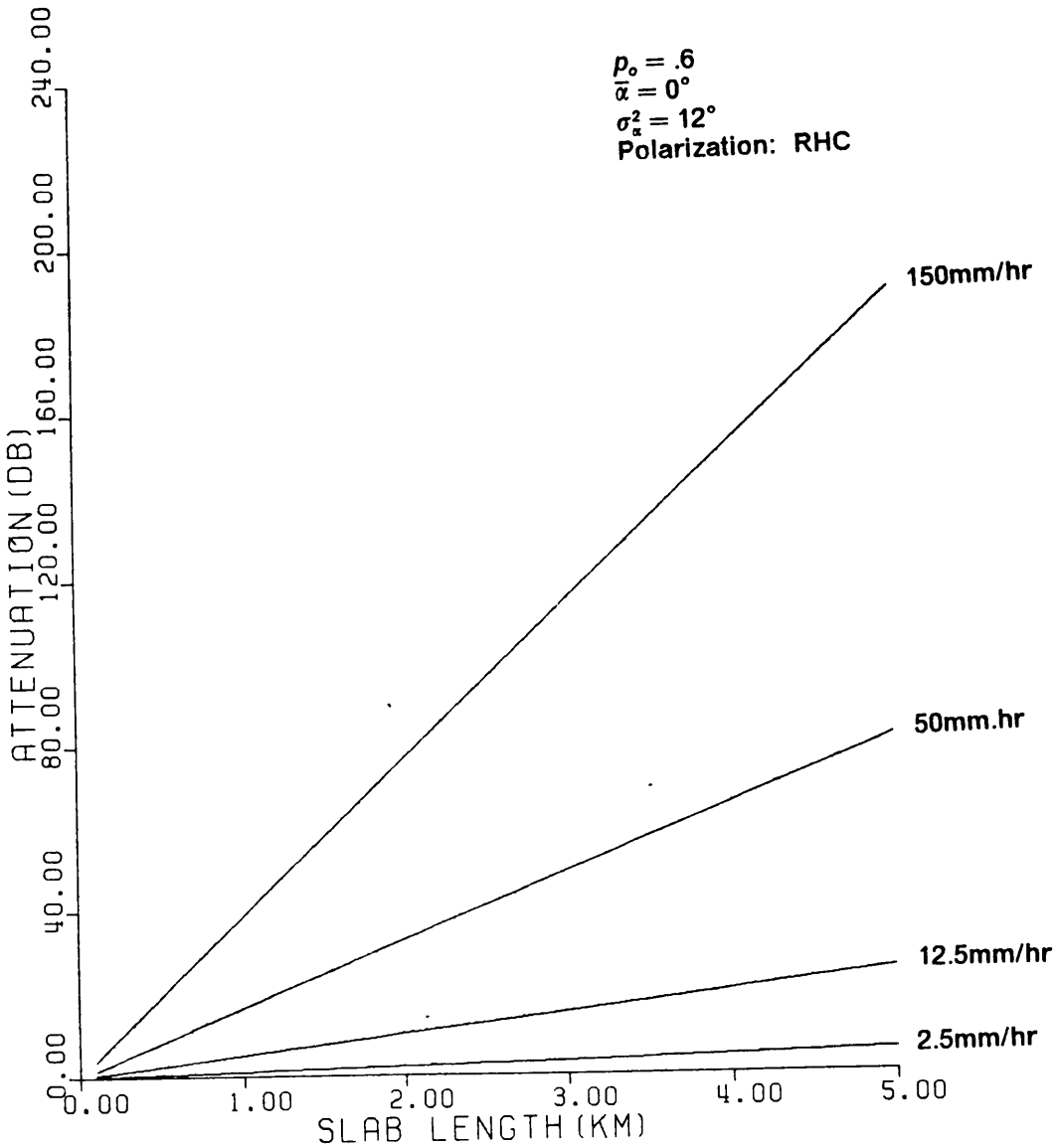

Attenuation vs Slab Length ; 45GHz
Figure 3.8

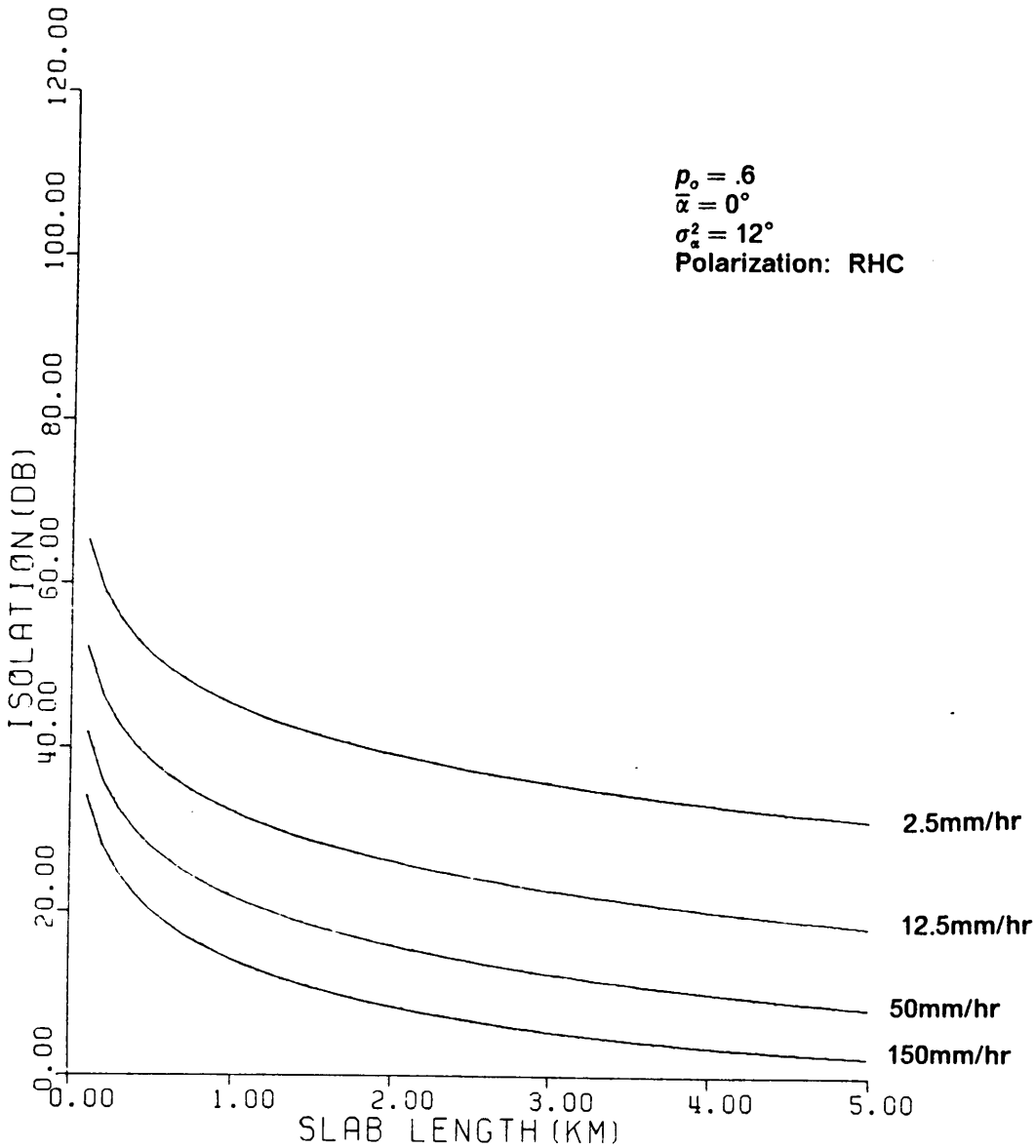

Isolation vs Slab Length ; 45GHz
Figure 3.9

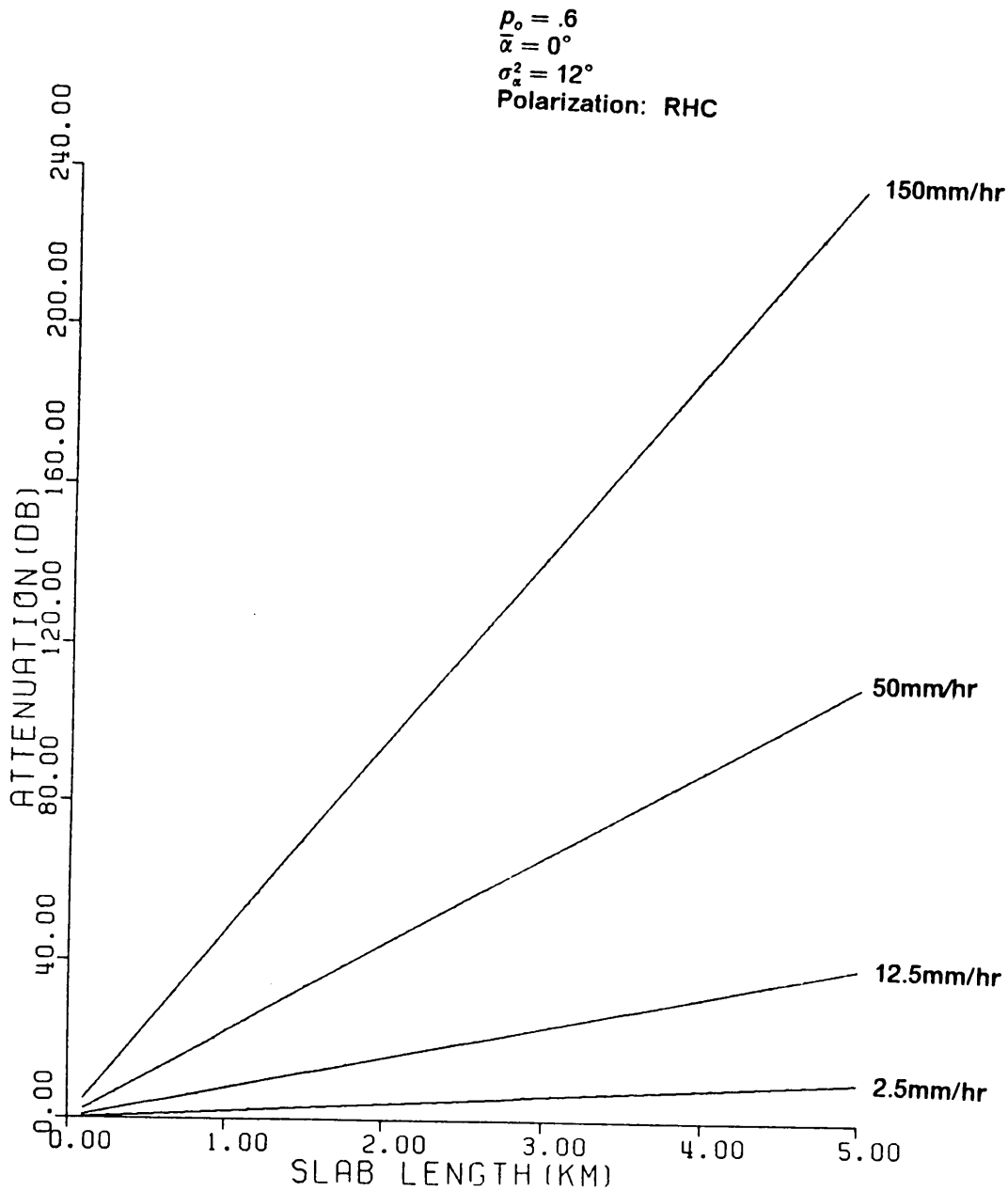

Attenuation vs Slab Length ; 70GHz

Figure 3.10

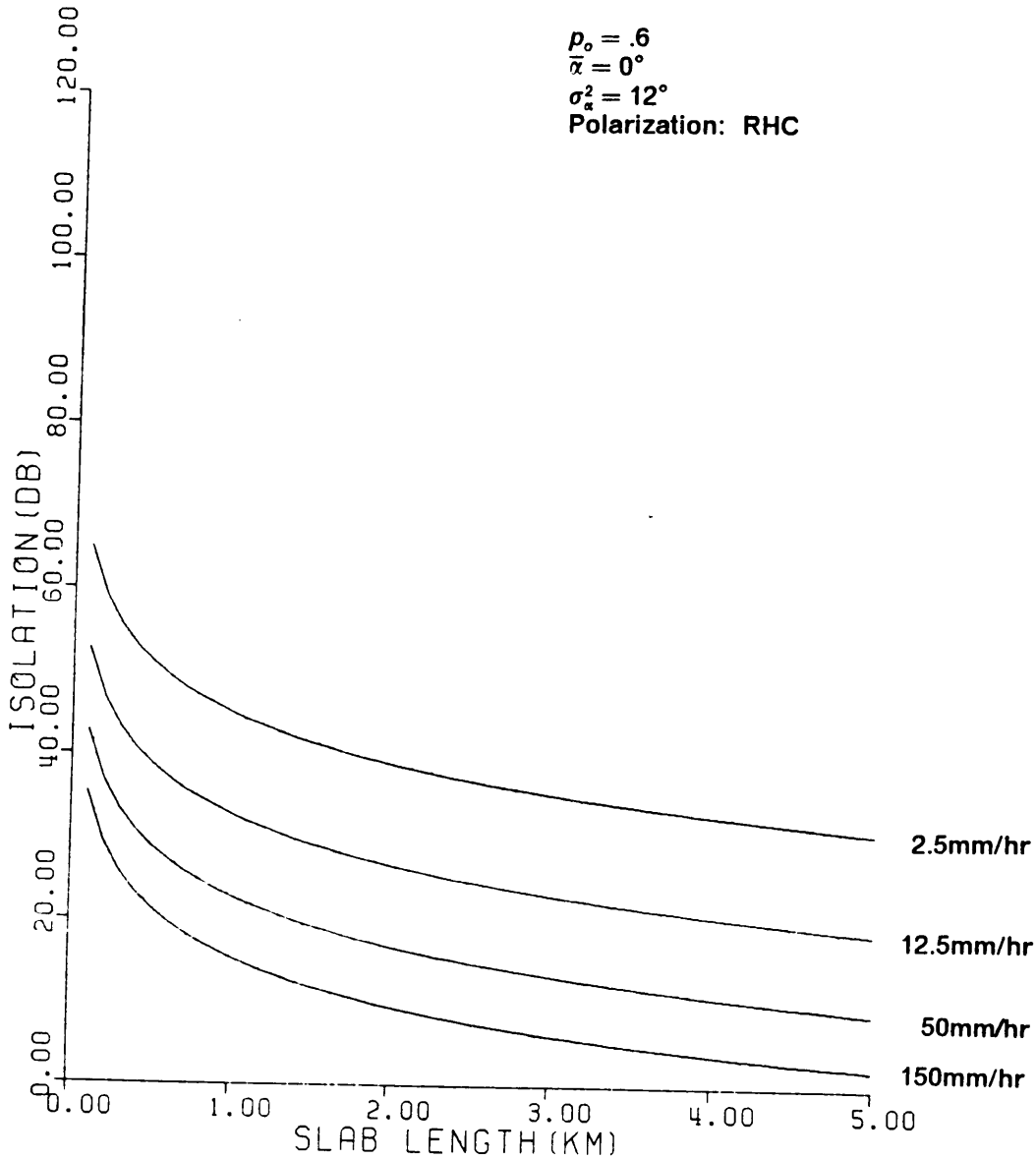

Isolation vs Slab Length ; 70GHz

Figure 3.11

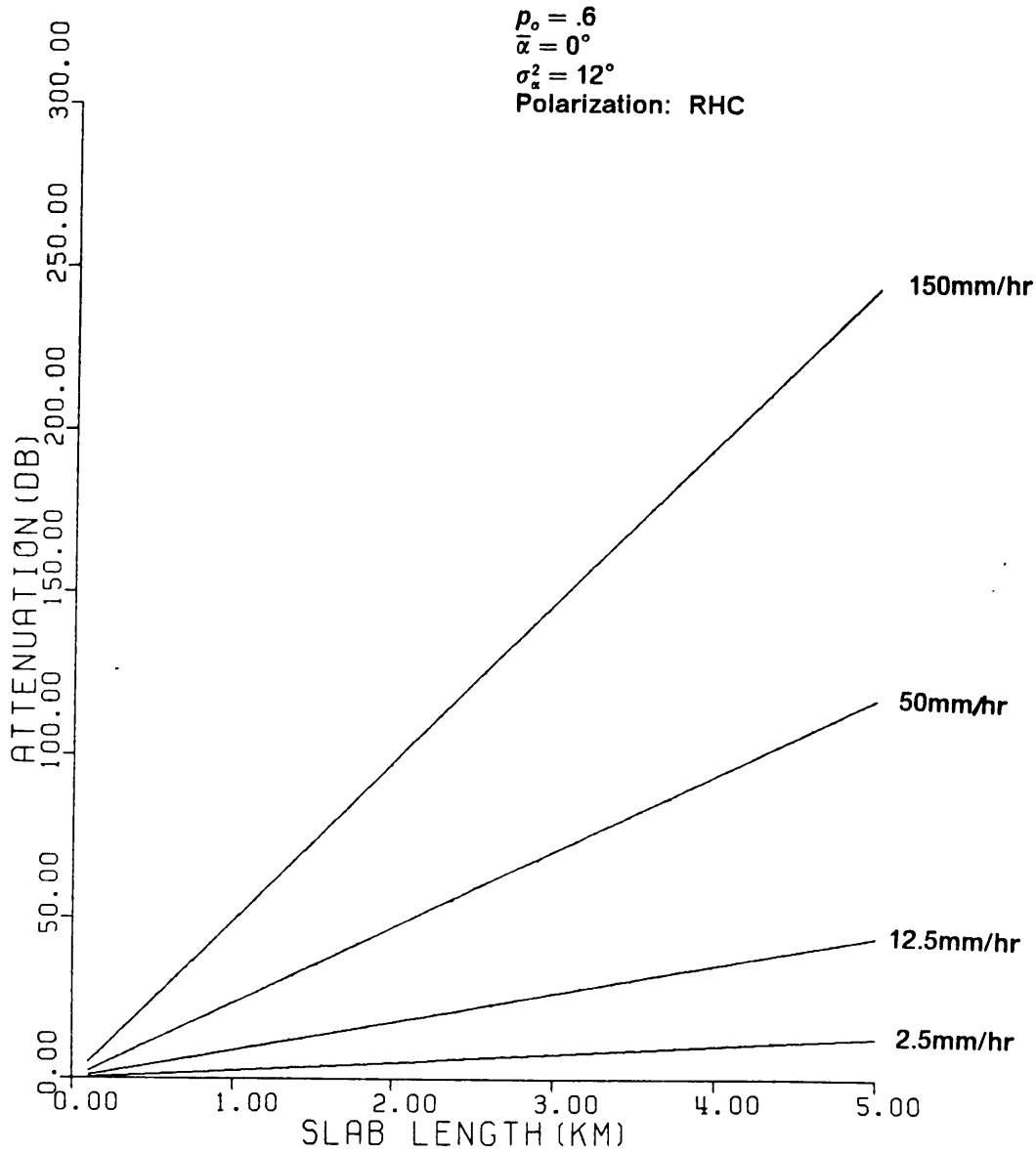
$p_o = .6$
$\bar{\alpha} = 0°$
$\sigma_\alpha^2 = 12°$
Polarization: RHC
150mm/hr
50mm/hr
12.5mm/hr
2.5mm/hr
ATTENUATION (DB)
0.00
50.00
100.00
150.00
200.00
250.00
300.00
0.00
1.00
2.00
3.00
4.00
5.00
SLAB LENGTH (KM)

Chapter 4 Incoherent Properties of Millimeter Wave Propagation Through Rain

As pointed out in section 3.1, the coherent part of the field in the presence of rain represents only a part of the total signal. For one's analysis to be complete, the incoherent portion of the signal must also be examined; in this chapter we consider the incoherent problem.

The organization of this chapter is similar to that of Chapter 3. We begin with a general statement of the probelm to be considered and then present Twersky's derivation of the total intensity. Following these preliminaries, the incoherent signal at the output of a receiver is derived for the cases of far field and near field scattering. We conclude the chapter with numerical computations of the received incoherent power vis-a-vis the received coherent power for various cases. The results of these computations will provide insight as to the conditions under which the incoherent effects of rain scattering should be taken into account.

4.1 Analysis of the Incoherent Signal-Statement of the Problem

The canonic problem we will study in this chapter is illustrated in Figure 4.1 where a normally incident plane wave is shown illuminating a rain cell. Our overall objective in this chapter will be to derive the intensity of the incoherent signal at the output of the receiver shown in Figure 4.1.

As in Chapter 3, we will model the raincell as a plane parallel slab of length d. In the present case however, we will make the simplifying assumption that all non-spherical raindrops are aligned and restrict our analysis to a scalar one. The joint probability of the scatterers is then given by

$$pho(\vec{\omega}) = \frac{n(\bar{a})p(s)}{N} \tag{4.1}$$

We should point out that by assuming the non-spherical drops are aligned we discount the effects raindrop canting has on the incoherent signal. We do however take into account polarization effects to the extent that we allow for a mix of spherical and spheroidal raindrops.

The assumptions that the raindrops are independently and identically distributed and uniformly distributed in posititon will be maintained. In addition, we will continue to assume a sparse scattering medium.

In most practical situations which can be modeled as shown in Figure 4.1, the receiving antenna will be a large circular aperture; large meaning the aperture's diameter is much greater than the wavelength. So for our analysis, the antenna shown will be taken as a large circular aperture which posesses a uniform phase aperture field distribution when used as a

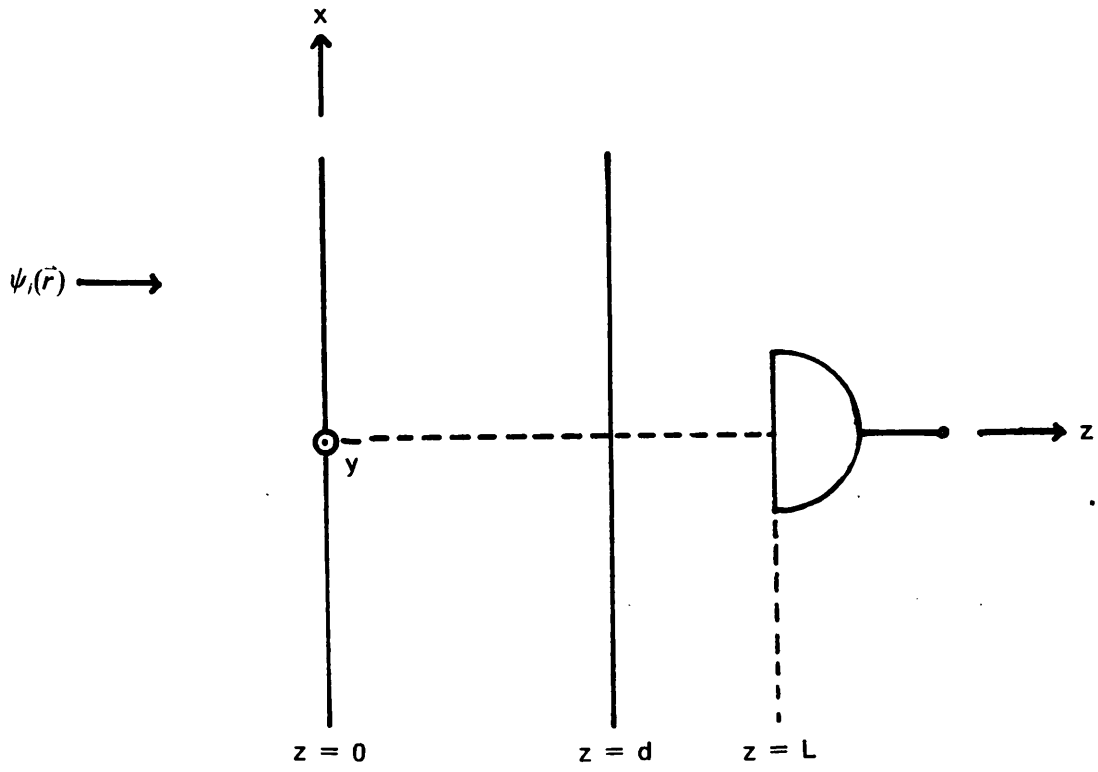

Geometry For the Analysis of the Incoherent Signal

Figure 4.1

transmitter. We will denote $\psi_a(x, y)$ as the function defining the taper of the aperture field; for convenience $\psi_a(x, y)$ is normalized so that

$$\left| \int_{S_a} \int \psi_a(\xi, \eta) d\xi d\eta \right|^2 = G_o \tag{4.2}$$

where G_o is the receiver's on axis gain expressed as a ratio and S_a indicates the integration is over the aperture surface.

The far field gain pattern of the receving terminal will be modeled using the well known Gaussian approximation

$$G(\theta_r) = G_o \exp(-\alpha_r \theta_r^2) \tag{4.3a}$$

where θ_r is in radians and is measured from the antenna's axis (see Figure 4.2) and α_r is a constant. α_r is related to the half power beamwidth of the antenna, HP by

$$\alpha_r = \frac{4}{(HP)^2 ln(2)} \quad ; HP \text{ in radians} \tag{4.3b}$$

Also, the constant α_r is approximately given in terms of the receiver's gain by [27]

$$\alpha_r = \frac{G_o}{4} \tag{4.3c}$$

4.2 The Total Intensity

In this section we begin our analysis of the incoherent aspect of the rain scatter problem by presenting the intplex integral equations which specify the total intensity of a signal. The intplex integral expressions we put forth are those derived by Twersky [44], [46], [58]. As a matter of review and to facilitate understanding of the physical significance of the equations, we also outline the steps Twersky used to derive them.

Consider the situation we have depicted in Figure 4.1. The scattering volume is illuminated by a normally incident plane wave with scalar field

$$\psi_i(\vec{r}) = \psi_0 e^{-jk_o z} \tag{4.4}$$

To derive the total intensity at a point $\vec{r}$ via the Twersky method, we begin with the fundamental equations.

$$\psi(\vec{r} = \psi_i(\vec{r}) + \sum_{j=1}^{N} \psi_s(\vec{r}, \vec{r}_j) \tag{4.5a}$$

$$\psi_s(\vec{r}, \vec{r}_j) = u(\vec{r}, \vec{r}_j)\psi(\vec{r}_j) \tag{4.5b}$$

where $\psi(\vec{r})$ is the field at $\vec{r}$ in the absence of a scatterer,

$\psi_s(\vec{r}, \vec{r}_j)$ the field scattered to $\vec{r}$ by the particle at $\vec{r}_j$ and $u(\vec{r}, \vec{r}_j)$ a scalar operator.

As shown in Chapter 3, the fundamental equations of (4.5) can, through iteration, be used to obtain the following series expansion for the total field at $\vec{r}$ (cf eq (3.16)):

$$\psi(\vec{r}) \overset{c}{+} \psi_i(\vec{r}) = \sum_{j=1}^{N} u(\vec{r}, \vec{r}_j)\psi_i(\vec{r}_j)$$

$$+ \sum_{j=1}^{N} \sum_{\substack{k=1 \\ (j)}}^{N} u(\vec{r}, \vec{r}_j)u(\vec{r}_j, \vec{r}_k)\psi_i(\vec{r}_k)$$

$$+ \sum_{j=1}^{N} \sum_{\substack{k=1 \\ (j)}}^{N} \sum_{\substack{\ell=1 \\ (j,k)}}^{N} u(\vec{r}, \vec{r}_j)u(\vec{r}_j, \vec{r}_k)u(\vec{r}_k, \vec{r}_\ell)\psi_i(\vec{r}_\ell)$$

$$+ \ldots \qquad (r.6)$$

Squaring the modulus of (4.6), we obtain as the total inensity at $\vec{r}$

$$|\psi(\vec{r})|^2 = \psi_i(\vec{r}) + \sum_{j=1}^{N} u(\vec{r}, \vec{r}_j)\psi_i(\vec{r}_j)$$

$$+ \sum_{j=1}^{N} \sum_{\substack{k=1 \\ (j)}}^{N} u(\vec{r}, \vec{r}_j)u(\vec{r}_j, \vec{r}_k)\psi_i(\vec{r}_k) + \ldots$$

$$x \quad \psi_i(\vec{r}) + \sum_{j=1}^{N} u(\vec{r}, \vec{r}_j)\psi_i(\vec{r}_j)$$

$$+ \sum_{j=1}^{N} \sum_{\substack{k=1 \\ (j)}}^{N} u(\vec{r}, \vec{r}_j)u(\vec{r}_j, \vec{r}_k)\psi_i(\vec{r}_k) + \ldots \qquad (4.7)$$

Let us now carry out the multiplication indicated by (4.7). Doing so and performing some extensive manipulations of the resulting expression, the intensity at $\vec{r}$ can be recast as

$$|\psi(\vec{r})|^2 = |\psi_i(\vec{r})|^2 + \psi_i(\vec{r})\sum_{j=1}^{N} U\ (\vec{r}, \vec{r}_j)\psi_i(\vec{r}_j)$$

$$+ \sum_{j=1}^{N} u(\vec{r}, \vec{r}_j)\psi_i(\vec{r}_j)\Psi\ (\vec{r}j)$$

$$+ \sum_{j=1}^{N} u(\vec{r}, \vec{r}_j)\psi_i(\vec{r}_j)u\ (\vec{r}, \vec{r}_j)\psi_l\ (\vec{r}_j)$$

$$+ \sum_{j=1}^{N} u(\vec{r}, \vec{r}_j)\psi_i(\vec{r}_j)\sum_{k=1}^{N} u\ (\vec{r}, \vec{r}_k)\psi_l\ (\vec{r}_k)$$

$$+ \sum_{j=1}^{N} \sum_{\substack{k=1 \\ (j)}}^{N} u(\vec{r}, \vec{r}_j)u(\vec{r}_j, \vec{r}_k)\psi_i(\vec{r}_k)\psi_i\ (\vec{r}_k)$$

$$+ \sum_{j=1}^{N} \sum_{\substack{k=1 \\ (j)}} u(\vec{r}, \vec{r}_j)\psi_i(\vec{r}_j) \begin{matrix} u\ (\vec{r}, \vec{r}_j)u\ (\vec{r}_j, \vec{r}_k)\psi_i(\vec{r}_k) \\ + u\ (\vec{r}, \vec{r}_k)u\ (\vec{r}_k, \vec{r}_j)\psi_i(\vec{r}_j) \end{matrix}$$

$$+ u(\vec{r}, \vec{r}_j)u(\vec{r}_j, \vec{r}_k)\psi_i(\vec{r}_k)$$
$$+ u(\vec{r}, \vec{r}_k)u(\vec{r}_k, \vec{r}_j)\psi_i(\vec{r}_j)$$
$$xu\ (\vec{r}, \vec{r}_j)\psi_i(\vec{r}_j)$$

$$+ u(\vec{r}, \vec{r}_j)u(\vec{r}_j, \vec{r}_k)\psi_i(\vec{r}_k)$$
$$x\, u(\vec{r}, \vec{r}_j)u(\vec{r}_j, \vec{r}_k)\psi_i(\vec{r}_k)$$

$$+ \ldots \tag{4.8}$$

The average total intensity is obtained by averaging (4.8) over the joint probability density of (4.1). Doing so and letting N approach infinity so that $(N-1)/N$, $(N-1)(N-2)/N^2$, etc. approach unity yields

$$<|\psi(\vec{r})|^2> = |\psi_i(\vec{r})|^2$$

$$+ \int d\vec{\omega}_j n(\vec{\omega}_j) \begin{matrix} \psi_i(\vec{r})u(\vec{r}, \vec{r}_j)\psi_i(\vec{r}_j) \\ + u(\vec{r}, \vec{r}_j)\psi_i(\vec{r}_j)\psi_i(\vec{r}_j) \end{matrix}$$

$$+ \int d\vec{\omega}_j \begin{matrix} n(\vec{\omega}_j)u(\vec{r}, \vec{r}_j)\psi_i(\vec{r}_j) \\ x\int d\vec{\omega}_k n(\omega_k)u(\vec{r}, \vec{r}_k)\psi(\vec{r}, \vec{r}_k) \end{matrix}$$

$$+ \iint d\vec{\omega}_j d\vec{\omega}_k n(\vec{\omega}_j)n(\vec{\omega}_k)$$

$$x\ \psi_i(\vec{r})u(\vec{r}, \vec{r}_j)u(rvecotr_j, \vec{f}_k)\psi_l(\vec{r}_k)$$

$$+ u(\vec{r}, \vec{r}_j)u(\vec{r}_j, \vec{r}_k)\psi_i(\vec{r}_k)\psi_i(\vec{r})$$

$$\begin{matrix} + u(\vec{r}, \vec{r}j)\psi_i(\vec{r}_j) \\ 13x\, u(\vec{r}, \vec{r}_j)u(\vec{r}_j, \vec{r}_k)\psi_i(\vec{r}_k) \\ + u(\vec{r}, \vec{r}_k)u(\vec{r}_k, \vec{r}_j)\psi_i(\vec{r}_j) \end{matrix}$$

$$+ \; u(\vec{r}, \vec{r}_j)u(\vec{r}_j, \vec{r}_k)\psi_i(\vec{r}_k)$$

$$+ \; u(\vec{r}, \vec{r}_k)u(\vec{r}_k, \vec{r}_j)\psi_i(\vec{r}_j)$$

$$x\, u(\vec{r}, \vec{r}_j)\psi_i(\vec{r}\, r_j)$$

$$+ \; u(\vec{r}, \vec{r}_j)u(\vec{r}_j)u(\vec{r}_j, \vec{r}_k)\psi_i(\vec{r}_k)$$

$$x\, u(\vec{r}, \vec{r}_j)u(\vec{r}_j, \vec{r}_k)\psi_i(\vec{r}_k)$$

$+ \; \ldots$ reqno (4.9)

As it stands, equation (4.9) is cumbersome and its physical significance is not apparent. However, Twersky recognized that it corresponds to the iterative expansion of the intplex integral equation

$$< |\psi(\vec{r})|^2 > \; = \; | < \psi(\vec{r}) > |^2 + \int |V(\vec{r}, \vec{r}')|^2 < |\psi(\vec{r}\, d')|^2 n(\vec{\omega}) d\vec{\omega} \tag{4.10}$$

where $v(\vec{r}, \vec{r}')$ is a scattering function satisfying the intplex integral equation

$$v(\vec{r}, \vec{r}') = u(\vec{r}, \vec{r}') + \int u(\vec{r}, \vec{r}'')v(\vec{r}'', \vec{r}')n(\vec{\omega}')d\omega' \tag{4.11}$$

and the coherent field $< \psi(\vec{r}) >$ is governed by equation (3.20), i.e.

$$< \psi(\vec{r}) > \; = \; \psi_i(\vec{r}) + \int u(\vec{r}, \vec{r}') < \psi(\vec{r}') > n(\vec{\omega}) d\vec{\omega} \tag{4.12}$$

Equations (4.10) and (4.11) are the Twersky intplex integral equations for the total intensity. In comparing (4.10) with equation (3.3), it is clear that in terms of physical quantitites, the first term on the right hand side of (4.10) is the coherent intensity and the second the

incoherent intensity. In addition, the operator $v(\vec{r}, \vec{r}')$ can be interpreted as the average of the scattering processes involved in propagation from $\vec{r}'$ to $\vec{r}$.

Although equations (4.10) and (4.11) conveniently express the total intensity, they cannot be solved explicitly; thus, it is necessary to make assumptions so that approximate solutions are obtained. For the case of a normally incident plane wave illuminating a plane parallel slab of scatterers, Twersky derived the following approximations for $v(\vec{r}, \vec{r}')$ and $< |\psi(\vec{r})|^2 >$ (see [2] for details of the derivation):

$$v(\vec{r}, \vec{r}') = \begin{cases} (\hat{z}, \hat{k}_s, \vec{\omega}) \dfrac{e^{-jkR}}{R} \\ f(\hat{z}, \hat{k}_s, \vec{\omega}) \dfrac{e^{-jk_0 R}}{R} \exp[-jk_1(d - z')] \end{cases} \tag{4.13a}$$

with

$$k_1 = \frac{2\pi}{k_o} \int f(0, \vec{\omega}) n(\vec{\omega}) d\vec{\omega} \tag{4.13b}$$

$$k = k_0 + k_1 \tag{4.13c}$$

$$\cos \theta' = \hat{z} \cdot \hat{k}_s \; ; \; \hat{k}_s = \frac{(\vec{r} - \vec{r}')}{R} \tag{4.13d}$$

and

$$< |\psi(\vec{r})|^2 > = |_o|^2 e^{\sigma_e z} \quad , \; o < z < d \tag{4.14a}$$

where

$$\sigma_a = \int C_a(\vec{\omega}) n(\vec{\omega}) d\vec{\omega} \qquad (4.14b)$$

and $C_a(\vec{\omega})$ is the absorbtion cross section of a particle having properites $\vec{\omega}$.

Note that as given by (4.13), $v(\vec{r}, \vec{r}')$ is identical to the far field representation of the operator $u(\vec{r}, \vec{r}')$ except that the wave number within the slab is k rather than k_0 . Physically then, the scattering function $v(\vec{r}, \vec{r}')$ describes scattering by a particle embedded in a medium with refractive index k/k_0 rather than in free space. Also observe that in (4.14) only the absorbtion characteristics of the scatterers affect the total intensity; this is not surprising since the total power must be conserved. Thus, the approximate solutions of (4.13) and (4.14) are intuitively "correct" in that they are consistent with what we would expect from a physical standpoint.

In deriving the approximation (4.13) and (4.14), Twersky used some approximations that are appropriate for "large" scatterers. Specifically, he assumed that backscattering is negligible in comparison to forward scattering and that scattered energy is concentrated at small angles in the forward direction. It has been found in tests involving random distributions of "large" scatterers that Twersky's approximate solutions bear experimental scrutiny as well [2], [50]. Because of this and the intuitive "correctness" of the approximations that we discussed in the preceding paragraph, (4.13) and (4.14) are often employed in studying millimeter wave propagation through raindrops (see for example [27]). Therefore, we will procede under the assumption that (4.13) and (4.14) are reasonable approximation and utilize them in the ramainder of our analysis.

4.3 Intensity of the Received Inchoherent Signal

In this section, we shall derive expressions for the intensity of the incoherent signal at the output of the receiver in Figure 4.1 for two cases. The first case we will look at is that of far field scattering; spcifically, the scattering volume in our generic problem will be taken to be entirely in the receving apterture's Fraunhofer region. This far field assumption is geneally used when studying the probelm of rain scatter; however, as pointed out insection 2.4, very large antennas can have extended near field regions. Therefore, we will also consider the situation that arises when the scattering volume is in the Fresnel region of the antenna. In this case, we will make the assumption that the receving antenna is very large in that $D > 100\lambda$, D being the receving aperture's diameter and λ the wavelength.

We begin our analysis of the received incoherent signal intensity with a review of our model of the antenna's receving characteristics. Recall from section 4.1 that the antenna's aperture field distriubtion is defined by

$$\left| \int_{S_a} \int \psi_a(\xi, \eta) d\xi d\eta \right|^2 = G_o \tag{4.15}$$

By describing the antenna in the above fashion, its receving characteristics can be modeled by using the Huygens-Kirchoff scalar diffraction integral and Helmholtz reciprocity theorom [51]. Specifically, consider and arbirary source at $\vec{r}' = (x', y', z')$ which radiates into the apterure shown in Figure 4.3. We denote $A(\vec{r})$ as the transmitted field of the source at an arbitrary point $\vec{r} = (x, y, z)$ and V as the antennas response to the source; in the source's far field radiation zone

$$A(\vec{r}) = A_o(\vec{r})\frac{e^{-jk_0|\,rvecttor-\vec{r}'|}}{|\vec{r}-\vec{r}'|} \tag{4.16}$$

with $A_o(\vec{r})$ describing the sources radiation pattern.

Assuming then that each point on the aperture is in the far field of the arbtrary source, V can be obtained by summing the contributions from each incremental element $d\varepsilon d\eta$ on the aperture, ie

$$V = \int_{S_a}\int \psi_a(\xi, \eta)A(\vec{r}')d\xi d\eta \tag{4.17a}$$

with

$$\vec{r}_1 = \xi(\eta, L) \tag{4.17b}$$

For notational convenience, we define the operator $f(\bullet)$ by

$$F[A(\vec{r})] = \int_{S_a}\int \psi_a(\xi, \eta)A(\vec{r}'d\xi d\eta) \tag{4.18}$$

Note that $F(\bullet)$ is linear and operates independently of the position coordinates of the source. Using the above description of the antenna's receving characteristics, we can derive a general expression for the intensity of the recieved incoherent signal.

4.3.1 Derivation of the Received Incoherent Signal Intesity

Consider the total field at a point $\vec{r}(\xi, \eta, L)$ on the aperture of the receiveing antenna; we will designate this field as $\psi(\vec{r})$. $\psi(\vec{r})$ will be the plex sum of the incident and scattered fields; thus,

$$\psi(\vec{r}) = \psi_i(\vec{r}) + \sum_{j=1}^{N} \psi_s(\vec{r}, \vec{r}_j) \tag{4.19}$$

where $\psi_s(\vec{r}, r_j)$ is the field scattered to $\vec{r}$ from $\vec{r}_j$. $\psi_s(\vec{r}, \vec{r}_j)$ will be random and can be expressed as the plex sum of a coherent component $<\psi_s(\vec{r}, \vec{r}_j)>$ and a zero-mean, fluctuating component. $\psi_s'(\vec{r}, \vec{r}_j)$. Thus, the total field at $\vec{r}$ can also be written as

$$\psi(\vec{r}) = \psi_i(\vec{r}) + \sum_{j=1}^{N} <\psi_s(\vec{r}, \vec{r}_j)> + \sum_{j=1}^{N} \psi_s^f(\vec{r}, \vec{r}_j) \tag{4.20}$$

Now let V_t be the voltage at the output of the receiving antenna. V_t is obtained by operating on $\psi(\vec{r})$ with $F(\bullet)$. Hence

$$V_t = F[\psi_i(\vec{r})] + \sum_{j=1}^{N} F[<\psi_x(\vec{r}, \vec{r}_j)>] + \sum_{j=1}^{N} F[\psi_s^f(\vec{r}, \vec{r}_j)] \tag{4.21}$$

So, the intensity of the received signal, which is the squared modulus of V_t, is given by

$$|V_t|^2 = |F[\psi_i(\vec{r})] + \sum_{j=1}^{N} F[<\psi_s(\vec{r}, \vec{r}_j)>]|^2$$

$$+\left\{F[\psi_i(\vec{r}\,]+\sum_{j=1}^{N}F[<\psi_s(\vec{r},\vec{r}_j)>]\right\}\left\{\sum_{j=1}^{N}F[\psi_s^f(\vec{r},\vec{r}_j)]\right\}$$

$$+\left\{F[\psi_i(\vec{r})]+\sum_{j=1}^{N}F[<\psi_s(\vec{r},\vec{r}_j)>]\right\}\left\{\sum_{j=1}^{N}F[\psi_s^f(\vec{r},\vec{r}_j)]\right\}$$

$$+\sum_{j=1}^{N}\sum_{k=1}^{N}F[\psi_s^f(\vec{r},\vec{r}_j]F\,[\psi_s^f(\vec{r},\vec{r}_k)] \tag{4.22}$$

We obtain the average intensity of the received signal by averaging (4.22) over the density of the scatterers, $\rho(\vec{\omega})$. Doing so and noting that

$$<\psi_s^f(\vec{r},\vec{r}_j)> \;=\; 0 \tag{4.23}$$

and that because $F(\bullet)$ is linear and operates independently of the position coordinates of the scatterers

$$<F[\psi_s^f(\vec{r},\vec{r}_j)]> \;=\; 0 \tag{4.24a}$$

$$<F[\psi_s^f(\vec{r},\vec{r}_k)]F\,[\psi_s^f(\vec{r},\vec{r}_j)]> \;=\; 0\;,\;\; \vec{r}_j \neq \vec{r}_k \tag{4.24b}$$

$$=\; <F[\psi_s(\vec{r},\vec{r}_j)]F\,[\psi_s(\vec{r},\vec{r}_j)]>\;,\vec{r}_j \;=\; \vec{r}_k \tag{4.24c}$$

we obtain

$$<|V_t|^2> \;=\; |F[\psi_i(\vec{r})]+\sum_{V=1}^{N}F[<\psi_s(\vec{r},\vec{r}_j)>]|^2$$

$$+ \int F[\psi_s^f(\vec{r}, \vec{r}')]F[\psi_s^f(\vec{r}, \vec{r}')]n(\vec{\omega}d\omega) \tag{4.25}$$

The first term on the right hand side of (4.25) is clearly the intensity of the recevied coherent signal and the second the received incoherent signal intensity; we will denote these components as I_c and I_f respectively. Following our discussion in section 3.4, the coherent signal intensity is immediately seen to be

$$I_c = G_o\psi_o e^{-\sigma_t d} \tag{4.26a}$$

where

$$\sigma_t = -\frac{4\pi}{k_0}\int I_m[f(0, \vec{\omega})]n(\vec{\omega})d\vec{\omega} \tag{4.26b}$$

or

$$\sigma_t = \int C_t(\vec{\omega})n(\vec{\omega})d\vec{\omega} \tag{4.26c}$$

and $C_t(\vec{\omega})$ is the total cross section of a particle with properties $\vec{\omega}$.

In order to determine I_f, a suitable expression for the fluctuating component of the scattered field must be obtained. To accomplish this, consider the total field at $\vec{r}$ as given by (4.20):

$$\psi(\vec{r}) = \psi_i(\vec{r} + \sum_{j=1}^{N} < \psi_s(\vec{r}, \vec{r}_j) > + \sum_{j=1}^{N} \psi_s f(\vec{r}, \vec{r}_j) \tag{4.27}$$

Averaging the squared modulus of $\psi(\vec{r})$ in (4.27) over the density of the scatterers we obtain for the total intensity at $\vec{r}$

$$< |\psi(\vec{r})|^2 > = |\psi_i(\vec{r}) + \sum_{j=1}^{N} < \psi_s(\vec{r}, \vec{r}_j) > |^2$$

$$+ \int \psi_s^f(\vec{r}, \vec{r}\,') \psi_s^f(\vec{r}, \vec{r}\, dprime) n(\vec{\omega}) d\vec{\omega} \tag{4.28}$$

Now, the total intensity at $\vec{r}$ will also follow the Twersky intplex integral equation

$$< |\psi(\vec{r})|^2 > = | < \psi(\vec{r}) > |^2 + \int V(\vec{r}, \vec{r}\,') V(\vec{r}, \vec{r}\,') < |\psi(\vec{r}\,')|^2 > n(\vec{\omega}) d\vec{\omega} \tag{4.29}$$

In comparing (4.28) and (4.29), it is readily deduced that the fluctuating field at $\vec{r}$ is given by

$$\psi_s^f(\vec{r}, \vec{r}\,') = \psi_1(\vec{r}\,') v(\vec{r}, \vec{r}\,') \tag{4.30a}$$

with

$$\psi_1(\vec{r}) \psi(\vec{r}\,') = < |\psi(\vec{r}\,')|^2 > \tag{4.30b}$$

Therefore, using (4.24) and (4.30) and noting that $F(\bullet)$ operates independently of $\vec{r}\,'$, we obtain

$$I_f = \int F[V(\vec{r}, \vec{r}\,')] F[V(\vec{r}, \vec{r}\,')] n(\vec{\omega}) d\vec{\omega} \tag{4.31}$$

Equation (4.31) is the general expression for the received incoherent signal intensity. We will use it to determine I_f for the far field and near field scattering cases.

4.3.2 Far Field Scattering

In Section 4.2, the following expression for the total intensity within the raincell and scattering function $v(\vec{r}, \vec{r}')$ were presented

$$< |\psi(\vec{r}')|^2 > = |\psi_o|^2 e^{-\sigma_e z'} \tag{4.32a}$$

$$v(\vec{r}, \vec{r}') = f(\hat{\vec{z}}, \hat{\vec{k}}_s, \omega) \frac{e^{-jk_0 R}}{R} \exp[-jk_1(d - z') \sec\theta', \ z > d \tag{4.32b}$$

where

$$R = |\vec{r} - \vec{r}'| \tag{4.32c}$$

$$\hat{k}_s = \frac{\vec{r} - \vec{r}'}{R} \tag{4.32d}$$

$$\cos\theta' = \hat{z} \cdot \hat{k}_s \tag{4.32e}$$

Also, in the far field of the receving aperture, $F[v(\vec{r}, \vec{r}']F^c[v(\vec{r}, \vec{r}')]$ can be written in terms of the antenna's far field gain pattern as

$$F[V(\vec{r}, \vec{r}')]F[V(\vec{r}, \vec{r}')] = G_o |V(\vec{r}, \vec{r}')|^2 e^{-\alpha_r \theta_r^2} \tag{4.33}$$

Substituting then (4.32) and (4.33) into (4.31), we obtain as the full expression of I_f in the case of far field scattering

$$I_f = G_o |\psi_o|^2 \int d\vec{\omega}_1 n(\vec{\omega}) \int_0^d dz' \int_{-\infty}^{\infty} \int dx' dy' \frac{e^{-\sigma_e z'}}{R^2}$$

$$x|f(\hat{z}, \hat{k}_s, \vec{\omega}_1)|^2 e^{-\alpha_r \theta_r^2} \exp[-\sigma_t(d - z') \sec \theta'] \tag{4.34a}$$

with

$$\vec{\omega}_1 = (\bar{a}, s) \tag{4.34b}$$

In order to evaluate the transverse integrals in (4.34), we convert the integration in x′, y′, and z′ to one in z′, θ_r and ϕ_r using (see Figure 4.4)

$$\theta' = \theta_r \tag{4.35a}$$

$$dxdy = R^2 \tan \theta_r d\theta_r d\phi_r \tag{4.35b}$$

$$(x', y', z') \in [(-\infty, \infty),(-\infty, \infty),(0, d)] \qquad (z', \theta_r, \phi_r) \in [(0, d),(0, \pi/w,(0, \pi)] \tag{4.35c}$$

Equation (4.34) then becomes

$$I_f = G_0|\psi_o|^2 \int d\vec{\omega}_1 \int n(\vec{\omega}) \int_d z' e^{-\sigma_s z'}$$

$$x \int_0^{2\pi} \int_o^{\pi/2} d\theta_r d\phi_r \tan \theta_r |f(\hat{z}, \hat{k}_s, \vec{\omega}_1)|^2 e - \alpha_r \theta_r^2$$

$$x \exp[-\sigma_t(d - z') \sec \theta_r] \tag{4.36}$$

For large antennas, effective contributions to the θ_r integral in (4.36) will be limited to small θ_r where

$$f(\hat{z}, \hat{k}_s, \vec{\omega}_1) \simeq f(0, \vec{\omega}_1) \tag{4.37a}$$

$$\sec\theta_r \simeq 1 + \frac{\theta_r^2}{2} \tag{4.37b}$$

$$\tan\theta_r \simeq \theta_r \tag{4.37c}$$

Making the approximations of (4.37) in (4.36) and extending the upper limit of integration in θ_r to infinity yields

$$I_f = 2\pi G_o |\psi_o|^2 e^{-\sigma_t d} \int |f(o, \vec{\omega}_1)|^2 n(\vec{\omega}) d\vec{\omega}_1$$

$$x \int_o^d \int_o^\infty \theta_r e^{\sigma_s z'} \exp\left\{ [\alpha_r + \frac{\sigma_t}{2}(d - z')\theta_r^2] \right\} d\theta_r dz' \tag{4.38}$$

where the intplex integral in ϕ_r has been evaluated and we have made the definition

$$\sigma_s = \int C_s(\vec{\omega}_1) n(\vec{\omega}_1) d\vec{\omega}_1 \tag{4.39a}$$

with $C_s(\vec{\omega})$ the scattering cross section of a raindrop with parameters ω_1 We have also noted that

$$\sigma_s = \sigma_t - \sigma_a \tag{4.39b}$$

The θ_r intplex integral in (4.6) is easily evaluated to give

$$I_f = \pi G_0 |\psi_0|^2 e^{-\sigma_t d} \int |f(0, \omega_1)|^2 n(\vec{\omega}) d\vec{\omega}_1$$

$$x\int_o^d \frac{e^{\sigma_t z'}}{\alpha_r + \frac{\sigma_t d}{2} - \frac{\sigma_t z'}{2}} dz' \tag{4.40}$$

In order to evaluate the z′ intplex integral in (4.40), we note that

$$\alpha_r + \frac{\sigma_t d}{2} > \frac{\sigma_t z}{2} \quad , \quad 0 < z < d \tag{4.41}$$

Thus [6]

$$\frac{1}{\alpha_r + \frac{\sigma_t d}{2} - \frac{\sigma_t z}{2}} = \frac{2}{2\alpha_r + \sigma_t d} \sum_{m=0}^{\infty} (-1)^m z^m q^m \tag{4.42a}$$

where

$$q = \frac{\sigma_t}{2\alpha_r + \sigma_t d} \tag{4.42b}$$

We shall truncate the series in (4.42) at an upper index M_o so that

$$\frac{1}{\alpha_r + \frac{\sigma_t d}{2} - \frac{\frac{\sigma_t z}{2}}{2\alpha_r + \sigma_t d} \sum_{m=0}^{M_o} (-1)^m z^m q^m} \tag{4.43}$$

Substituting (4.43) into (4.40) yields

$$I_f = \frac{2\pi}{2\alpha_r + \sigma_t d} G_0 |\psi_0|^2 e^{-\sigma_t d} \int |f(0, \vec{\omega}_1)|^2 n(\vec{\omega}) d\vec{\omega}_1$$

$$x\sum_{m=0}^{M_o}(-1)^m q^m \int_o^d (z')^m e^{\sigma_s z'} dz' \tag{4.44}$$

The z′ intplex integral in (4.44) can be evaluated using the indefinite integral [52]

$$\int z^m e^{ax} dx = e^{ax}\sum_{n=0}^{m}(-1)^n \frac{m! x^{m-n}}{(m-n)! a^{n+1}} \tag{4.45}$$

We then obtain

$$I_f = \frac{2\pi}{\sigma_s(2\alpha_r + \sigma_t d)} G_o |\psi_o|^2 e^{-\sigma_t d} \int |f(o, \vec{\omega}_1|^2 n(\vec{\omega}) d\vec{\omega}_1$$

$$x\left\{ e^{\sigma_s d}\sum_{m=0}^{M_o}\sum_{n=0}^{m}\left[(-1)^{m+n}\frac{m!}{(m-n)!}\frac{q^m d^{m-n}}{\sigma_s^n}\right] - 1\right\} \tag{4.46}$$

With (4.46) we have derived the intensity of the incoherent signal at the output of the receiver under far field scattering conditions. Let us now consider the case of near field scattering.

4.3.3 Near Field Scattering

When the plane-parallel slab of rain drops in our canonic problem lies in the Fresnel region of the receiving aperture, the far field approximation given in (4.33) is not valid. Rather,

the quadratic phase term in the scattering function $v(\vec{r}, \vec{r}')$ must be retained in order to approximate $F[v(\vec{r}, \vec{r}')]$. Specifically recall from (4.32) that

$$v(\vec{r}, \vec{r}') = f(\hat{z}, \hat{k}_s, \vec{\omega}_1)\frac{e^{-js_0R}}{R}\exp[-jk_1(d-z')\sec\theta'], \; z > d \tag{4.47a}$$

with (see Figure 4.5)

$$R = [\xi - x')^2 + (\eta - y')^2 + (L - z')^2]^{1/2} \tag{4.47b}$$

$$\cos\theta' = \hat{z} \cdot \hat{k}_s = \frac{L - z'}{R} \tag{4.47c}$$

In the antenna's Fresnel region, R can be approximated by [16]

$$R \simeq (L - z') + (\xi - x')^2 + \frac{(\eta - y')^2}{2(L - z'} \tag{4.48a}$$

for phase variation and by

$$R \simeq (L - z') \tag{4.48b}$$

for amplitude variation. Also, since $\sec\theta' = R/(L - z')$, it is appropriate to approximate it as

$$\sec\theta' \simeq 1 + \frac{(\xi - z')^2 + (\eta - y')^2}{2(L - z')^2} \tag{4.49}$$

If we now substitute (4.48) and (4.49) into (4.47), we obtain the following Fresnel region approximation for $F[v(\vec{r}, \vec{r}')]$:

$$F[v(\vec{r}, \vec{r}')] = \frac{1}{L - z'}\exp[-jk_o(L - z')]\exp[-jk_1(d - z')]$$

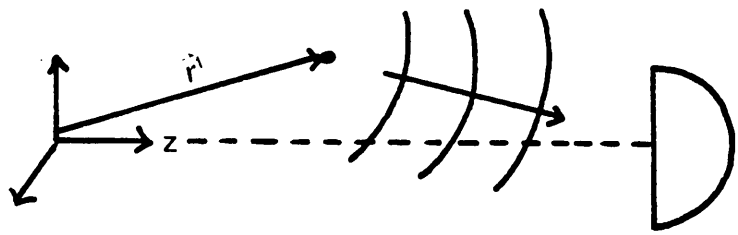

Arbitrary Source at the $\vec{r}'$ Radiating Into The Aperture

Figure 4.3

$$x\int_{S_a}\int \psi_a(\xi,\eta) f(\hat{z},\hat{k}_s,\vec{\omega}_1)$$

$$x\exp\left\{\frac{Q(z')}{2(l-z')^2}[(\xi-z')^2+(n-y')^2]\right\}d\xi d\eta \tag{4.50a}$$

where

$$Q(z') = -j[s_0(L-z') + k_1(d-z')] \tag{4.50b}$$

Substituting then (4.50) into (4.31) , we obtain as the full expression for the intensity of the received incoherent signal

$$I_f = |\psi_o|^2 e^{-\sigma_t d}\int d\vec{\omega}_1 n(\vec{\omega})\int_o^d dz' \frac{e^{\sigma_s z'}}{(l-z')^2}\int_{-\infty}^{\infty}\int dx'dy'$$

$$x\int_{S_a}\int d\xi_1 d\eta_1 \psi_a(\xi_1,\eta_1) f(\hat{z},\hat{k}_s^{(1)},\vec{\omega})\exp\left\{\frac{Q(\hat{z})}{2(l-z')^2[(\xi_1-x')^2+(\eta_1-y')^2]}\right\}$$

$$x\int_{S_a}\int d\xi_2 d\eta_2 \psi_a(\xi_2,\eta_2) f(\hat{z},\hat{k}_s^{(2)},\vec{\omega}_1)\exp\left\{\frac{Q(z')}{2(L-z')^2}[(\xi_2-z')^2+(\eta_2+y'^2]\right\} \tag{4.51}$$

where $\hat{k}_s^{(1)}$ and $\hat{k}_s^{(2)}$ are unit vectors from $\vec{r}'$ to $(\xi_1, \eta_1, :)$ and (ξ_2, η_2, L) respectively.

Equation (4.51) can be simplified considerably. To do this we first observe that the scattering pattern of a raindrop will be much broader than a very large antenna's angular pattern in the Fresnel region. Therefore, it is reasonable to approximate the scattering

amplitude $f(\hat{z}, \hat{k}_s^{(\omega)}, \bar{a})$ in (4.51) with the forward scattering amplitude and rewrite the equation as

$$I_f = |\psi_0|^2 e^{-\sigma_t d} \int |f(0, \vec{\omega}_1)|^2 n(\vec{\omega}) d\vec{\omega}_1 \int_o^d dz' \frac{e^{\sigma_{z'}}}{(L-z')^2} \int_{-\infty}^{\infty} \int dx' dy'$$

$$S_a \int d\xi_1 d\eta_1 \psi_a(\xi_1, \eta_1) \exp\left\{ \frac{Q(z')}{2(L-z')^2[(\xi_1 - x')^2 + (\eta_1 - y')^2]} \right\}$$

$$x \int_{S_a} \int d\xi_2 d\eta_2 \psi_a(\xi_2, \eta_2) \exp\left\{ \frac{Q(z')}{2(l-z')^2} [(\xi_2 - x')^2 + (\eta_2 - y')^2] \right\} \tag{4.52}$$

We now exchange orders of integration in (4.52) and perform some algebra to rearrange terms in the exponentials so that the equation can be recast

$$I_f = |\psi_0|^2 e^{-\sigma_t d} \int |f(o, \vec{\omega}_1|^2 n(\vec{\omega}) d\vec{\omega}_1 \int_o^{d/dz'} \frac{e^{\sigma_s z'}}{L-z')^2}$$

$$x \int_{S_a} \int \int_{S_a} \int d\xi_1 d\eta_1 d\xi_2 d\eta_2 \psi_a(\xi_1, \eta_1) \psi_a(\xi_2, \eta_2)$$

$$x \exp\left\{ |Q \frac{(z'|^2}{r Q_r(z')(L-z')^2} [(\xi_1 - \xi_2)^2 + (\eta_1 - \eta_2)^2] \right\}$$

$$x \int_{-\infty}^{\infty} \int dx' dy' \exp \frac{Q_r(z')}{(L-z')^2} \left[x' - \frac{Q(z')\xi_1 + Q(z')\xi_2}{2Q_r(z')} \right]^2$$

$$+\left[y' - \frac{Q(z')\eta_1 + Q(z')\eta_s}{2Q_r(z')}\right]^2 \tag{4.53}$$

where $Q_r(z')$ is the real part of $Q(z')$. $Q_r(z')$ is negative; hence, we can evaluate the integrals in x′ and y′ using the elementary result [42]

$$\int_{(-\infty)}^{\infty} \exp[-p^2(x-\mu)^2]dx = \frac{\sqrt{\pi}}{p} \tag{4.54}$$

We then obtain

$$I_f = -\pi|\psi_o|^2 e^{-\sigma_t d}\int |f(0,\vec{\omega}_1)|^2 n(\vec{\omega})d\vec{\omega}_1 \int_o^d dz' \frac{E\sigma_s z'}{Q_r(z')}$$

$$x\int_{S_a}\int\int\int d\xi_1 d\eta_1 d\xi_2 d\eta_2 \psi_a(\xi_1,\eta_1)\psi_a(\xi_2,\eta_2)$$

$$x\ \exp\left\{\frac{|Q(z')|^2}{4Q_r(z')(L-z')^2}[(\xi_1-\xi_2)^2+(\eta_1-\eta_2)]\right\} \tag{4.55}$$

We can obtain an approximate solution to the integral in ε_1, ε_2, η_1 and η_2 in (4.55) by using Laplace's method [7]. Laplace's method is an asymptotic technique for evaluating (approximately definite integrals possessing rapidly decaying integrans and when applied to the present case yields (see Appendix E)

$$\int_{S_a}\int\int_{S_a}\int d\xi_1, d\eta_1, d\xi_2, d\eta_2 \psi_a(\xi_1,\eta_1)\psi_a(\xi_2,\eta_2)$$

$$x \exp\left\{\frac{|Q(z')|^2}{4Q_r(z')(L-z')^2}[(\xi_1 - zi_2)^2 + (\eta_1 - \eta_2^2]\right\}$$

$$\simeq -\frac{16\pi^2}{\lambda^2}\frac{Q_r(z')(l-z')}{|Q(z')|^2} \tag{4.56}$$

Substituting now (4.56) into (4.55) yields

$$I_f = \frac{16\pi^3}{\lambda^2}|\psi_o|^2 e^{-\sigma_t d}\int |f(0, \vec{\omega}_1)|^2 n(\vec{\omega}) d\vec{\omega}_1$$

$$x\int_o^d \left[\frac{(L-z')}{|Q(z')|}\right]^2 e^{\sigma_s z'} dz' \tag{4.57}$$

If we now observe that

$$\frac{L-z')}{|Q(z')|} \simeq \frac{1}{s_0} \tag{4.68a}$$

$$k_o = \frac{2\pi}{\lambda} \tag{4.58b}$$

(4.57) can be further reduced to

$$I_f = 4\pi|\psi_o|^2 e^{-\sigma_t d}\int |f(0, \vec{\omega}_1)|^2 n(\vec{\omega}) d\vec{\omega}_1$$

$$x\int_o^d e^{\sigma_s z'} dz' \tag{4.59}$$

Evaluating the intplex integral in z′ of (4.59), we finally obtain for I_f the rather simple expression

$$I_f = 4\pi |\psi_o|^2 e^{-\sigma_t d}\left[\frac{e^{\sigma_s d}-1}{\sigma_s}\right]\int |f(o,\omega_1|^2 n(\vec{\omega})d\vec{\omega}_1 \tag{4.60}$$

Equation (4.60) is probably the most significant result of our investigation in this treatise. In it note the conspicuous absence of L which defines the distance between the slab of scatterers and the antenna. This indicates that the incoherent intensity at the receiver's output is independent of the location of the scatterers in relation to the antenna. To further establish the validity of this observation, recall equation (4.46) for the recevied incoherent intensity under the assumption of far field scattering:

$$I_f = \pi G_0 |\psi_o|^2 e^{-\sigma_t d}\int |f(0,\vec{\omega}_1)|^2 n(\vec{\omega})d\vec{\omega}_1$$

$$x\int_o^d \frac{e^{\sigma_s z'}}{\alpha_r + \frac{\sigma_t d}{2} - \frac{\sigma_t z'}{2}}dz' \tag{4.61}$$

For very large antennas and practical values of d

$$\alpha_r >> \frac{\sigma_t d}{2} - \frac{\sigma_t z'}{2} \simeq (4.63)$$

and, hence

$$\alpha_r + \frac{\sigma_t d}{2} - \frac{\sigma_t z'}{2} \simeq \alpha_r \tag{4.63}$$

making the approximation of (4.67) in (4.66) yields

$$I_f = \pi \frac{G_o}{\alpha_r} |\psi_o|^2 e^{-\sigma_s d} \int |f(o, \vec{\omega})|^2 n(\vec{\omega}) d\vec{\omega}_1$$

$$x \int_o^d e^{\sigma_s z'} dz' \tag{4.64}$$

Noting from (4.3) that $G_0 = 4\alpha_r$ and evaluating the z′ intplex integral in (4.64) gives

$$I_f = 4\pi |\psi_0|^2 e^{-\sigma_t d} \left[\frac{e^{\sigma_s d} - 1}{\sigma_s} \right] \int |f(0, \vec{\omega}_1)|^2 n(\vec{\omega}) d\vec{\omega}_1 \tag{4.65}$$

which is identical to (4.60). We conclude therfore that, from a practical standpoint, scatterer location vis-a-vis a receiver has no effect on the incohrent output during a rain event. This coupled with our finding in section (3.4) regarding the coherent field establishes the validity of restricting attention to far field scattering when analyzing the effects of rain scatter at millimeter wave frequencies.

4.4 Calculations of the Received Incoherent Intesity

Our objective in this section will be to gain some insight as to the conditions under which the incoherent effects of a rain event should be taken into account. To do this, we have computed the ratio of the received coherent to incoherent intensities for various situations using the results of the previous section. This quantity can be thought of as a signal-to-noise ratio. and is given analytically by (cf (4.26) and (4.46)

$$\frac{I_c}{I_f} = \frac{2\pi}{\sigma_s(2\alpha_r + \sigma_t d)} \int |f(o, \vec{\omega}_1)|^2 n(\vec{\omega}) d\vec{omega} ave_1$$

$$x \left[e^{\sigma_s d} \sum_{m=0 M_o} \sum_{n=0}^{m} (-1)^{m+n} \frac{M!}{m-n)!} Q^m \frac{d^{m-n}}{\sigma_s^n} - 1 \right]^{-1} \qquad (4.66)$$

We computed values of I_c/I_f for various receiving antenna gains (G_o = 30, 40, *and* 45 *dB*) and frequencies (30, 45, 75 and 90 GHz) and for rain rates which are light (2.5 mm/hr), moderate (12.5 mm/hr), heavy (50 mm/hr) and very heavy (150 mm/hr.). In calculating the data we assumed uniform rain rates and used the Marshall-Palmer drop size distribution (see (3.78)); the program used is in Appendix G. Plots of the computed data are presented in Figures 4.6 through 4.17. In these plots, the circled points correspond to where $A = exp(\sigma_t, d)$ is at 40 dB. (A is the attenuation of the coherent field at the slab length and rain rate corresponding to a circled point.)

In considering the plots in Figures 4.6 through 4.17, it can be seen that in almost all instances the power in the coherent signal is significantly greater than that in the incoherent one for A less than the value indicated. For this reason it is often assumed that incoherent effects can usually be neglected at millimeter wave frequencies. However, the incoherent signal results from multiple scattering phenomena and can be considered a phase delayed copy of the coherent signal. For this reason, the incoherent effects are probably best looked at by treating the fluctuating signal in the same manner as one would treat multipath [11]. So let us define Δ by

$$\Delta = \frac{|<v>|}{|<v>| - |_f|} = \left[1 - |/<v>|\right]^{-1} \qquad (4.67a)$$

or

$$\Delta = \left[1 - (I_c/I_f)^{-1/2}\right]^{-1} \tag{4.67b}$$

Δ is an additional attenuation of the signal that will occur when the fluctuating and coherent signals are in phase quadrature (a "worst case" scenerio). By looking at the relationship between the coherent and incoherent signals from this standpoint rather than by simply considering the ration I_c/I_f, the incoherent effects are found to be significant for heavy and very heavy rain rates. To illustrate, we have compiled tables 4.1 through 4.6 which indicate values of Δ at the circled points shown in teh plots. Based on the data presented in these tables, it can be concluded that, the fluctuating signal accompanying heavy rainfall can lead to more severe fades than one would expect from a coherent analysis alone. We conclude therefore that the incoherent effects caused by heavy rainfall should be considered when planning a millimeter wave system if such rainfall is expected over the link.

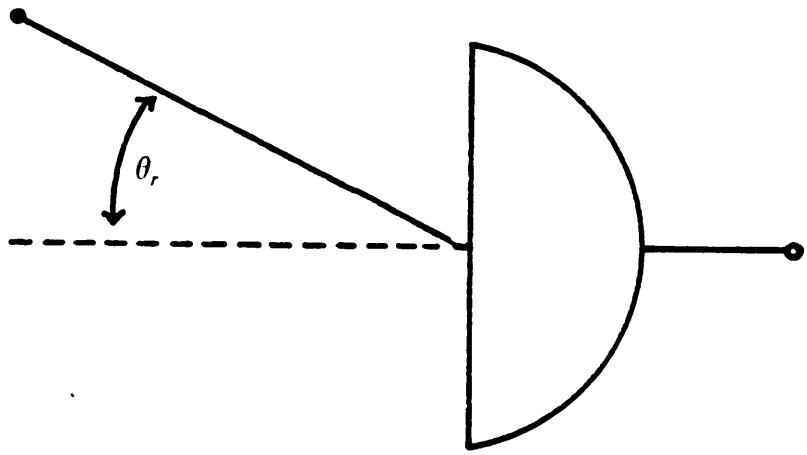

Definition of the variable θ_r

Figure 4.2

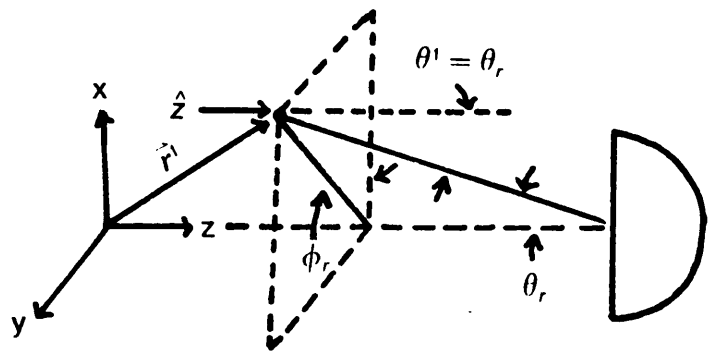

Geometry For Change of Coordinate Systems in (4.35)

Figure 4.4

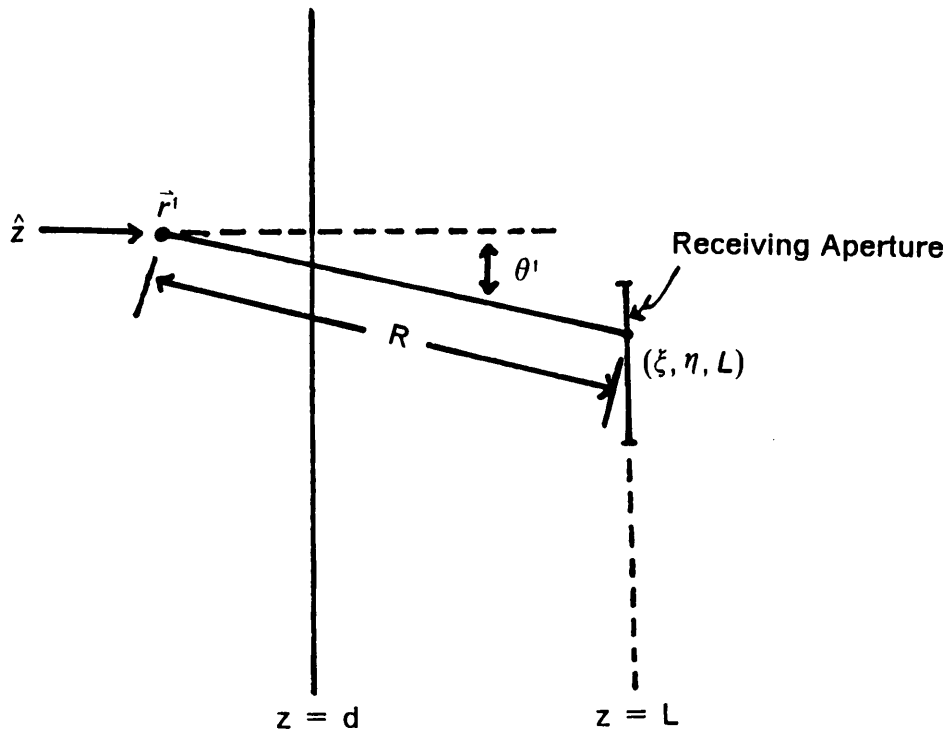

Geometry Showing R and θ' in (4.70)

Figure 4.5

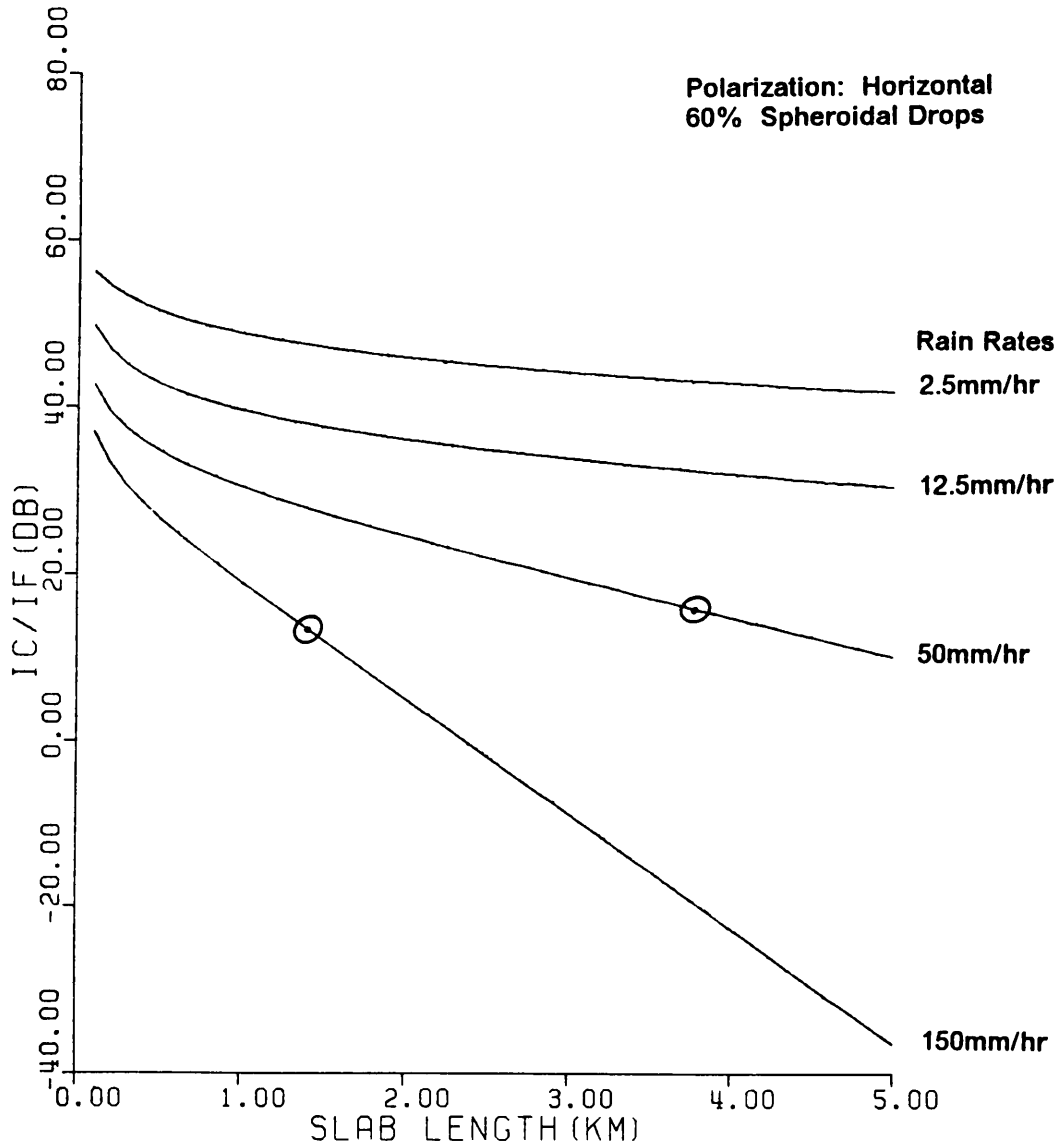

Ratio of Coherent to Incoherent Power at 30GHz and 60 = 35 dB

Figure 4.6

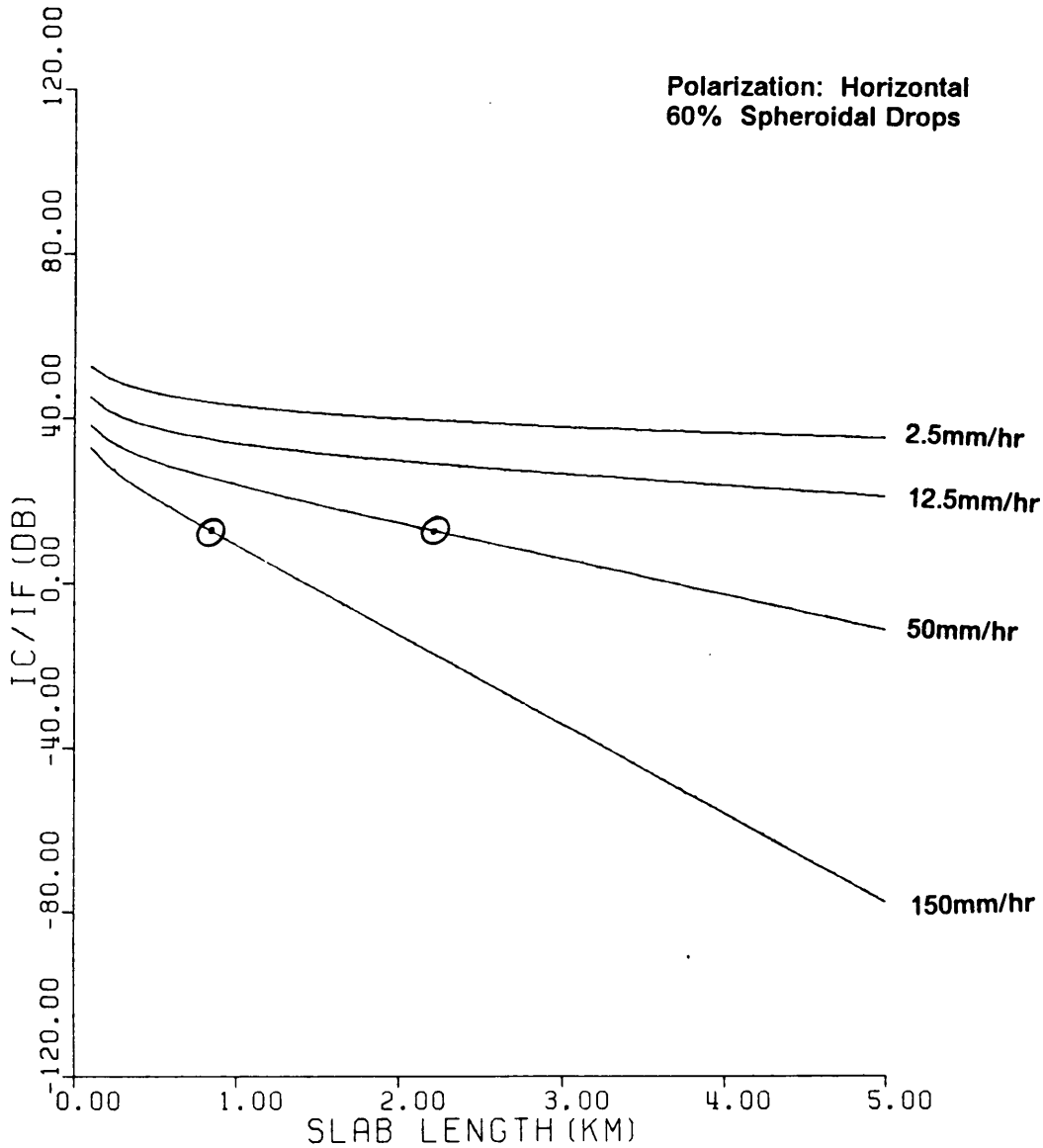

Ratio of Coherent to Incoherent Power at 46GHz and 60 = 35dB

Figure 4.7

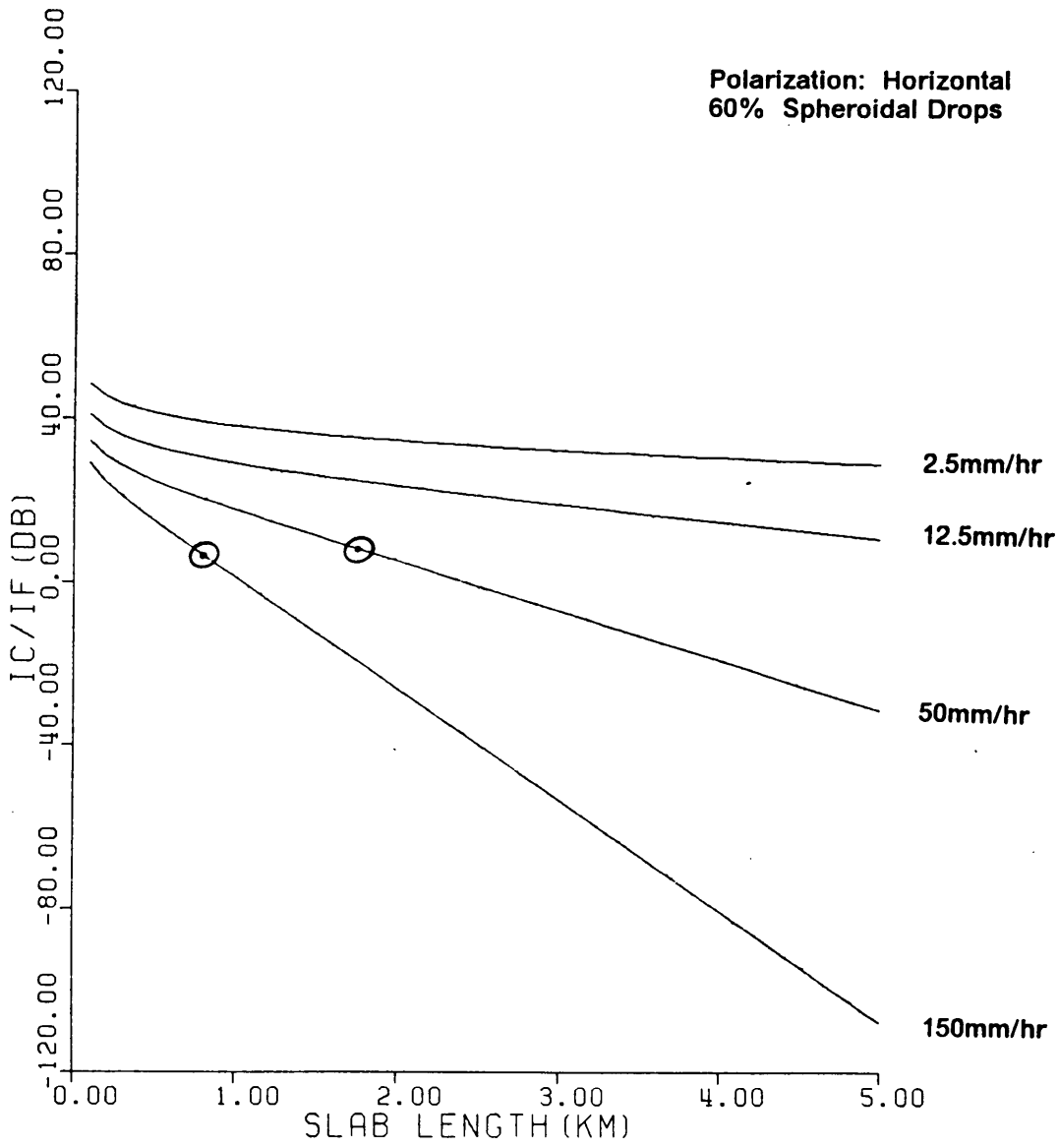

Ratio of Coherent to Incoherent Power at 70GHz and 60 = 35 db

Figure 4.8

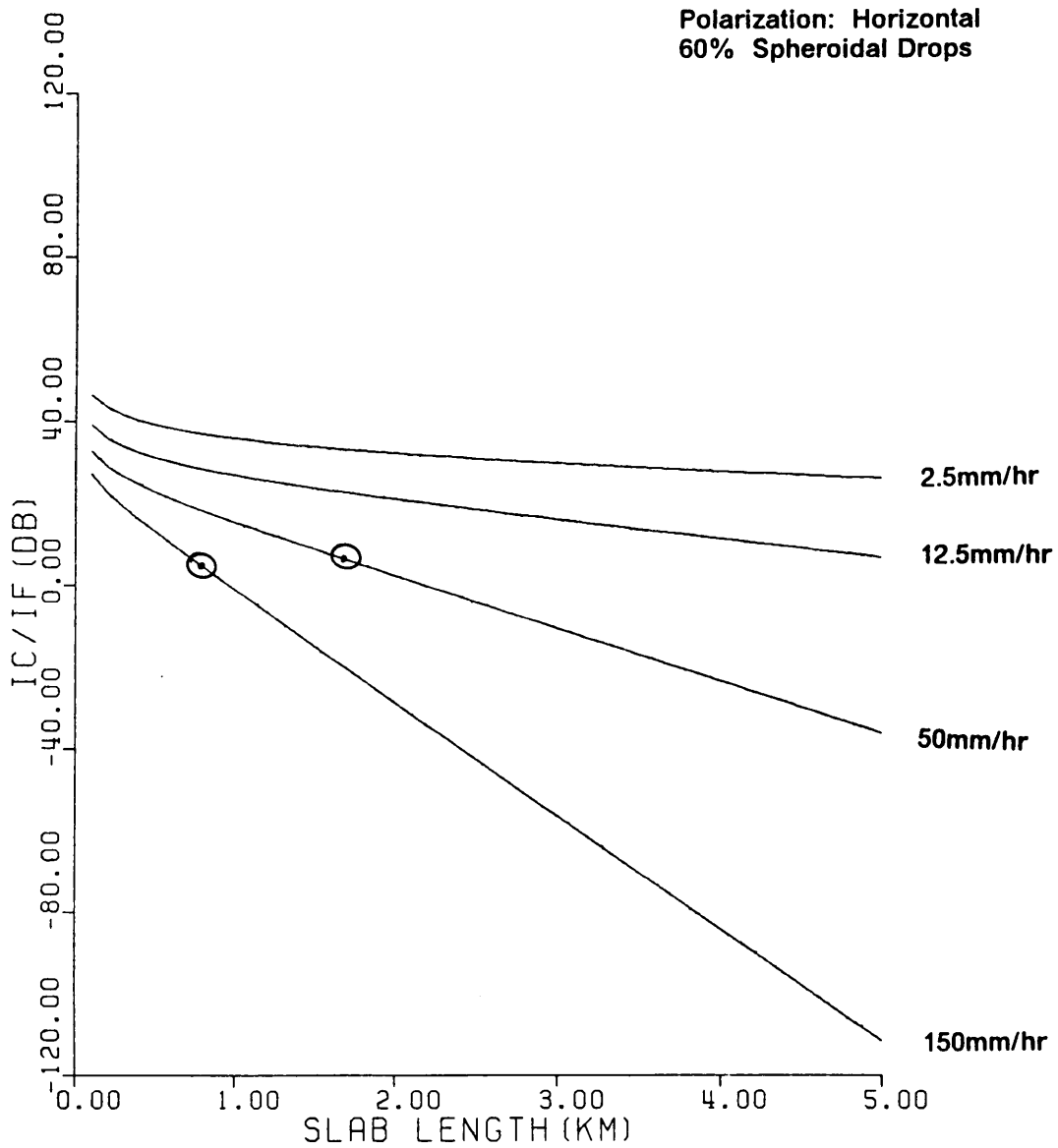

Ratio of Coherent to Incoherent Power at 90GHz and 60 = 35 dB

Figure 4.9

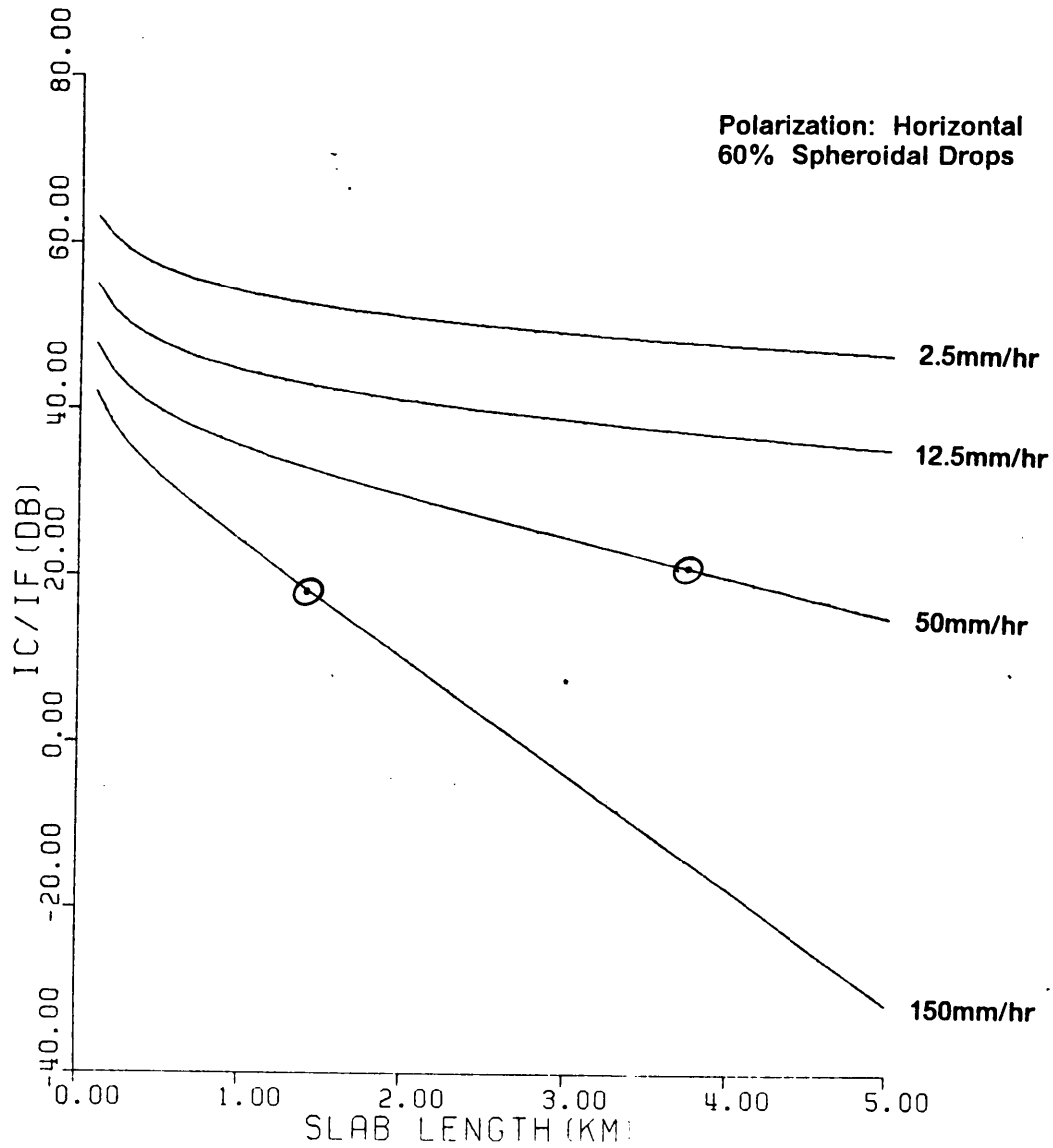

Ratio of Coherent to Incoherent Power at 30GHz and 60 = 40 dB

Figure 4.10

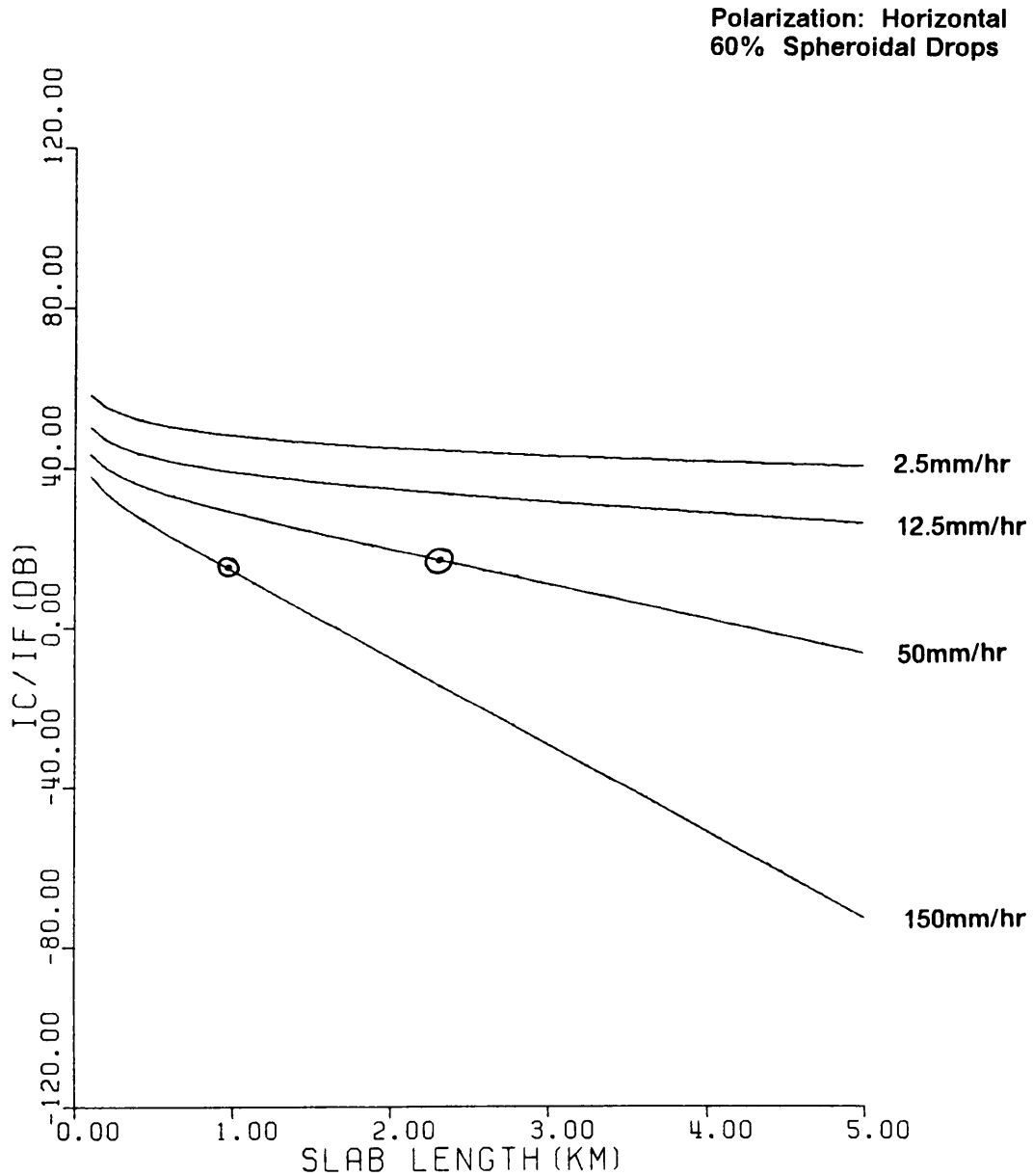

Ratio of Coherent to Incoherent Power at 45GHz and 60 = 40 dB

Figure 4.11

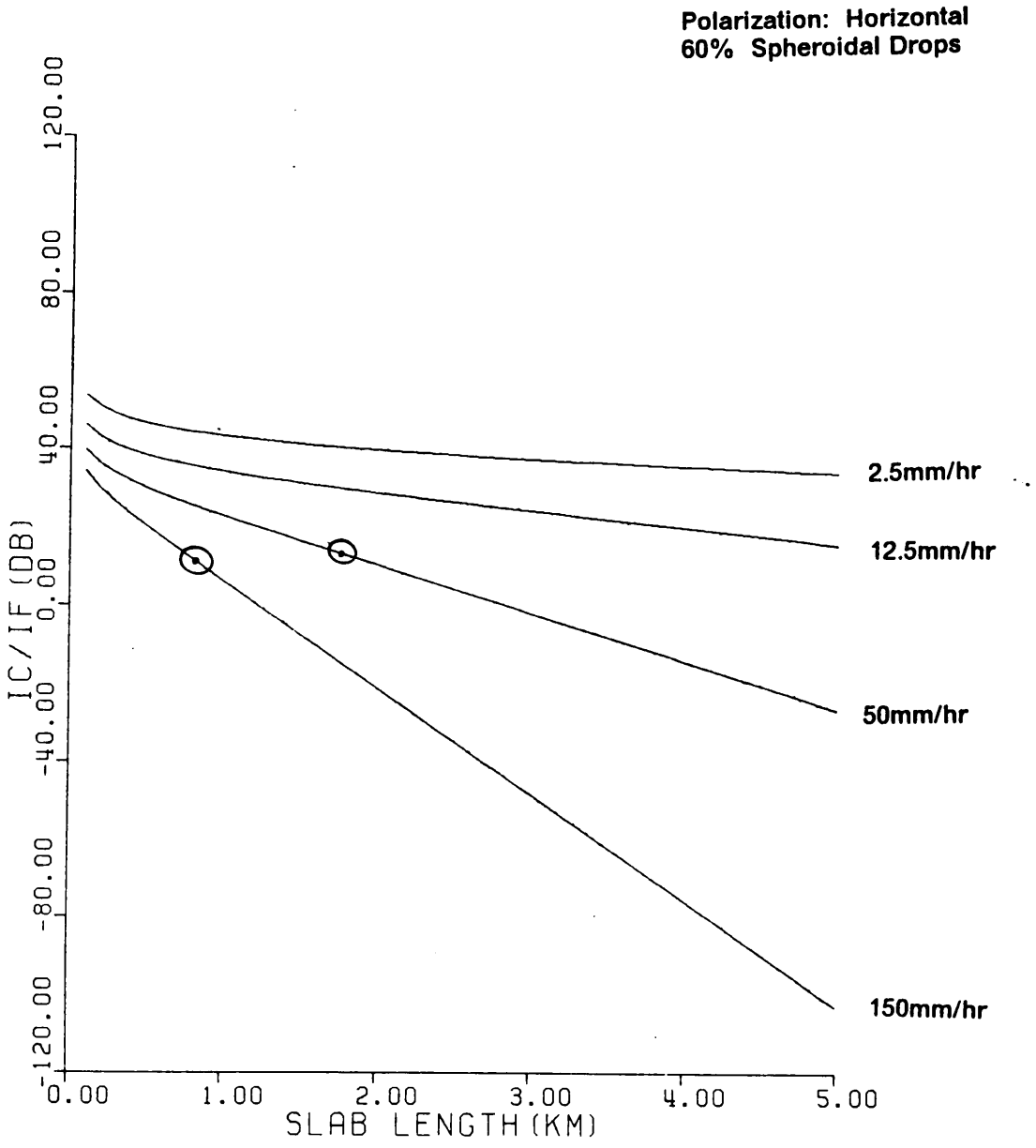

Ratio of Coherent to Incoherent Power at 70GHz and 60 = 45 dB

Figure 4.12

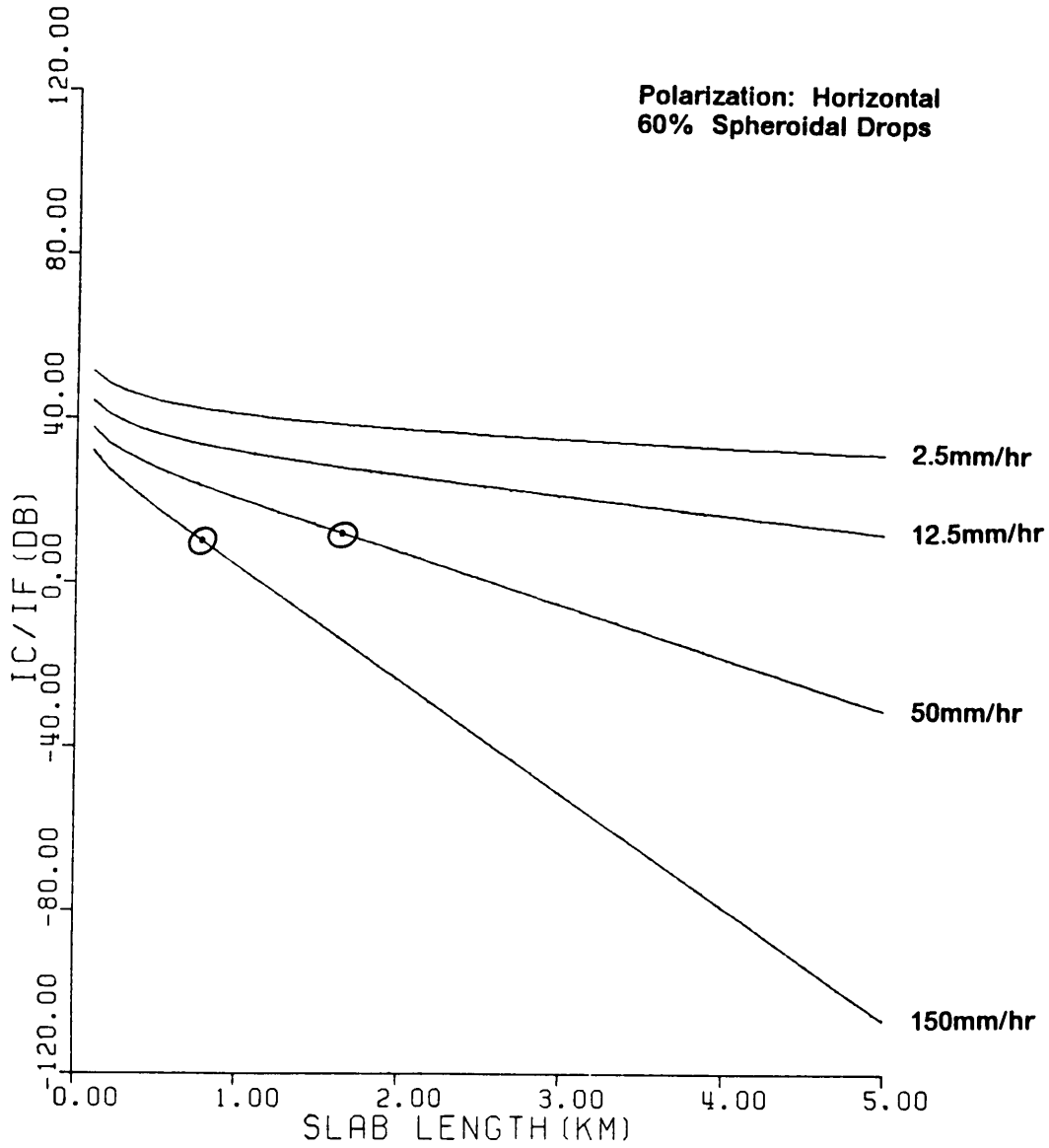

Ratio of Coherent to Incoherent Power at 90GHz and 60 = 40 db

Figure 4.13

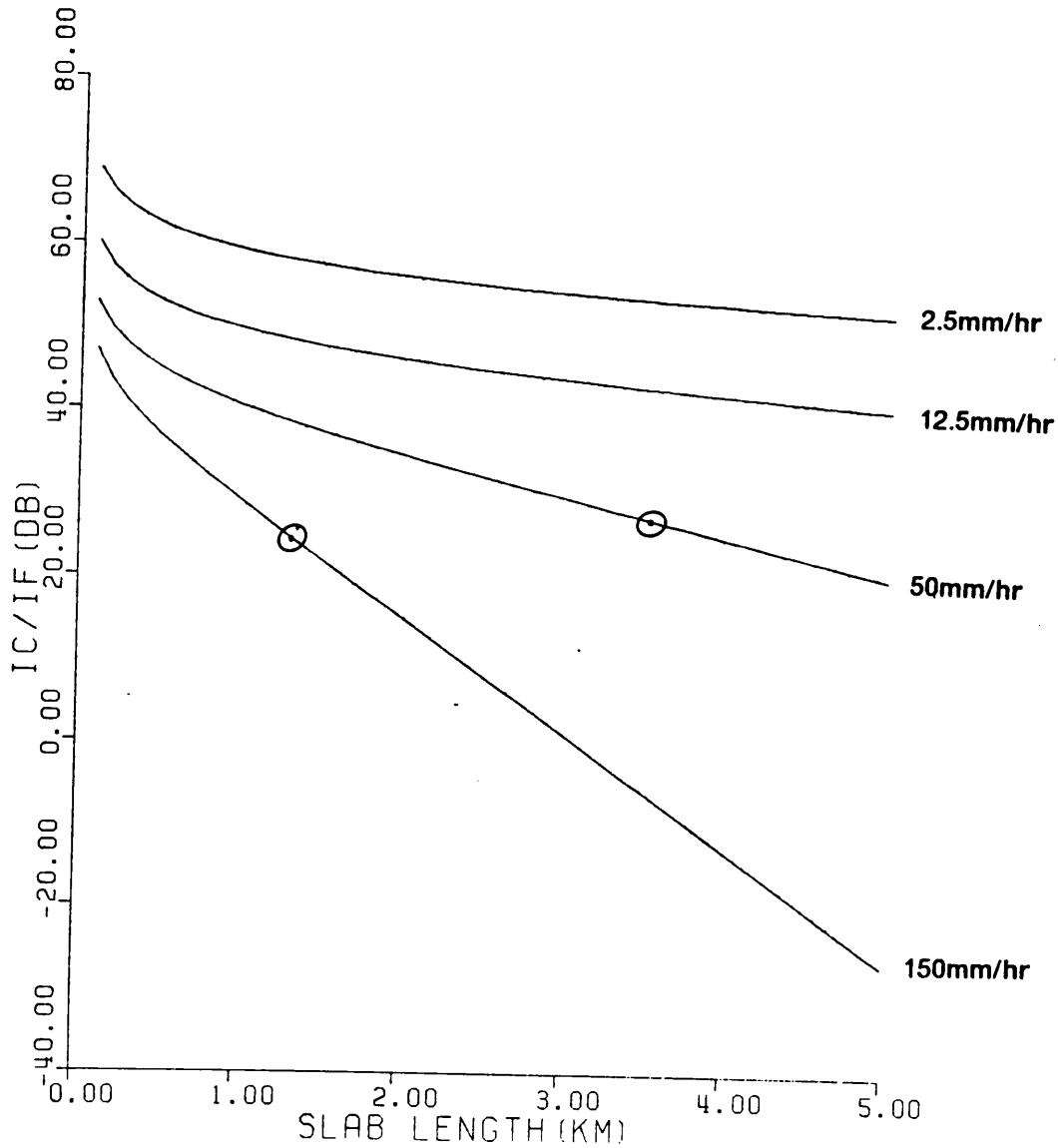

Ratio of Coherent to Incoherent Power at 30GHz and 60 = 45 dB

Figure 4.14

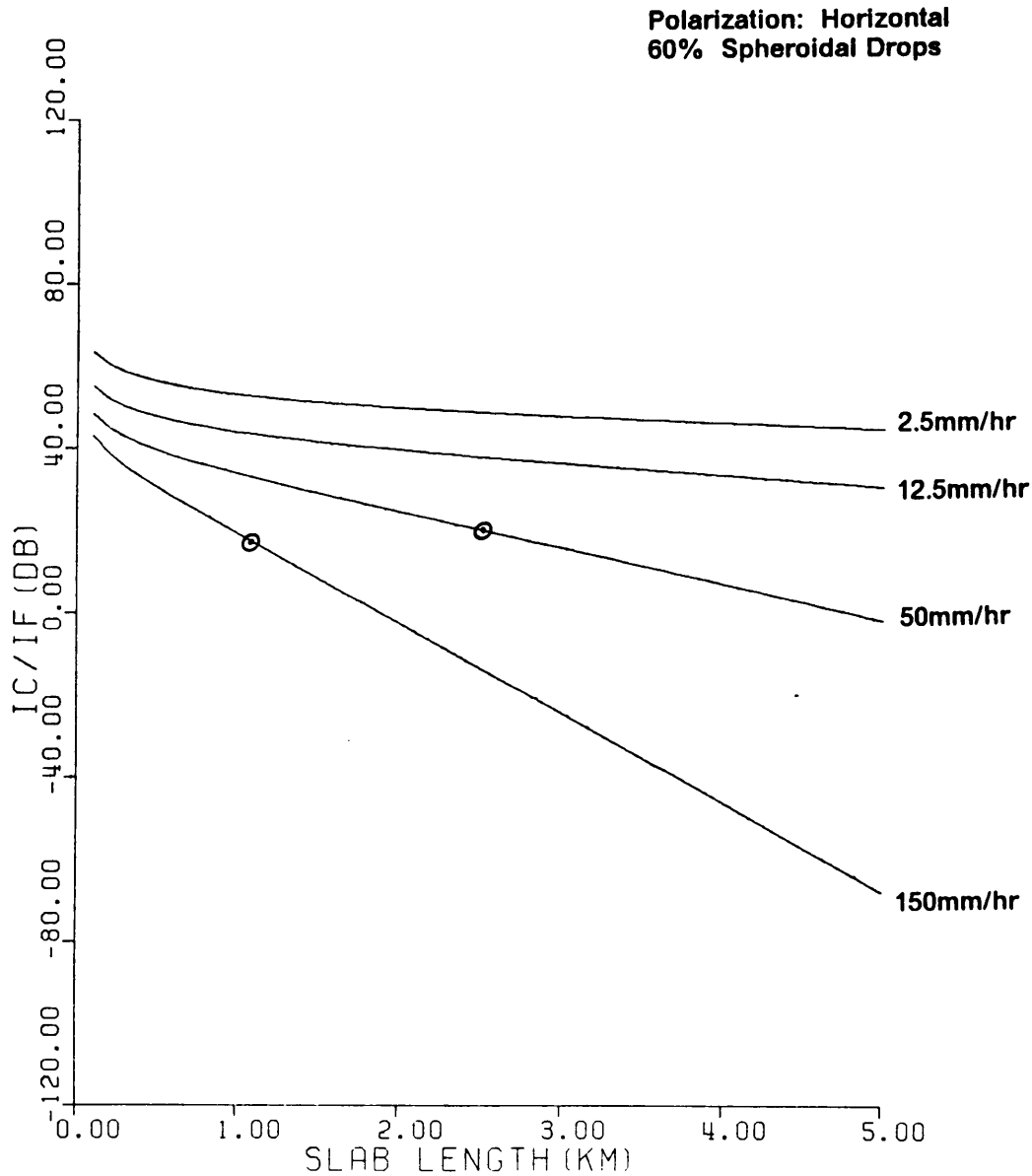

Ratio of Coherent to Incoherent Power at 45GHz and 60 = 45 dB

Figure 4.15

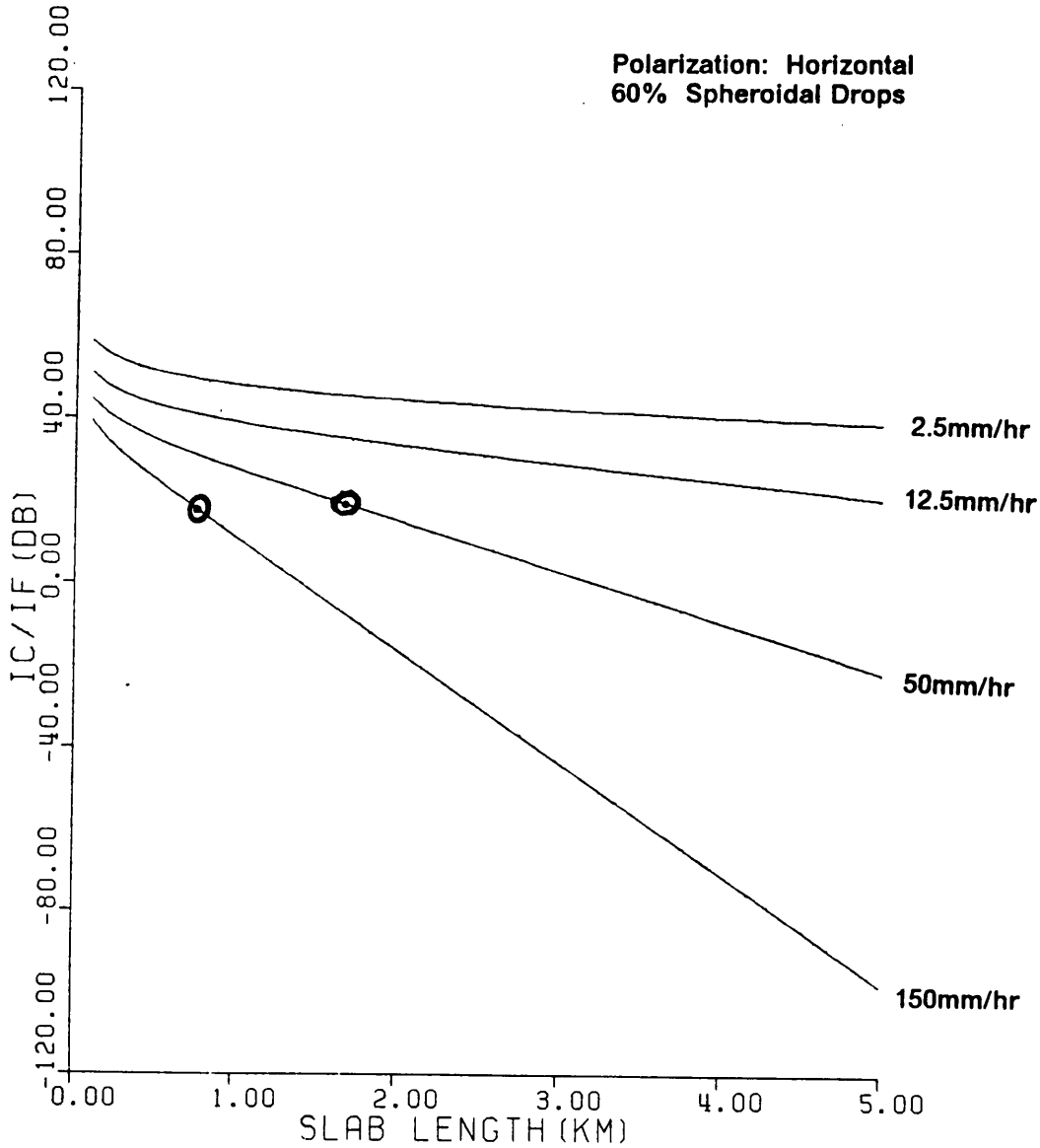

Ratio of Coherent to Incoherent Power at 70GHz and 60 = 45 dB

Figure 4.16

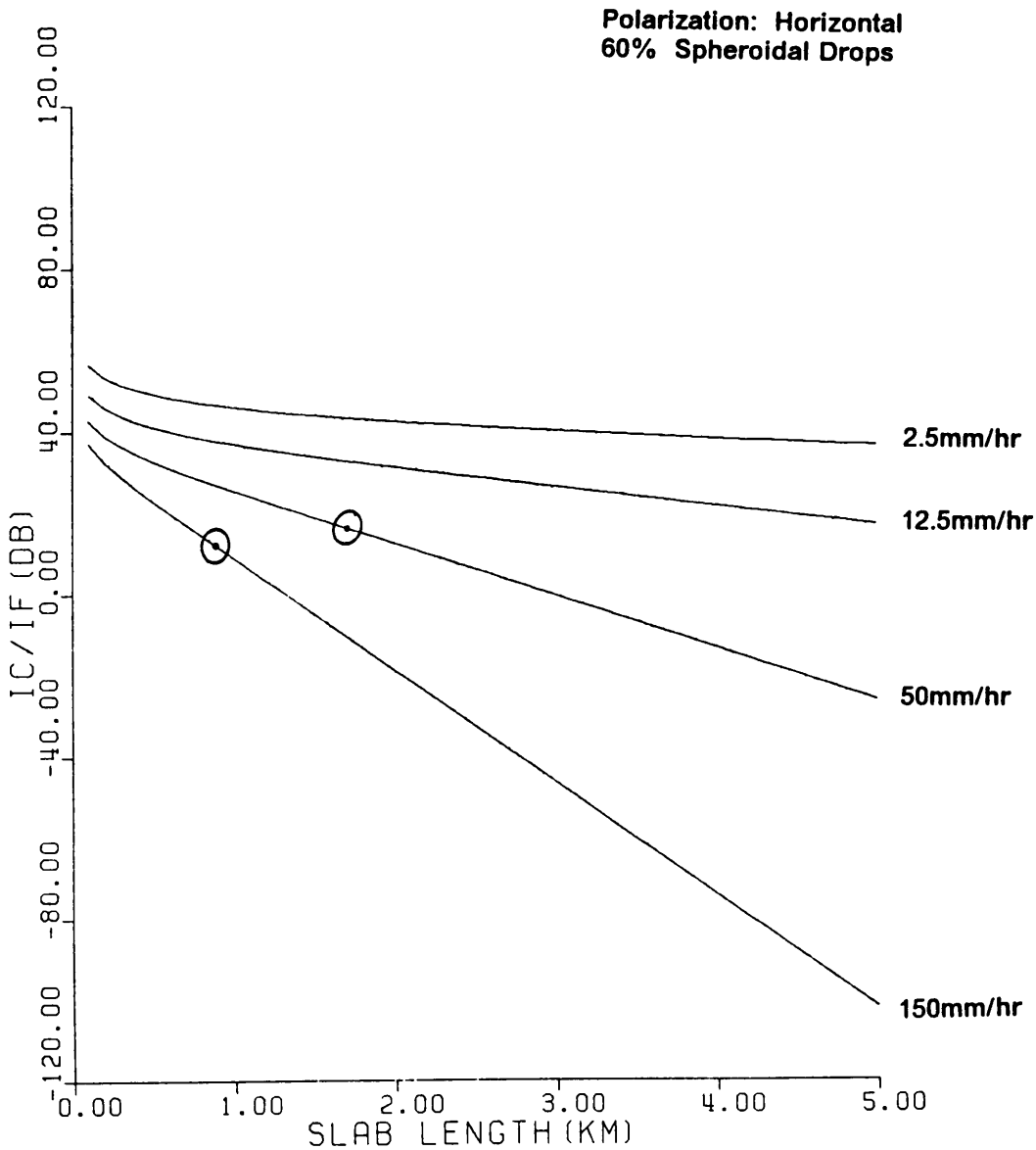

Ratio of Coherent to Incoherent Power at 90GHz and 60 = 45 dB

Figure 4.17

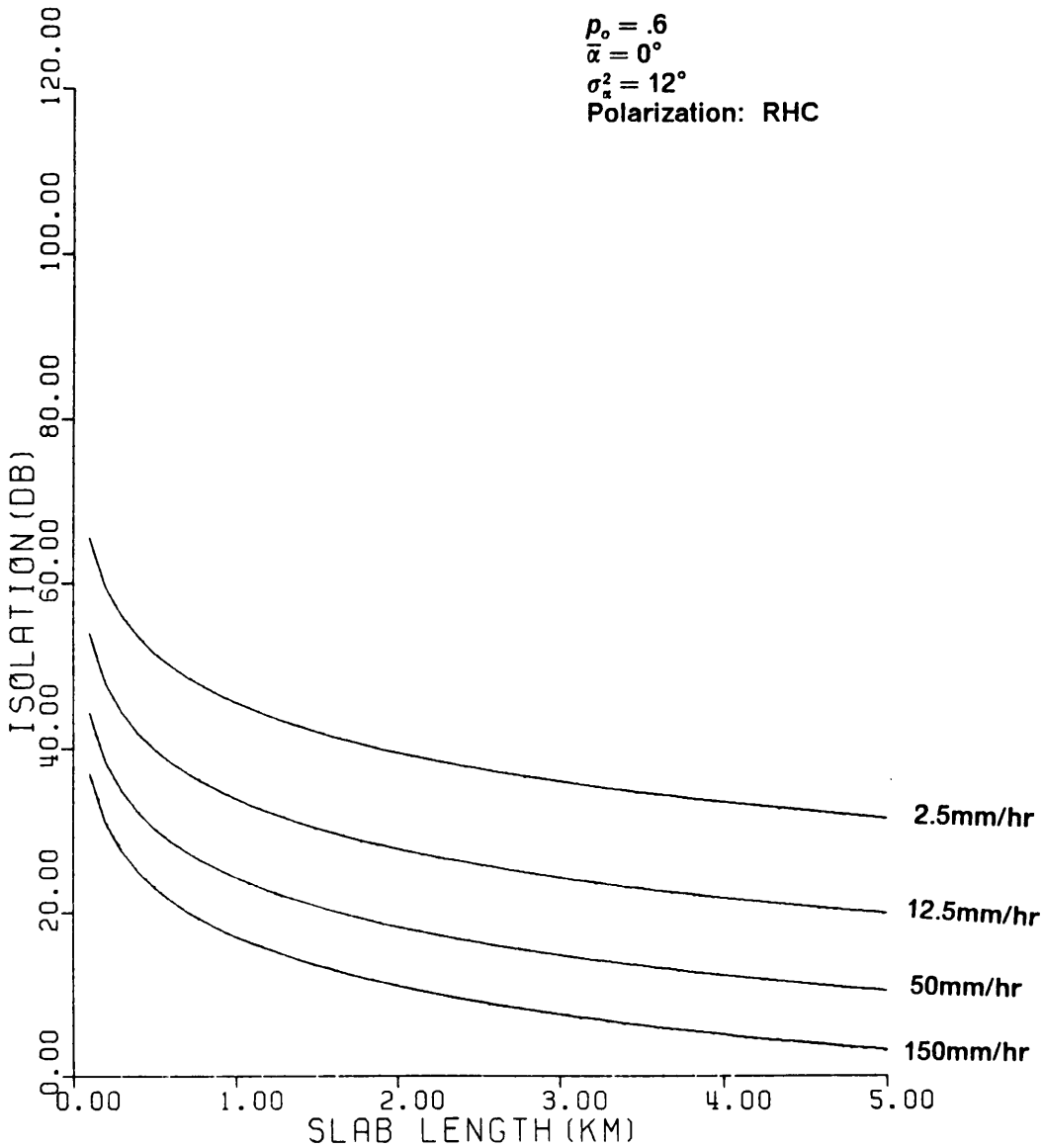
$p_o = .6$
$\bar{\alpha} = 0°$
$\sigma_\alpha^2 = 12°$
Polarization: RHC
ISOLATION (DB)
0.00
20.00
40.00
60.00
80.00
100.00
120.00
0.00
1.00
2.00
3.00
4.00
5.00
SLAB LENGTH (KM)
2.5mm/hr
12.5mm/hr
50mm/hr
150mm/hr

Frequency (GHz)	$I_c/I_r(dB)$	$\Delta(dB)$
30	16.4	1.4
45	11.9	2.6
70	8.3	4.2
90	6.8	5.3

Values of $\Delta = \left[1 - \{I_c/I_r\}^{1/2}\right]^{-1}$ for 60 = 35 dB and 50mm/hr Rain Rate (A = 40 dB)

Table 4.1

Frequency (GHz)	$I_c/I_r(dB)$	$\Delta(dB)$
30	13.7	2.0
45	9.4	3.6
70	6.2	5.8
90	4.6	7.7

Values of $\Delta = \left[1 - \{I_c/I_r\}^{1/2}\right]^{-1}$ for 60 = 35 dB and 150mm/hr Rain Rate (A = 40 dB)

Table 4.2

Frequency (GHz)	$I_c/I_r(dB)$	$\Delta(dB)$
30	21.4	.8
45	16.4	1.4
70	13.3	2.1
90	11.8	2.6

Values of $\Delta = \left[1 - \{I_c/I_r\}^{11/2}\right]^{-1}$ for 60 = 40 dB and 50mm/hr Rain Rate (A = 40 dB)

Table 4.3

Frequency (GHz)	$I_c/I_r(dB)$	$\Delta(dB)$
30	18.7	1.1
45	14.1	1.8
70	11.2	2.8
90	9.6	3.5

Values of $\Delta = \left[1 - \{I_c/I_r\}^{11/2}\right]^{-1}$ for 60 = 40 dB and 150mm/hr Rain Rate (A = 40 dB)

Table 4.4

Frequency (GHz)	$I_c/I_r(dB)$	$\Delta(dB)$
30	26.4	.4
45	21.4	.8
70	18.3	1.1
90	16.8	1.4

Values of $\Delta = \left[1 - \{I_c/I_r\}^{11/2}\right]^{-1}$ for 60 = 45 dB and 50mm/hr Rain Rate (A = 40 dB)

Table 4.5

Frequency (GHz)	$I_c/I_r(dB)$	$\Delta(dB)$
30	23.7	.6
45	19.4	1.0
70	16.2	1.5
90	14.6	1.8

Values of $\Lambda = \left[1 - \{I_c/I_r\}^{11/2}\right]^{-1}$ for 60 = 45 dB and 150mm/hr Rain Rate (A = 40 dB)

Table 4.6

Chapter 5 Conclusion

Within this treatise, we have provided a thorough analysis of the millimeter wave ram scatter problem. We began with a detailed look at scattering by an individual raindrop and developed formulae for quantifying the scattering properties of spherical and non-spherical raindrops. From there we proceded to examine both the coherent and the more difficult incoherent problems associated with the propagation of millimeter waves through randomly distributed raindrops. In studying these problems, we used analytical techniques which allowed us to study an area that researchers have generally avoided in the past: rain scatter in an antenna's near field.

As a result of our analysis, several important contributions have been made and some significant results realized. These contributions and results can be summarized as follows:

1. We have presented scattering data for non-spherical raindrops at some higher frequencies in the millimeter wave region. In addition, the code used to generate the data is appended to this dissertation and can be used to obtain data at other frequencies.
2. Inso far as the coherent aspect of the rain scatter problem is concerned, arguments about near field vs far vield scattering are pointless. Specifically, we have shown that the average output of a system for a given raincell will be identical for near and far field scattering.

3. We have provided theoretical data which gives predicted values of isolation and attenuation of the coherent signal at higher frequencies in the millimeter wave band. Also, the computer program we used to obtain the data is attached to this treatise and can be used to study other cases.

4. Our analysis of the incoherent problem associated with rain scatter has shown that for all practical purposes, near field and far field scatteing are identical. Put another way, the incoherent power at th output of a receiviner will be the same regardless of whether a given raincell is in the receiving antenna's Fraunhofer or Fresnel region.

5. We have put forth computer generated data which quantifies the relationship between the coherent and incoherent signals at a receiver's output. In analysing this data, we concluded that incoherent effects should be taken into account in the design of millimeter wave radio systems.

We now conlcude this dissertation iwth a listing of some possible research areas that are related to ours and that we feel warrent further study:

1. Application of teh Extended Boundary Condition Method in the analysis of scattering by frozen and melting huydrometeors at millimeter wave frequencies.

2. The analysis of scattering by media consistingnot only of rain by of frozen and melting hudrometeors as well.

3. Investigation of raincell models in which the properties of raindrops are not assumed to be statistically independent.

4. Statistical modeling of the amplitudes and phases of incoherent signals so that their effects on a system's performance can be more accurately portrayed.

5. Investigation of atmospheric phenomena associated with rain which can be of particular concern for systems employing very large aperture antennas. An example would be varying refractive indicies caused by termperature gradients that can accompany rain events [66]. :eol

REFERENCES

1. M. Abramowitz and I. Stegun, Editors, Handbook of Mathematical Functions, NBS Applied Mathematics Series 55, US Printing office, 1964.

2. P.W. Barber, "Resonance electromagnetic absorbtion by nonspherical dielectric objects,: IEEE Trans. on Microwave Theory and Techniques, vol. MTT-25, pp. 373-381, May 1977.

3. P.W. Barber and C. Yeh, "Scattering of electromagnetic waves by arbitrarily shaped dielectric bodies," App. Opt., vol. 14, pp. 2864-2872, Dec. 1975.

4. L. P Bayvel and A. R. Jones, Electromagnetic Scattering and its Applications, Applied Science, Lond, 1981.

5. C.M. Bender and S.A. Orszag, Advanced Mathematical Methods for Scientist and Engineers, McGraw-Hill, New York, 1978.

6. W.H. Beyer, Editor, CRC Standard Mathematical TAbles, CRC Press, Boca Raton, 1984.

7. N. Bleistein and R.A. Handelsman, Asymptotic Expansion of Integrals, Holt, Rinehart and Winston, New York, 1975.

8. M. Born and E. Wolf, Principles of Optics, Pergamon, Oxford, 1975.

9. V.N. Bringi, V.V. Varandan and V.K. Varandan, "Coherent Wave Attenuation by a random distribution of particles," Radio Science, vol. 17, pp. 946-952, Sept. - Oct 1982.

10. W.L. Brogan, Modern Control Theory, Prentice-Hall, Englewood Cliffs, NJ, 1982.

11. C. Capsoni and A. Paraboni, "Properties of the forward-scattered incoherent radiation through intense precipitiation," IEEE Trans. on Ant. and Prop., vol. AP-26, pp. 804-809, Nov. 1978.

12. R.E. Collin and F.J. Zucker, Antenna Theory, pt. 1, McGraw-Hill, New York, 1969.

13. L. Flatto, Advanced Calculus, Williams and Wilkins, Baltimore, 1976.

14. L. Foldy, "The multiple scattering of waves," Physical Review, vol. 67, pp. 107-121, Feb. 1945.

15. J.N. Franklin, Matrix Theory, Prentice-Hall, Englewood Cliffs, 1968.

16. J.W. Goodman, Introduction to Fourier Optics, McGraw-Hill, New York, 1968.

17. I.S. Gradshteyn and I.M. Ryzhik, Tables of Integrals, Series and Product, Academic Press, Orlando, Fl., 1980.

18. R.F. Harrington, Time-Harmonic Electromagnetic Fields, McGraw-Hill, New York, 1961.

19. W.H. Hayt Jr., Engineering Electromagnetics, McGraw-Hill, New York, 1967.

20. A.R. Holt, "The scattering of electromagnetic waves by single hydrometeors," Radio Science, vol. 17, pp. 929-945, Setp. - Oct. 1982.

21. A.R. Holt, N.K. Uzumoglu and B.G. Evans, "An integral equation solution of the scattering of electromagnetic radiation by dielectric spheroids and ellipsoids," IEEE Trans on Ant. and Prop., vol. AP-26, pp. 706-712, Setp. 1978.

22. A. Ishimaru, "Theory and application of wave propagation and scattering in random media," Proc. of the IEEE, vol. 65, pp. 1030 - 1060, July 1977.

23. A. Ishimaru, Wave Propagation and Scattering in Random Media Academic Press, New York, 1978.

24. A. Ishimaru, R.L-T. Cheung, "Multiple-scattering effect on radiometric determination of rain attenuation at millimeter wavelengths," Radio Science, vol. 15, pp. 507-516, May-June 1980.

25. A. Ishimaru, R.L-T. Cheung, "Multiple scattering effects on wave propagation due to rain," Ann. Telecomm, vol. 35, Nov. - Dec. 1980.

26. A. Ishimaru, D. Lesselier, C. Yeh, "Mudltiple scattering calculations for nonspherical particles based on the vector radiative transfer theory," Radio Science, vol. 19, pp. 1356-1366, Sept. - Oct. 1984.

27. A. Ishimaru and J.C. Lin, "Multiple scattering effects on wave propagationthrough rain," AGARD Confernece Proceedings, No. 107 on Telecommunications Aspects of Frequencies Between 10 and 100 GHz, pp. 1-1 to 1-13, Sept. 1972.

28. A. Ishimaru, R. Woo, J.W. Armstrong and D.C. Blackman, "Multiple scattering caluclations of rain effects," Radio Science, vol. 17, pp. 1425-1433, Nov. - Dec. 1982.

29. H. Jasik, Editor, Antenna Engineering Handbook, McGraw-Hill, New York, 1961.

30. L.W. Johnson and R.D. Riess, Numerical Analysis, Addison-Wesley, Reading, Mass., 1982

31. W. Kaplan, Operational Methods for Linear Systems, Addison-Wesley, Reading, Mass. 1962.

32. J.D. Kraus, Radio Astronomy, Cygnus-Quasar, 1986.

33. M. Lax, "Multiple Scatter of Waves," Reviews of Modern Physics, vol. 23, pp. 287-310, Oct. 1951.

34. J.A. Morrison and M.J. Cross, "Scattering of a plane electromagnetic wave by axisymetric raindrops," B.S.T.J., vol. 53, pp. 955-1019, July - Aug. 1974.

35. R.M. Morse and H. Feshback, Methods of Theoretical Physics, McGraw-Hill, New York, 1953.

36. T. Oguchi, "Attenuation of electromagnetic waves due to rain with distorted raindrops," Journal Radio Res. Lab. (Japan), Vol. 7, pp. 467-485, Setp. 1960.

37. T. Oguchi, "Attenuation of electromagnetic waves due to rain with distorted drops (Part II)," J. Radio Res. Lab. (Japan), vol. 11, pp. 19-44, Jan. 1964.

38. T. Oguchi, "Attenuation and phase rotation of radio waves due to rain: calucaltions at 19.3 and 82 GHz fro spherical raindrops," Ann. Telecomm., Nov. - Dec. 1980.

39. T. Oguchi, "Electromagnetic wave propagation and scattering in rain and other hydrometeors," Proc. of the IEEE, vol. 71, pp. 1029-1079, Sept. 1983.

40. T. Oguchi, "Effects of incoherent scattering and attenuation and depolariztaion of millimeter and optical waves due to hydrometeors," Radio Science, vol. 21, pp. 717-730, July - Aug. 1986.

41. D.T. Paris, W.M. Leach Jr. and E.B. Joy, "Basic theory of probe-compensated near-field measurements," IEEE Trans. on Ant. and Prop., vol. AP-26, pp. 373-379, May 1978.

42. T. Pratt and C.W. Bostian, Satellite Communications, John Wiley and Sons, New York, 1986.

43. Y. Rahmat-Samii, "Antenna design notes," IEEE Trans. on Ant. and Prop., vol. AP-27, pp. 571-574, July 1979.

44. P.S. Ray, "Broadband complex refactive indicies of ice and water," Apl. Opt., pp. 1836-1844, Aug. 1972.

45. D.F. Riddle, Calculus and Analytic Geometry, Wadsworth, Belmont, CA., 1970.

46. D.V. Rogers and R.L. Olsen, "Multiple scattering in coherent radiowave propagation through rain," COMSAT Tech. Rev., pp. 385-401, Fall 1983.

47. S.A. Schelkunoff, Electromagnetic Waves, D. Von Nostrand, New York, 1943.

48. S. Silver, Editor, Microwave Antenna Theory and Design, M.I.T. Radiation Laboratory Series, vol. 12, McGraw-Hill, New York, 1949.

49. J.A. Stratton, Electromagnetic Theory, McGraw-Hill, New York, 1941.

50. W.L. Stutzman, "A Review of Theoryetical Modeling of Millimeter Wave Propagation Through Precipitiation," Interim Report for NASA Cotnract NAS5-22577, VPI&SU EE Detp., May 1980.

51. P.T. Thompson, "Tabulation of the forward scattering amplutdes of spheroidal raindrops over the frequency range 2 to 30 GHz," NATO Document, 1980.

52. A.I. Tsolakis, "Multiple Scattering of Electromagnetic Waves by Distributions of Particles with Applications to Radio Wave Propagation through Precipition," Ph.D. Dissertation, Jan. 1982.

53. A.I. Tsolakis and W.L. Stutzman, "Multiple scattering of electromagnetic waves by rain," Radio Science, vol. 17, pp. 1495-1502, Nov. - Dec. 1982.

54. V. Twersky, "Multiple Scattering of Waves," J. Res. Nati. Bur. Stds. Sect. D 64, pp. 715-730, 1960.

55. V. Twersky, "On Propagtion in Random Media of Discrete Scatterers," Proc. Am. Math. Sec. Symp. on Stoch. Prc. in Math. Phys. and Eng., vol. 16, pp. 84-116, 1964.

56. V. Twersky, "Theory and Microwave Measurements of Higher Statistical Moments of Randomly Scattered Fields," Electromagnetic Scattering, (ed. by R.L. Rowell and R.S. Stein), Gordon and Breach Science Publsishers, New York, pp. 579.-695, 1967.

57. N.K. Uzunogly and B.G. Evans, "Multiple scattering effects in electromagnetic wave propagation through a medium containing precipitation," J. Phys. A: Math Gen., vol. 11, pp. 767-776, Apr. 1978.

58. H.C. van de Hulst, Light Scattering by Small Particles, John Wiley, New York, 1957.

59. P.M. van den Berg and J.T. Fokkema, "The Rayleigh hypothesis in the theory and diffraction by a cylindrical obstacle," IEEE Trans. on Ant. and Prop., vol. AP-27, pp. 577-583, May 1979.

60. V.V. Varadan and V.K. Varadan, "Multiple scattering of electromagnetic waves by randomly distributed and oriented dielectric scatterers," Phys. Rev. D., vol. 21, pp. 388-394, Jan. 1980.

61. W.J. Vogel, J.H. Davis and C.E. Mayer, "Line of sight observations at 86 GHz with a very large and small antenna," IEEE Trans. on Ant. and Prop., vol. AP-32, pp. 113-118, Feb. 1984.

62. C. Warner and A. Hizal, "Scattering and depolarization of microwaves by spheroidal riandrops, Radio Science, vol. 11, pp. 921-930, Nov. 1976.

63. P.C. Waterman, Proc. IEEE, vol. 53, p. 805, 1965.

64. P.C. Waterman, "Symmetry, Unitarity and geometry in electromagnetic scattering," Phys. Rev. D, vol. 3, pp. 825-836, Feb. 1971.

Appendix A

Spherical Mode Expansions for Plane Waves

In this appendix, we seek vector spherical harmonic expandions of the plane waves

$$\vec{E}_1 = (\cos\alpha\hat{x} - \sin\alpha\hat{z})\exp[-jk_0(x\sin\alpha + z\cos\alpha)] \tag{A.1}$$

$$\vec{E}_2 = \hat{y}\exp[-jk_0(x\sin\alpha + z\cos\alpha)] \tag{A.2}$$

Let $\vec{E}_2$ and $\vec{E}_{12}$ be defined by

$$\vec{E}_{1x} = \hat{x}\exp[-jk_0(x\sin\alpha + z\cos\alpha)] \tag{A.3}$$

$$\vec{E}_{1z} = \hat{z}\exp[-jk_0(x\sin\alpha + z\cos\alpha)] \tag{A.4}$$

So that

$$\vec{E}_1 = \cos\alpha\vec{E}_{1x} - \sin\alpha\vec{E}_{1z} \tag{A.5}$$

We assume expansions of the form

$$\vec{E} = \sum_{\nu}\sum_{\ell=1}^{\infty}\sum_{m=o}^{\ell}\left[E_{\nu\ell m}\vec{M}^{(1)}_{\nu\ell m}(k_0 r) + \eta_{\nu\ell m}\vec{N}^{(1)}_{\nu}\ell m(k_0 r)\right] \tag{A.6}$$

Where $\vec{E} = \vec{E}_{1x}, \vec{E}_{1z}$ or $\vec{E}_2$; $\nu = e$ or 0

$$\vec{M}^{e}_{o\ell m}(kr) = \mp z_\ell(kr)p^m_\ell(\cos\theta)\frac{\sin}{\sin\theta}_{\cos} m\phi\hat{\theta} - z_\ell(kr)\frac{d}{d}\theta P^m_\ell(\cos\theta)^{\cos}_{\sin} m\phi\hat{\theta} \tag{A.7}$$

$$\begin{aligned}\vec{N}e_{\ell om}(kr) = {} & \ell(\ell+1)z_\ell\frac{(kr)}{kr}P^m_\ell(\cos\theta)^{\cos}_{\sin} m\phi\hat{r} \\ & + \frac{1}{kr}\frac{\dot{\partial}}{\partial}r\ [rZ_\ell(kr)]\frac{d}{d}\theta P^m_\ell(\cos\theta)^{\cos}_{\sin} m\phi\hat{\theta} \\ & \mp \frac{1}{kr}\frac{\partial}{\partial}r[rZ_\ell(kr)] \mp^m_\ell\frac{(\cos\theta)}{\sin}\theta^{\sin}_{\cos} m\phi\hat{\phi}\end{aligned} \tag{A.8}$$

and the (1) superscript indicates $z_\ell = j_\ell$

Using orthogonality relationships for the trigonometric and associated Legendre functions [16], the unknown coefficients ξ and η in (A.6) are found to be

$$\xi_{\nu}\ell m = \varepsilon_m \pi 2 \frac{\ell+1}{\ell(\ell+1)} \frac{(\ell+m)!}{(\ell-m)!} \frac{1}{j_{\ell}^2(k_0 r)} \int_o^{2\pi}\int_o^{\pi} \vec{E} \cdot \vec{M}_{\nu\ell}^{(1)} m(k_0 r) \sin\theta d\theta d\phi \qquad (A.9)$$

$$\eta_{\nu\ell m} = \varepsilon_m \pi \frac{(2\ell+1)^2}{\ell(\ell+1)} \frac{(\ell+m)!}{(\ell-m)!} \left[(\ell+1) j_{\ell-1}^2(k_0 r) + \ell j_{\ell+1}^2(k_0 r\right]^{-1} \qquad (A.10)$$

$$x \int_o^{2\pi}\int_o^{\pi} \vec{E} \cdot \vec{N}^{(1)}{}_{\nu}\ell m(k_0 r) \sin\theta d\theta d\phi$$

with $\varepsilon_M = 1$ when $m = o$ and $\varepsilon_m = 2$ when $m > o$.

Consider then the integrals

$$I_{1_o^e} = \int_o^{2\pi}\int_o^{\pi} \vec{E} \cdot \vec{M}_{o}^{(1)\ell m}(k_0 r) \sin\theta d\theta d\phi \qquad (A.11)$$

$$I_{2_o^e} = \int_o^{2\pi}\int_o^{\pi} \vec{E} \cdot \vec{N}_{o}^{(1)\ell m}(k_0 r) \sin\theta d\theta d\phi \qquad (A.12)$$

for $\vec{E} = \vec{E}_{1x}$. Converting $\vec{E}$1x spherical coordinates and substituting (A.7) into (A.11) yeilds

$$I_{1_o^e} = j(k_0 r) \int_o^{2\pi}\int_o^{\pi} \left[\mp m \frac{P_{\ell}^m}{\sin\theta} \cos\theta \begin{matrix}\sin\\ \cos\end{matrix} m\phi \sin\phi + \frac{d}{d\theta} P_{\ell}^m(\cos\theta) \begin{matrix}\cos\\ \sin\end{matrix} m\phi \sin\phi \right] \qquad (A.13)$$
$$x \exp\left[-jk_0 r(\sin\alpha \sin\theta \cos\phi + \sin\theta \sin\alpha)\right] x \sin\theta d\theta d\phi$$

The multiple intplex integralin (A.13) can be evaluated. To do so we first use the trigonometric identities [6]

$$\begin{matrix}\sin\\ \cos\end{matrix} m\phi \cos\phi = \frac{1}{2}\left[\begin{matrix}\sin\\ \cos\end{matrix}(m+1)\phi - \begin{matrix}\sin\\ \cos\end{matrix}(m-1)\phi\right] \tag{A.14a}$$

$$\begin{matrix}\sin\\ \cos\end{matrix} m\phi \sin\phi = \frac{1}{2}\left[\mp\begin{matrix}\sin\\ \cos\end{matrix}(m+1)\phi \mp \begin{matrix}\cos\\ \sin\end{matrix}(m-1)\phi\right] \tag{A.14b}$$

and the recurrence relations [50]

$$\cos\theta m\frac{P_\ell^m}{\sin\theta} = \frac{1}{2}\left[P_\ell^{m+1}(\cos\theta) + (\ell+m)(\ell-m+1)P_\ell^{m-1}(\cos\theta)\right] \tag{A.15a}$$

$$\frac{d}{d}\theta P_\ell^m(\cos\theta) = \frac{1}{2}\left[(\ell+m)(\ell-m+1)P_\ell^{m-1}(\cos\theta)\right] \tag{A.15b}$$

to recast (A.13) as

$$I_{1_o^e} = \mp\frac{j\ell(k_0 r)}{2}\int_o^{2\pi}\int_o^{\pi}\left[(\ell+m)(\ell-m+1)P_\ell^{m-1}(\cos\theta)\begin{matrix}\sin\\ \cos\end{matrix}(m-1)\phi\right. \tag{A.16}$$

$$\left. + P_\ell^m(\cos\theta)\begin{matrix}\cos\\ \sin\end{matrix}(m+1)\phi\right] x \exp\left[-jk_0 r(\sin\alpha\sin\theta\cos\phi + \sin\theta\sin\alpha)\right]$$

$$x \sin\theta d\theta d\phi$$

The integrals in (A.16) can be evaluated using the identity [16]

$$\int_0^{2\pi}\int_0^{\pi} P_\ell^m(\cos\theta)\begin{matrix}\sin\\ \cos\end{matrix} m\phi \exp\{-jkr[\sin\alpha\sin\theta\cos(\phi-\beta) + \cos\alpha\cos\theta]\} \tag{A.17}$$

$$x \sin\theta d\theta d\phi = 4\pi j^{-\ell} j_\ell(kr) P_\ell^m(\cos\alpha) \begin{matrix}\sin \\ \cos\end{matrix} m\beta$$

We then obtain

$$I_{1e} = 0 \tag{A.18a}$$

$$I_{1o} = 4\pi j^{-\ell} j_\ell^{-2}(k_0 r) \frac{m \cos\alpha P_\ell^m(\cos\alpha)}{\sin\alpha} \tag{A.18b}$$

Consider now $I_2^{\begin{matrix}e\\o\end{matrix}}$ for $\vec{E} = \vec{E}_{/1x}$. Converting $\vec{E}_{1x}$ to spherical coordinates and expressing $\vec{N}$ by (A.8), (A.12) becomes

$$I_{2_o^e} = \int_0^{2\pi}\int_o^{\pi}\left\{\ell(\ell+1)j_\ell(k_0r)\frac{}{k_0r}\sin\theta P_\ell^m(\cos\theta)\begin{matrix}\cos\\ \sin\end{matrix} m\pi\cos\pi \right. \tag{A.19}$$

$$+\frac{1}{k_0}r\frac{\partial}{\partial r}[Rj_\ell(k_0r)]\cos\theta\frac{d}{d}\theta P_\ell^m(\cos\theta)\begin{matrix}\cos\\ \sin\end{matrix} m\phi\cos\phi]$$

$$\mp\frac{i}{k_0r}\frac{\partial}{\partial r}[Rj_\ell(k_0r)]\frac{mP_\ell^m(\cos\theta)}{\sin\theta}\begin{matrix}\sin\\ \cos\end{matrix} m\phi\sin\phi\{$$

$$x\exp[-jk_0r(\sin\alpha\sin\theta\cos\phi+\cos\alpha\cos\phi)]\sin\theta d\theta d\phi$$

We now make use of the trigonometric identities of (A.15) and the recurrence relations in (A.16) and note that [17]

$$\frac{J_\ell(\delta)}{\delta} = \frac{1}{2\ell+1}[j_{\ell-1}(\delta)+j_{\ell+1}(\delta)] \tag{A.20a}$$

$$\frac{d}{d\delta}J_{\ell(\delta)} = \frac{i}{2}\ell+1[\ell j_{\ell-1}(\delta)-(\ell+1)j_{\ell+1}(\delta)righr] \tag{A.20b}$$

Then, after some algebra, (A.19) can be rewritten as

$$I_{2_o^e} = \frac{1}{2(2\ell+1)}\int_o^{2\pi}\int_o^{\pi}\left\{(l+1)j_\ell-1(k_0r)\left[(\ell+m)(\ell+m-1)P_{\ell-1}^{m-1}(\cos\theta)\begin{matrix}\cos\\ \sin\end{matrix}(m-1)\phi\right.\right. \tag{A.21}$$

$$+\ell j_{\ell+1}(k_0r)\left[P_{\ell+1}^{m+1}(\cos\theta)\begin{matrix}\cos\\ \sin\end{matrix}(m+1)\phi-(\ell-m+1)(\ell-m+2)P_{(\ell+1}^{m-1}(\cos\theta)\begin{matrix}\cos\\ \sin\end{matrix}(m-1)\phi\right]$$

$$x\exp[-jk_0r(\sin\alpha\sin\theta\cos\phi+\cos\alpha\cos\theta)]\sin\theta d\theta d\phi$$

Using then (A.17) to evaluate the intplex integralin (A.21) yields

$$I_{2e} = \frac{4\pi j^{-}(\ell-1)}{2}(2\ell+1)\Big\{(\ell+1)j^2_{\ell-1}(k_0r) \tag{A.22a}$$

$$\Big[(\ell+m)x(\ell+m-1)P^{m-1}_{\ell-1}(\cos\alpha) - P^{m+1}_{\ell-1}(\cos\alpha)\Big]$$

$$+\ell j^2_{\ell+1}(k_0r)\Big[(\ell-m+1)(\ell-m+2)P^{m-1}_{\ell+1}(\cos\alpha) - P^{m+1}_{\ell+1}(\cos\alpha)\Big]$$

$$I_{20} = 0 \tag{A.22b}$$

By using (A.16), the expression for I_{2e} can also be written as

$$I_{2e} = 4\pi\frac{j^{-(\ell-1)}}{2\ell+1}\Big\{(\cos\alpha)\frac{d}{d\alpha}P^m_\ell(\cos\alpha)\Big[(\ell+1)j^2_{\ell-1}(k_0r) + \ell j^2_{\ell+1}(k_0r)\Big] \tag{A.23}$$

$$+\ell(\ell+1)(\sin\alpha)P^m_\ell(\cos\alpha)\Big[j^2_{\ell-1)}(k_0r) - j^2_{\ell+1}(k_0r)\Big]\Big\}$$

Thus, with (A.6), (A.9) through (A.12), (A.18), (A.22) and (A.23) we find the modal expansion of $\vec{E}_{1x}$ to be

$$\vec{E}_{1x} = \sum_{\ell=1}^{\infty}\sum_{m=0}^{\ell}\Big[\xi^x_{\ell m}\vec{M}^{(1)}_{o_e m}(k_0r) + \eta^x_{\ell m}\vec{N}^{(1)}_{e_e m}(k_0r)\Big] \tag{A.24a}$$

with

$$\xi^x_{\ell m} = \varepsilon_m j^{-}\ell\frac{2\ell+1}{\ell(\ell+1)}\frac{(\ell-m)!}{(\ell+m)!}\quad\frac{M\cos\alpha P^m_\ell(\cos\alpha)}{\sin\alpha} \tag{A.24b}$$

$$\eta^x_{\ell m} = \varepsilon m j^{-(\ell-1)}\frac{(2\ell+1}{\ell}(\ell+1)\frac{\ell-m)!}{(\ell+m)!}\quad\cos\alpha\frac{d}{d}\alpha\ P^m_\ell(\cos\alpha) + Q\sin\alpha\ P^m_\ell(\cos\alpha) \tag{A.24c}$$

and

$$Q = \varepsilon_m j^{-(\ell-1)}(2\ell+1)\&lit.-m)!\overline{M}\ell+m)!$$

$$x\left[\frac{(\ell+1)j^2_{\ell-1}(k_0r)+\ell j^2_{\ell-1}(k_0r)}{j^2_{\ell-1}(k_0r)-j^2_{\ell+1}(k_0r)}\right] \qquad (A.24d)$$

Similarly it is found that

$$\vec{E}_{1z}=\sum_{\ell-1}^{\infty}\sum_{m}=o\infty\left[\varepsilon^z_{\ell m}\vec{M}^{(1)}_{o\ell m(k_0)}+\eta^z_{\ell m}\vec{N}^{(1)}_{e\ell m(k_0r)}\right] \qquad (A.25a)$$

with

$$\varepsilon^z_{\ell m}=-\varepsilon_m j^{-\ell}\frac{(2\ell+1)}{\ell(\ell+1)}\ \frac{(\ell-m)!}{(\ell+m)!}mP^m_\ell(\cos\alpha) \qquad (A.25b)$$

$$\eta^z_{\ell m}=-\varepsilon mj^{-(\ell-1)}\frac{(2\ell+1)}{\ell(\ell+1)}\ \frac{(\ell-m)!}{(\ell+m)!}\ \sin\alpha\ \frac{d}{d\alpha}\ mP^m_\ell(\cos\alpha) \qquad (A.25c)$$

and that

$$\vec{E}_2=\sum fro\ell-1o\infty\ \sum_m=o\ell\ \left[\varepsilon^{(2)}_\ell m\vec{M}^{(1)}{}_o\ell m(k_0r+\eta^{(2)}_\ell m\bar{}\, n^{(1)}_{e\ell m}(k_0r)\right] \qquad (A.26a)$$

with

$$\varepsilon^{(2)}_\ell m=\varepsilon mj^{-}\ell\ \frac{(2\ell+1)}{\ell(\ell+1)}\ \frac{(\ell-m)!}{(\ell+m)!}\ \frac{d}{d}\alpha\ P^m_\ell(\cos\alpha) \qquad (A.26b)$$

$$\eta^{(2)}_\ell m=\varepsilon mj^{-}(\ell-1)\ \frac{(2\ell+1)}{\ell(\ell+1)}\ \frac{(\ell-m)!}{(\ell+m)!}\ mP^m_\ell\ \frac{(\cos\alpha)}{\sin}\alpha \qquad (A.26c)$$

Substituting now (A.24) and (A.25) into (A.5), we find the spherical hormonic expandion of $\vec{E}_1$ is

$$\vec{E}_1 = \sum_{\ell-1}^{\infty} \sum_{m} = o\ell \left[\varepsilon_\ell^{(1)} m \vec{M}^{(1)}{}_o \ell m(k_0 r + \eta_\ell^{(1)} m \vec{n}_{e\ell m}^{(1)}(k_0 r) \right] \tag{A.27a}$$

where

$$\varepsilon_\ell^{(2)} m = \varepsilon m j^{-} \ell \quad \frac{(2\ell+1)}{\ell(\ell+1)} \quad \frac{(\ell-m)!}{(\ell+m)!} \quad m P_\ell^m \quad \frac{(\cos\alpha)}{\sin}\alpha \tag{A.27b}$$

$$\eta_\ell^{(2)} m = \varepsilon m j^{-}(\ell-1) \quad \frac{(2\ell+1)}{\ell(\ell+1)} \quad \frac{(\ell-m)!}{(\ell-m)!} \quad \frac{d}{d}\alpha \quad P_\ell^m(\cos\alpha) \tag{A.27c}$$

We note that at =0 [16]

$$m P_\ell^m \frac{(\cos\alpha)}{\sin}\alpha = \frac{d}{d}\alpha \quad P_\ell^m(\cos\alpha) = \begin{cases} 0, m \neq 1 \\ \frac{1}{2}\ell(\ell+1), m = 1 \end{cases} \tag{A.28}$$

$\vec{E}_1$ then reduces to

$$\vec{E}_1 = \hat{x} e^{-j} Ksubo Z = \sum^{\infty} j^{-l} \ell = 1 \frac{2\ell+1}{\ell(\ell+1)} \left[\vec{M}_o^{(1)} \ell 1(k_0 r) + j \vec{N}_o^{(1)} \ell 1(k_0 r) \right] \tag{A.29}$$

Appendix B

Mie Theory Program

The Mie theory program compiles the forward scattering amplitudes and scattering cross sections of spherical scatterers having radii .025 through .35cm in steps of .025cm. The contents of this Appendix are a flow chart of the program and descriptions of the subprograms used, the program listing and output for frequencies of 30, 45, 70 and 90 GHz.

B.1 Program Flow Chart and Descriptions of Subprograms

The flow chart for the Mie Theory program is shown in given in Figure B.1. The subprograms used are as follows:

(1)!FUNCTION SBEST (X,N): Computes the spherical Bessel function *jsunn*(x) with x real using backward recursion.

(2) FUNCTION SBSST (X,N): Computes the spherical Bessel function $j_n(x)$ with x real from its Taylor series [17]. Values obtained are used as starting points for backward recursion in SBEST.

(3) FUNCTION CBESJ (Y, N): Computes the spherical Bessel function $j_n(y)$, y complex, using backward recursion.

(4) FUNCTION CBESST (Y, N): Computes the spherical Bessel function $j_n(y)$, y complex, from its Taylor series. Values are used to begin backward recursion in CBESJ.

(5) FUNCTION SBESY (X, N): Computes the spherical Bessel function $Y_N(x)$, x real, using forward recursion.

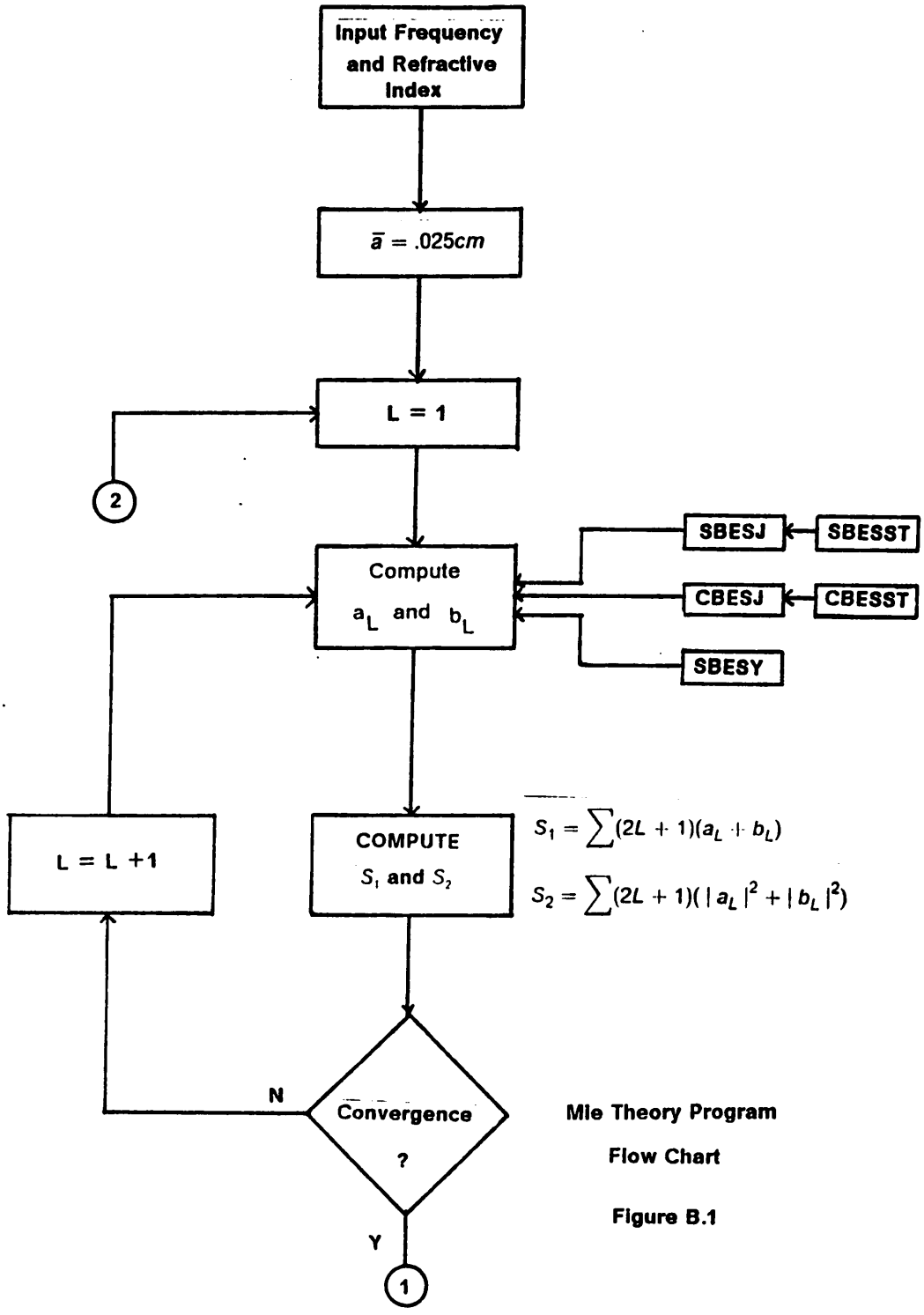

Mie Theory Program

Flow Chart

Figure B.1

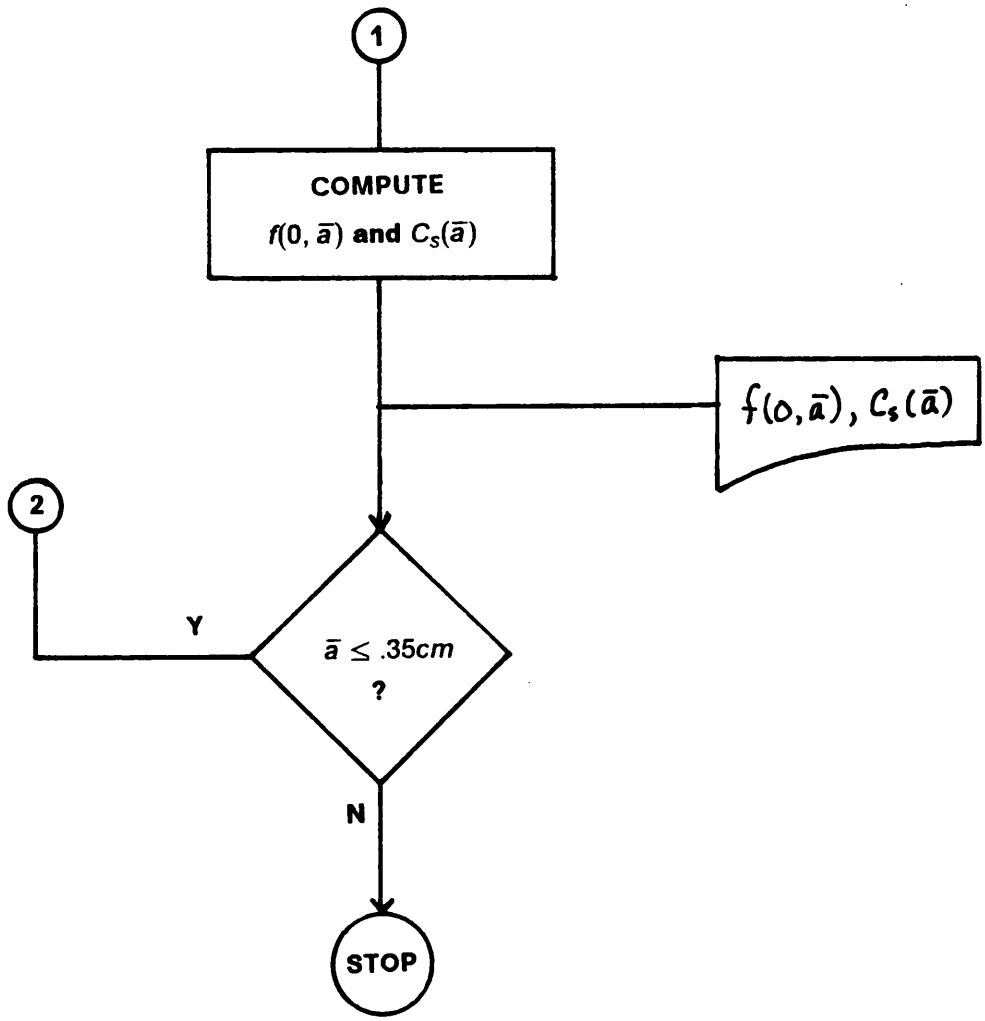

Flow Chart for Mie Theory Program (Cont'd)

Figure B.1

```
C****** SCATTERING PARAMETERS - SPHERICAL RAINDROPS ***************
C                                                                  *
C    THIS PROGRAM COMPUTES SCATTERING PARAMETERS FOR SPHERICAL     *
C  RAINDROPS USING THE MIE THEORY.  THE PARAMETERS COMPUTED ARE    *
C  THE FORWARD SCATTERING AMPLITUDE AND THE SCATTERING CROSS       *
C  SECTION COMPUTATIONS ARE MADE FOR DROP RADII OF .025(.025).350  *
C  CM.                                                             *
C                                                                  *
C    USER INPUTS TO THE PROGRAM ARE:                               *
C                                                                  *
C            FREQ= FREQUENCY OF OPERATION IN GHZ.                  *
C                                                                  *
C            RIRE(RIIM)= REAL(IMAG) PART OF THE REFRACTIVE         *
C                        INDEX OF WATER AT THE FREQUENCY AND       *
C                        TEMPERATURE OF INTEREST.                  *
C******************************************************************

      COMPLEX IMAG,RI,FFOR,Y,HX,GY,JY
      COMPLEX CBESJ,Q1,Q2,Q3,Q4,AL,BL
      REAL K0,JX

C  INPUT DATA.

      IMAG=(0.,1.)
      PI=3.1415927
   66 CONTINUE
      READ(5,*,END=500)FREQ,RIRE,RIIM
      WRITE(6,100)FREQ,RIRE,RIIM
      RI=CMPLX(RIRE,RIIM)
      K0=2.*PI*FREQ/30.
      RAD=.025
  608 X=K0*RAD
      Y=X*RI

C  COMPUTE MIE COEFFICIENTS AL AND BL.

      FFOR=(0.,0.)
      SCRS=0.
      SCRS0=0.
      L=1
   70 TLP1=2*L+1
      JX=SBESJ(X,L)
      JY=CBESJ(Y,L)
      GX=((L+1)*SBESJ(X,L-1)-L*SBESJ(X,L+1))/TLP1
      GY=((L+1)*CBESJ(Y,L-1)-L*CBESJ(Y,L+1))/TLP1
      Q1=JX*GY
      Q2=GX*JY
      Q3=JY*CMPLX(GX,-((L+1)*SBESY(X,L-1)-L*SBESY(X,L+1))/TLP1)
      Q4=GY*CMPLX(JX,-1.*SBESY(X,L))
      AL=(RI*Q1-Q2)/(Q3-RI*Q4)
      BL=(RI*Q2-Q1)/(Q4-RI*Q3)

C  COMPUTE SCATTERING PARAMETERS AND CHECK FOR CONVERGENCE.

      FFOR=FFOR+TLP1*(AL+BL)
```

```
      SCRS=SCRS+TLP1*(CABS(AL)**2+CABS(BL)**2)
      IF(ABS((SCRS-SCRS0)/SCRS).GT.1.0E-05) THEN
         L=L+1
         SCRS0=SCRS
         GO TO 70
      ENDIF
      FFOR=IMAG*FFOR/(2.*K0)
      FR=REAL(FFOR)
      FI=AIMAG(FFOR)
      SCRS=2.*PI*SCRS/K0**2
      WRITE(6,101)RAD,FR,FI,SCRS
      RAD=RAD+.025
      IF(RAD.LE.(.350)) GO TO 608
      WRITE(6,102)
      GO TO 66
  100 FORMAT(1X,'FREQUENCY=',F5.1,' GHZ',/,1X,
     &'REFRACTIVE INDEX= (',F6.4,',',F7.4,')',//,1X,'RADIUS',
     &12X,'F(0)',16X,'SCRS',/,2X,'(CM)',13X,'(CM)',15X,'(CMSQ)')
  101 FORMAT(2X,F4.3,3X,'(',E10.4,',',E11.4,')',3X,E10.4)
  102 FORMAT(1X,46('*'),/)
  500 STOP
      END



      FUNCTION SBESJ(X,N)
      Z=SIN(X)/X
      IF(N.EQ.0) THEN
         SBESJ=Z
         RETURN
      ENDIF
      IF(ABS(.5*X*X/FLOAT(2*N+3)).LT.1.0) THEN
         SBESJ=SBESST(X,N)
         RETURN
      ENDIF
      M=X+10.
      IF(M.LE.N) M=N+5
      Q2=SBESST(X,M+1)
      Q1=SBESST(X,M)
      MM=M
      DO 1 I=1,M
      IF(MM.EQ.N) QN=Q0
      Q0=(2*MM+1)*Q1/X-Q2
      Q2=Q1
      Q1=Q0
    1 MM=MM-1
      SBESJ=Z*QN/Q0
      RETURN
      END



      FUNCTION SBESST(X,N)
```

```
      F=1.
      DO 1 I=1,N
    1 F=F*X/FLOAT(2*I+1)
      K1=1
      K2=2*N+3
      Z=-.5*X*X
      Q1=1.
      Q2=Z/FLOAT(K2)
    2 Q1=Q1+Q2
      IF(ABS(Q2).GT.1.0E-09) THEN
         K1=K1+1
         K2=K2+2
         Q2=Q2*Z/FLOAT(K1*K2)
         GO TO 2
      ENDIF
      SBESST=F*Q1
      RETURN
      END



      COMPLEX FUNCTION CBESJ(Y,N)
      COMPLEX Y,Z,Q0,Q1,Q2,QN,CBESST
      Z=CSIN(Y)/Y
      IF(N.EQ.0) THEN
         CBESJ=Z
         RETURN
      ENDIF
      IF(CABS(.5*Y*Y/FLOAT(2*N+3)).LT.1.0) THEN
         CBESJ=CBESST(Y,N)
         RETURN
      ENDIF
      M=CABS(Y)+10.
      IF(M.LE.N) M=N+5
      Q2=CBESST(Y,M+1)
      Q1=CBESST(Y,M)
      MM=M
      DO 1 I=1,M
      IF(MM.EQ.N) QN=Q0
      Q0=(2*MM+1)*Q1/Y-Q2
      Q2=Q1
      Q1=Q0
    1 MM=MM-1
      CBESJ=Z*QN/Q0
      RETURN
      END



      COMPLEX FUNCTION CBESST(Y,N)
      COMPLEX Y,Z,F,Q1,Q2
      F=(1.,0.)
      DO 1 I=1,N
```

```
1 F=F*Y/FLOAT(2*I+1)
  K1=1
  K2=2*N+3
  Z=-.5*Y*Y
  Q1=(1.,0.)
  Q2=Z/FLOAT(K2)
2 Q1=Q1+Q2
  IF(CABS(Q2).GT.1.0E-09) THEN
     K1=K1+1
     K2=K2+2
     Q2=Q2*Z/FLOAT(K1*K2)
     GO TO 2
  ENDIF
  CBESST=F*Q1
  RETURN
  END



  FUNCTION SBESY(X,N)
  Z0=-1.*COS(X)/X
  IF(N.EQ.0) THEN
     SBESY=Z0
     RETURN
  ENDIF
  Z1=Z0/X-SIN(X)/X
  IF(N.EQ.1) THEN
     SBESY=Z1
     RETURN
  ENDIF
  DO 1 I=2,N
  NN=I-1
  SBESY=(2*NN+1)*Z1/X-Z0
  Z0=Z1
1 Z1=SBESY
  RETURN
  END
```

FREQUENCY= 30.0 GHZ
REFRACTIVE INDEX= (5.5810,-2.8482)

RADIUS (CM)	F(0) (CM)	SCRS (CMSQ)
.025	(0.6082E-03,-0.5658E-04)	0.2998E-05
.050	(0.5167E-02,-0.1161E-02)	0.2125E-03
.075	(0.1624E-01,-0.7731E-02)	0.2886E-02
.100	(0.3319E-01,-0.2391E-01)	0.1739E-01
.125	(0.5065E-01,-0.5659E-01)	0.5632E-01
.150	(0.5688E-01,-0.1011E+00)	0.1172E+00
.175	(0.5184E-01,-0.1446E+00)	0.1804E+00
.200	(0.4674E-01,-0.1821E+00)	0.2340E+00
.225	(0.4898E-01,-0.2207E+00)	0.2858E+00
.250	(0.5666E-01,-0.2683E+00)	0.3481E+00
.275	(0.6272E-01,-0.3272E+00)	0.4275E+00
.300	(0.6217E-01,-0.3924E+00)	0.5193E+00
.325	(0.5709E-01,-0.4578E+00)	0.6137E+00
.350	(0.5327E-01,-0.5225E+00)	0.7068E+00

****

FREQUENCY= 45.0 GHZ
REFRACTIVE INDEX= (4.6241,-2.6437)

RADIUS (CM)	F(0) (CM)	SCRS (CMSQ)
.025	(0.1380E-02,-0.2101E-03)	0.1542E-04
.050	(0.1132E-01,-0.4679E-02)	0.1206E-02
.075	(0.3034E-01,-0.2681E-01)	0.1495E-01
.100	(0.3776E-01,-0.7094E-01)	0.5224E-01
.125	(0.3196E-01,-0.1120E+00)	0.9059E-01
.150	(0.3291E-01,-0.1512E+00)	0.1247E+00
.175	(0.4026E-01,-0.2038E+00)	0.1689E+00
.200	(0.4023E-01,-0.2691E+00)	0.2274E+00
.225	(0.3488E-01,-0.3348E+00)	0.2885E+00
.250	(0.3449E-01,-0.4036E+00)	0.3507E+00
.275	(0.3642E-01,-0.4840E+00)	0.4225E+00
.300	(0.3308E-01,-0.5732E+00)	0.5045E+00
.325	(0.2748E-01,-0.6647E+00)	0.5901E+00
.350	(0.2524E-01,-0.7613E+00)	0.6792E+00

****

FREQUENCY= 70.0 GHZ
REFRACTIVE INDEX= (3.7873,-2.2394)

RADIUS (CM)	F(0) (CM)	SCRS (CMSQ)
.025	(0.3367E-02,-0.9015E-03)	0.9337E-04
.050	(0.2180E-01,-0.2061E-01)	0.7165E-02
.075	(0.2075E-01,-0.6619E-01)	0.3157E-01
.100	(0.2161E-01,-0.1069E+00)	0.5290E-01
.125	(0.2422E-01,-0.1685E+00)	0.8543E-01
.150	(0.1906E-01,-0.2353E+00)	0.1231E+00
.175	(0.1948E-01,-0.3133E+00)	0.1656E+00
.200	(0.1393E-01,-0.4040E+00)	0.2168E+00

```
 .225   (0.9815E-02,-0.5010E+00)   0.2717E+00
 .250   (0.5132E-02,-0.6122E+00)   0.3344E+00
 .275   (-.2427E-02,-0.7308E+00)   0.4027E+00
 .300   (-.7997E-02,-0.8605E+00)   0.4766E+00
 .325   (-.1664E-01,-0.1001E+01)   0.5577E+00
 .350   (-.2472E-01,-0.1150E+01)   0.6438E+00
**********************************************

FREQUENCY= 90.0 GHZ
REFRACTIVE INDEX= (3.4162,-1.9758)

RADIUS            F(0)                SCRS
 (CM)             (CM)               (CMSQ)
 .025   (0.5520E-02,-0.2126E-02)   0.2609E-03
 .050   (0.1936E-01,-0.3814E-01)   0.1270E-01
 .075   (0.1549E-01,-0.7888E-01)   0.2896E-01
 .100   (0.1666E-01,-0.1404E+00)   0.5334E-01
 .125   (0.1290E-01,-0.2097E+00)   0.8236E-01
 .150   (0.9099E-02,-0.2971E+00)   0.1188E+00
 .175   (0.3509E-02,-0.3939E+00)   0.1601E+00
 .200   (-.3341E-02,-0.5070E+00)   0.2084E+00
 .225   (-.1090E-01,-0.6308E+00)   0.2619E+00
 .250   (-.2011E-01,-0.7694E+00)   0.3220E+00
 .275   (-.2964E-01,-0.9195E+00)   0.3875E+00
 .300   (-.4083E-01,-0.1084E+01)   0.4595E+00
 .325   (-.5222E-01,-0.1260E+01)   0.5369E+00
 .350   (-.6518E-01,-0.1449E+01)   0.6206E+00
**********************************************
```

Appendix C Extended Boundary Condition Method (ECBM) Program

The EBCM program computes the forward scattering amplitudes and scattering cross sections for oblate spheroidal raindrops using the equations derived in Section 2.4. The parameters are calculated fro drop equivolumetric radii of .025(.025).350 cm and angles of incidence $\alpha = 0(15)90$ degrees. Computations at $\alpha \neq 90°$ are made for polarizations 1 and 2 defined in Section 2.4.

This appendix is in three parts. In section 1, the expressions for the surface integrals of (2.58) which are used in the EBCM program are presented. Section 2 provides a flow chart of the program and descriptions of the subprograms used. Section 3 gives a listing of the program and computed parameters for 30, 45, 70 and 90 GHz.

C2. Expressions for the Surface Integrals of (2.58)

To obtain expressions for the surface integrals in (2.58), the outward normal unit vector at the surface of a scatterer must be expressed analytically. To accomplish this we note that for the geometry employed, the surface of an oblate spheroid can be expressed parametrically as

$$r = R(\theta) \tag{C.1}$$

The outward normal unit vector $\hat{n}$ can then be obtained from [13]

$$\hat{n} = \frac{\nabla[r - R(\theta)]}{|\nabla[r - R(\theta)]|} \tag{c.2}$$

To obtain an expression for $R(\theta)$, consider the equation defining the surface of an oblate spheroid having semiminor and semimajor axes a and b respectively [46]:

$$\frac{x^2}{b^2} + \frac{y^2}{b^2} + \frac{z^2}{a^2} = 1 \tag{C.3}$$

where the minor axis is alligned with he z-axis. After converting (C.3) to spherical coordinates using

$$x = r\sin\theta\cos\phi \tag{C.4a}$$

$$y = r\sin\theta\sin\phi \tag{C.4b}$$

$$z = r\cos\theta \tag{C.4c}$$

and doing some algebra , its found that

$$r = \left[\frac{a^2b^2}{b^2 + (a^2 - b^2)\sin^2\theta} = R(\theta)\right. \tag{C.5}$$

We assumed the following linear relationship between the spheroid's axial ratio and equivolumetric radius [34], [51]:

$$\frac{a}{b} = 1 - \bar{a} \tag{C.6}$$

where $\bar{a}$ is the equivolumetric radius in cm which, by definition, is related to a and b by

$$\bar{a} = (ab^2)^{1/3} \tag{C.7}$$

Using (C.6) and (C.7), equation (C.5) can be rewritten as

$$R(\theta) = \bar{a}(1 - \bar{a})^{1/3}[1 - \nu\sin\theta]^{-1/2} \tag{C.8a}$$

where

$$\nu = \bar{a}(2 - \bar{a}) \tag{C.8b}$$

Substituting $R(\theta)$ as given by (C.8) into (C.2), we find the outward normal unit vector can be expressed as

$$\hat{n} = V_r\hat{r} + V_\theta\hat{\theta} \tag{C.9a}$$

where

$$V_r = \left[1 + \left(\frac{\nu\sin\theta\cos\theta}{1 - \nu\sin^2\theta}\right)^2\right]^{-1/2} \tag{C.9b}$$

$$v_\theta = -v_r\frac{\nu\sin\theta\cos\theta}{1 - \nu\sin^2\theta} \tag{C.9c}$$

Now consider the surface plex integral $I^{(i)}$ *given by* (2.58) *when:* $f.\vec{E}_i = \vec{E}_1$:

$$I_1^{(i)} = \int_S \hat{n} \cdot \vec{N}^{(i)}_{o\ell m}(k_o r')x\vec{M}^{(1)}_{o\rho m}(nk_o r')d\vec{r}' \tag{C.10}$$

where the 1 subscript on $I_1^{(i)}$ indicates $\vec{E}_i = \vec{E}_1$ and we have noted $\sigma = 0$ in this case.

Using (2.18) to express the vector harmonics and (C.9) the normal unit vector $\hat{n}$ in (C.10) we find that

$$I_1^{(i)} = \int_0^{2\pi}\int_0^{\pi} V_r H_\ell(k_o R)j_\rho(nk_o R)\left(\frac{dP_\ell^m}{d\theta}\frac{dP_\rho^m}{d\theta} + \frac{m^2 P_\ell^m P_\rho^m}{\sin^2\theta}\right)$$

$$- V_\theta \ell(\ell+1) Z_\ell \frac{(k_o R}{k_o R} j_\rho(nk_o R) P^m_{\&ltl.} \frac{dP^m_\ell}{d\theta}$$

$$xR^2 \sin\theta d\theta d\phi \qquad (C.12)$$

where

$$z_\ell(k_o R) = \begin{matrix} j_\ell(k_o R) & , i = 1 \\ h^{(i)}_\ell(k_o r) & , i = 2 \end{matrix} \qquad (C.13)$$

and we have used the notation

$$R = R(\theta) \qquad (C.14a)$$

$$P^m_\ell = P^m_\ell(\cos\theta) \qquad (C.14)$$

$$H_\ell(k_o R) = \frac{1}{k_o R} \frac{\partial}{\partial R}[R z_\ell(k_o R)] \qquad (C.14c)$$

The plex integral in ϕ of (C.12) can be evaluated to give

$$0 \quad , \quad m = 0$$

$$- \pi \int_o^\pi V_r h_\ell(k_o R) j^\rho(nk_o R) \left(\frac{dP^m_\ell}{d\theta} \frac{dP^m_\rho}{d\theta} + \frac{m^2 P^m_\ell P^m_\rho}{\sin^2\theta} \right)$$

$$I^{(i)}_1 = \qquad (C.15)$$

$$- V_\theta \ell(\ell+1) \frac{z_\ell(k_o R)}{k_o R} j_\rho(nk_o R) P^m_\ell \frac{dP^m_\ell}{d\theta}$$

$$xR^2 \sin\theta d\theta \quad , m \neq 0$$

Similarly, it is found that the remaining surface integrals are given by

$$\tilde{I}^{(i)}_2 = I^{(i)}_1 \text{:df..in.in15:df.} - 2\pi \int V_r H_\ell(k_o R) j_\rho(nk_o R) \frac{dP^m_\ell}{d\theta} \frac{dP^m_\ell}{d\theta} \qquad (C.15b)$$

$$- V\ell(\ell+1) z_\ell \frac{(k_o R}{k_o R} j_\rho(nx_o R) P^m_\ell \frac{dP^m_\rho}{d\theta}$$

$$I^{(i)}_2 = \tilde{I}^{(i)}_1 \qquad (C.15c)$$

x R sup 2 sin theta d theta , m = 0 I sub 1 sup <(i)> , m ≠ 0

$$0 \quad , \quad m = 0$$

$$\pi \int_o^\pi v_r z_\ell(k_o R) G_\rho(nk_o R) \left(\frac{dP^m_\ell}{d\theta} \frac{dP^m_\rho}{d\theta} \frac{m^2 P^m_\ell P^m_\rho}{\sin^2\theta} \right.$$

$$J^{(i)}_1 = \tilde{J}^{(i)}_2 = \qquad (C.16a)$$

$$- V_\theta p(p+1) z_\ell(k_o R) \frac{j_\rho(nk_oR)}{nk_oR} \frac{dP_\ell^m}{d\theta} P_\rho^m$$

$$xR^2 \sin\theta d\theta \quad , \quad m \neq 0$$

$$2\pi \int_o^\pi v_r z_\ell(k_oR) G_\rho(nk_oR) \frac{dP_\ell^m}{d\theta} \frac{dP_\rho^m}{d\theta}$$

$$- v_\theta P(\rho+1) z_\ell(k_oR) \frac{j_\rho(nk_oR)}{nk_oR} \frac{dP_\ell^m}{d\theta} P_\rho^m$$

$$J_2^{(i)} = \tilde{J}_1^{(i)} = \qquad \textbf{(C.16b)}$$

x R sup 2 sin theta d theta , m = 0 J sub 1 sup <(i)> , m ≠ 0

0 , $m = 0$

$$- \pi \int_o^\pi v_r h_\ell(k_oR) G_\rho(nk_oR) \left(\frac{dPsb\ell^m}{d\theta} \frac{mP_\rho^m}{\sin\theta} + \frac{mP_\ell^m}{\sin\theta} \frac{dP_{\rho m}}{d\theta} \right)$$

$$J_1^{(i)} = \tilde{J}_2^{(i)} = \qquad \textbf{(C.17a)}$$

- nu sub theta left lb p (p + 1) H sub ℓ (k sub o R) < j sub rho (n k sub o R)> over < k sub o R> + ℓ (ℓ + 1) <z sub ℓ (k sub o R)> over < k sub o R> G sub rho (n k sub o R) right rb

$$x \frac{mP_\ell^m P_\rho^m}{\sin\theta} \; R^2 \sin\theta d\theta, \quad , \quad m \neq 0$$

$$J_2^{(i)} = \tilde{J}_1^{(i)} = - J_1^{(i)} \qquad \textbf{(C.17b)}$$

0 , $m = 0$

$$k_1^{(i)} = \tilde{k}_2^{(i)} = - \pi \int_o^\pi v_r z_\ell(k_oR) j_\rho(nk_oR) \left(\frac{mP_\ell^m}{\sin\theta} \frac{dP_\ell^m}{d\theta} + \frac{dP_\ell^m}{d\theta} \frac{mP_\rho^m}{sign\theta} \right) \qquad \textbf{(C.18a)}$$

$$xR^2 \sin\theta d\theta \quad , \quad m \neq 0$$

$$k_2^{(i)} = \tilde{k}_1^{(i)} = - k_1^{(i)}$$

C.2. Program Flow Chart and Descriptions of Subprograms

The flow chart for the EBCM program is given in Figure C.1. The functions and subroutines composing subprogram lists A, B and C which are shown in Figure C.1 are as follows:

(a) Subprogram List A

(1) SUBROUTINE QPTS: Computes and stores the quadrature nodes for numerical evaluation of the surface integrals given in Section C.1. The nodes are calculated for a composite eight point Gaussian quadrature scheme. The subprogram also computes v_r, v_θ, $k_o R$, $\cos\theta$ *and* $R^2 \sin\theta$ at the quadrature nodes.

(2) BLOCKDATA WGTSNDS: Inputs the weights and nodes for eight point Gaussian quadrature.

(b) Subprogram List B

(1) SUBROUTINE BESFIL: Computes and stores the Bessel functions in the surface integrals at the quadrature nodes. The functions computed are : $j_\ell(k_o R)$, $G_\ell(k_o R)$, $g_\ell^{(2)}(k_o R)$, $F_\ell(k_o R)$, $j_\ell(nk_o R)$, *and* $G_\ell(nk_o R)$.

(2) FUNCTION SBEST (X , N) : Computes the spherical Bessel function (first kind) of degree N and real argument x using backward recursion. Starting values for the recursion process area computed in the function subprogram SBESST using Taylor series expansions.

(3) FUNCTION CBESJ (Y , N): Computes the spherical Bessel function (first kind) of degree N and complex argument Y. Backward recursion is used with starting values obtained in CBESST using series expansion.

(c) Subprogram List C

(1) SUBROUTINE LGNFIL: Stores the functions $P_\ell^m(\cos\theta)$, $\frac{d}{d\theta}P_\ell^m(\cos\theta)$ *and* $mP_\ell^m\frac{(\cos\theta}{\sin\theta}$ evaluated at the quadrature nodes.

(2) SUBROUTINE CHIFIL: Stores the surface integrals given in Section C.1.

(3) SUBROUTINE MATFIL: Fills the matricies $\underline{S}_m$ and $\tilde{S}barudner_m$ given in (2.71)

(4) SUBROUTINE FACTOR: Performs an L-U decomposition [43] of the matrix $\underline{S}_m$.

(5) SUBROUTINE VECFIL: Fills the vector of expansion coefficients of the incident field , : xi barunder sub m in (2.71).

(6) SUBROUTINE SOLVE: Solves for the expansion coefficients fo the internal field , $\underline{c}_m$ in (2.71).

(7) SUBROUTINE COEFF: Computes the expansion coefficients of the scattered field.

```
C****** SCATTERING PARAMETERS - OBLATE SPHEROIDAL RAINDROPS *********
C                                                                     *
C    THIS PROGRAM USES THE EBCM TO COMPUTE SCATTERING PARAMETERS      *
C  FOR OBLATE SPHEROIDAL RAINDROPS.  THE PARAMETERS COMPUTED ARE      *
C  THE FORWARD SCATTERING AMPLITUDE AND SCATTREING CROSS SECTION.     *
C  COMPUTATIONS ARE MADE FOR DROP RADII OF .025(.025).350 CM AND      *
C  ANGLES OF INCIDENCE 0(15)90 DEGREES.                               *
C                                                                     *
C    USER INPUTS TO THE PROGRAM ARE:                                  *
C                                                                     *
C            FREQ= FREQUENCY OF OPERATION IN GHZ.                     *
C                                                                     *
C            RIRE(RIIM)= REAL(IMAG) PART OF THE REFRACTIVE            *
C                        INDEX OF WATER AT THE FREQUENCY              *
C                        AND TEMPERATURE OF INTEREST.                 *
C*********************************************************************

      COMPLEX*16 K,FSAMP,AB(60),Y(60),CD(60),SNTRNL(0:30,60,60)
      COMPLEX*16 NTRNL(60,60),SCTR(60,60),FSAMPO,KR(248)
      COMPLEX*16 BESSEL(6,30,248),CHI(0:30,30,30,4,2)
      COMPLEX IMAG,RI
      REAL*8 SCRS,WGTS(8),NDS(8),PI,KO,CSALFA,R(248)
      REAL*8 LGNDR(3,30,248),VR(248),VTH(248)
      REAL*8 R2TAU(248),ETA(248),KOR(248)
      REAL MAX
      INTEGER IPIVOT(0:30,59)

      COMMON /BLOC1/ K,KO,EVR,IPOL
      COMMON /BLOC2/ CSALFA,IMAG
      COMMON /BLOC3/ WGTS,NDS,PI
      COMMON /BLOC4/ M,LMIN,LMAX,ISAVE
      COMMON /BLOC5/ RI
      COMMON /BLOC6/ AB,CD,SCTR
      COMMON /BLOC7/ FSAMP,SCRS
      COMMON /BLOC8/ NTRNL,SNTRNL,IPIVOT,N,IER
      COMMON /BLOC9/ NQI,NQP
      COMMON /BLOC10/ VR,VTH,R2TAU
      COMMON /BLOC11/ BESSEL
      COMMON /BLOC12/ LGNDR
      COMMON /BLOC13/ ETA
      COMMON /BLOC14/ KOR,KR
      COMMON /BLOC15/ CHI
      COMMON /BLOC16/ Y

      IMAG=(0.,1.)
      PI=3.141592653589793
   66 CONTINUE
      READ(5,*,END=500)FREQ,RIRE,RIIM
      RI=CMPLX(RIRE,RIIM)
      KO=2.*PI*FREQ/30.
      K=KO*RI
      EVR=.025
  777 WRITE(6,100)FREQ,RIRE,RIIM,EVR
      NU1=EVR*(2.-EVR)
      NU2=EVR*DBLE((1.-EVR)**(2./3.))
```

```
C  CHOOSE INITIAL LMAX.

      RAD=EVR/(1.-EVR)**(1./3.)
      LMAX=2.*K0*RAD+1.
   55 Z0=FLOAT(LMAX)+.5
      Z1=(EXP(1.)*K0*RAD/(2.*Z0))**Z0
      IF(Z1.GT.5.0E-05) THEN
         LMAX=LMAX+1
         GO TO 55
      ENDIF
      LLL=LMAX
      LL=LMAX+8
      NQI=LL+1
      NQP=8*NQI

C  DETERMINE THE QUADRATURE NODES AND COMPUTE THE SPHERICAL
C  BESSEL FUNCTIONS.

      CALL QPTS
      CALL BESFIL

C  ALPHA=0 DEGREES.

      ISAVE=0
      IPOL=1
      CSALFA=1.
      M=1
      LMIN=1
      FSAMP0=(0.,0.)
   70 FSAMP=(0.,0.)
      SCRS=0.
      N=2*LMAX

CC  COMPUTE SURFACE INTEGRALS FOR AZIMUTHAL MODE M=1.

      CALL LGNFIL
      CALL CHIFIL

CC  COMPUTE T-MATRIX FOR AZIMUTHAL MODE M=1.

      CALL MATFIL(NTRNL,2,1)
      CALL FACTOR
      IF(IER.EQ.2) GO TO 700
      CALL MATFIL(SCTR,1,1)
      CALL VECFIL
      CALL SOLVE

CC  COMPUTE EXPANSION COEFFICIENTS FOR THE SCATTERED FIELD.

      CALL COEFF(M,N)

CC   CALCULATE SCATTERING PARAMETERS AND CHECK FOR CONVERGENCE.

      CALL PARAM
```

```
      TESTR=DABS(DREAL(FSAMP-FSAMP0)/DREAL(FSAMP))
      TESTI=DABS(DIMAG(FSAMP-FSAMP0)/DIMAG(FSAMP))
      IF(TESTR.GT.1.0E-03.OR.TESTI.GT.1.0E-03) THEN
         LLL=LLL+1
         IF(LLL.GT.LL) GO TO 201
         LMAX=LMAX+1
         FSAMP0=FSAMP
         ISAVE=1
         GO TO 70
      ENDIF
  201 TEST=MAX(TESTR,TESTI)
      FSAMPR=DREAL(FSAMP)/K0
      FSAMPI=DIMAG(FSAMP)/K0
      CRSS=SCRS*PI/K0**2
      WRITE(6,101)FSAMPR,FSAMPI,CRSS,TEST,LMAX

C  COMPUTE SURFACE INTEGRALS FOR AZIMUTHAL MODE M=0.

      ISAVE=0
      M=0
      LMIN=1
      N=LMAX
      CALL LGNFIL
      CALL CHIFIL
      CALL MATFIL(NTRNL,2,1)
      CALL FACTOR

C  POLARIZATIONS 1 AND 2, ALPHA=15(15)90 DEGREES.

      MMAX=1
  333 WRITE(6,105)IPOL
      ALPHA=15.
  305 CONTINUE
      IF(ALPHA.EQ.90.) THEN
         CSALFA=0.
      ELSE
         CSALFA=DCOS(PI*ALPHA/180.)
      ENDIF
      FSAMP=(0.,0.)
      FSAMP0=(0.,0.)
      SCRS=0.
      M=0
  304 LMIN=M
      IF(M.EQ.0) LMIN=1
      N=2*(LMAX-LMIN+1)
      IF(M.EQ.0) N=LMAX
      IF(M.LE.MMAX) GO TO 733

CC  COMPUTE SURFACE INTEGRALS.

      CALL LGNFIL
      CALL CHIFIL
  733 CONTINUE

CC  COMPUTE T-MATRICIES.
```

```
      IF(M.LE.MMAX.AND.IPOL.EQ.1) GO TO 744
      CALL MATFIL(NTRNL,2,IPOL)
      CALL FACTOR
      IF(IER.EQ.2) GO TO 700
  744 CONTINUE
      CALL MATFIL(SCTR,1,IPOL)
      CALL VECFIL
      CALL SOLVE

CC    COMPUTE EXPANSION COEFFICIENTS FOR THE SCATTERED FIELD.

      CALL COEFF(M,N)

CC    COMPUTE SCATTERING PARAMETERS AND CHECK FOR CONVERGENCE.

      CALL PARAM
      TESTR=DABS(DREAL(FSAMP-FSAMPO)/DREAL(FSAMP))
      TESTI=DABS(DIMAG(FSAMP-FSAMPO)/DIMAG(FSAMP))
      IF(TESTR.GT.1.0E-03.OR.TESTI.GT.1.0E-03) THEN
         M=M+1
         FSAMPO=FSAMP
         IF(M.LE.LMAX) GO TO 304
      ENDIF
      TEST=MAX(TESTR,TESTI)
      FSAMPR=DREAL(FSAMP)/K0
      FSAMPI=DIMAG(FSAMP)/K0
      CRSS=SCRS*PI/K0**2
      WRITE(6,102)ALPHA,FSAMPR,FSAMPI,CRSS,TEST,M
      IF(M.GT.MMAX) MMAX=M
      ALPHA=ALPHA+15.
      IF(ALPHA.LE.90.) GO TO 305
      IPOL=IPOL+1
      IF(IPOL.EQ.2) GO TO 333
      WRITE(6,104)

      EVR=EVR+.025
      IF(EVR.LE.(.350)) GO TO 777
      GO TO 66
  700 WRITE(6,103)IPOL,M
      WRITE(6,104)

  100 FORMAT(26X,'FREQUENCY=',F4.1,' GHZ',/,22X,'REF INDEX=(',
     &F6.4,',',F7.4,')',/,20X,'EQUIVOLUMETRIC RADIUS=',F5.3,
     &' CM',/,20X,30('-'))
  101 FORMAT(//,1X,'ALPHA=0 DEGREES:',//,22X,'F(0,0)',17X,'SCRS',/,
     &23X,'(CM)',17X,'(CMSQ)',8X,'TEST',5X,'LMAX',/,12X,'(',E11.5,
     &',',E12.5,')',3X,E11.5,3X,E10.4,3X,I2)
  105 FORMAT(//,1X,'POLARIZATION ',I1,':',//,3X,'ALPHA',12X,
     &'F(0,ALPHA)',15X,'SCRS',/,1X,'(DEGREES)',13X,'(CM)',17X,
     &'(CMSQ)',8X,'TEST',5X,'MMAX')
  102 FORMAT(3X,F4.1,5X,'(',E11.5,',',E12.5,')',3X,E11.5,3X,
     &E10.4,3X,I2)
  103 FORMAT(1X,'IER=2 FOR POLARIZATION ',I1,' M = ',I2)
  104 FORMAT(1X,70('*'),/)
```

```
500 STOP
    END


    SUBROUTINE MATFIL(C,IBES,IPOL)
    COMPLEX RI
    COMPLEX*16 C(60,60),CHI(0:30,30,30,4,2),D1,D2,D3,D4
    INTEGER P
    COMMON /BLOC4/ M,LMIN,LMAX,ISAVE
    COMMON /BLOC5/ RI
    COMMON /BLOC15/ CHI

    IMAX=LMAX-LMIN+1
    I=1
    DO 1 L=LMIN,LMAX
    II=I+IMAX
    J=1
    DO 2 P=LMIN,LMAX
    JJ=J+IMAX
    D1=CHI(M,L,P,1,IBES)
    D2=CHI(M,L,P,2,IBES)
    IF(M.EQ.0) THEN
       IF(IPOL.EQ.1) C(I,J)=D2+RI*D1
       IF(IPOL.EQ.2) C(I,J)=D1+RI*D2
    ELSE
       D3=CHI(M,L,P,3,IBES)
       D4=CHI(M,L,P,4,IBES)
       C(I,J)=D1+RI*D2
       C(I,JJ)=D3+RI*D4
       C(II,J)=-(D4+RI*D3)
       C(II,JJ)=D2+RI*D1
       IF(IPOL.EQ.2) THEN
          C(I,JJ)=-C(I,JJ)
          C(II,J)=-C(II,J)
       ENDIF
    ENDIF
  2 J=J+1
  1 I=I+1
    RETURN
    END


-
      SUBROUTINE CHIFIL
      COMPLEX*16 CHI(0:30,30,30,4,2),NTGRL
      INTEGER P
      COMMON /BLOC4/ M,LMIN,LMAX,ISAVE
      COMMON /BLOC15/ CHI

      IF(ISAVE.EQ.1) GO TO 100
-     DO 1 L=LMIN,LMAX
-     DO 1 P=LMIN,LMAX
```

```
      DO 1 IBES=1,2
      DO 1 I=1,4
      IF((I.EQ.3.OR.I.EQ.4).AND.M.EQ.0) GO TO 1
      CHI(M,L,P,I,IBES)=NTGRL(M,L,P,I,IBES)
    1 CONTINUE

  100 LMAXM1=LMAX-1
      DO 2 I=1,4
      DO 2 IBES=1,2
      DO 3 L=LMIN,LMAXM1
      CHI(M,L,LMAX,I,IBES)=NTGRL(M,L,LMAX,I,IBES)
    3 CHI(M,LMAX,L,I,IBES)=NTGRL(M,LMAX,L,I,IBES)
    2 CHI(M,LMAX,LMAX,I,IBES)=NTGRL(M,LMAX,LMAX,I,IBES)
      RETURN
      END



      SUBROUTINE VECFIL
      COMPLEX*16 K,Y(60)
      COMPLEX IMAG,FJML
      REAL*8 K0,CSALFA,LGNDR2,LGNDR3,FA,FB
      COMMON /BLOC1/ K,K0,EVR,IPOL
      COMMON /BLOC2/ CSALFA,IMAG
      COMMON /BLOC4/ M,LMIN,LMAX,ISAVE
      COMMON /BLOC16/ Y
      I=1
      DO 2 L=LMIN,LMAX
      FA=LGNDR2(L,M,CSALFA)
      FB=LGNDR3(L,M,CSALFA)
      FJML=4.*IMAG**(-L)
      II=I+LMAX-LMIN+1
      IF(IPOL.EQ.1) THEN
         IF(M.EQ.0) THEN
            Y(I)=IMAG*FJML*FB
         ELSE
            Y(I)=FJML*FA
            Y(II)=IMAG*FJML*FB
         ENDIF
      ELSE
         Y(I)=-FJML*FB
         IF(M.NE.0) Y(II)=IMAG*FJML*FA
      ENDIF
    2 I=I+1
      RETURN
      END



      SUBROUTINE FACTOR
      COMPLEX*16 C(60,60),SC(0:30,60,60),Q,Z,TEMP
      INTEGER IPIVOT(0:30,59)
      COMMON /BLOC4/ M,LMIN,LMAX,ISAVE
```

```
      COMMON /BLOC8/ C,SC,IPIVOT,N,IER
      IER=1
      NM1=N-1
      DO 1 I=1,N
      DO 1 J=1,N
    1 SC(M,I,J)=C(I,J)
      DO 8 I=1,NM1
      PIVOT=0.
      DO 3 J=I,N
      RTEMP=CDABS(SC(M,J,I))
      IF(PIVOT.GE.RTEMP) GO TO 3
      PIVOT=RTEMP
      IPIVOT(M,I)=J
    3 CONTINUE
      IF(PIVOT.EQ.0.) GO TO 13
      IF (IPIVOT(M,I).EQ.I) GO TO 5
      DO 4 K=I,N
      TEMP=SC(M,I,K)
      SC(M,I,K)=SC(M,IPIVOT(M,I),K)
    4 SC(M,IPIVOT(M,I),K)=TEMP
    5 IP1=I+1
      DO 7 K=IP1,N
      Q=-SC(M,K,I)/SC(M,I,I)
      SC(M,K,I)=Q
      DO 6 J=IP1,N
    6 SC(M,K,J)=Q*SC(M,I,J)+SC(M,K,J)
    7 CONTINUE
    8 CONTINUE
      Z=(0.,0.)
      IF(SC(M,N,N).EQ.Z) GO TO 13
      RETURN
   13 IER=2
      RETURN
      END



      SUBROUTINE SOLVE
      COMPLEX*16 SC(0:30,60,60),Y(60),CD(60),Q,TEMP
      COMPLEX*16 AB(60),SCTR(60,60),C(60,60)
      INTEGER IPIVOT(0:30,59)
      COMMON /BLOC4/ M,LMIN,LMAX,ISAVE
      COMMON /BLOC6/ AB,CD,SCTR
      COMMON /BLOC8/ C,SC,IPIVOT,N,IER
      COMMON /BLOC16/ Y
      NP1=N+1
      NM1=N-1
      DO 1 I=1,NM1
      TEMP=Y(I)
      Y(I)=Y(IPIVOT(M,I))
      Y(IPIVOT(M,I))=TEMP
      IP1=I+1
      DO 4 J=IP1,N
    4 Y(J)=Y(J)+Y(I)*SC(M,J,I)
```

```
 1 CONTINUE
   CD(N)=Y(N)/SC(M,N,N)
   DO 10 K=1,NM1
   Q=(0.,0.)
   DO 9 J=1,K
 9 Q=Q+SC(M,N-K,NP1-J)*CD(NP1-J)
10 CD(N-K)=(Y(N-K)-Q)/SC(M,N-K,N-K)
   RETURN
   END



   SUBROUTINE COEFF(M,N)
   COMPLEX*16 AB(60),CD(60),SCTR(60,60)
   COMMON /BLOC6/ AB,CD,SCTR
   DO 20 I=1,N
   AB(I)=(0.,0.)
   DO 20 J=1,N
20 AB(I)=AB(I)-SCTR(I,J)*CD(J)
   RETURN
   END



   SUBROUTINE PARAM
   COMPLEX*16 FSAMP,AB(60),CD(60),SCTR(60,60),K
   COMPLEX IMAG,JL
   REAL*8 FA,FB,LGNDR2,LGNDR3,D,D1,D2
   REAL*8 SCRS,KO,CSALFA,PI,FACT
   COMMON /BLOC1/ K,KO,EVR,IPOL
   COMMON /BLOC2/ CSALFA,IMAG
   COMMON /BLOC4/ M,LMIN,LMAX,ISAVE
   COMMON /BLOC6/ AB,CD,SCTR
   COMMON /BLOC7/ FSAMP,SCRS
   PI=3.141592653589793
   I=1
   DO 21 L=LMIN,LMAX
   II=I+LMAX-LMIN+1
   FA=LGNDR2(L,M,CSALFA)
   FB=LGNDR3(L,M,CSALFA)
   JL=IMAG**L
   D1=(2*L+1)*FACT(L-M)
   D2=4*L*(L+1)*FACT(L+M)
   D=D1/D2
   IF(M.NE.0) D=2.*D
   IF(M.EQ.0) THEN
      IF(IPOL.EQ.1) FSAMP=FSAMP+JL*D*AB(I)*FB
      IF(IPOL.EQ.2) FSAMP=FSAMP-IMAG*JL*D*AB(I)*FB
      SCRS=SCRS+D*CDABS(AB(I))**2
   ELSE
      IF(IPOL.EQ.1) FSAMP=FSAMP+JL*D*(AB(II)*FB+IMAG*AB(I)*FA)
      IF(IPOL.EQ.2) FSAMP=FSAMP+JL*D*(AB(II)*FA-IMAG*AB(I)*FB)
      SCRS=SCRS+D*(CDABS(AB(I))**2+CDABS(AB(II))**2)
```

```
      ENDIF
   21 I=I+1
      RETURN
      END



      SUBROUTINE BESFIL
      COMPLEX*16 BESSEL(6,30,248),CBESJ,Y,KR(248),BES3(0:31)
      COMPLEX MIMAG
      REAL*8 KOR(248),BES1(0:31),BES2(0:31),SBESJ,SBESY,X
      COMMON /BLOC9/ NQI,NQP
      COMMON /BLOC11/ BESSEL
      COMMON /BLOC14/ KOR,KR
      MIMAG=(0.,-1.)
      NQIM1=NQI-1
      NQIM2=NQI-2
      DO 1 NP=1,NQP
      X=KOR(NP)
      Y=KR(NP)
      BES2(0)=-1.*DCOS(X)/X
      BES2(1)=BES2(0)/X-DSIN(X)/X
      DO 51 L=2,NQI
   51 BES2(L)=(2*L-1)*BES2(L-1)/X-BES2(L-2)
      BES1(NQI)=SBESJ(X,NQI)
      BES1(NQIM1)=SBESJ(X,NQIM1)
      BES3(NQI)=CBESJ(Y,NQI)
      BES3(NQIM1)=CBESJ(Y,NQIM1)
      L=NQIM2
      DO 52 I=0,NQIM2
      TLP3=2*L+3
      BES1(L)=TLP3*BES1(L+1)/X-BES1(L+2)
      BES3(L)=TLP3*BES3(L+1)/Y-BES3(L+2)
   52 L=L-1
      DO 53 L=0,NQI
      BES1(L)=DSIN(X)*BES1(L)/(X*BES1(0))
   53 BES3(L)=CDSIN(Y)*BES3(L)/(Y*BES3(0))
      DO 4 L=1,NQIM1
      TLP1=2*L+1
      BESSEL(1,L,NP)=BES1(L)
      BESSEL(2,L,NP)=BES1(L)+MIMAG*BES2(L)
      BESSEL(3,L,NP)=((L+1)*BES1(L-1)-L*BES1(L+1))/TLP1
      BESSEL(4,L,NP)=BESSEL(3,L,NP)+MIMAG*((L+1)*BES2(L-1)-L*
     &BES2(L+1))/TLP1
      BESSEL(5,L,NP)=BES3(L)
    4 BESSEL(6,L,NP)=((L+1)*BES3(L-1)-L*BES3(L+1))/TLP1
    1 CONTINUE
      RETURN
      END



      SUBROUTINE LGNFIL
```

```
      REAL*8 LGNDR(3,30,248),LGNDR1,LGNDR2,LGNDR3,ETA(248)
      COMMON /BLOC4/ M,LMIN,LMAX,ISAVE
      COMMON /BLOC9/ NQI,NQP
      COMMON /BLOC12/ LGNDR
      COMMON /BLOC13/ ETA
      LL=LMIN
      IF(ISAVE.EQ.1) LL=LMAX
      DO 1 NP=1,NQP
      DO 1 L=LL,LMAX
      LGNDR(1,L,NP)=LGNDR1(L,M,ETA(NP))
      LGNDR(2,L,NP)=LGNDR2(L,M,ETA(NP))
    1 LGNDR(3,L,NP)=LGNDR3(L,M,ETA(NP))
      RETURN
      END



      SUBROUTINE QPTS
      COMPLEX*16 K,KR(248)
      REAL*8 D1,ARG,PI,WGTS(8),NDS(8),ETA(248),TAU,FTHTA,R
      REAL*8 R2TAU(248),KOR(248),VR(248),VTH(248),KO,NET
      REAL NU
      COMMON /BLOC1/ K,KO,EVR,IPOL
      COMMON /BLOC3/ WGTS,NDS,PI
      COMMON /BLOC9/ NQI,NQP
      COMMON /BLOC10/ VR,VTH,R2TAU
      COMMON /BLOC13/ ETA
      COMMON /BLOC14/ KOR,KR
      D1=1.
      NP=1
      DO 2 I=1,NQI
      DO 3 J=1,8
      ARG=PI*(NDS(J)+DBLE(2.*I-1.))/(2.*NQI)
      ETA(NP)=DCOS(ARG)
      TAU=DSQRT(D1-ETA(NP)**2)
      NU=EVR*(2.-EVR)
      NET=NU*ETA(NP)*TAU
      FTHTA=D1-NU*TAU**2
      R=EVR*(D1-DBLE(EVR))**(2./3.)/DSQRT(FTHTA)
      R2TAU(NP)=TAU*R**2
      KOR(NP)=KO*R
      KR(NP)=K*R
      VR(NP)=D1/DSQRT(D1+(NET/FTHTA)**2)
      VTH(NP)=VR(NP)*NET/FTHTA
    3 NP=NP+1
    2 CONTINUE
      RETURN
      END



      REAL FUNCTION FACT*8(N)
      FACT=1.
```

```
      IF(N.EQ.0.OR.N.EQ.1) RETURN
      DO 1 I=2,N
    1 FACT=I*FACT
      RETURN
      END



      REAL FUNCTION MAX(A,B)
      IF(A.GE.B) MAX=A
      IF(B.GT.A) MAX=B
      RETURN
      END


      COMPLEX FUNCTION NTGRL*16(M,L,P,N,IBES)
      COMPLEX*16 NTGRND
      REAL*8 NDS(8),WGTS(8),PI
      INTEGER P
      COMMON /BLOC3/ WGTS,NDS,PI
      COMMON /BLOC9/ NQI,NQP
      NP=1
      NTGRL=(0.,0.)
      DO 1 I=1,NQI
      DO 2 J=1,8
      NTGRL=NTGRL+WGTS(J)*NTGRND(M,L,P,N,IBES,NP)
    2 NP=NP+1
    1 CONTINUE
      NTGRL=-NTGRL*PI*PI/(2.*NQI)
      RETURN
      END



      COMPLEX FUNCTION NTGRND*16(M,L,P,N,IBES,NP)
      COMPLEX*16 BESSEL(6,30,248),Y,FBES,KR(248)
      REAL*8 X,VR(248),VTH(248),R2TAU(248),R2,V1,V2
      REAL*8 LGNDR(3,30,248),FLGNDR,KOR(248)
      INTEGER P
      COMMON /BLOC10/ VR,VTH,R2TAU
      COMMON /BLOC11/ BESSEL
      COMMON /BLOC12/ LGNDR
      COMMON /BLOC14/ KOR,KR
      R2=R2TAU(NP)
      X=KOR(NP)
      Y=KR(NP)
      V1=VR(NP)
      V2=VTH(NP)
      IF(N.EQ.1.OR.N.EQ.2) THEN
         IF(M.EQ.0) THEN
            FLGNDR=LGNDR(3,L,NP)*LGNDR(3,P,NP)
         ELSE
```

```
      FLGNDR=LGNDR(2,L,NP)*LGNDR(2,P,NP)+
&           LGNDR(3,L,NP)*LGNDR(3,P,NP)
    ENDIF
    FBES=BESSEL(5,P,NP)*BESSEL(IBES,L,NP)
    IF(N.EQ.1) THEN
      NTGRND=(V1*BESSEL(IBES+2,L,NP)*BESSEL(5,P,NP)*
&           FLGNDR+V2*L*(L+1)*FBES*LGNDR(1,L,NP)*
&           LGNDR(3,P,NP)/X)*R2
    ELSE
      NTGRND=-(V1*BESSEL(IBES,L,NP)*BESSEL(6,P,NP)*FLGNDR+
&           V2*P*(P+1)*FBES*LGNDR(3,L,NP)*LGNDR(1,P,NP)/Y)*R2
    ENDIF
 ELSE
    FLGNDR=LGNDR(2,L,NP)*LGNDR(3,P,NP)+
&         LGNDR(3,L,NP)*LGNDR(2,P,NP)
    IF(N.EQ.3) THEN
      NTGRND=(V1*BESSEL(IBES+2,L,NP)*BESSEL(6,P,NP)*
&           FLGNDR+V2*(P*(P+1)*BESSEL(IBES+2,L,NP)*
&           BESSEL(5,P,NP)*LGNDR(2,L,NP)*
&           LGNDR(1,P,NP)/Y+L*(L+1)*BESSEL(IBES,L,NP)*
&           BESSEL(6,P,NP)*LGNDR(1,L,NP)*
&           LGNDR(2,P,NP)/X))*R2
    ELSE
      NTGRND=V1*BESSEL(IBES,L,NP)*BESSEL(5,P,NP)*
&           FLGNDR*R2
    ENDIF
 ENDIF
 RETURN
 END



 REAL FUNCTION LGNDR1*8(N,M,ETA)
 REAL*8 FACT,ETA,DP1,DM1,D0
 DP1=DBLE(1.)
 DM1=DBLE(-1.)
 D0=DBLE(0.)
 IF(M.GT.N) THEN
   LGNDR1=0.
   RETURN
 ENDIF
 IF(ETA.EQ.DP1.OR.ETA.EQ.DM1) GO TO 200
 KMAX=(N-M)/2
 IF(ETA.EQ.D0) THEN
    IF((FLOAT(N-M)/2.).NE.FLOAT(KMAX)) THEN
      LGNDR1=0.
    ELSE
      LGNDR1=(-1.)**KMAX*FACT(2*N-2*KMAX)/
&           (FACT(KMAX)*FACT(N-KMAX)*2.**N)
    ENDIF
    RETURN
 ELSE
     LGNDR1=0.
     DO 1 K=0,KMAX
```

```
     1     LGNDR1=LGNDR1+(-1.)**K*FACT(2*N-2*K)*ETA**(N-M-2*K)/
      &          (FACT(K)*FACT(N-K)*FACT(N-M-2*K))
           IF(M.EQ.0) THEN
              LGNDR1=LGNDR1/2.**N
           ELSE
              LGNDR1=(DP1-ETA**2)**(FLOAT(M)/2.)*LGNDR1/2.**N
           ENDIF
           RETURN
        ENDIF
   200 CONTINUE
        IF(M.NE.0) THEN
           LGNDR1=0.
        ELSE
           IF(ETA.EQ.DP1) LGNDR1=1.
           IF(ETA.EQ.DM1) LGNDR1=(-1.)**N
        ENDIF
        RETURN
        END



        REAL FUNCTION LGNDR2*8(N,M,ETA)
        REAL*8 LGNDR1,FACT,ETA,DP1,DM1,D0
        DP1=DBLE(1.)
        DM1=DBLE(-1.)
        D0=DBLE(0.)
        IF(M.EQ.0) THEN
          LGNDR2=0.
          RETURN
        ENDIF
        IF(ETA.EQ.DP1.OR.ETA.EQ.DM1) GO TO 200
        IF(ETA.EQ.D0) GO TO 300
        KMAX=(N-M)/2
        LGNDR2=0.
        DO 1 K=0,KMAX
      1 LGNDR2=LGNDR2+(-1.)**K*FACT(2*N-2*K)*ETA**(N-M-2*K)/
       &(FACT(K)*FACT(N-K)*FACT(N-M-2*K))
        IF(M.EQ.1) THEN
           LGNDR2=LGNDR2/2.**N
        ELSE
           LGNDR2=M*(DP1-ETA**2)**(FLOAT(M-1)/2.)*LGNDR2/2.**N
        ENDIF
        RETURN
   200 CONTINUE
        IF(M.NE.1) THEN
           LGNDR2=0.
           RETURN
        ENDIF
        IF(ETA.EQ.DP1) PN0=1.
        IF(ETA.EQ.DM1) PN0=(-1.)**N
        LGNDR2=ETA*(N*(N+1)*PN0)/2.
        RETURN
   300 LGNDR2=M*LGNDR1(N,M,D0)
        RETURN
```

```
      END



      REAL FUNCTION LGNDR3*8(N,M,ETA)
      REAL*8 LGNDR1,ETA,DP1,DM1
      DP1=DBLE(1.)
      DM1=DBLE(-1.)
      IF(M.NE.0) THEN
        LGNDR3=((N-M+1)*(N+M)*LGNDR1(N,M-1,ETA)-LGNDR1(N,M+1,ETA))/2.
      ELSE
        IF(ETA.EQ.DP1.OR.ETA.EQ.DM1) THEN
          LGNDR3=0.
        ELSE
          LGNDR3=-((N+1)*ETA*LGNDR1(N,M,ETA)-(N-M+1)*
     &             LGNDR1(N+1,M,ETA))/DSQRT(DP1-ETA**2)
        ENDIF
      ENDIF
      RETURN
      END



      REAL FUNCTION SBESJ*8(X,N)
      REAL*8 X,Z,SBESST,Q0,Q1,Q2,QN
      Z=DSIN(X)/X
      IF(N.EQ.0) THEN
         SBESJ=Z
         RETURN
      ENDIF
      IF(.5*X*X/(2.*N+3.).LT.1.0) THEN
         SBESJ=SBESST(X,N)
         RETURN
      ENDIF
      M=X+10.
      IF(M.LE.N) M=N+5
      Q2=SBESST(X,M+1)
      Q1=SBESST(X,M)
      MM=M
      DO 1 I=1,M
      IF(MM.EQ.N) QN=Q0
      Q0=(2*MM+1)*Q1/X-Q2
      Q2=Q1
      Q1=Q0
    1 MM=MM-1
      SBESJ=Z*QN/Q0
      RETURN
      END



      REAL FUNCTION SBESST*8(X,N)
```

```
      REAL*8 X,F,Q1,Q2,Z
      F=1.
      DO 1 I=1,N
    1 F=F*X/(2.*I+1.)
      K1=1
      K2=2*N+3
      Z=-.5*X*X
      Q1=1.
      Q2=Z/FLOAT(K2)
    2 Q1=Q1+Q2
      IF(DABS(Q2).GT.1.0D-16) THEN
         K1=K1+1
         K2=K2+2
         Q2=Q2*Z/FLOAT(K1*K2)
         GO TO 2
      ENDIF
      SBESST=F*Q1
      RETURN
      END



      COMPLEX FUNCTION CBESJ*16(Y,N)
      COMPLEX*16 Y,Z,Q0,Q1,Q2,QN,CBESST
      Z=CDSIN(Y)/Y
      IF(N.EQ.0) THEN
         CBESJ=Z
         RETURN
      ENDIF
      IF(CDABS(.5*Y*Y/(2.*N+3.)).LT.1.0) THEN
         CBESJ=CBESST(Y,N)
         RETURN
      ENDIF
      M=CDABS(Y)+10.
      IF(M.LE.N) M=N+5
      Q2=CBESST(Y,M+1)
      Q1=CBESST(Y,M)
      MM=M
      DO 1 I=1,M
      IF(MM.EQ.N) QN=Q0
      Q0=(2*MM+1)*Q1/Y-Q2
      Q2=Q1
      Q1=Q0
    1 MM=MM-1
      CBESJ=Z*QN/Q0
      RETURN
      END



      COMPLEX FUNCTION CBESST*16(Y,N)
      COMPLEX*16 Y,Z,F,Q1,Q2
      F=(1.,0.)
```

```
      DO 1 I=1,N
    1 F=F*Y/(2.*I+1.)
      K1=1
      K2=2*N+3
      Z=-.5*Y*Y
      Q1=(1.,0.)
      Q2=Z/FLOAT(K2)
    2 Q1=Q1+Q2
      IF(CDABS(Q2).GT.1.0D-16) THEN
         K1=K1+1
         K2=K2+2
         Q2=Q2*Z/FLOAT(K1*K2)
         GO TO 2
      ENDIF
      CBESST=F*Q1
      RETURN
      END



      BLOCK DATA WTSNDS
      COMMON /BLOC3/ WGTS,NDS,PI
      REAL*8 WGTS(8),NDS(8),PI
      DATA WGTS/.101228536290376,.222381034453374,.313706645877887,
     &.362683783378362,.362683783378362,.313706645877887,
     &.222381034453374,.101228536290376/
      DATA NDS/-.960289856497536,-.796666477413627,-.525532409916329,
     &-.18343464249565,.18343464249565,.525532409916329,
     &.796666477413627,.960289856497536/
      END
```

FREQUENCY=30.0 GHZ
REF INDEX=(5.5810,-2.8482)
EQUIVOLUMETRIC RADIUS=0.025 CM

ALPHA=0 DEGREES:

F(0,0) (CM)	SCRS (CMSQ)	TEST	LMAX
(0.61405E-03,-0.57195E-04)	0.30587E-05	0.1106E-06	5

POLARIZATION 1:

ALPHA (DEGREES)	F(0,ALPHA) (CM)	SCRS (CMSQ)	TEST	MMAX
15.0	(0.61288E-03,-0.57043E-04)	0.30469E-05	0.1291E-03	2
30.0	(0.60967E-03,-0.56629E-04)	0.30146E-05	0.3900E-03	2
45.0	(0.60529E-03,-0.56063E-04)	0.29705E-05	0.5269E-03	2
60.0	(0.60091E-03,-0.55497E-04)	0.29264E-05	0.4913E-03	2
75.0	(0.59771E-03,-0.55082E-04)	0.28942E-05	0.4153E-03	2
90.0	(0.59653E-03,-0.54931E-04)	0.28823E-05	0.3676E-03	2

POLARIZATION 2:

ALPHA (DEGREES)	F(0,ALPHA) (CM)	SCRS (CMSQ)	TEST	MMAX
15.0	(0.61406E-03,-0.57227E-04)	0.30587E-05	0.1379E-03	2
30.0	(0.61410E-03,-0.57314E-04)	0.30586E-05	0.5135E-03	2
45.0	(0.61416E-03,-0.57433E-04)	0.30584E-05	0.4272E-06	3
60.0	(0.61421E-03,-0.57553E-04)	0.30583E-05	0.9592E-06	3
75.0	(0.61425E-03,-0.57640E-04)	0.30582E-05	0.1482E-05	3
90.0	(0.61426E-03,-0.57672E-04)	0.30582E-05	0.1701E-05	3

****

FREQUENCY=30.0 GHZ
REF INDEX=(5.5810,-2.8482)
EQUIVOLUMETRIC RADIUS=0.050 CM

ALPHA=0 DEGREES:

F(0,0) (CM)	SCRS (CMSQ)	TEST	LMAX
(0.52761E-02,-0.11657E-02)	0.22188E-03	0.1987E-05	5

POLARIZATION 1:

ALPHA (DEGREES)	F(0,ALPHA) (CM)	SCRS (CMSQ)	TEST	MMAX
15.0	(0.52551E-02,-0.11621E-02)	0.22010E-03	0.5098E-03	2

```
  30.0     (0.51979E-02,-0.11523E-02)   0.21525E-03   0.1298E-05    3
  45.0     (0.51197E-02,-0.11389E-02)   0.20864E-03   0.3560E-05    3
  60.0     (0.50416E-02,-0.11255E-02)   0.20203E-03   0.4249E-05    3
  75.0     (0.49845E-02,-0.11157E-02)   0.19719E-03   0.5009E-05    3
  90.0     (0.49636E-02,-0.11121E-02)   0.19542E-03   0.5364E-05    3

POLARIZATION 2:

  ALPHA          F(0,ALPHA)                SCRS
(DEGREES)          (CM)                   (CMSQ)        TEST      MMAX
  15.0     (0.52760E-02,-0.11685E-02)   0.22188E-03   0.5420E-03    2
  30.0     (0.52758E-02,-0.11762E-02)   0.22190E-03   0.1684E-05    3
  45.0     (0.52755E-02,-0.11866E-02)   0.22193E-03   0.6682E-05    3
  60.0     (0.52753E-02,-0.11970E-02)   0.22195E-03   0.1491E-04    3
  75.0     (0.52751E-02,-0.12046E-02)   0.22197E-03   0.2295E-04    3
  90.0     (0.52750E-02,-0.12074E-02)   0.22198E-03   0.2630E-04    3
**********************************************************************

                    FREQUENCY=30.0 GHZ
                  REF INDEX=(5.5810,-2.8482)
                EQUIVOLUMETRIC RADIUS=0.075 CM
                ------------------------------

ALPHA=0 DEGREES:

                    F(0,0)                   SCRS
                     (CM)                   (CMSQ)        TEST      LMAX
          (0.17007E-01,-0.78356E-02)   0.30933E-02   0.3460E-06    6

POLARIZATION 1:

  ALPHA          F(0,ALPHA)                SCRS
(DEGREES)          (CM)                   (CMSQ)        TEST      MMAX
  15.0     (0.16883E-01,-0.77986E-02)   0.30547E-02   0.6484E-06    3
  30.0     (0.16544E-01,-0.76977E-02)   0.29493E-02   0.7450E-05    3
  45.0     (0.16083E-01,-0.75602E-02)   0.28057E-02   0.2087E-04    3
  60.0     (0.15622E-01,-0.74231E-02)   0.26627E-02   0.2603E-04    3
  75.0     (0.15285E-01,-0.73230E-02)   0.25582E-02   0.3266E-04    3
  90.0     (0.15162E-01,-0.72865E-02)   0.25201E-02   0.3654E-04    3

POLARIZATION 2:

  ALPHA          F(0,ALPHA)                SCRS
(DEGREES)          (CM)                   (CMSQ)        TEST      MMAX
  15.0     (0.16986E-01,-0.78552E-02)   0.30938E-02   0.6872E-06    3
  30.0     (0.16929E-01,-0.79087E-02)   0.30952E-02   0.9497E-05    3
  45.0     (0.16851E-01,-0.79818E-02)   0.30971E-02   0.3758E-04    3
  60.0     (0.16773E-01,-0.80549E-02)   0.30990E-02   0.8365E-04    3
  75.0     (0.16716E-01,-0.81084E-02)   0.31004E-02   0.1284E-03    3
  90.0     (0.16695E-01,-0.81279E-02)   0.31009E-02   0.1471E-03    3
**********************************************************************
```

FREQUENCY=30.0 GHZ
REF INDEX=(5.5810,-2.8482)
EQUIVOLUMETRIC RADIUS=0.100 CM

ALPHA=0 DEGREES:

F(0,0) (CM)	SCRS (CMSQ)	TEST	LMAX
(0.35950E-01,-0.25300E-01)	0.19429E-01	0.3210E-05	6

POLARIZATION 1:

ALPHA (DEGREES)	F(0,ALPHA) (CM)	SCRS (CMSQ)	TEST	MMAX
15.0	(0.35529E-01,-0.25032E-01)	0.19078E-01	0.2404E-05	3
30.0	(0.34383E-01,-0.24301E-01)	0.18122E-01	0.2780E-04	3
45.0	(0.32823E-01,-0.23310E-01)	0.16826E-01	0.7852E-04	3
60.0	(0.31271E-01,-0.22326E-01)	0.15539E-01	0.1088E-03	3
75.0	(0.30139E-01,-0.21611E-01)	0.14604E-01	0.1657E-03	3
90.0	(0.29726E-01,-0.21350E-01)	0.14263E-01	0.1893E-03	3

POLARIZATION 2:

ALPHA (DEGREES)	F(0,ALPHA) (CM)	SCRS (CMSQ)	TEST	MMAX
15.0	(0.35846E-01,-0.25329E-01)	0.19412E-01	0.2545E-05	3
30.0	(0.35561E-01,-0.25407E-01)	0.19368E-01	0.3527E-04	3
45.0	(0.35174E-01,-0.25513E-01)	0.19307E-01	0.1402E-03	3
60.0	(0.34786E-01,-0.25620E-01)	0.19246E-01	0.3134E-03	3
75.0	(0.34503E-01,-0.25698E-01)	0.19202E-01	0.4828E-03	3
90.0	(0.34399E-01,-0.25726E-01)	0.19186E-01	0.5537E-03	3

****

FREQUENCY=30.0 GHZ
REF INDEX=(5.5810,-2.8482)
EQUIVOLUMETRIC RADIUS=0.125 CM

ALPHA=0 DEGREES:

F(0,0) (CM)	SCRS (CMSQ)	TEST	LMAX
(0.55696E-01,-0.62862E-01)	0.65520E-01	0.3243E-05	7

POLARIZATION 1:

ALPHA (DEGREES)	F(0,ALPHA) (CM)	SCRS (CMSQ)	TEST	MMAX

15.0	(0.54985E-01,-0.61796E-01)	0.64026E-01	0.7201E-05	3
30.0	(0.53048E-01,-0.58904E-01)	0.59975E-01	0.8134E-04	3
45.0	(0.50413E-01,-0.55000E-01)	0.54511E-01	0.2174E-03	3
60.0	(0.47791E-01,-0.51151E-01)	0.49125E-01	0.3479E-03	3
75.0	(0.45880E-01,-0.48368E-01)	0.45233E-01	0.5465E-03	3
90.0	(0.45182E-01,-0.47356E-01)	0.43819E-01	0.6315E-03	3

POLARIZATION 2:

ALPHA (DEGREES)	F(0,ALPHA) (CM)	SCRS (CMSQ)	TEST	MMAX
15.0	(0.55391E-01,-0.62807E-01)	0.65338E-01	0.7719E-05	3
30.0	(0.54562E-01,-0.62656E-01)	0.64843E-01	0.1088E-03	3
45.0	(0.53436E-01,-0.62449E-01)	0.64173E-01	0.4422E-03	3
60.0	(0.52316E-01,-0.62243E-01)	0.63509E-01	0.9203E-05	4
75.0	(0.51501E-01,-0.62091E-01)	0.63027E-01	0.1774E-04	4
90.0	(0.51203E-01,-0.62036E-01)	0.62852E-01	0.2185E-04	4

****

FREQUENCY=30.0 GHZ
REF INDEX=(5.5810,-2.8482)
EQUIVOLUMETRIC RADIUS=0.150 CM

ALPHA=0 DEGREES:

F(0,0) (CM)	SCRS (CMSQ)	TEST	LMAX
(0.61077E-01,-0.11510E+00)	0.13901E+00	0.1522E-04	7

POLARIZATION 1:

ALPHA (DEGREES)	F(0,ALPHA) (CM)	SCRS (CMSQ)	TEST	MMAX
15.0	(0.60615E-01,-0.11281E+00)	0.13551E+00	0.2149E-04	3
30.0	(0.59331E-01,-0.10663E+00)	0.12608E+00	0.2277E-03	3
45.0	(0.57529E-01,-0.98345E-01)	0.11345E+00	0.5235E-03	3
60.0	(0.55673E-01,-0.90244E-01)	0.10113E+00	0.8179E-03	3
75.0	(0.54281E-01,-0.84430E-01)	0.92297E-01	0.1887E-04	4
90.0	(0.53765E-01,-0.82326E-01)	0.89104E-01	0.2345E-04	4

POLARIZATION 2:

ALPHA (DEGREES)	F(0,ALPHA) (CM)	SCRS (CMSQ)	TEST	MMAX
15.0	(0.60552E-01,-0.11474E+00)	0.13832E+00	0.2372E-04	3
30.0	(0.59127E-01,-0.11376E+00)	0.13646E+00	0.3437E-03	3
45.0	(0.57201E-01,-0.11245E+00)	0.13394E+00	0.1347E-04	4
60.0	(0.55296E-01,-0.11115E+00)	0.13147E+00	0.4656E-04	4
75.0	(0.53917E-01,-0.11022E+00)	0.12969E+00	0.9126E-04	4
90.0	(0.53415E-01,-0.10988E+00)	0.12904E+00	0.1131E-03	4

****

FREQUENCY=30.0 GHZ
REF INDEX=(5.5810,-2.8482)
EQUIVOLUMETRIC RADIUS=0.175 CM

ALPHA=0 DEGREES:

F(0,0) (CM)	SCRS (CMSQ)	TEST	LMAX
(0.52761E-01,-0.16621E+00)	0.21670E+00	0.1565E-04	8

POLARIZATION 1:

ALPHA (DEGREES)	F(0,ALPHA) (CM)	SCRS (CMSQ)	TEST	MMAX
15.0	(0.53049E-01,-0.16275E+00)	0.21094E+00	0.6776E-04	3
30.0	(0.53708E-01,-0.15343E+00)	0.19545E+00	0.6592E-03	3
45.0	(0.54316E-01,-0.14104E+00)	0.17492E+00	0.2226E-04	4
60.0	(0.54594E-01,-0.12901E+00)	0.15509E+00	0.3201E-04	4
75.0	(0.54596E-01,-0.12044E+00)	0.14101E+00	0.6290E-04	4
90.0	(0.54555E-01,-0.11735E+00)	0.13595E+00	0.7808E-04	4

POLARIZATION 2:

ALPHA (DEGREES)	F(0,ALPHA) (CM)	SCRS (CMSQ)	TEST	MMAX
15.0	(0.52143E-01,-0.16532E+00)	0.21506E+00	0.7758E-04	3
30.0	(0.50463E-01,-0.16292E+00)	0.21064E+00	0.7635E-05	4
45.0	(0.48181E-01,-0.15973E+00)	0.20474E+00	0.6443E-04	4
60.0	(0.45917E-01,-0.15664E+00)	0.19899E+00	0.2298E-03	4
75.0	(0.44270E-01,-0.15443E+00)	0.19488E+00	0.4612E-03	4
90.0	(0.43669E-01,-0.15364E+00)	0.19340E+00	0.5767E-03	4

****

FREQUENCY=30.0 GHZ
REF INDEX=(5.5810,-2.8482)
EQUIVOLUMETRIC RADIUS=0.200 CM

ALPHA=0 DEGREES:

F(0,0) (CM)	SCRS (CMSQ)	TEST	LMAX
(0.43510E-01,-0.21202E+00)	0.28685E+00	0.8485E-04	8

POLARIZATION 1:

ALPHA	F(0,ALPHA)	SCRS

(DEGREES)	(CM)	(CMSQ)	TEST	MMAX
15.0	(0.44787E-01,-0.20746E+00)	0.27871E+00	0.2005E-03	3
30.0	(0.47888E-01,-0.19519E+00)	0.25692E+00	0.1676E-04	4
45.0	(0.51241E-01,-0.17885E+00)	0.22816E+00	0.6318E-04	4
60.0	(0.53621E-01,-0.16299E+00)	0.20056E+00	0.8803E-04	4
75.0	(0.54775E-01,-0.15168E+00)	0.18107E+00	0.1884E-03	4
90.0	(0.55078E-01,-0.14761E+00)	0.17408E+00	0.3286E-03	4

POLARIZATION 2:

ALPHA (DEGREES)	F(0,ALPHA) (CM)	SCRS (CMSQ)	TEST	MMAX
15.0	(0.43098E-01,-0.21049E+00)	0.28394E+00	0.2379E-03	3
30.0	(0.41933E-01,-0.20641E+00)	0.27613E+00	0.3031E-04	4
45.0	(0.40258E-01,-0.20104E+00)	0.26580E+00	0.2584E-03	4
60.0	(0.38488E-01,-0.19590E+00)	0.25586E+00	0.9313E-03	4
75.0	(0.37137E-01,-0.19229E+00)	0.24882E+00	0.3626E-04	5
90.0	(0.36631E-01,-0.19099E+00)	0.24630E+00	0.4847E-04	5

****

FREQUENCY=30.0 GHZ
REF INDEX=(5.5810,-2.8482)
EQUIVOLUMETRIC RADIUS=0.225 CM

ALPHA=0 DEGREES:

F(0,0) (CM)	SCRS (CMSQ)	TEST	LMAX
(0.40358E-01,-0.25970E+00)	0.35756E+00	0.8953E-04	9

POLARIZATION 1:

ALPHA (DEGREES)	F(0,ALPHA) (CM)	SCRS (CMSQ)	TEST	MMAX
15.0	(0.42884E-01,-0.25409E+00)	0.34689E+00	0.4841E-03	3
30.0	(0.48933E-01,-0.23879E+00)	0.31819E+00	0.4466E-04	4
45.0	(0.55271E-01,-0.21801E+00)	0.28002E+00	0.1390E-03	4
60.0	(0.59522E-01,-0.19740E+00)	0.24306E+00	0.2077E-03	4
75.0	(0.61395E-01,-0.18245E+00)	0.21677E+00	0.7009E-03	4
90.0	(0.61830E-01,-0.17702E+00)	0.20731E+00	0.2022E-04	5

POLARIZATION 2:

ALPHA (DEGREES)	F(0,ALPHA) (CM)	SCRS (CMSQ)	TEST	MMAX
15.0	(0.40459E-01,-0.25777E+00)	0.35352E+00	0.5917E-03	3
30.0	(0.40558E-01,-0.25261E+00)	0.34273E+00	0.9135E-04	4
45.0	(0.40295E-01,-0.24587E+00)	0.32852E+00	0.7590E-03	4
60.0	(0.39599E-01,-0.23945E+00)	0.31490E+00	0.5428E-04	5
75.0	(0.38829E-01,-0.23494E+00)	0.30529E+00	0.1333E-03	5

90.0	(0.38494E-01,-0.23333E+00)	0.30185E+00	0.1777E-03	5

****

FREQUENCY=30.0 GHZ
REF INDEX=(5.5810,-2.8482)
EQUIVOLUMETRIC RADIUS=0.250 CM

ALPHA=0 DEGREES:

F(0,0) (CM)	SCRS (CMSQ)	TEST	LMAX
(0.42026E-01,-0.31660E+00)	0.43998E+00	0.4620E-03	9

POLARIZATION 1:

ALPHA (DEGREES)	F(0,ALPHA) (CM)	SCRS (CMSQ)	TEST	MMAX
15.0	(0.45981E-01,-0.31015E+00)	0.42694E+00	0.9848E-03	3
30.0	(0.55388E-01,-0.29201E+00)	0.39117E+00	0.9899E-04	4
45.0	(0.65096E-01,-0.26617E+00)	0.34222E+00	0.2585E-03	4
60.0	(0.71437E-01,-0.23935E+00)	0.29342E+00	0.4295E-03	4
75.0	(0.74099E-01,-0.21925E+00)	0.25794E+00	0.4258E-04	5
90.0	(0.74678E-01,-0.21182E+00)	0.24502E+00	0.7447E-04	5

POLARIZATION 2:

ALPHA (DEGREES)	F(0,ALPHA) (CM)	SCRS (CMSQ)	TEST	MMAX
15.0	(0.42531E-01,-0.31478E+00)	0.43557E+00	0.4313E-05	4
30.0	(0.43496E-01,-0.30984E+00)	0.42362E+00	0.2260E-03	4
45.0	(0.43887E-01,-0.30314E+00)	0.40760E+00	0.3186E-04	5
60.0	(0.43295E-01,-0.29652E+00)	0.39192E+00	0.1656E-03	5
75.0	(0.42289E-01,-0.29173E+00)	0.38068E+00	0.4091E-03	5
90.0	(0.41807E-01,-0.28998E+00)	0.37662E+00	0.5473E-03	5

****

FREQUENCY=30.0 GHZ
REF INDEX=(5.5810,-2.8482)
EQUIVOLUMETRIC RADIUS=0.275 CM

ALPHA=0 DEGREES:

F(0,0) (CM)	SCRS (CMSQ)	TEST	LMAX
(0.43263E-01,-0.38553E+00)	0.53990E+00	0.2522E-03	11

POLARIZATION 1:

ALPHA (DEGREES)	F(0,ALPHA) (CM)	SCRS (CMSQ)	TEST	MMAX
15.0	(0.48511E-01,-0.37843E+00)	0.52484E+00	0.8009E-05	4
30.0	(0.61130E-01,-0.35751E+00)	0.48226E+00	0.2108E-03	4
45.0	(0.74465E-01,-0.32585E+00)	0.42132E+00	0.4706E-03	4
60.0	(0.83551E-01,-0.29134E+00)	0.35817E+00	0.8485E-03	4
75.0	(0.87664E-01,-0.26471E+00)	0.31108E+00	0.1347E-03	5
90.0	(0.88658E-01,-0.25472E+00)	0.29375E+00	0.2211E-03	5

POLARIZATION 2:

ALPHA (DEGREES)	F(0,ALPHA) (CM)	SCRS (CMSQ)	TEST	MMAX
15.0	(0.43440E-01,-0.38402E+00)	0.53574E+00	0.1037E-04	4
30.0	(0.43337E-01,-0.37958E+00)	0.52395E+00	0.5566E-03	4
45.0	(0.41911E-01,-0.37279E+00)	0.50701E+00	0.9961E-04	5
60.0	(0.39154E-01,-0.36532E+00)	0.48931E+00	0.5472E-03	5
75.0	(0.36382E-01,-0.35951E+00)	0.47599E+00	0.3810E-04	6
90.0	(0.35220E-01,-0.35731E+00)	0.47105E+00	0.5564E-04	6

****

FREQUENCY=30.0 GHZ
REF INDEX=(5.5810,-2.8482)
EQUIVOLUMETRIC RADIUS=0.300 CM

ALPHA=0 DEGREES:

F(0,0) (CM)	SCRS (CMSQ)	TEST	LMAX
(0.39793E-01,-0.46392E+00)	0.65518E+00	0.3059E-03	12

POLARIZATION 1:

ALPHA (DEGREES)	F(0,ALPHA) (CM)	SCRS (CMSQ)	TEST	MMAX
15.0	(0.46130E-01,-0.45607E+00)	0.63825E+00	0.1951E-04	4
30.0	(0.61765E-01,-0.43185E+00)	0.58852E+00	0.4701E-03	4
45.0	(0.79041E-01,-0.39324E+00)	0.51400E+00	0.9137E-03	4
60.0	(0.91503E-01,-0.34970E+00)	0.43414E+00	0.6286E-04	5
75.0	(0.97549E-01,-0.31553E+00)	0.37355E+00	0.3779E-03	5
90.0	(0.99114E-01,-0.30264E+00)	0.35109E+00	0.5965E-03	5

POLARIZATION 2:

ALPHA (DEGREES)	F(0,ALPHA) (CM)	SCRS (CMSQ)	TEST	MMAX
15.0	(0.38968E-01,-0.46214E+00)	0.65087E+00	0.2695E-04	4
30.0	(0.36266E-01,-0.45644E+00)	0.63775E+00	0.1942E-04	5
45.0	(0.31575E-01,-0.44695E+00)	0.61710E+00	0.3634E-03	5
60.0	(0.25823E-01,-0.43591E+00)	0.59401E+00	0.6001E-04	6

```
   75.0     (0.20994E-01,-0.42707E+00)   0.57592E+00   0.2197E-03    6
   90.0     (0.19104E-01,-0.42371E+00)   0.56910E+00   0.3411E-03    6
*************************************************************************

                    FREQUENCY=30.0 GHZ
                  REF INDEX=(5.5810,-2.8482)
                EQUIVOLUMETRIC RADIUS=0.325 CM
                ------------------------------

 ALPHA=0 DEGREES:

                      F(0,0)                      SCRS
                       (CM)                      (CMSQ)          TEST        LMAX
          (0.32316E-01,-0.54758E+00)   0.78012E+00   0.7457E-03    13

 POLARIZATION 1:

  ALPHA                F(0,ALPHA)                  SCRS
 (DEGREES)              (CM)                      (CMSQ)          TEST        MMAX
   15.0     (0.39691E-01,-0.53883E+00)   0.76128E+00   0.5045E-04    4
   30.0     (0.58549E-01,-0.51069E+00)   0.70361E+00   0.1637E-04    5
   45.0     (0.80398E-01,-0.46387E+00)   0.61322E+00   0.6048E-04    5
   60.0     (0.96687E-01,-0.40967E+00)   0.51353E+00   0.1792E-03    5
   75.0     (0.10462E+00,-0.36659E+00)   0.43691E+00   0.9621E-03    5
   90.0     (0.10663E+00,-0.35029E+00)   0.40840E+00   0.5608E-04    6

 POLARIZATION 2:

  ALPHA                F(0,ALPHA)                  SCRS
 (DEGREES)              (CM)                      (CMSQ)          TEST        MMAX
   15.0     (0.30519E-01,-0.54474E+00)   0.77468E+00   0.7682E-04    4
   30.0     (0.25644E-01,-0.53578E+00)   0.75746E+00   0.7098E-04    5
   45.0     (0.18864E-01,-0.52126E+00)   0.72934E+00   0.3304E-04    6
   60.0     (0.11677E-01,-0.50481E+00)   0.69726E+00   0.4046E-03    6
   75.0     (0.60260E-02,-0.49193E+00)   0.67198E+00   0.6668E-04    7
   90.0     (0.38588E-02,-0.48710E+00)   0.66246E+00   0.1573E-03    7
*************************************************************************

                    FREQUENCY=30.0 GHZ
                  REF INDEX=(5.5810,-2.8482)
                EQUIVOLUMETRIC RADIUS=0.350 CM
                ------------------------------

 ALPHA=0 DEGREES:

                      F(0,0)                      SCRS
                       (CM)                      (CMSQ)          TEST        LMAX
          (0.24827E-01,-0.63553E+00)   0.91235E+00   0.5502E-03    14

 POLARIZATION 1:
```

ALPHA (DEGREES)	F(0,ALPHA) (CM)	SCRS (CMSQ)	TEST	MMAX
15.0	(0.33119E-01,-0.62589E+00)	0.89167E+00	0.1303E-03	4
30.0	(0.55376E-01,-0.59360E+00)	0.82543E+00	0.4127E-04	5
45.0	(0.82572E-01,-0.53749E+00)	0.71648E+00	0.1271E-03	5
60.0	(0.10333E+00,-0.47056E+00)	0.59265E+00	0.4535E-03	5
75.0	(0.11321E+00,-0.41645E+00)	0.49607E+00	0.9468E-04	6
90.0	(0.11558E+00,-0.39581E+00)	0.45993E+00	0.1574E-03	6

POLARIZATION 2:

ALPHA (DEGREES)	F(0,ALPHA) (CM)	SCRS (CMSQ)	TEST	MMAX
15.0	(0.22434E-01,-0.63134E+00)	0.90527E+00	0.2251E-03	4
30.0	(0.16537E-01,-0.61877E+00)	0.88291E+00	0.2698E-03	5
45.0	(0.92324E-02,-0.59945E+00)	0.84650E+00	0.1927E-03	6
60.0	(0.18275E-02,-0.57842E+00)	0.80515E+00	0.2016E-03	7
75.0	(-.41176E-02,-0.56233E+00)	0.77275E+00	0.3274E-03	7
90.0	(-.64582E-02,-0.55634E+00)	0.76057E+00	0.3147E-03	7

****

FREQUENCY=45.0 GHZ
REF INDEX=(4.6241,-2.6437)
EQUIVOLUMETRIC RADIUS=0.025 CM

ALPHA=0 DEGREES:

F(0,0) (CM)	SCRS (CMSQ)	TEST	LMAX
(0.13937E-02,-0.21231E-03)	0.15739E-04	0.1166E-06	5

POLARIZATION 1:

ALPHA (DEGREES)	F(0,ALPHA) (CM)	SCRS (CMSQ)	TEST	MMAX
15.0	(0.13911E-02,-0.21176E-03)	0.15677E-04	0.2869E-03	2
30.0	(0.13838E-02,-0.21026E-03)	0.15508E-04	0.8666E-03	2
45.0	(0.13738E-02,-0.20821E-03)	0.15277E-04	0.1092E-05	3
60.0	(0.13638E-02,-0.20616E-03)	0.15046E-04	0.1258E-05	3
75.0	(0.13565E-02,-0.20466E-03)	0.14878E-04	0.9638E-03	2
90.0	(0.13538E-02,-0.20411E-03)	0.14816E-04	0.8788E-03	2

POLARIZATION 2:

ALPHA (DEGREES)	F(0,ALPHA) (CM)	SCRS (CMSQ)	TEST	MMAX
15.0	(0.13938E-02,-0.21244E-03)	0.15739E-04	0.3064E-03	2
30.0	(0.13938E-02,-0.21279E-03)	0.15738E-04	0.5337E-06	3
45.0	(0.13939E-02,-0.21327E-03)	0.15736E-04	0.2128E-05	3
60.0	(0.13940E-02,-0.21375E-03)	0.15735E-04	0.4771E-05	3
75.0	(0.13941E-02,-0.21410E-03)	0.15734E-04	0.7365E-05	3
90.0	(0.13941E-02,-0.21423E-03)	0.15733E-04	0.8453E-05	3

****

FREQUENCY=45.0 GHZ
REF INDEX=(4.6241,-2.6437)
EQUIVOLUMETRIC RADIUS=0.050 CM

ALPHA=0 DEGREES:

F(0,0) (CM)	SCRS (CMSQ)	TEST	LMAX
(0.11620E-01,-0.47411E-02)	0.12633E-02	0.5677E-07	6

POLARIZATION 1:

ALPHA (DEGREES)	F(0,ALPHA) (CM)	SCRS (CMSQ)	TEST	MMAX
15.0	(0.11568E-01,-0.47219E-02)	0.12525E-02	0.5895E-06	3

30.0	(0.11426E-01,-0.46694E-02)	0.12228E-02	0.6693E-05	3
45.0	(0.11233E-01,-0.45978E-02)	0.11824E-02	0.1836E-04	3
60.0	(0.11040E-01,-0.45263E-02)	0.11420E-02	0.2202E-04	3
75.0	(0.10899E-01,-0.44741E-02)	0.11125E-02	0.2477E-04	3
90.0	(0.10847E-01,-0.44550E-02)	0.11017E-02	0.2687E-04	3

POLARIZATION 2:

ALPHA (DEGREES)	F(0,ALPHA) (CM)	SCRS (CMSQ)	TEST	MMAX
15.0	(0.11615E-01,-0.47490E-02)	0.12633E-02	0.6275E-06	3
30.0	(0.11600E-01,-0.47706E-02)	0.12632E-02	0.8678E-05	3
45.0	(0.11581E-01,-0.48000E-02)	0.12631E-02	0.3438E-04	3
60.0	(0.11561E-01,-0.48294E-02)	0.12630E-02	0.7661E-04	3
75.0	(0.11547E-01,-0.48509E-02)	0.12629E-02	0.1177E-03	3
90.0	(0.11542E-01,-0.48588E-02)	0.12629E-02	0.1349E-03	3

****

FREQUENCY=45.0 GHZ
REF INDEX=(4.6241,-2.6437)
EQUIVOLUMETRIC RADIUS=0.075 CM

ALPHA=0 DEGREES:

F(0,0) (CM)	SCRS (CMSQ)	TEST	LMAX
(0.31954E-01,-0.28151E-01)	0.16242E-01	0.8001E-07	7

POLARIZATION 1:

ALPHA (DEGREES)	F(0,ALPHA) (CM)	SCRS (CMSQ)	TEST	MMAX
15.0	(0.31709E-01,-0.27891E-01)	0.16014E-01	0.3831E-05	3
30.0	(0.31042E-01,-0.27183E-01)	0.15394E-01	0.4350E-04	3
45.0	(0.30133E-01,-0.26221E-01)	0.14551E-01	0.1193E-03	3
60.0	(0.29228E-01,-0.25266E-01)	0.13714E-01	0.1425E-03	3
75.0	(0.28567E-01,-0.24571E-01)	0.13106E-01	0.1867E-03	3
90.0	(0.28326E-01,-0.24318E-01)	0.12883E-01	0.2106E-03	3

POLARIZATION 2:

ALPHA (DEGREES)	F(0,ALPHA) (CM)	SCRS (CMSQ)	TEST	MMAX
15.0	(0.31881E-01,-0.28165E-01)	0.16228E-01	0.4079E-05	3
30.0	(0.31681E-01,-0.28203E-01)	0.16188E-01	0.5652E-04	3
45.0	(0.31409E-01,-0.28255E-01)	0.16135E-01	0.2245E-03	3
60.0	(0.31137E-01,-0.28307E-01)	0.16081E-01	0.5017E-03	3
75.0	(0.30939E-01,-0.28345E-01)	0.16042E-01	0.7726E-03	3
90.0	(0.30866E-01,-0.28358E-01)	0.16028E-01	0.8860E-03	3

****

FREQUENCY=45.0 GHZ
REF INDEX=(4.6241,-2.6437)
EQUIVOLUMETRIC RADIUS=0.100 CM

ALPHA=0 DEGREES:

F(0,0) (CM)	SCRS (CMSQ)	TEST	LMAX
(0.39334E-01,-0.76675E-01)	0.58178E-01	0.7063E-06	7

POLARIZATION 1:

ALPHA (DEGREES)	F(0,ALPHA) (CM)	SCRS (CMSQ)	TEST	MMAX
15.0	(0.39204E-01,-0.75698E-01)	0.57202E-01	0.2223E-04	3
30.0	(0.38842E-01,-0.73048E-01)	0.54557E-01	0.2406E-03	3
45.0	(0.38329E-01,-0.69474E-01)	0.50993E-01	0.5980E-03	3
60.0	(0.37795E-01,-0.65952E-01)	0.47484E-01	0.5821E-03	3
75.0	(0.37392E-01,-0.63406E-01)	0.44950E-01	0.8793E-03	3
90.0	(0.37242E-01,-0.62482E-01)	0.44030E-01	0.1290E-04	4

POLARIZATION 2:

ALPHA (DEGREES)	F(0,ALPHA) (CM)	SCRS (CMSQ)	TEST	MMAX
15.0	(0.39109E-01,-0.76538E-01)	0.57993E-01	0.2420E-04	3
30.0	(0.38497E-01,-0.76167E-01)	0.57490E-01	0.3418E-03	3
45.0	(0.37665E-01,-0.75665E-01)	0.56809E-01	0.1214E-04	4
60.0	(0.36839E-01,-0.75167E-01)	0.56135E-01	0.4113E-04	4
75.0	(0.36238E-01,-0.74806E-01)	0.55647E-01	0.7944E-04	4
90.0	(0.36018E-01,-0.74674E-01)	0.55469E-01	0.9794E-04	4

****

FREQUENCY=45.0 GHZ
REF INDEX=(4.6241,-2.6437)
EQUIVOLUMETRIC RADIUS=0.125 CM

ALPHA=0 DEGREES:

F(0,0) (CM)	SCRS (CMSQ)	TEST	LMAX
(0.31007E-01,-0.12227E+00)	0.10225E+00	0.2276E-05	8

POLARIZATION 1:

ALPHA (DEGREES)	F(0,ALPHA) (CM)	SCRS (CMSQ)	TEST	MMAX

15.0	(0.31418E-01,-0.12066E+00)	0.10043E+00	0.1201E-03	3
30.0	(0.32471E-01,-0.11630E+00)	0.95516E-01	0.9334E-05	4
45.0	(0.33747E-01,-0.11044E+00)	0.88940E-01	0.4313E-04	4
60.0	(0.34841E-01,-0.10468E+00)	0.82525E-01	0.5437E-04	4
75.0	(0.35528E-01,-0.10053E+00)	0.77928E-01	0.7033E-04	4
90.0	(0.35756E-01,-0.99028E-01)	0.76266E-01	0.8581E-04	4

POLARIZATION 2:

ALPHA (DEGREES)	F(0,ALPHA) (CM)	SCRS (CMSQ)	TEST	MMAX
15.0	(0.30790E-01,-0.12181E+00)	0.10167E+00	0.1364E-03	3
30.0	(0.30197E-01,-0.12055E+00)	0.10009E+00	0.1427E-04	4
45.0	(0.29384E-01,-0.11886E+00)	0.97963E-01	0.1164E-03	4
60.0	(0.28566E-01,-0.11722E+00)	0.95882E-01	0.4014E-03	4
75.0	(0.27966E-01,-0.11604E+00)	0.94385E-01	0.7856E-03	4
90.0	(0.27745E-01,-0.11561E+00)	0.93842E-01	0.9733E-03	4

****

FREQUENCY=45.0 GHZ
REF INDEX=(4.6241,-2.6437)
EQUIVOLUMETRIC RADIUS=0.150 CM

ALPHA=0 DEGREES:

F(0,0) (CM)	SCRS (CMSQ)	TEST	LMAX
(0.28735E-01,-0.16601E+00)	0.14324E+00	0.8329E-06	9

POLARIZATION 1:

ALPHA (DEGREES)	F(0,ALPHA) (CM)	SCRS (CMSQ)	TEST	MMAX
15.0	(0.29803E-01,-0.16382E+00)	0.14047E+00	0.4298E-03	3
30.0	(0.32495E-01,-0.15782E+00)	0.13296E+00	0.4275E-04	4
45.0	(0.35647E-01,-0.14959E+00)	0.12285E+00	0.1616E-03	4
60.0	(0.38217E-01,-0.14133E+00)	0.11292E+00	0.1581E-03	4
75.0	(0.39745E-01,-0.13528E+00)	0.10576E+00	0.3501E-03	4
90.0	(0.40232E-01,-0.13306E+00)	0.10317E+00	0.6404E-03	4

POLARIZATION 2:

ALPHA (DEGREES)	F(0,ALPHA) (CM)	SCRS (CMSQ)	TEST	MMAX
15.0	(0.28752E-01,-0.16532E+00)	0.14222E+00	0.5065E-03	3
30.0	(0.28758E-01,-0.16347E+00)	0.13948E+00	0.7510E-04	4
45.0	(0.28664E-01,-0.16101E+00)	0.13583E+00	0.6078E-03	4
60.0	(0.28459E-01,-0.15863E+00)	0.13227E+00	0.3966E-04	5
75.0	(0.28241E-01,-0.15693E+00)	0.12972E+00	0.9484E-04	5
90.0	(0.28147E-01,-0.15632E+00)	0.12880E+00	0.1252E-03	5

****

FREQUENCY=45.0 GHZ
REF INDEX=(4.6241,-2.6437)
EQUIVOLUMETRIC RADIUS=0.175 CM

ALPHA=0 DEGREES:

F(0,0) (CM)	SCRS (CMSQ)	TEST	LMAX
(0.32933E-01,-0.22322E+00)	0.19460E+00	0.8512E-05	9

POLARIZATION 1:

ALPHA (DEGREES)	F(0,ALPHA) (CM)	SCRS (CMSQ)	TEST	MMAX
15.0	(0.34734E-01,-0.22051E+00)	0.19089E+00	0.4108E-05	4
30.0	(0.39270E-01,-0.21280E+00)	0.18059E+00	0.1283E-03	4
45.0	(0.44581E-01,-0.20162E+00)	0.16623E+00	0.3938E-03	4
60.0	(0.48913E-01,-0.18977E+00)	0.15159E+00	0.4601E-03	4
75.0	(0.51487E-01,-0.18074E+00)	0.14075E+00	0.3418E-04	5
90.0	(0.52307E-01,-0.17737E+00)	0.13675E+00	0.6747E-04	5

POLARIZATION 2:

ALPHA (DEGREES)	F(0,ALPHA) (CM)	SCRS (CMSQ)	TEST	MMAX
15.0	(0.32983E-01,-0.22268E+00)	0.19352E+00	0.4905E-05	4
30.0	(0.32993E-01,-0.22115E+00)	0.19056E+00	0.2587E-03	4
45.0	(0.32724E-01,-0.21899E+00)	0.18648E+00	0.3803E-04	5
60.0	(0.32148E-01,-0.21674E+00)	0.18237E+00	0.1951E-03	5
75.0	(0.31542E-01,-0.21505E+00)	0.17934E+00	0.4744E-03	5
90.0	(0.31284E-01,-0.21442E+00)	0.17824E+00	0.6301E-03	5

****

FREQUENCY=45.0 GHZ
REF INDEX=(4.6241,-2.6437)
EQUIVOLUMETRIC RADIUS=0.200 CM

ALPHA=0 DEGREES:

F(0,0) (CM)	SCRS (CMSQ)	TEST	LMAX
(0.31666E-01,-0.29511E+00)	0.26107E+00	0.9249E-04	10

POLARIZATION 1:

ALPHA	F(0,ALPHA)	SCRS

(DEGREES)	(CM)	(CMSQ)	TEST	MMAX
15.0	(0.34081E-01,-0.29180E+00)	0.25646E+00	0.1382E-04	4
30.0	(0.40343E-01,-0.28203E+00)	0.24326E+00	0.3910E-03	4
45.0	(0.48053E-01,-0.26716E+00)	0.22403E+00	0.9649E-03	4
60.0	(0.54731E-01,-0.25078E+00)	0.20369E+00	0.4250E-04	5
75.0	(0.58932E-01,-0.23797E+00)	0.18824E+00	0.2129E-03	5
90.0	(0.60321E-01,-0.23313E+00)	0.18249E+00	0.3583E-03	5

POLARIZATION 2:

ALPHA (DEGREES)	F(0,ALPHA) (CM)	SCRS (CMSQ)	TEST	MMAX
15.0	(0.31106E-01,-0.29443E+00)	0.25993E+00	0.1745E-04	4
30.0	(0.29490E-01,-0.29236E+00)	0.25660E+00	0.9718E-03	4
45.0	(0.27083E-01,-0.28910E+00)	0.25159E+00	0.2024E-03	5
60.0	(0.24459E-01,-0.28541E+00)	0.24612E+00	0.2747E-04	6
75.0	(0.22408E-01,-0.28246E+00)	0.24187E+00	0.8827E-04	6
90.0	(0.21631E-01,-0.28134E+00)	0.24026E+00	0.1288E-03	6

****

FREQUENCY=45.0 GHZ
REF INDEX=(4.6241,-2.6437)
EQUIVOLUMETRIC RADIUS=0.225 CM

ALPHA=0 DEGREES:

F(0,0) (CM)	SCRS (CMSQ)	TEST	LMAX
(0.24762E-01,-0.37181E+00)	0.33436E+00	0.7024E-03	10

POLARIZATION 1:

ALPHA (DEGREES)	F(0,ALPHA) (CM)	SCRS (CMSQ)	TEST	MMAX
15.0	(0.27805E-01,-0.36767E+00)	0.32868E+00	0.5023E-04	4
30.0	(0.35980E-01,-0.35519E+00)	0.31195E+00	0.1986E-04	5
45.0	(0.46534E-01,-0.33562E+00)	0.28665E+00	0.9133E-04	5
60.0	(0.55991E-01,-0.31353E+00)	0.25908E+00	0.1312E-03	5
75.0	(0.62015E-01,-0.29599E+00)	0.23778E+00	0.9421E-03	5
90.0	(0.64001E-01,-0.28933E+00)	0.22980E+00	0.5029E-04	6

POLARIZATION 2:

ALPHA (DEGREES)	F(0,ALPHA) (CM)	SCRS (CMSQ)	TEST	MMAX
15.0	(0.23701E-01,-0.37033E+00)	0.33259E+00	0.6867E-04	4
30.0	(0.20918E-01,-0.36603E+00)	0.32731E+00	0.6126E-04	5
45.0	(0.17311E-01,-0.35964E+00)	0.31924E+00	0.2495E-04	6
60.0	(0.13821E-01,-0.35278E+00)	0.31033E+00	0.2333E-03	6
75.0	(0.11284E-01,-0.34753E+00)	0.30339E+00	0.8388E-03	6

```
  90.0     (0.10352E-01,-0.34557E+00)   0.30077E+00   0.3895E-04    7
**********************************************************************

                        FREQUENCY=45.0 GHZ
                    REF INDEX=(4.6241,-2.6437)
                  EQUIVOLUMETRIC RADIUS=0.250 CM
                  ------------------------------

ALPHA=0 DEGREES:

                      F(0,0)                    SCRS
                       (CM)                    (CMSQ)        TEST      LMAX
          (0.21041E-01,-0.45377E+00)   0.41255E+00   0.1784E-03    12

POLARIZATION 1:

  ALPHA            F(0,ALPHA)                SCRS
(DEGREES)           (CM)                    (CMSQ)        TEST      MMAX
  15.0     (0.24676E-01,-0.44872E+00)   0.40561E+00   0.1542E-03    4
  30.0     (0.34899E-01,-0.43319E+00)   0.38464E+00   0.6399E-04    5
  45.0     (0.48833E-01,-0.40812E+00)   0.35174E+00   0.2294E-03    5
  60.0     (0.61766E-01,-0.37895E+00)   0.31477E+00   0.5858E-03    5
  75.0     (0.70100E-01,-0.35526E+00)   0.28563E+00   0.1275E-03    6
  90.0     (0.72849E-01,-0.34614E+00)   0.27461E+00   0.2137E-03    6

POLARIZATION 2:

  ALPHA            F(0,ALPHA)                SCRS
(DEGREES)           (CM)                    (CMSQ)        TEST      MMAX
  15.0     (0.19767E-01,-0.45157E+00)   0.41006E+00   0.2258E-03    4
  30.0     (0.16508E-01,-0.44546E+00)   0.40279E+00   0.2571E-03    5
  45.0     (0.12362E-01,-0.43693E+00)   0.39187E+00   0.1432E-03    6
  60.0     (0.82806E-02,-0.42815E+00)   0.37998E+00   0.4586E-04    7
  75.0     (0.51868E-02,-0.42158E+00)   0.37076E+00   0.2651E-03    7
  90.0     (0.40136E-02,-0.41915E+00)   0.36729E+00   0.5146E-03    7
**********************************************************************

                        FREQUENCY=45.0 GHZ
                    REF INDEX=(4.6241,-2.6437)
                  EQUIVOLUMETRIC RADIUS=0.275 CM
                  ------------------------------

ALPHA=0 DEGREES:

                      F(0,0)                    SCRS
                       (CM)                    (CMSQ)        TEST      LMAX
          (0.21202E-01,-0.54894E+00)   0.50242E+00   0.9958E-04    13

POLARIZATION 1:
```

ALPHA (DEGREES)	F(0,ALPHA) (CM)	SCRS (CMSQ)	TEST	MMAX
15.0	(0.25082E-01,-0.54270E+00)	0.49389E+00	0.3807E-03	4
30.0	(0.36796E-01,-0.52348E+00)	0.46775E+00	0.1758E-03	5
45.0	(0.54110E-01,-0.49197E+00)	0.42584E+00	0.5205E-03	5
60.0	(0.71132E-01,-0.45446E+00)	0.37769E+00	0.6839E-04	6
75.0	(0.82457E-01,-0.42341E+00)	0.33915E+00	0.4412E-03	6
90.0	(0.86239E-01,-0.41135E+00)	0.32445E+00	0.7064E-03	6

POLARIZATION 2:

ALPHA (DEGREES)	F(0,ALPHA) (CM)	SCRS (CMSQ)	TEST	MMAX
15.0	(0.19160E-01,-0.54616E+00)	0.49942E+00	0.5863E-03	4
30.0	(0.13671E-01,-0.53854E+00)	0.49070E+00	0.9362E-03	5
45.0	(0.61890E-02,-0.52784E+00)	0.47755E+00	0.2479E-04	7
60.0	(-.15159E-02,-0.51654E+00)	0.46292E+00	0.3020E-04	8
75.0	(-.74167E-02,-0.50781E+00)	0.45129E+00	0.8137E-03	7
90.0	(-.96457E-02,-0.50451E+00)	0.44685E+00	0.9366E-03	7

****

FREQUENCY=45.0 GHZ
REF INDEX=(4.6241,-2.6437)
EQUIVOLUMETRIC RADIUS=0.300 CM

ALPHA=0 DEGREES:

F(0,0) (CM)	SCRS (CMSQ)	TEST	LMAX
(0.19129E-01,-0.65924E+00)	0.60764E+00	0.2566E-03	14

POLARIZATION 1:

ALPHA (DEGREES)	F(0,ALPHA) (CM)	SCRS (CMSQ)	TEST	MMAX
15.0	(0.23034E-01,-0.65101E+00)	0.59666E+00	0.9267E-03	4
30.0	(0.35954E-01,-0.62644E+00)	0.56361E+00	0.4922E-03	5
45.0	(0.56787E-01,-0.58681E+00)	0.51095E+00	0.5318E-04	6
60.0	(0.78233E-01,-0.53925E+00)	0.44988E+00	0.2526E-03	6
75.0	(0.92628E-01,-0.49935E+00)	0.40043E+00	0.6629E-04	7
90.0	(0.97397E-01,-0.48371E+00)	0.38146E+00	0.1135E-03	7

POLARIZATION 2:

ALPHA (DEGREES)	F(0,ALPHA) (CM)	SCRS (CMSQ)	TEST	MMAX
15.0	(0.15651E-01,-0.65503E+00)	0.60352E+00	0.1218E-04	5
30.0	(0.63750E-02,-0.64337E+00)	0.59160E+00	0.1076E-03	6
45.0	(-.58061E-02,-0.62675E+00)	0.57340E+00	0.1047E-03	7
60.0	(-.17581E-01,-0.60914E+00)	0.55279E+00	0.3730E-03	7

75.0	(-.26086E-01,-0.59558E+00)	0.53622E+00	0.8899E-03	7
90.0	(-.29198E-01,-0.59048E+00)	0.52985E+00	0.5294E-04	8

****

FREQUENCY=45.0 GHZ
REF INDEX=(4.6241,-2.6437)
EQUIVOLUMETRIC RADIUS=0.325 CM

ALPHA=0 DEGREES:

F(0,0) (CM)	SCRS (CMSQ)	TEST	LMAX
(0.13505E-01,-0.78026E+00)	0.72503E+00	0.1633E-03	17

POLARIZATION 1:

ALPHA (DEGREES)	F(0,ALPHA) (CM)	SCRS (CMSQ)	TEST	MMAX
15.0	(0.17759E-01,-0.76924E+00)	0.71059E+00	0.2438E-04	5
30.0	(0.32463E-01,-0.73783E+00)	0.66881E+00	0.3212E-04	6
45.0	(0.57399E-01,-0.68854E+00)	0.60352E+00	0.1371E-03	6
60.0	(0.83925E-01,-0.62872E+00)	0.52682E+00	0.7647E-03	6
75.0	(0.10189E+00,-0.57746E+00)	0.46353E+00	0.2290E-03	7
90.0	(0.10781E+00,-0.55712E+00)	0.43898E+00	0.3785E-03	7

POLARIZATION 2:

ALPHA (DEGREES)	F(0,ALPHA) (CM)	SCRS (CMSQ)	TEST	MMAX
15.0	(0.89431E-02,-0.77357E+00)	0.71876E+00	0.5727E-04	5
30.0	(-.29647E-02,-0.75555E+00)	0.70119E+00	0.7144E-03	6
45.0	(-.18064E-01,-0.73120E+00)	0.67548E+00	0.1208E-03	7
60.0	(-.32295E-01,-0.70678E+00)	0.64730E+00	0.7119E-03	7
75.0	(-.42559E-01,-0.68871E+00)	0.62503E+00	0.9499E-04	8
90.0	(-.46349E-01,-0.68204E+00)	0.61654E+00	0.1387E-03	8

****

FREQUENCY=45.0 GHZ
REF INDEX=(4.6241,-2.6437)
EQUIVOLUMETRIC RADIUS=0.350 CM

ALPHA=0 DEGREES:

F(0,0) (CM)	SCRS (CMSQ)	TEST	LMAX
(0.88744E-02,-0.91161E+00)	0.85308E+00	0.6161E-04	19

POLARIZATION 1:

ALPHA (DEGREES)	F(0,ALPHA) (CM)	SCRS (CMSQ)	TEST	MMAX
15.0	(0.13868E-01,-0.89738E+00)	0.83448E+00	0.7843E-04	5
30.0	(0.30568E-01,-0.85824E+00)	0.78258E+00	0.9728E-04	6
45.0	(0.59610E-01,-0.79795E+00)	0.70267E+00	0.3484E-03	6
60.0	(0.92082E-01,-0.72371E+00)	0.60717E+00	0.1185E-03	7
75.0	(0.11484E+00,-0.65890E+00)	0.52685E+00	0.6722E-03	7
90.0	(0.12242E+00,-0.63295E+00)	0.49542E+00	0.6666E-04	8

POLARIZATION 2:

ALPHA (DEGREES)	F(0,ALPHA) (CM)	SCRS (CMSQ)	TEST	MMAX
15.0	(0.37727E-02,-0.90232E+00)	0.84433E+00	0.3410E-03	5
30.0	(-.10123E-01,-0.87803E+00)	0.82072E+00	0.6060E-03	6
45.0	(-.29079E-01,-0.84649E+00)	0.78781E+00	0.2475E-03	7
60.0	(-.48385E-01,-0.81552E+00)	0.75255E+00	0.7337E-04	8
75.0	(-.63072E-01,-0.79256E+00)	0.72469E+00	0.2406E-03	8
90.0	(-.68619E-01,-0.78402E+00)	0.71403E+00	0.3490E-03	8

****

FREQUENCY=70.0 GHZ
REF INDEX=(3.7873,-2.2394)
EQUIVOLUMETRIC RADIUS=0.025 CM

ALPHA=0 DEGREES:

F(0,0) (CM)	SCRS (CMSQ)	TEST	LMAX
(0.34008E-02,-0.91129E-03)	0.95389E-04	0.1912E-08	6

POLARIZATION 1:

ALPHA (DEGREES)	F(0,ALPHA) (CM)	SCRS (CMSQ)	TEST	MMAX
15.0	(0.33943E-02,-0.90886E-03)	0.94999E-04	0.6811E-03	2
30.0	(0.33763E-02,-0.90221E-03)	0.93936E-04	0.2316E-05	3
45.0	(0.33518E-02,-0.89314E-03)	0.92484E-04	0.6248E-05	3
60.0	(0.33272E-02,-0.88406E-03)	0.91032E-04	0.7239E-05	3
75.0	(0.33093E-02,-0.87743E-03)	0.89971E-04	0.6084E-05	3
90.0	(0.33027E-02,-0.87500E-03)	0.89582E-04	0.5685E-05	3

POLARIZATION 2:

ALPHA (DEGREES)	F(0,ALPHA) (CM)	SCRS (CMSQ)	TEST	MMAX
15.0	(0.34008E-02,-0.91183E-03)	0.95383E-04	0.7273E-03	2
30.0	(0.34007E-02,-0.91330E-03)	0.95369E-04	0.3049E-05	3
45.0	(0.34005E-02,-0.91530E-03)	0.95349E-04	0.1212E-04	3
60.0	(0.34003E-02,-0.91731E-03)	0.95329E-04	0.2712E-04	3
75.0	(0.34002E-02,-0.91877E-03)	0.95315E-04	0.4179E-04	3
90.0	(0.34001E-02,-0.91931E-03)	0.95310E-04	0.4793E-04	3

****

FREQUENCY=70.0 GHZ
REF INDEX=(3.7873,-2.2394)
EQUIVOLUMETRIC RADIUS=0.050 CM

ALPHA=0 DEGREES:

F(0,0) (CM)	SCRS (CMSQ)	TEST	LMAX
(0.22394E-01,-0.21244E-01)	0.75422E-02	0.6712E-08	7

POLARIZATION 1:

ALPHA (DEGREES)	F(0,ALPHA) (CM)	SCRS (CMSQ)	TEST	MMAX
15.0	(0.22305E-01,-0.21115E-01)	0.74733E-02	0.4261E-05	3

30.0	(0.22060E-01,-0.20762E-01)	0.72857E-02	0.4792E-04	3
45.0	(0.21726E-01,-0.20282E-01)	0.70305E-02	0.1297E-03	3
60.0	(0.21394E-01,-0.19805E-01)	0.67766E-02	0.1537E-03	3
75.0	(0.21150E-01,-0.19457E-01)	0.65916E-02	0.1358E-03	3
90.0	(0.21061E-01,-0.19330E-01)	0.65240E-02	0.1486E-03	3

POLARIZATION 2:

ALPHA (DEGREES)	F(0,ALPHA) (CM)	SCRS (CMSQ)	TEST	MMAX
15.0	(0.22365E-01,-0.21253E-01)	0.75382E-02	0.4548E-05	3
30.0	(0.22286E-01,-0.21277E-01)	0.75275E-02	0.6278E-04	3
45.0	(0.22178E-01,-0.21309E-01)	0.75129E-02	0.2481E-03	3
60.0	(0.22071E-01,-0.21341E-01)	0.74983E-02	0.5514E-03	3
75.0	(0.21992E-01,-0.21365E-01)	0.74877E-02	0.8457E-03	3
90.0	(0.21963E-01,-0.21373E-01)	0.74838E-02	0.9684E-03	3

****

FREQUENCY=70.0 GHZ
REF INDEX=(3.7873,-2.2394)
EQUIVOLUMETRIC RADIUS=0.075 CM

ALPHA=0 DEGREES:

F(0,0) (CM)	SCRS (CMSQ)	TEST	LMAX
(0.20670E-01,-0.69346E-01)	0.33817E-01	0.5418E-07	8

POLARIZATION 1:

ALPHA (DEGREES)	F(0,ALPHA) (CM)	SCRS (CMSQ)	TEST	MMAX
15.0	(0.20785E-01,-0.68830E-01)	0.33461E-01	0.7578E-04	3
30.0	(0.21088E-01,-0.67431E-01)	0.32496E-01	0.7970E-03	3
45.0	(0.21477E-01,-0.65537E-01)	0.31192E-01	0.2481E-04	4
60.0	(0.21838E-01,-0.63664E-01)	0.29906E-01	0.4056E-04	4
75.0	(0.22083E-01,-0.62307E-01)	0.28975E-01	0.2344E-04	4
90.0	(0.22169E-01,-0.61813E-01)	0.28637E-01	0.2798E-04	4

POLARIZATION 2:

ALPHA (DEGREES)	F(0,ALPHA) (CM)	SCRS (CMSQ)	TEST	MMAX
15.0	(0.20567E-01,-0.69226E-01)	0.33717E-01	0.8314E-04	3
30.0	(0.20286E-01,-0.68900E-01)	0.33445E-01	0.6806E-05	4
45.0	(0.19903E-01,-0.68459E-01)	0.33077E-01	0.5417E-04	4
60.0	(0.19521E-01,-0.68023E-01)	0.32713E-01	0.1820E-03	4
75.0	(0.19243E-01,-0.67707E-01)	0.32449E-01	0.3495E-03	4
90.0	(0.19141E-01,-0.67592E-01)	0.32353E-01	0.4299E-03	4

****

FREQUENCY=70.0 GHZ
REF INDEX=(3.7873,-2.2394)
EQUIVOLUMETRIC RADIUS=0.100 CM

ALPHA=0 DEGREES:

F(0,0) (CM)	SCRS (CMSQ)	TEST	LMAX
(0.19571E-01,-0.11231E+00)	0.57461E-01	0.1612E-06	9

POLARIZATION 1:

ALPHA (DEGREES)	F(0,ALPHA) (CM)	SCRS (CMSQ)	TEST	MMAX
15.0	(0.20046E-01,-0.11149E+00)	0.56782E-01	0.5236E-03	3
30.0	(0.21282E-01,-0.10922E+00)	0.54931E-01	0.5782E-04	4
45.0	(0.22827E-01,-0.10607E+00)	0.52410E-01	0.2479E-03	4
60.0	(0.24211E-01,-0.10285E+00)	0.49900E-01	0.2715E-03	4
75.0	(0.25125E-01,-0.10047E+00)	0.48069E-01	0.2836E-03	4
90.0	(0.25439E-01,-0.99589E-01)	0.47401E-01	0.4174E-03	4

POLARIZATION 2:

ALPHA (DEGREES)	F(0,ALPHA) (CM)	SCRS (CMSQ)	TEST	MMAX
15.0	(0.19575E-01,-0.11210E+00)	0.57224E-01	0.6002E-03	3
30.0	(0.19576E-01,-0.11153E+00)	0.56583E-01	0.9133E-04	4
45.0	(0.19545E-01,-0.11076E+00)	0.55718E-01	0.7200E-03	4
60.0	(0.19479E-01,-0.11000E+00)	0.54865E-01	0.4703E-04	5
75.0	(0.19409E-01,-0.10945E+00)	0.54249E-01	0.1106E-03	5
90.0	(0.19380E-01,-0.10925E+00)	0.54025E-01	0.1451E-03	5

****

FREQUENCY=70.0 GHZ
REF INDEX=(3.7873,-2.2394)
EQUIVOLUMETRIC RADIUS=0.125 CM

ALPHA=0 DEGREES:

F(0,0) (CM)	SCRS (CMSQ)	TEST	LMAX
(0.21450E-01,-0.17661E+00)	0.92382E-01	0.4162E-05	9

POLARIZATION 1:

ALPHA (DEGREES)	F(0,ALPHA) (CM)	SCRS (CMSQ)	TEST	MMAX

15.0	(0.22274E-01,-0.17544E+00)	0.91353E-01	0.9748E-05	4
30.0	(0.24467E-01,-0.17209E+00)	0.88476E-01	0.3164E-03	4
45.0	(0.27315E-01,-0.16720E+00)	0.84400E-01	0.2919E-04	5
60.0	(0.29983E-01,-0.16196E+00)	0.80176E-01	0.7720E-03	4
75.0	(0.31819E-01,-0.15794E+00)	0.77001E-01	0.5492E-04	5
90.0	(0.32465E-01,-0.15643E+00)	0.75824E-01	0.1316E-03	5

POLARIZATION 2:

ALPHA (DEGREES)	F(0,ALPHA) (CM)	SCRS (CMSQ)	TEST	MMAX
15.0	(0.21197E-01,-0.17641E+00)	0.92135E-01	0.1152E-04	4
30.0	(0.20487E-01,-0.17583E+00)	0.91437E-01	0.6166E-03	4
45.0	(0.19476E-01,-0.17495E+00)	0.90433E-01	0.1098E-03	5
60.0	(0.18420E-01,-0.17399E+00)	0.89375E-01	0.5729E-03	5
75.0	(0.17619E-01,-0.17324E+00)	0.88569E-01	0.3735E-04	6
90.0	(0.17320E-01,-0.17295E+00)	0.88268E-01	0.5321E-04	6

****

FREQUENCY=70.0 GHZ
REF INDEX=(3.7873,-2.2394)
EQUIVOLUMETRIC RADIUS=0.150 CM

ALPHA=0 DEGREES:

F(0,0) (CM)	SCRS (CMSQ)	TEST	LMAX
(0.15341E-01,-0.24947E+00)	0.13446E+00	0.6013E-05	10

POLARIZATION 1:

ALPHA (DEGREES)	F(0,ALPHA) (CM)	SCRS (CMSQ)	TEST	MMAX
15.0	(0.16544E-01,-0.24775E+00)	0.13297E+00	0.6461E-04	4
30.0	(0.19842E-01,-0.24275E+00)	0.12872E+00	0.3021E-04	5
45.0	(0.24315E-01,-0.23529E+00)	0.12249E+00	0.1746E-03	5
60.0	(0.28658E-01,-0.22714E+00)	0.11585E+00	0.1289E-03	5
75.0	(0.31705E-01,-0.22076E+00)	0.11076E+00	0.9615E-03	5
90.0	(0.32784E-01,-0.21834E+00)	0.10885E+00	0.4706E-04	6

POLARIZATION 2:

ALPHA (DEGREES)	F(0,ALPHA) (CM)	SCRS (CMSQ)	TEST	MMAX
15.0	(0.14832E-01,-0.24880E+00)	0.13396E+00	0.8290E-04	4
30.0	(0.13486E-01,-0.24693E+00)	0.13252E+00	0.7352E-04	5
45.0	(0.11730E-01,-0.24433E+00)	0.13043E+00	0.2833E-04	6
60.0	(0.10044E-01,-0.24167E+00)	0.12821E+00	0.2416E-03	6
75.0	(0.88407E-02,-0.23969E+00)	0.12652E+00	0.7947E-03	6
90.0	(0.84047E-02,-0.23896E+00)	0.12589E+00	0.3568E-04	7

```
**********************************************************************

                    FREQUENCY=70.0 GHZ
                  REF INDEX=(3.7873,-2.2394)
                EQUIVOLUMETRIC RADIUS=0.175 CM
                ------------------------------

ALPHA=0 DEGREES:

                    F(0,0)                  SCRS
                     (CM)                  (CMSQ)        TEST      LMAX
          (0.14704E-01,-0.33431E+00)   0.18253E+00   0.8831E-04    11

POLARIZATION 1:

  ALPHA          F(0,ALPHA)                SCRS
(DEGREES)          (CM)                   (CMSQ)        TEST      MMAX
  15.0     (0.16243E-01,-0.33188E+00)   0.18040E+00   0.2595E-03    4
  30.0     (0.20646E-01,-0.32482E+00)   0.17426E+00   0.1425E-03    5
  45.0     (0.26980E-01,-0.31412E+00)   0.16510E+00   0.6111E-03    5
  60.0     (0.33461E-01,-0.30219E+00)   0.15511E+00   0.8653E-03    5
  75.0     (0.38170E-01,-0.29267E+00)   0.14731E+00   0.2431E-03    6
  90.0     (0.39867E-01,-0.28902E+00)   0.14437E+00   0.4256E-03    6

POLARIZATION 2:

  ALPHA          F(0,ALPHA)                SCRS
(DEGREES)          (CM)                   (CMSQ)        TEST      MMAX
  15.0     (0.13860E-01,-0.33333E+00)   0.18180E+00   0.3559E-03    4
  30.0     (0.11549E-01,-0.33067E+00)   0.17978E+00   0.4632E-03    5
  45.0     (0.83666E-02,-0.32703E+00)   0.17686E+00   0.2926E-03    6
  60.0     (0.51289E-02,-0.32334E+00)   0.17378E+00   0.1118E-03    7
  75.0     (0.27112E-02,-0.32060E+00)   0.17141E+00   0.7525E-03    7
  90.0     (0.18145E-02,-0.31958E+00)   0.17052E+00   0.5437E-04    8
**********************************************************************

                    FREQUENCY=70.0 GHZ
                  REF INDEX=(3.7873,-2.2394)
                EQUIVOLUMETRIC RADIUS=0.200 CM
                ------------------------------

ALPHA=0 DEGREES:

                    F(0,0)                  SCRS
                     (CM)                  (CMSQ)        TEST      LMAX
          (0.10274E-01,-0.43686E+00)   0.24182E+00   0.3586E-03    12

POLARIZATION 1:

  ALPHA          F(0,ALPHA)                SCRS
```

(DEGREES)	(CM)	(CMSQ)	TEST	MMAX
15.0	(0.12083E-01,-0.43325E+00)	0.23875E+00	0.8886E-05	5
30.0	(0.17477E-01,-0.42294E+00)	0.22997E+00	0.6860E-03	5
45.0	(0.25676E-01,-0.40762E+00)	0.21701E+00	0.1052E-03	6
60.0	(0.34434E-01,-0.39055E+00)	0.20283E+00	0.2254E-03	6
75.0	(0.40944E-01,-0.37682E+00)	0.19166E+00	0.7010E-04	7
90.0	(0.43310E-01,-0.37152E+00)	0.18741E+00	0.1275E-03	7

POLARIZATION 2:

ALPHA (DEGREES)	F(0,ALPHA) (CM)	SCRS (CMSQ)	TEST	MMAX
15.0	(0.86367E-02,-0.43494E+00)	0.24065E+00	0.1457E-04	5
30.0	(0.42256E-02,-0.42965E+00)	0.23732E+00	0.1088E-03	6
45.0	(-.16433E-02,-0.42237E+00)	0.23251E+00	0.2436E-03	7
60.0	(-.73359E-02,-0.41500E+00)	0.22736E+00	0.5792E-03	7
75.0	(-.11405E-01,-0.40954E+00)	0.22336E+00	0.5355E-04	8
90.0	(-.12877E-01,-0.40754E+00)	0.22185E+00	0.7553E-04	8

****

FREQUENCY=70.0 GHZ
REF INDEX=(3.7873,-2.2394)
EQUIVOLUMETRIC RADIUS=0.225 CM

ALPHA=0 DEGREES:

F(0,0) (CM)	SCRS (CMSQ)	TEST	LMAX
(0.52488E-02,-0.54998E+00)	0.30825E+00	0.6742E-03	13

POLARIZATION 1:

ALPHA (DEGREES)	F(0,ALPHA) (CM)	SCRS (CMSQ)	TEST	MMAX
15.0	(0.75400E-02,-0.54481E+00)	0.30389E+00	0.5345E-04	5
30.0	(0.14349E-01,-0.53035E+00)	0.29164E+00	0.7730E-04	6
45.0	(0.24895E-01,-0.50913E+00)	0.27371E+00	0.3742E-03	6
60.0	(0.36579E-01,-0.48539E+00)	0.25393E+00	0.5647E-04	7
75.0	(0.45550E-01,-0.46606E+00)	0.23813E+00	0.4601E-03	7
90.0	(0.48866E-01,-0.45853E+00)	0.23206E+00	0.7670E-03	7

POLARIZATION 2:

ALPHA (DEGREES)	F(0,ALPHA) (CM)	SCRS (CMSQ)	TEST	MMAX
15.0	(0.31978E-02,-0.54677E+00)	0.30631E+00	0.1496E-03	5
30.0	(-.24334E-02,-0.53823E+00)	0.30101E+00	0.8970E-03	6
45.0	(-.10207E-01,-0.52698E+00)	0.29365E+00	0.2329E-03	7
60.0	(-.18114E-01,-0.51607E+00)	0.28604E+00	0.5831E-04	8
75.0	(-.24019E-01,-0.50822E+00)	0.28025E+00	0.1888E-03	8

```
 90.0     (-.26209E-01,-0.50535E+00)   0.27808E+00   0.2737E-03    8
**************************************************************************

                        FREQUENCY=70.0 GHZ
                     REF INDEX=(3.7873,-2.2394)
                   EQUIVOLUMETRIC RADIUS=0.250 CM
                   ------------------------------

ALPHA=0 DEGREES:

                    F(0,0)                    SCRS
                     (CM)                     (CMSQ)        TEST      LMAX
          (0.21925E-02,-0.68111E+00)   0.38486E+00   0.1877E-03    15

POLARIZATION 1:

  ALPHA          F(0,ALPHA)                 SCRS
(DEGREES)          (CM)                     (CMSQ)        TEST      MMAX
  15.0     (0.48892E-02,-0.67404E+00)   0.37893E+00   0.2556E-03     5
  30.0     (0.12842E-01,-0.65429E+00)   0.36235E+00   0.3353E-03     6
  45.0     (0.25509E-01,-0.62551E+00)   0.33819E+00   0.6618E-04     7
  60.0     (0.40204E-01,-0.59346E+00)   0.31151E+00   0.3725E-03     7
  75.0     (0.51823E-01,-0.56724E+00)   0.29009E+00   0.1304E-03     8
  90.0     (0.56158E-01,-0.55698E+00)   0.28183E+00   0.2286E-03     8

POLARIZATION 2:

  ALPHA          F(0,ALPHA)                 SCRS
(DEGREES)          (CM)                     (CMSQ)        TEST      MMAX
  15.0     (-.78266E-03,-0.67649E+00)   0.38217E+00   0.1721E-04     6
  30.0     (-.92400E-02,-0.66392E+00)   0.37477E+00   0.9670E-03     6
  45.0     (-.21328E-01,-0.64683E+00)   0.36434E+00   0.5491E-03     7
  60.0     (-.33745E-01,-0.62974E+00)   0.35334E+00   0.1891E-03     8
  75.0     (-.42931E-01,-0.61718E+00)   0.34482E+00   0.6222E-03     8
  90.0     (-.46304E-01,-0.61258E+00)   0.34160E+00   0.9036E-03     8
**************************************************************************

                        FREQUENCY=70.0 GHZ
                     REF INDEX=(3.7873,-2.2394)
                   EQUIVOLUMETRIC RADIUS=0.275 CM
                   ------------------------------

ALPHA=0 DEGREES:

                    F(0,0)                    SCRS
                     (CM)                     (CMSQ)        TEST      LMAX
          (-.40222E-02,-0.82871E+00)   0.47243E+00   0.9110E-03    17

POLARIZATION 1:
```

ALPHA (DEGREES)	F(0,ALPHA) (CM)	SCRS (CMSQ)	TEST	MMAX
15.0	(-.80599E-03,-0.81913E+00)	0.46452E+00	0.5191E-04	6
30.0	(0.86040E-02,-0.79237E+00)	0.44238E+00	0.5119E-04	7
45.0	(0.23760E-01,-0.75376E+00)	0.41032E+00	0.2340E-03	7
60.0	(0.41947E-01,-0.71097E+00)	0.37498E+00	0.1005E-03	8
75.0	(0.56808E-01,-0.67569E+00)	0.34633E+00	0.6634E-03	8
90.0	(0.62444E-01,-0.66177E+00)	0.33519E+00	0.7276E-04	9

POLARIZATION 2:

ALPHA (DEGREES)	F(0,ALPHA) (CM)	SCRS (CMSQ)	TEST	MMAX
15.0	(-.79114E-02,-0.82170E+00)	0.46851E+00	0.4611E-03	5
30.0	(-.18827E-01,-0.80262E+00)	0.45762E+00	0.4879E-04	7
45.0	(-.34317E-01,-0.77700E+00)	0.44231E+00	0.6462E-04	8
60.0	(-.50412E-01,-0.75206E+00)	0.42643E+00	0.6365E-03	8
75.0	(-.62591E-01,-0.73422E+00)	0.41433E+00	0.1402E-03	9
90.0	(-.67142E-01,-0.72776E+00)	0.40979E+00	0.2179E-03	9

****

FREQUENCY=70.0 GHZ
REF INDEX=(3.7873,-2.2394)
EQUIVOLUMETRIC RADIUS=0.300 CM

ALPHA=0 DEGREES:

F(0,0) (CM)	SCRS (CMSQ)	TEST	LMAX
(-.85832E-02,-0.99247E+00)	0.56983E+00	0.6318E-03	18

POLARIZATION 1:

ALPHA (DEGREES)	F(0,ALPHA) (CM)	SCRS (CMSQ)	TEST	MMAX
15.0	(-.48204E-02,-0.98001E+00)	0.55958E+00	0.2724E-04	6
30.0	(0.61599E-02,-0.94495E+00)	0.53072E+00	0.2731E-03	7
45.0	(0.23909E-01,-0.89443E+00)	0.48901E+00	0.7384E-03	7
60.0	(0.45970E-01,-0.83869E+00)	0.44309E+00	0.4818E-03	8
75.0	(0.64591E-01,-0.79262E+00)	0.40569E+00	0.2041E-03	9
90.0	(0.71743E-01,-0.77435E+00)	0.39107E+00	0.3550E-03	9

POLARIZATION 2:

ALPHA (DEGREES)	F(0,ALPHA) (CM)	SCRS (CMSQ)	TEST	MMAX
15.0	(-.13276E-01,-0.98296E+00)	0.56453E+00	0.5577E-03	5
30.0	(-.26921E-01,-0.95706E+00)	0.54983E+00	0.1351E-03	7
45.0	(-.47478E-01,-0.92191E+00)	0.52922E+00	0.2128E-03	8
60.0	(-.69880E-01,-0.88699E+00)	0.50770E+00	0.1309E-03	9

```
 75.0     (-.87155E-01,-0.86152E+00)   0.49110E+00   0.5168E-03    9
 90.0     (-.93626E-01,-0.85221E+00)   0.48482E+00   0.7907E-03    9
*****************************************************************

                    FREQUENCY=70.0 GHZ
                  REF INDEX=(3.7873,-2.2394)
                EQUIVOLUMETRIC RADIUS=0.325 CM
                ------------------------------

ALPHA=0 DEGREES:

                    F(0,0)                    SCRS
                     (CM)                    (CMSQ)        TEST      LMAX
          (-.13322E-01,-0.11775E+01)   0.68016E+00   0.1128E-03    19

POLARIZATION 1:

  ALPHA                F(0,ALPHA)                SCRS
(DEGREES)               (CM)                    (CMSQ)        TEST      MMAX
  15.0     (-.91821E-02,-0.11614E+01)   0.66704E+00   0.3493E-04    6
  30.0     (0.32476E-02,-0.11160E+01)   0.63000E+00   0.5864E-04    8
  45.0     (0.23562E-01,-0.10506E+01)   0.57656E+00   0.1568E-03    8
  60.0     (0.49577E-01,-0.97885E+00)   0.51783E+00   0.1377E-03    9
  75.0     (0.72329E-01,-0.91913E+00)   0.46966E+00   0.8673E-03    9
  90.0     (0.81215E-01,-0.89523E+00)   0.45068E+00   0.1206E-03    10

POLARIZATION 2:

  ALPHA                F(0,ALPHA)                SCRS
(DEGREES)               (CM)                    (CMSQ)        TEST      MMAX
  15.0     (-.19445E-01,-0.11647E+01)   0.67319E+00   0.7597E-03    5
  30.0     (-.37086E-01,-0.11292E+01)   0.65355E+00   0.3465E-03    7
  45.0     (-.63304E-01,-0.10802E+01)   0.62549E+00   0.6445E-03    8
  60.0     (-.91773E-01,-0.10317E+01)   0.59598E+00   0.4587E-03    9
  75.0     (-.11397E+00,-0.99687E+00)   0.57333E+00   0.1422E-03    10
  90.0     (-.12238E+00,-0.98425E+00)   0.56478E+00   0.2313E-03    10
*****************************************************************

                    FREQUENCY=70.0 GHZ
                  REF INDEX=(3.7873,-2.2394)
                EQUIVOLUMETRIC RADIUS=0.350 CM
                ------------------------------

ALPHA=0 DEGREES:

                    F(0,0)                    SCRS
                     (CM)                    (CMSQ)        TEST      LMAX
          (-.19369E-01,-0.13820E+01)   0.80313E+00   0.7558E-03    21

 POLARIZATION 1:
```

ALPHA (DEGREES)	F(0,ALPHA) (CM)	SCRS (CMSQ)	TEST	MMAX
15.0	(-.14663E-01,-0.13614E+01)	0.78649E+00	0.4439E-04	6
30.0	(-.41171E-03,-0.13036E+01)	0.73966E+00	0.5381E-04	9
45.0	(0.22789E-01,-0.12202E+01)	0.67203E+00	0.5441E-03	8
60.0	(0.53342E-01,-0.11290E+01)	0.59783E+00	0.5719E-03	9
75.0	(0.81085E-01,-0.10530E+01)	0.53673E+00	0.2973E-03	10
90.0	(0.92094E-01,-0.10225E+01)	0.51254E+00	0.5192E-03	10

POLARIZATION 2:

ALPHA (DEGREES)	F(0,ALPHA) (CM)	SCRS (CMSQ)	TEST	MMAX
15.0	(-.26553E-01,-0.13648E+01)	0.79387E+00	0.9980E-03	5
30.0	(-.47312E-01,-0.13178E+01)	0.76794E+00	0.8194E-03	7
45.0	(-.79292E-01,-0.12532E+01)	0.73109E+00	0.1160E-03	9
60.0	(-.11588E+00,-0.11887E+01)	0.69237E+00	0.1143E-03	10
75.0	(-.14532E+00,-0.11417E+01)	0.66244E+00	0.5209E-03	10
90.0	(-.15659E+00,-0.11246E+01)	0.65109E+00	0.8293E-03	10

****

FREQUENCY=90.0 GHZ
REF INDEX=(3.4162,-1.9758)
EQUIVOLUMETRIC RADIUS=0.025 CM

ALPHA=0 DEGREES:

F(0,0) (CM)	SCRS (CMSQ)	TEST	LMAX
(0.55752E-02,-0.21510E-02)	0.26678E-03	0.2822E-08	6

POLARIZATION 1:

ALPHA (DEGREES)	F(0,ALPHA) (CM)	SCRS (CMSQ)	TEST	MMAX
15.0	(0.55646E-02,-0.21450E-02)	0.26566E-03	0.5590E-06	3
30.0	(0.55355E-02,-0.21286E-02)	0.26260E-03	0.6285E-05	3
45.0	(0.54959E-02,-0.21062E-02)	0.25843E-03	0.1695E-04	3
60.0	(0.54563E-02,-0.20839E-02)	0.25426E-03	0.1975E-04	3
75.0	(0.54273E-02,-0.20676E-02)	0.25121E-03	0.1525E-04	3
90.0	(0.54167E-02,-0.20616E-02)	0.25009E-03	0.1452E-04	3

POLARIZATION 2:

ALPHA (DEGREES)	F(0,ALPHA) (CM)	SCRS (CMSQ)	TEST	MMAX
15.0	(0.55749E-02,-0.21521E-02)	0.26676E-03	0.5971E-06	3
30.0	(0.55739E-02,-0.21553E-02)	0.26669E-03	0.8265E-05	3
45.0	(0.55727E-02,-0.21596E-02)	0.26661E-03	0.3278E-04	3
60.0	(0.55714E-02,-0.21639E-02)	0.26652E-03	0.7315E-04	3
75.0	(0.55705E-02,-0.21671E-02)	0.26645E-03	0.1125E-03	3
90.0	(0.55702E-02,-0.21682E-02)	0.26643E-03	0.1289E-03	3

****

FREQUENCY=90.0 GHZ
REF INDEX=(3.4162,-1.9758)
EQUIVOLUMETRIC RADIUS=0.050 CM

ALPHA=0 DEGREES:

F(0,0) (CM)	SCRS (CMSQ)	TEST	LMAX
(0.19601E-01,-0.39246E-01)	0.13284E-01	0.2310E-07	7

POLARIZATION 1:

ALPHA (DEGREES)	F(0,ALPHA) (CM)	SCRS (CMSQ)	TEST	MMAX
15.0	(0.19600E-01,-0.39039E-01)	0.13183E-01	0.2144E-04	3

30.0	(0.19593E-01,-0.38477E-01)	0.12908E-01	0.2360E-03	3
45.0	(0.19582E-01,-0.37714E-01)	0.12535E-01	0.6192E-03	3
60.0	(0.19568E-01,-0.36956E-01)	0.12164E-01	0.7065E-03	3
75.0	(0.19556E-01,-0.36404E-01)	0.11895E-01	0.4286E-03	3
90.0	(0.19552E-01,-0.36203E-01)	0.11797E-01	0.4695E-03	3

POLARIZATION 2:

ALPHA (DEGREES)	F(0,ALPHA) (CM)	SCRS (CMSQ)	TEST	MMAX
15.0	(0.19552E-01,-0.39233E-01)	0.13269E-01	0.2306E-04	3
30.0	(0.19418E-01,-0.39199E-01)	0.13227E-01	0.3181E-03	3
45.0	(0.19234E-01,-0.39152E-01)	0.13171E-01	0.1027E-04	4
60.0	(0.19051E-01,-0.39105E-01)	0.13114E-01	0.3419E-04	4
75.0	(0.18917E-01,-0.39072E-01)	0.13073E-01	0.6518E-04	4
90.0	(0.18869E-01,-0.39059E-01)	0.13058E-01	0.7997E-04	4

****

FREQUENCY=90.0 GHZ
REF INDEX=(3.4162,-1.9758)
EQUIVOLUMETRIC RADIUS=0.075 CM

ALPHA=0 DEGREES:

F(0,0) (CM)	SCRS (CMSQ)	TEST	LMAX
(0.14520E-01,-0.81689E-01)	0.30767E-01	0.3941E-06	8

POLARIZATION 1:

ALPHA (DEGREES)	F(0,ALPHA) (CM)	SCRS (CMSQ)	TEST	MMAX
15.0	(0.14756E-01,-0.81259E-01)	0.30500E-01	0.4422E-03	3
30.0	(0.15379E-01,-0.80076E-01)	0.29770E-01	0.4598E-04	4
45.0	(0.16176E-01,-0.78444E-01)	0.28778E-01	0.2155E-03	4
60.0	(0.16911E-01,-0.76795E-01)	0.27791E-01	0.3078E-03	4
75.0	(0.17411E-01,-0.75576E-01)	0.27071E-01	0.1738E-03	4
90.0	(0.17586E-01,-0.75128E-01)	0.26808E-01	0.2061E-03	4

POLARIZATION 2:

ALPHA (DEGREES)	F(0,ALPHA) (CM)	SCRS (CMSQ)	TEST	MMAX
15.0	(0.14504E-01,-0.81574E-01)	0.30670E-01	0.4958E-03	3
30.0	(0.14456E-01,-0.81260E-01)	0.30407E-01	0.6769E-04	4
45.0	(0.14381E-01,-0.80837E-01)	0.30051E-01	0.5282E-03	4
60.0	(0.14295E-01,-0.80421E-01)	0.29698E-01	0.3090E-04	5
75.0	(0.14225E-01,-0.80121E-01)	0.29443E-01	0.7246E-04	5
90.0	(0.14198E-01,-0.80011E-01)	0.29351E-01	0.9489E-04	5

****

FREQUENCY=90.0 GHZ
REF INDEX=(3.4162,-1.9758)
EQUIVOLUMETRIC RADIUS=0.100 CM

ALPHA=0 DEGREES:

F(0,0) (CM)	SCRS (CMSQ)	TEST	LMAX
(0.15296E-01,-0.14513E+00)	0.56467E-01	0.6821E-07	10

POLARIZATION 1:

ALPHA (DEGREES)	F(0,ALPHA) (CM)	SCRS (CMSQ)	TEST	MMAX
15.0	(0.15780E-01,-0.14443E+00)	0.55999E-01	0.1348E-04	4
30.0	(0.17086E-01,-0.14246E+00)	0.54694E-01	0.4513E-03	4
45.0	(0.18828E-01,-0.13960E+00)	0.52856E-01	0.4568E-04	5
60.0	(0.20513E-01,-0.13658E+00)	0.50961E-01	0.8773E-03	4
75.0	(0.21710E-01,-0.13428E+00)	0.49539E-01	0.5781E-04	5
90.0	(0.22138E-01,-0.13341E+00)	0.49013E-01	0.1201E-03	5

POLARIZATION 2:

ALPHA (DEGREES)	F(0,ALPHA) (CM)	SCRS (CMSQ)	TEST	MMAX
15.0	(0.15078E-01,-0.14499E+00)	0.56350E-01	0.1572E-04	4
30.0	(0.14479E-01,-0.14457E+00)	0.56020E-01	0.8365E-03	4
45.0	(0.13657E-01,-0.14397E+00)	0.55548E-01	0.1537E-03	5
60.0	(0.12828E-01,-0.14333E+00)	0.55054E-01	0.7967E-03	5
75.0	(0.12217E-01,-0.14284E+00)	0.54679E-01	0.5359E-04	6
90.0	(0.11993E-01,-0.14265E+00)	0.54539E-01	0.7624E-04	6

****

FREQUENCY=90.0 GHZ
REF INDEX=(3.4162,-1.9758)
EQUIVOLUMETRIC RADIUS=0.125 CM

ALPHA=0 DEGREES:

F(0,0) (CM)	SCRS (CMSQ)	TEST	LMAX
(0.10702E-01,-0.21899E+00)	0.88180E-01	0.4582E-05	10

POLARIZATION 1:

ALPHA (DEGREES)	F(0,ALPHA) (CM)	SCRS (CMSQ)	TEST	MMAX

15.0	(0.11470E-01,-0.21784E+00)	0.87409E-01	0.1261E-03	4
30.0	(0.13599E-01,-0.21456E+00)	0.85227E-01	0.6791E-04	5
45.0	(0.16554E-01,-0.20975E+00)	0.82068E-01	0.4024E-03	5
60.0	(0.19518E-01,-0.20456E+00)	0.78719E-01	0.2158E-03	5
75.0	(0.21665E-01,-0.20052E+00)	0.76156E-01	0.3902E-04	6
90.0	(0.22443E-01,-0.19899E+00)	0.75196E-01	0.9545E-04	6

POLARIZATION 2:

ALPHA (DEGREES)	F(0,ALPHA) (CM)	SCRS (CMSQ)	TEST	MMAX
15.0	(0.10329E-01,-0.21853E+00)	0.87906E-01	0.1608E-03	4
30.0	(0.93219E-02,-0.21727E+00)	0.87144E-01	0.1613E-03	5
45.0	(0.79686E-02,-0.21557E+00)	0.86065E-01	0.7023E-04	6
60.0	(0.66290E-02,-0.21389E+00)	0.84946E-01	0.6068E-03	6
75.0	(0.56506E-02,-0.21266E+00)	0.84102E-01	0.6564E-04	7
90.0	(0.52919E-02,-0.21222E+00)	0.83789E-01	0.1045E-03	7

****

FREQUENCY=90.0 GHZ
REF INDEX=(3.4162,-1.9758)
EQUIVOLUMETRIC RADIUS=0.150 CM

ALPHA=0 DEGREES:

F(0,0) (CM)	SCRS (CMSQ)	TEST	LMAX
(0.76968E-02,-0.31293E+00)	0.12821E+00	0.3468E-04	11

POLARIZATION 1:

ALPHA (DEGREES)	F(0,ALPHA) (CM)	SCRS (CMSQ)	TEST	MMAX
15.0	(0.86800E-02,-0.31108E+00)	0.12698E+00	0.7769E-03	4
30.0	(0.11517E-01,-0.30582E+00)	0.12351E+00	0.5084E-03	5
45.0	(0.15687E-01,-0.29816E+00)	0.11849E+00	0.9635E-04	6
60.0	(0.20093E-01,-0.28989E+00)	0.11314E+00	0.5654E-04	6
75.0	(0.23403E-01,-0.28340E+00)	0.10901E+00	0.8726E-03	6
90.0	(0.24621E-01,-0.28093E+00)	0.10745E+00	0.5657E-04	7

POLARIZATION 2:

ALPHA (DEGREES)	F(0,ALPHA) (CM)	SCRS (CMSQ)	TEST	MMAX
15.0	(0.67918E-02,-0.31201E+00)	0.12777E+00	0.8487E-05	5
30.0	(0.43252E-02,-0.30949E+00)	0.12652E+00	0.4438E-04	6
45.0	(0.97569E-03,-0.30601E+00)	0.12475E+00	0.1528E-03	7
60.0	(-.23448E-02,-0.30248E+00)	0.12287E+00	0.6714E-03	7
75.0	(-.47551E-02,-0.29986E+00)	0.12144E+00	0.4210E-04	8
90.0	(-.56331E-02,-0.29890E+00)	0.12090E+00	0.5653E-04	8

****

FREQUENCY=90.0 GHZ
REF INDEX=(3.4162,-1.9758)
EQUIVOLUMETRIC RADIUS=0.175 CM

ALPHA=0 DEGREES:

F(0,0) (CM)	SCRS (CMSQ)	TEST	LMAX
(0.19718E-02,-0.42069E+00)	0.17546E+00	0.1457E-03	13

POLARIZATION 1:

ALPHA (DEGREES)	F(0,ALPHA) (CM)	SCRS (CMSQ)	TEST	MMAX
15.0	(0.32945E-02,-0.41775E+00)	0.17355E+00	0.8006E-04	5
30.0	(0.71270E-02,-0.40956E+00)	0.16820E+00	0.1051E-03	6
45.0	(0.12874E-01,-0.39776E+00)	0.16052E+00	0.5723E-03	6
60.0	(0.19147E-01,-0.38502E+00)	0.15230E+00	0.2544E-04	7
75.0	(0.24001E-01,-0.37496E+00)	0.14589E+00	0.4308E-03	7
90.0	(0.25818E-01,-0.37111E+00)	0.14345E+00	0.7519E-03	7

POLARIZATION 2:

ALPHA (DEGREES)	F(0,ALPHA) (CM)	SCRS (CMSQ)	TEST	MMAX
15.0	(0.69477E-03,-0.41887E+00)	0.17462E+00	0.4480E-03	5
30.0	(-.28231E-02,-0.41399E+00)	0.17232E+00	0.4953E-03	6
45.0	(-.77015E-02,-0.40752E+00)	0.16913E+00	0.1908E-03	7
60.0	(-.12673E-01,-0.40123E+00)	0.16586E+00	0.4919E-04	8
75.0	(-.16379E-01,-0.39672E+00)	0.16342E+00	0.1628E-03	8
90.0	(-.17750E-01,-0.39508E+00)	0.16250E+00	0.2374E-03	8

****

FREQUENCY=90.0 GHZ
REF INDEX=(3.4162,-1.9758)
EQUIVOLUMETRIC RADIUS=0.200 CM

ALPHA=0 DEGREES:

F(0,0) (CM)	SCRS (CMSQ)	TEST	LMAX
(-.28944E-02,-0.54880E+00)	0.23154E+00	0.1279E-03	14

POLARIZATION 1:

ALPHA	F(0,ALPHA)	SCRS

(DEGREES)	(CM)	(CMSQ)	TEST	MMAX
15.0	(-.12900E-02,-0.54441E+00)	0.22873E+00	0.7967E-03	5
30.0	(0.33807E-02,-0.53218E+00)	0.22088E+00	0.2944E-04	7
45.0	(0.10572E-01,-0.51471E+00)	0.20967E+00	0.1694E-03	7
60.0	(0.18735E-01,-0.49595E+00)	0.19768E+00	0.5711E-03	7
75.0	(0.25242E-01,-0.48114E+00)	0.18831E+00	0.2077E-03	8
90.0	(0.27712E-01,-0.47545E+00)	0.18474E+00	0.3698E-03	8

POLARIZATION 2:

ALPHA (DEGREES)	F(0,ALPHA) (CM)	SCRS (CMSQ)	TEST	MMAX
15.0	(-.49659E-02,-0.54579E+00)	0.23025E+00	0.2513E-03	5
30.0	(-.10751E-01,-0.53758E+00)	0.22666E+00	0.7327E-03	6
45.0	(-.18869E-01,-0.52638E+00)	0.22163E+00	0.5595E-03	7
60.0	(-.27137E-01,-0.51524E+00)	0.21638E+00	0.2141E-03	8
75.0	(-.33245E-01,-0.50713E+00)	0.21239E+00	0.7266E-03	8
90.0	(-.35487E-01,-0.50418E+00)	0.21090E+00	0.6221E-04	9

****

FREQUENCY=90.0 GHZ
REF INDEX=(3.4162,-1.9758)
EQUIVOLUMETRIC RADIUS=0.225 CM

ALPHA=0 DEGREES:

F(0,0) (CM)	SCRS (CMSQ)	TEST	LMAX
(-.95341E-02,-0.69387E+00)	0.29611E+00	0.8404E-03	14

POLARIZATION 1:

ALPHA (DEGREES)	F(0,ALPHA) (CM)	SCRS (CMSQ)	TEST	MMAX
15.0	(-.75266E-02,-0.68754E+00)	0.29210E+00	0.3565E-03	5
30.0	(-.17047E-02,-0.66992E+00)	0.28093E+00	0.3190E-03	7
45.0	(0.73102E-02,-0.64485E+00)	0.26502E+00	0.9541E-03	7
60.0	(0.17829E-01,-0.61807E+00)	0.24802E+00	0.2596E-03	8
75.0	(0.26496E-01,-0.59691E+00)	0.23469E+00	0.1019E-03	9
90.0	(0.29850E-01,-0.58876E+00)	0.22959E+00	0.1849E-03	9

POLARIZATION 2:

ALPHA (DEGREES)	F(0,ALPHA) (CM)	SCRS (CMSQ)	TEST	MMAX
15.0	(-.12216E-01,-0.68909E+00)	0.29408E+00	0.2855E-03	5
30.0	(-.19798E-01,-0.67612E+00)	0.28848E+00	0.5679E-04	7
45.0	(-.30785E-01,-0.65870E+00)	0.28072E+00	0.9272E-04	8
60.0	(-.42498E-01,-0.64161E+00)	0.27277E+00	0.9521E-03	8
75.0	(-.51501E-01,-0.62927E+00)	0.26678E+00	0.2262E-03	9

90.0	(-.54883E-01,-0.62479E+00)	0.26455E+00	0.3521E-03	9

****

FREQUENCY=90.0 GHZ
REF INDEX=(3.4162,-1.9758)
EQUIVOLUMETRIC RADIUS=0.250 CM

ALPHA=0 DEGREES:

F(0,0) (CM)	SCRS (CMSQ)	TEST	LMAX
(-.15374E-01,-0.86060E+00)	0.37032E+00	0.7597E-04	16

POLARIZATION 1:

ALPHA (DEGREES)	F(0,ALPHA) (CM)	SCRS (CMSQ)	TEST	MMAX
15.0	(-.13059E-01,-0.85179E+00)	0.36482E+00	0.4522E-03	5
30.0	(-.62543E-02,-0.82721E+00)	0.34945E+00	0.3999E-03	7
45.0	(0.44495E-02,-0.79229E+00)	0.32756E+00	0.4143E-03	8
60.0	(0.17289E-01,-0.75512E+00)	0.30424E+00	0.1174E-03	9
75.0	(0.28187E-01,-0.72571E+00)	0.28590E+00	0.7877E-03	9
90.0	(0.32472E-01,-0.71434E+00)	0.27886E+00	0.9392E-04	10

POLARIZATION 2:

ALPHA (DEGREES)	F(0,ALPHA) (CM)	SCRS (CMSQ)	TEST	MMAX
15.0	(-.19112E-01,-0.85360E+00)	0.36744E+00	0.4450E-03	5
30.0	(-.29750E-01,-0.83434E+00)	0.35941E+00	0.1863E-03	7
45.0	(-.45220E-01,-0.80789E+00)	0.34806E+00	0.3716E-03	8
60.0	(-.61653E-01,-0.78156E+00)	0.33624E+00	0.2656E-03	9
75.0	(-.74235E-01,-0.76252E+00)	0.32727E+00	0.7848E-04	10
90.0	(-.78954E-01,-0.75562E+00)	0.32390E+00	0.1298E-03	10

****

FREQUENCY=90.0 GHZ
REF INDEX=(3.4162,-1.9758)
EQUIVOLUMETRIC RADIUS=0.275 CM

ALPHA=0 DEGREES:

F(0,0) (CM)	SCRS (CMSQ)	TEST	LMAX
(-.22511E-01,-0.10476E+01)	0.45449E+00	0.7270E-03	17

POLARIZATION 1:

ALPHA (DEGREES)	F(0,ALPHA) (CM)	SCRS (CMSQ)	TEST	MMAX
15.0	(-.19764E-01,-0.10357E+01)	0.44709E+00	0.5395E-03	5
30.0	(-.11685E-01,-0.10023E+01)	0.42642E+00	0.7754E-03	7
45.0	(0.10313E-02,-0.95484E+00)	0.39699E+00	0.4925E-03	9
60.0	(0.16604E-01,-0.90449E+00)	0.36567E+00	0.9272E-03	9
75.0	(0.30249E-01,-0.86470E+00)	0.34100E+00	0.3830E-03	10
90.0	(0.35717E-01,-0.84929E+00)	0.33151E+00	0.6568E-03	10

POLARIZATION 2:

ALPHA (DEGREES)	F(0,ALPHA) (CM)	SCRS (CMSQ)	TEST	MMAX
15.0	(-.27121E-01,-0.10376E+01)	0.45040E+00	0.6665E-03	5
30.0	(-.40369E-01,-0.10102E+01)	0.43902E+00	0.5480E-03	7
45.0	(-.60274E-01,-0.97269E+00)	0.42301E+00	0.8165E-04	9
60.0	(-.82418E-01,-0.93523E+00)	0.40639E+00	0.8364E-04	10
75.0	(-.99977E-01,-0.90791E+00)	0.39375E+00	0.3998E-03	10
90.0	(-.10666E+00,-0.89795E+00)	0.38900E+00	0.6469E-03	10

****

FREQUENCY=90.0 GHZ
REF INDEX=(3.4162,-1.9758)
EQUIVOLUMETRIC RADIUS=0.300 CM

ALPHA=0 DEGREES:

F(0,0) (CM)	SCRS (CMSQ)	TEST	LMAX
(-.28852E-01,-0.12586E+01)	0.54952E+00	0.1191E-04	20

POLARIZATION 1:

ALPHA (DEGREES)	F(0,ALPHA) (CM)	SCRS (CMSQ)	TEST	MMAX
15.0	(-.25743E-01,-0.12427E+01)	0.53980E+00	0.6064E-03	5
30.0	(-.16552E-01,-0.11985E+01)	0.51265E+00	0.1007E-03	8
45.0	(-.19194E-02,-0.11355E+01)	0.47396E+00	0.9667E-03	9
60.0	(0.16344E-01,-0.10686E+01)	0.43280E+00	0.4262E-03	10
75.0	(0.32893E-01,-0.10157E+01)	0.40029E+00	0.1908E-03	11
90.0	(0.39680E-01,-0.99507E+00)	0.38772E+00	0.3375E-03	11

POLARIZATION 2:

ALPHA (DEGREES)	F(0,ALPHA) (CM)	SCRS (CMSQ)	TEST	MMAX
15.0	(-.34737E-01,-0.12450E+01)	0.54404E+00	0.4117E-04	6
30.0	(-.51791E-01,-0.12073E+01)	0.52866E+00	0.7630E-04	8
45.0	(-.77469E-01,-0.11549E+01)	0.50668E+00	0.3302E-03	9
60.0	(-.10614E+00,-0.11022E+01)	0.48358E+00	0.3846E-03	10

75.0	(-.12918E+00,-0.10639E+01)	0.46594E+00	0.1636E-03	11
90.0	(-.13806E+00,-0.10500E+01)	0.45931E+00	0.2795E-03	11

****

FREQUENCY=90.0 GHZ
REF INDEX=(3.4162,-1.9758)
EQUIVOLUMETRIC RADIUS=0.325 CM

ALPHA=0 DEGREES:

F(0,0) (CM)	SCRS (CMSQ)	TEST	LMAX
(-.36137E-01,-0.14938E+01)	0.65623E+00	0.3459E-03	20

POLARIZATION 1:

ALPHA (DEGREES)	F(0,ALPHA) (CM)	SCRS (CMSQ)	TEST	MMAX
15.0	(-.32528E-01,-0.14732E+01)	0.64369E+00	0.5252E-03	5
30.0	(-.21952E-01,-0.14156E+01)	0.60864E+00	0.2365E-03	8
45.0	(-.51500E-02,-0.13334E+01)	0.55862E+00	0.1093E-03	10
60.0	(0.16104E-01,-0.12462E+01)	0.50538E+00	0.2024E-03	11
75.0	(0.35928E-01,-0.11772E+01)	0.46331E+00	0.9848E-04	12
90.0	(0.44206E-01,-0.11503E+01)	0.44701E+00	0.1802E-03	12

POLARIZATION 2:

ALPHA (DEGREES)	F(0,ALPHA) (CM)	SCRS (CMSQ)	TEST	MMAX
15.0	(-.43147E-01,-0.14755E+01)	0.64892E+00	0.7323E-04	6
30.0	(-.63635E-01,-0.14251E+01)	0.62842E+00	0.2242E-03	8
45.0	(-.95422E-01,-0.13549E+01)	0.59911E+00	0.8617E-04	10
60.0	(-.13225E+00,-0.12835E+01)	0.56811E+00	0.1404E-03	11
75.0	(-.16250E+00,-0.12311E+01)	0.54420E+00	0.7461E-03	11
90.0	(-.17423E+00,-0.12119E+01)	0.53517E+00	0.1293E-03	12

****

FREQUENCY=90.0 GHZ
REF INDEX=(3.4162,-1.9758)
EQUIVOLUMETRIC RADIUS=0.350 CM

ALPHA=0 DEGREES:

F(0,0) (CM)	SCRS (CMSQ)	TEST	LMAX
(-.42577E-01,-0.17559E+01)	0.77544E+00	0.3763E-03	24

POLARIZATION 1:

ALPHA (DEGREES)	F(0,ALPHA) (CM)	SCRS (CMSQ)	TEST	MMAX
15.0	(-.38582E-01,-0.17297E+01)	0.75954E+00	0.3543E-03	5
30.0	(-.26800E-01,-0.16560E+01)	0.71505E+00	0.5309E-03	7
45.0	(-.78914E-02,-0.15508E+01)	0.65146E+00	0.5283E-03	9
60.0	(0.16345E-01,-0.14388E+01)	0.58370E+00	0.9744E-04	12
75.0	(0.39808E-01,-0.13500E+01)	0.53000E+00	0.5741E-03	12
90.0	(0.49883E-01,-0.13152E+01)	0.50911E+00	0.9850E-03	12

POLARIZATION 2:

ALPHA (DEGREES)	F(0,ALPHA) (CM)	SCRS (CMSQ)	TEST	MMAX
15.0	(-.51055E-01,-0.17323E+01)	0.76606E+00	0.1305E-03	6
30.0	(-.76040E-01,-0.16665E+01)	0.73956E+00	0.5399E-03	8
45.0	(-.11496E+00,-0.15738E+01)	0.70116E+00	0.3408E-03	10
60.0	(-.16077E+00,-0.14790E+01)	0.66015E+00	0.6027E-03	11
75.0	(-.19948E+00,-0.14092E+01)	0.62839E+00	0.3461E-03	12
90.0	(-.21481E+00,-0.13836E+01)	0.61636E+00	0.6043E-03	12

****

BLANK PAGE

BLANK PAGE

BLANK PAGE

BLANK PAGE

BLANK PAGE

Appendix D Derivation of the Scattered Field's Plane Wave Spectrum

In this Appendix, we derive the plane wave spectrum of the field scattered by the particle shown in Figure D.1. The particle is positioned at $\vec{r}' = (x', y', z')$ and illuminated by a plane wave having electric field vector

$$\vec{E}_i(\vec{r}) = \vec{E}_0 e^{-jk_0 z} \tag{D.1a}$$

$$\vec{E}_0 = E_{0x}\hat{x} + E_{0y}\hat{y} \tag{d.1b}$$

The plane wave spectrum of the scattered field $\vec{E}_s(\vec{r}, \vec{r}')$ is given by the inverse Fourier Transform [39]

$$\vec{A}(\vec{k}; z) = \frac{1}{4\pi_2} \int_{-\infty}^{\infty} \vec{E}_S^c(\vec{r}, \vec{r}') \exp(j\vec{k} \cdot \vec{r}) dxdy \tag{D.2a}$$

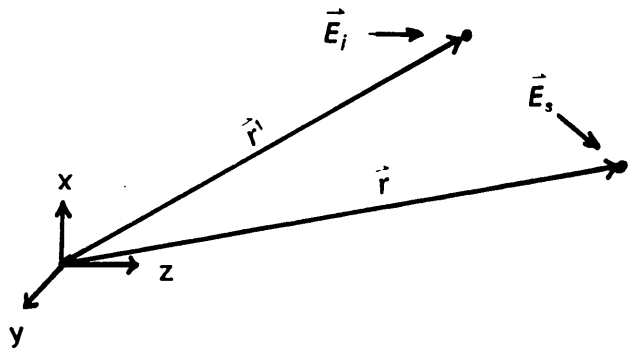

Geometry for Computing Scattered Field's Plane Wave Spectrum

Figure D.1

where the c superscript indicates the scattered field is resolved into its rectangular components and

$$\vec{r} = (x, y, L) \tag{D.2b}$$

$$\vec{k} = (k_x, k_y, k_z) \tag{D.2c}$$

$$k_2 = \sqrt{k_0^2 - k_x^2 - k_y^2} \tag{D.2d}$$

The scattered field is given in terms of the particle's tensor scattering amplitude $\underline{f}(\hat{z}, \hat{k}_s)$ i.e.

$$\vec{E}_s(\vec{r}, \vec{r}') = \underline{f}(\hat{z}, \hat{k}_s) \cdot \vec{E}_i(\vec{r}') \frac{e^{-jk_0R}}{R} \tag{D.3a}$$

where

$$R = \sqrt{(x - x')^2 + (y - y')^2 + (L - z')^2} \tag{D.3b}$$

$$\hat{k}_s = \frac{1}{R}[(x - x')\hat{x} + (y - \hat{y})\hat{y} + (L - z')\hat{z}] \tag{D.3c}$$

$$\hat{k}_s - [\underline{f}(\hat{z}, \hat{k}_s) \cdot \vec{E}] = 0 \tag{D.3d}$$

As given by (D.3), the scattered field is resolved into angular components which are referenced to a spherical coordinate system (r_1, θ_1, ϕ_1) centered at $\vec{r}'$ (see Figure D.2). It is converted to rectangular components through the transformation

$$\vec{E}_s^{\zeta}(\vec{r}, \vec{r}') = {}^c\underline{T}^s(\theta_1, \phi_1)\underline{f}(\hat{z}, \hat{k}_s) \cdot \vec{E}_i(\vec{r}') \frac{e^{-jk_0R}}{R} \tag{D.4}$$

where ${}^c\underline{T}^s(\theta_1, \phi_1)$ converts angular spherical components to cartesian components [55]:

$$^{c}\underline{\underline{I}}^{s}(\theta_1,\ \phi_1) = \begin{bmatrix} \cos\theta_1 \cos\phi_1 & -\sin\phi_1 \\ \cos\theta_1 \sin\phi_1 & \cos\phi_1 \\ -\sin\phi_1 & 0 \end{bmatrix} \tag{D.5}$$

substituting (*e/4) into (E.2) yields

$$\vec{A}(\vec{k};\ L) = \frac{e^{jk_0 L}}{4\pi^2} \int_{-\infty}^{\infty} \int c\underline{\underline{I}}^{s}(\theta_1,\ \phi_1)\underline{\underline{I}}(\hat{z},\ \hat{k}_s) \frac{e^{-jk_0 R}}{R}$$

x exp (j k sub x x + j k sub u u) d x d y bullet E vector sub i (r vector prime) reqno

(D.6)

In (D.6) we make the variable substitutions

$$k_x = k_0 u_x \tag{D.7a}$$

$$ksyby = k_0 u_u \tag{D.7b}$$

$$\xi = (x - x')/(l - z') \tag{D.7c}$$

$$\eta = (y - y')/(L - z') \tag{D.7d}$$

Also we define $\underline{Q}(\xi,\ \eta)$ and $\Phi(\xi, \eta)$ by

$$\underline{Q}(\xi,\ \eta) = \frac{1}{R^c}\underline{\underline{I}}^{s}(\theta_1,\ \phi_1) \Big|_{\substack{(x-x')=\xi(L-z') \\ (y-y')=\eta((L-z')}} \tag{D.8a}$$

$$\Phi(\xi,\ \eta) = \sqrt{\xi^2 + \eta^2 + 1} - \xi U_x - \eta U_y \tag{D.8b}$$

Equation (E.b) can then be recast as

$$\vec{A}(\vec{k};\ L) = L - z')\frac{2}{4\pi}\exp(jk_x x' + jk_u u' + jk_z L_1)$$

$$x \int_{-\infty}^{} \infty \underline{Q}(\xi,\ \eta) f(\hat{z},\ \hat{k}_s) \exp[-jk_0(L - z')\Phi(\xi,\ \eta)]$$

d xi d eta bullet E vector sub i (r vector prime) reqno (D.9)

Under the assumption that the plane z=L is in the far field of the particle, the plex integral in (D.9) can be evaluated by stationary phase with $\xi_o, \eta_o)$ being the stationary point, the stationary phase solution to (D.9) is [54]

$$\vec{A}(\vec{k};\ L) = \frac{-j(L - z')}{2\pi k_0}\exp[jk_x x' + jk_y y' + jk_x L - jk_0(L - z')\Phi(\xi_o,\ \eta_o)]$$

$$x\underline{Q}(\xi_o, \eta_o) fbarudner(\hat{z}, \hat{k}_{so}[\Phi_{\xi\xi}(\xi_o,\ \eta_o)\Phi_{\eta\eta}(\xi_o, \eta_o) - \Phi^2_{\xi\eta}(\xi_o, \eta_o)]^{-1/2}$$

$$\cdot \vec{E}_i(\vec{r}') \qquad (D.10)$$

where $\hat{k}_{so}$ is also $\hat{k}_s$ evaluated at $(\xi_o,\ \eta_o)$

The coordinates of the stationary point are defined by

$$\Phi_\xi(\xi_o,\ \eta_o) = \Phi_\eta(\xi_o,\ \eta_o) = 0 \qquad (D.11)$$

solving (D.11) for ξ_o and η_o gives

$$\xi_o = \frac{U_x}{\sqrt{1 - U_x^2 - U_y^2}} \qquad (D.12a)$$

$$o = \frac{U_y}{\sqrt{1 - U_x^2 - U_y^2}} \tag{D.12b}$$

After doing the necessary differentiation, suing (D.12) and performing some algebra we obtain

$$\Phi(\xi_o,\ \eta_o) = \sqrt{1 - U_x^2 - U_y^2} \tag{D.13a}$$

$$\underline{Q}(\xi_o,\ \eta_o) = \frac{\sqrt{1 - U_x^2 - U_y^2}}{(L - z')\sqrt{U_x^2 + U_y^2}} \begin{bmatrix} U_x\sqrt{1 - U_x^2 - U_y^2} & -U_y \\ Usyby\sqrt{1 - U_x^2 - U_y^2} & U_x \\ -(u_x^2 U_y^2) & 0 \end{bmatrix} \tag{D.13c}$$

$$s0 = \vec{k}/k_o = \hat{k} \tag{D.13d}$$

Substituting (D.13) into (D.10) and simplifying yields

$$\vec{A}(\vec{k};\ L) = -\frac{j}{2\pi k_0} \exp(j\vec{k} \cdot \vec{r}')\underline{U}(\vec{k})[(\hat{z},\ \hat{k}) \cdot \vec{E}_i(\vec{r}') \tag{D.14a}$$

where

$$\underline{U}(\vec{k}) = \frac{1}{\sqrt{k_x^2 + k_y^2}} \begin{bmatrix} k_x & -k_0 k_y/k_z \\ k_y & k_0 k_x/k_z \\ -(k_x^2 + k_y^2)/k_z & 0 \end{bmatrix} \tag{D.14b}$$

Appendix E Program for Computing the Attenuation and Isolation of the Coherent Field

This Appenix contains the program used to obtain the plots of attenuationand isolation vs. slab length provided in Chapter 3, Section 3.5. The program computes and plots the data for rain rates of 2.5, 12.5, 50 and 150 mm/hr.

E.1 Program Flow Chart and Program Listing

The flow chart for the program is in Figure E.1. SUBROUTINE FSAMPS computes forward scatteringamplitudes for spherical raindrops and SUBROUTINE PLOTT plots the attenuation andisolation versus slab length d. The spherical Bessel function programs are SBESJ, SBESST, CBESJ, CBESST and SBESY which were described in Appendix B.

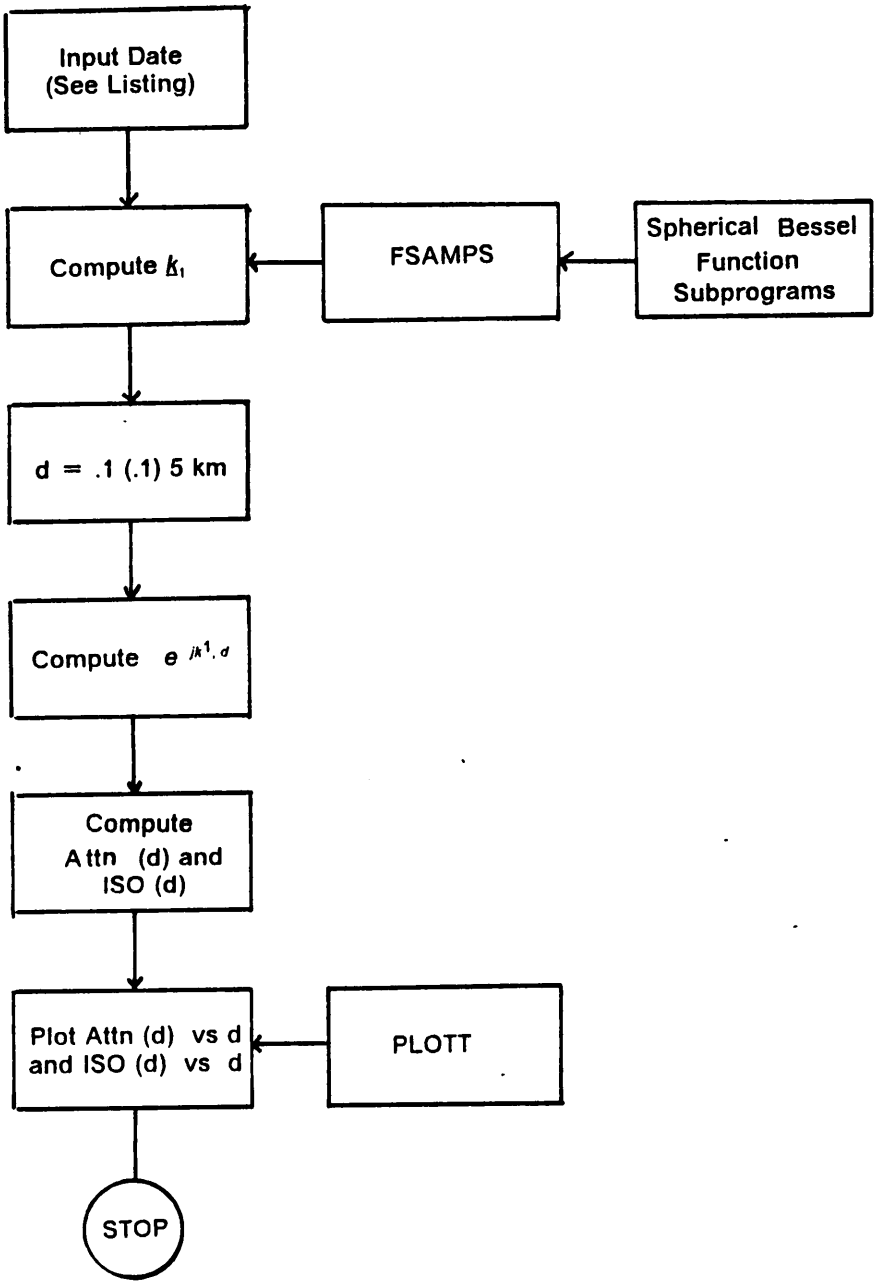

Flow Chart for Attenuation and Isolation Program

Figure E.1

```
C***** ATTENUATION AND DEPOLARIZATION OF THE COHERENT FIELD **********
C                                                                     *
C    THIS PROGRAM COMPUTES AND PLOTS THE ATTENUATION OF THE VECTOR    *
C  COHERENT FIELD PROPOGATING THROUGH A RAIN CELL.  IT ALSO COM-      *
C  PUTES AND PLOTS THE ISOLATION BETWEEN THE CO AND CROSS POLAR-      *
C  IZED COMPONENTS OF THE FIELD.  CALCULATIONS ARE MADE FOR RAIN      *
C  RATES OF 2.5,12.5,50 AND 150 MM/HR                                 *
C                                                                     *
C    USER INPUTS TO THE PROGRAM ARE:                                  *
C                                                                     *
C            GMA,DLTA= ARRAYS DEFINING THE POLARIZATION               *
C                      OF THE ANTENNA.                                *
C                                                                     *
C            F= ARRAY CONTAINING THE FORWARD SCATTERING               *
C               AMPLITUDES (IN METERS) OF OBLATE SPHERE-              *
C               OIDAL RAINDROPS HAVING EVR'S .25(.25)3.5              *
C               MM.                                                   *
C                                                                     *
C            FREQ= FREQUENCY(GHZ)                                     *
C                                                                     *
C                                                                     *
C            RIRE,RIIM= REAL AND IMAGINARY PARTS OF THE               *
C                       REFRACTIVE INDEX OF WATER AT THE              *
C                       FREQUENCY OF OPERATION.                       *
C                                                                     *
C            PO= FRACTION OF THE TOTAL NUMBER OF RAIN-                *
C                DROPS IN THE RAIN CELL WHICH ARE SPHER-              *
C                ICAL.                                                *
C                                                                     *
C            MCA= MEAN CANTING ANGLE OF THE OBLATE DROPS              *
C                 (DEGREES).                                          *
C                                                                     *
C            SDVCA= STANDARD DEVIATION OF OBLATE DROP CANT-           *
C                   ING ANGLE (DEGREES).                              *
C                                                                     *
C*********************************************************************

      COMPLEX IMAG,F(0:2,14),RSPNS(2,2),E0(2),RI,S(0:2)
      COMPLEX K11,K12,K22,KP,KSQRT,LMBDA1,LMBDA2,L1ML2
      COMPLEX EL1D,EL2D,MATEXP(2,2),V0(2),V(2)
      REAL K0,MCA,GMA(2),DLTA(2),MCAR,DKM(52)
      REAL RRATE(4),ISO(202),ATTN(202)
      COMMON /BLOC1/ DKM,ATTN,ISO
      COMMON /BLOC2/ IMAG,K0,RI,F

C  INPUT DATA.

      DATA RRATE/2.5,12.5,50.,150./
      IMAG=(0.,1.)
      PI=3.1415927
      DTR=PI/180.
      N0=16000

      READ(5,*)FREQ,RIRE,RIIM
      READ(5,*)PO,MCA,SDVCA
```

```
      READ(5,*) GMA(1),DLTA(1),GMA(2),DLTA(2)
      DO 67 I=1,14
      READ(5,*)F1RE,F1IM,F2RE,F2IM
      F(1,I)=CMPLX(F1RE,F1IM)
   67 F(2,I)=CMPLX(F2RE,F2IM)
      WRITE(6,100)FREQ,PO,MCA,SDVCA

      P1=1-PO
      KO=20.*PI*FREQ/3.
      MCAR=MCA*DTR
      VARCA=(SDVCA*DTR)**2
      RI=CMPLX(RIRE,RIIM)
      DO 68 I=1,2
      RSPNS(I,1)=COS(GMA(I)*DTR)
      RSPNS(I,2)=SIN(GMA(I)*DTR)*CEXP(-IMAG*DLTA(I)*DTR)
   68 EO(I)=CONJG(RSPNS(1,I))
      IMIN=1
      IMAX=50
      DO 603 II=1,4
      BETA=8.2*RRATE(II)**(-.21)

C  COMPUTE THE ELEMENTS AND EIGENVALUES OF THE MATRIX K1.

      QO=PI*NO/(12.*KO)
      Q1=1.+EXP(-2.*VARCA)*COS(2.*MCAR)
      Q2=1.-EXP(-2.*VARCA)*COS(2.*MCAR)
      CALL FSAMPS
      DO 1 I=0,2
      S(I)=4.*F(I,1)*EXP(-.25*BETA)+F(I,14)*EXP(-3.5*BETA)
      DO 1 J=1,6
    1 S(I)=S(I)+2.*F(I,2*J)*EXP(-.5*BETA*J)+4.*F(I,2*J+1)
     &*EXP(-(.5*J+.25)*BETA)
      K11=QO*(2.*PO*S(0)+P1*(Q1*S(1)+Q2*S(2)))
      K22=QO*(2.*PO*S(0)+P1*(Q1*S(2)+Q2*S(1)))
      K12=QO*P1*(S(2)-S(1))*EXP(-2.*VARCA)*SIN(2.*MCAR)
      KP=K11+K22
      KSQRT=CSQRT((K11-K22)**2+4.*K12*K12)
      LMBDA1=(KP+KSQRT)/2.
      LMBDA2=(KP-KSQRT)/2.

      D=100.
      DO 2 I=IMIN,IMAX

C  DETERMINE THE MATRIX EXPONENTIAL EXP(-J*K1*D) FOR SLAB LENGTH D.

      EL1D=CEXP(-IMAG*LMBDA1*D)
      EL2D=CEXP(-IMAG*LMBDA2*D)
      L1ML2=LMBDA1-LMBDA2
      MATEXP(1,1)=((LMBDA1-K11)*EL2D-(LMBDA2-K11)*EL1D)/L1ML2
      MATEXP(2,2)=((LMBDA1-K22)*EL2D-(LMBDA2-K22)*EL1D)/L1ML2
      MATEXP(1,2)=K12*(EL1D-EL2D)/L1ML2
      MATEXP(2,1)=MATEXP(1,2)

C  COMPUTE THE ATTENUATION AND ISOLATION.
```

```
      CALL MVMULT(MATEXP,E0,V0)
      CALL MVMULT(RSPNS,V0,V)
      VC2=CABS(V(1))**2
      VX2=CABS(V(2))**2
      ATTN(I)=-10.*ALOG10(VC2)
      IF(VX2.EQ.0.) THEN
         ISO(I)=99.
      ELSE
         ISO(I)=10.*ALOG10(VC2/VX2)
      ENDIF
    2 D=D+100.
      IMIN=IMIN+50
  603 IMAX=IMAX+50

C  OUTPUT DATA.

      DO 17 I=1,50
   17 DKM(I)=.1*I
      JMIN=10
      JMAX=50
      DO 18 I=1,4
      WRITE(6,102)RRATE(I)
      II=10
      DO 19 J=JMIN,JMAX,10
      WRITE(6,101)DKM(II),ATTN(J),ISO(J)
   19 II=II+10
      JMIN=JMIN+50
      JMAX=JMAX+50
   18 WRITE(6,104)

      CALL PLOTT

  100 FORMAT(1X,'FREQUENCY:',F5.1,' GHZ',/,1X,
     &'FRACTION SPHERICAL DROPS:',F5.2,/,1X,
     &'MEAN CANTING ANGLE:',F5.1,' DEG',/,1X,
     &'STD. DEV. OF CANTING ANGLE:',F5.1,' DEG',/)
  101 FORMAT(7X,F3.1,5X,F6.2,4X,F7.2)
  102 FORMAT(1X,'RAIN RATE:',F6.1,' MM/HR',//,6X,'D(KM)',3X,
     &'ATTN(DB)',3X,'ISO(DB)')
  104 FORMAT(//)
      STOP
      END



      SUBROUTINE PLOTT
      REAL DKM(52),ATTN(202),ISO(202),ATTN1(52),ISO1(52)
      COMMON /BLOC1/ DKM,ATTN,ISO
      CALL PLOTS(0,0,50)
      CALL SCALE(DKM,5.,50,1)
      CALL SCALE(ATTN,6.,200,1)
      CALL SCALE(ISO,6.,200,1)
      CALL PLOT(2.,2.,-3)
      CALL AXIS(0.,0.,'SLAB LENGTH(KM)',-15,5.,0.,DKM(51),DKM(52))
      CALL AXIS(0.,0.,'ATTENUATION(DB)',15,6.,90.,ATTN(201),
```

```
     &ATTN(202))
      DO 1 I=1,50
    1 ATTN1(I)=ATTN(I)
      ATTN1(51)=ATTN(201)
      ATTN1(52)=ATTN(202)
      CALL LINE(DKM,ATTN1,50,1,0,0)
      DO 2 J=1,3
      CALL PLOT(0.,0.,-3)
      DO 3 I=1,50
    3 ATTN1(I)=ATTN(50*J+I)
    2 CALL LINE(DKM,ATTN1,50,1,0,0)
      CALL PLOT(8.5,0.,-3)
      CALL AXIS(0.,0.,'SLAB LENGTH(KM)',-15,5.,0.,DKM(51),DKM(52))
      CALL AXIS(0.,0.,'ISOLATION(DB)',13,6.,90.,ISO(201),ISO(202))
      DO 4 I=1,50
    4 ISO1(I)=ISO(I)
      ISO1(51)=ISO(201)
      ISO1(52)=ISO(202)
      CALL LINE(DKM,ISO1,50,1,0,0)
      DO 5 J=1,3
      CALL PLOT(0.,0.,-3)
      DO 6 I=1,50
    6 ISO1(I)=ISO(50*J+I)
    5 CALL LINE(DKM,ISO1,50,1,0,0)
      CALL PLOT(0.,0.,999)
      RETURN
      END


      SUBROUTINE FSAMPS
      COMPLEX IMAG,RI,SUM,SUM0,Y,F(0:2,14),JY,GY,CBESJ
      COMPLEX Q1,Q2,Q3,Q4,AL,BL
      REAL K0,JX
      COMMON /BLOC2/ IMAG,K0,RI,F
      RAD=.25
      DO 1 I=1,14
      X=K0*RAD/1000.
      Y=X*RI
      SUM0=(0.,0.)
      SUM=(0.,0.)
      L=1
   70 TLP1=2*L+1
      JX=SBESJ(X,L)
      JY=CBESJ(Y,L)
      GX=((L+1)*SBESJ(X,L-1)-L*SBESJ(X,L+1))/TLP1
      GY=((L+1)*CBESJ(Y,L-1)-L*CBESJ(Y,L+1))/TLP1
      Q1=JX*GY
      Q2=GX*JY
      Q3=JY*CMPLX(GX,-((L+1)*SBESY(X,L-1)-L*SBESY(X,L+1))/TLP1)
      Q4=GY*CMPLX(JX,-1.*SBESY(X,L))
      AL=(RI*Q1-Q2)/(Q3-RI*Q4)
      BL=(RI*Q2-Q1)/(Q4-RI*Q3)
      SUM=SUM+TLP1*(AL+BL)
      IF(CABS((SUM-SUM0)/SUM).GT.1.0E-06) THEN
```

```
      L=L+1
      SUMO=SUM
      GO TO 70
    ENDIF
    F(0,I)=IMAG*SUM/(2.*K0)
  1 RAD=RAD+.25
    RETURN
    END


    SUBROUTINE MVMULT(A,X,B)
    COMPLEX A(2,2),X(2),B(2)
    DO 1 I=1,2
    B(I)=(0.,0.)
    DO 1 J=1,2
  1 B(I)=B(I)+A(I,J)*X(J)
    RETURN
    END



    FUNCTION SBESJ(X,N)
    Z=SIN(X)/X
    IF(N.EQ.0) THEN
      SBESJ=Z
      RETURN
    ENDIF
    IF(ABS(.5*X*X/FLOAT(2*N+3)).LT.1.0) THEN
      SBESJ=SBESST(X,N)
      RETURN
    ENDIF
    M=X+10.
    IF(M.LE.N) M=N+5
    Q2=SBESST(X,M+1)
    Q1=SBESST(X,M)
    MM=M
    DO 1 I=1,M
    IF(MM.EQ.N) QN=Q0
    Q0=(2*MM+1)*Q1/X-Q2
    Q2=Q1
    Q1=Q0
  1 MM=MM-1
    SBESJ=Z*QN/Q0
    RETURN
    END



    FUNCTION SBESST(X,N)
    F=1.
    DO 1 I=1,N
  1 F=F*X/FLOAT(2*I+1)
```

```
      K1=1
      K2=2*N+3
      Z=-.5*X*X
      Q1=1.
      Q2=Z/FLOAT(K2)
    2 Q1=Q1+Q2
      IF(ABS(Q2).GT.1.0E-09) THEN
         K1=K1+1
         K2=K2+2
         Q2=Q2*Z/FLOAT(K1*K2)
         GO TO 2
      ENDIF
      SBESST=F*Q1
      RETURN
      END



      COMPLEX FUNCTION CBESJ(Y,N)
      COMPLEX Y,Z,Q0,Q1,Q2,QN,CBESST
      Z=CSIN(Y)/Y
      IF(N.EQ.0) THEN
         CBESJ=Z
         RETURN
      ENDIF
      IF(CABS(.5*Y*Y/FLOAT(2*N+3)).LT.1.0) THEN
         CBESJ=CBESST(Y,N)
         RETURN
      ENDIF
      M=CABS(Y)+10.
      IF(M.LE.N) M=N+5
      Q2=CBESST(Y,M+1)
      Q1=CBESST(Y,M)
      MM=M
      DO 1 I=1,M
      IF(MM.EQ.N) QN=Q0
      Q0=(2*MM+1)*Q1/Y-Q2
      Q2=Q1
      Q1=Q0
    1 MM=MM-1
      CBESJ=Z*QN/Q0
      RETURN
      END



      COMPLEX FUNCTION CBESST(Y,N)
      COMPLEX Y,Z,F,Q1,Q2
      F=(1.,0.)
      DO 1 I=1,N
    1 F=F*Y/FLOAT(2*I+1)
      K1=1
      K2=2*N+3
```

```
      Z=-.5*Y*Y
      Q1=(1.,0.)
      Q2=Z/FLOAT(K2)
    2 Q1=Q1+Q2
      IF(CABS(Q2).GT.1.0E-09) THEN
         K1=K1+1
         K2=K2+2
         Q2=Q2*Z/FLOAT(K1*K2)
         GO TO 2
      ENDIF
      CBESST=F*Q1
      RETURN
      END



      FUNCTION SBESY(X,N)
      Z0=-1.*COS(X)/X
      IF(N.EQ.0) THEN
         SBESY=Z0
         RETURN
      ENDIF
      Z1=Z0/X-SIN(X)/X
      IF(N.EQ.1) THEN
         SBESY=Z1
         RETURN
      ENDIF
      DO 1 I=2,N
      NN=I-1
      SBESY=(2*NN+1)*Z1/X-Z0
      Z0=Z1
    1 Z1=SBESY
      RETURN
      END
```

Appendix F

Derivation of the Approximation in Equation (4.56) we seek an approximate solution to

$$I_1(z') = \iiiint \psi_a(\xi_2, \eta_2)$$

$$x \exp\left\{ | Q \frac{(z'|^2}{4Q_r(z')(L - z')^2} \left[(\xi_i - \xi_2)^2 + (\eta_1 - \eta_2)^2 \right] \right\}$$

$$d\xi_1 d\eta_1 d\xi_2 d\eta_2 \qquad (F.1)$$

where S_a indicates integration over the surface of a large circular aperture and

$$(z') = -j[k_0)L - z') + k_1(d - z')] \qquad (F.2a)$$

$$Q_r(z') = R_e[Q(z')] < 1 \qquad (F.2b)$$

Let R_a be the radius of the aperture and define x by

BLANK PAGE

$$U_1 = (\xi_{12'} - \xi_{1'})/\sqrt{2}\ rqno(F.9a)$$

$$U_2 = (\xi_{1'} + \xi_{2'})/\sqrt{2} \qquad (F.9b)$$

$$V_1 = (\eta_{2'} - \eta_{1'}/\sqrt{2} \qquad (F.9c)$$

$$V_2 = (\eta_{1'} + \eta_{1'})/\sqrt{2} \qquad (F.9d)$$

$$\xi_{1'} = (U_2 - U_1)/\sqrt{2}\,) \qquad (F.10)a$$

$$\xi_{2'} = (U_1 + U_2)/\sqrt{2} \qquad (F.10b)$$

$$\eta_{1'} = (V_2 - V_1)/\sqrt{2} \qquad (F.10c)$$

/

$$\eta_{2'} = (V_1 + V_2)/\sqrt{2} \qquad (F.10d)$$

Then, the plex integral in (F.6) can be recast as

$$I_2(x) = \sum_{i=1}^{z}\sum_{j=1}^{3}\int\int\int\int G(U_1, V_1, U_2, V_2)\exp[-2x(U_1^2 + V_1^2)]$$

$$+ \sum_{i=3}^{4}\sum_{j=1}^{3}\int\int\int\int G(U_1, V_1, U_2, V_2,)\exp[x_x(u_1^2 + V_1^2]$$

$$dV_2 dV_1 \qquad (F.11)$$

where

$$G(U_1,\ V_1,\ U_2,\ V_2) = F[U_2 - U_1)/\sqrt{2},\ (V_2 - V_1)\sqrt{2,}\ (U_1, + U_2)/\sqrt{2},(V_1 + V_2)/\sqrt{2} \qquad (F.12)$$

and the domains T_i, A_i and B_i are as shown in Figure F.1, F.2 and F.2 respectively.

Let us define $J_{ij}(x)$ and k_{ij} by

$$J_{ij}(x)\iiiint G(U_1, V_1, U_2, V_2)\exp[-2x(U_1^2 + V_1^2)]$$

$$dU_2dU_1dV_1dV_2\ ;\ i = 1, 2; j = 1, 2, 3 \qquad (F.13a)$$

$$K_{ij}(x) = \iiiint G(U_1, V_1, U_2, V_2)\exp[-2x(U^2 + V^2]$$

$$dU_2dU_1dV_2dV_1\ ;\ i = 3, 4;\ j = 1, 2, 3, \qquad (F.13b)$$

and consider $J_{12}(x)$. From Figure F.1 and F.2 we deduce that

$$J_{12}(x) = \int_{-\sqrt{2}}^{o}\int_{o}^{V_1+\sqrt{2}} \int_{U_{22}(U_1, V_1, V_2)} \quad V_{12}(V_1, V_2 \int_{U_{21}(U_1, V_1, V_2)} G(U_1, V_1, U_2, V_2) \quad U_{11}(V_i, V_2V_1 + \sqrt{2} \int_{U_{11}(V_1, V_2)}$$

$$x\exp[-2x9U_1^2 + V_1^2)]dU_2dU_1dV_2dV_1 \qquad (F.14a)$$

with

$$U_{11}(V_1, V_2) = \frac{1}{1}\sqrt{2}\,[f(\eta_2) - f(\eta_1)] = -\frac{1}{\sqrt{2}}\Big\{[1 - \frac{1}{2}(V_1 + V_2)^2]^{1/2}$$

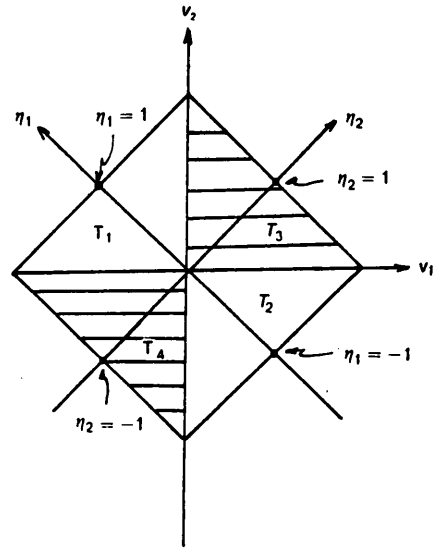

Domain T_1, T_2, T_3 and T_4 for
Integration in V_1 and V_2

Figure F.1

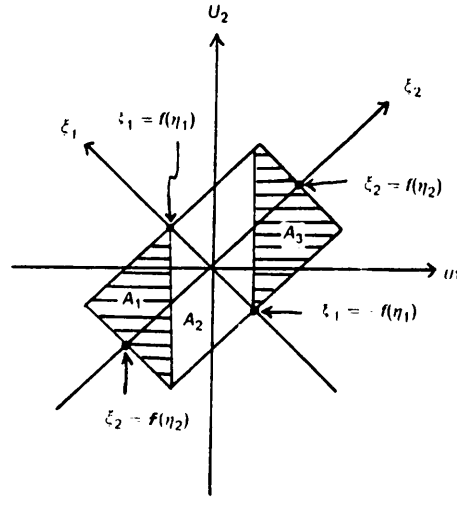

Domains A_1, A_2 and A_3 for Integration
In U_1 and U_2 $(f(\eta_2) > f(\eta_1); |\eta_1| < |\eta_2|)$

Figure F.2

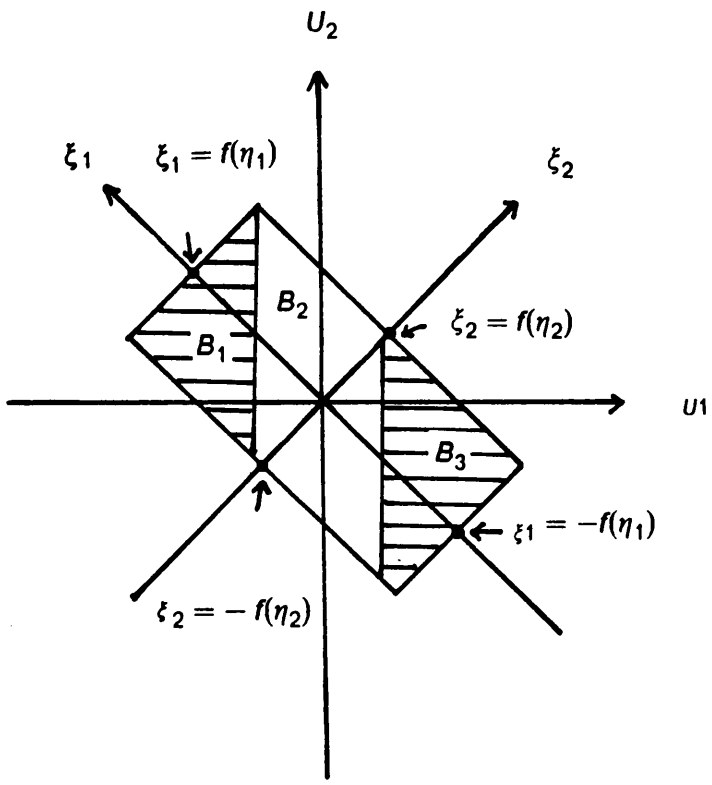

Domains B_1, B_2 and B_3 for Integration
In U_2 and U_1 $(f(\eta_1) > f(\eta_2);\ |\eta_1| > |\eta_2|)$

Figure F.3

$$U_1 = -\frac{1}{\sqrt{2}}\left[1 - \frac{1}{2}\left\{2v_1 + \sqrt{2}\right\}^2\right]^{\frac{1}{2}}$$

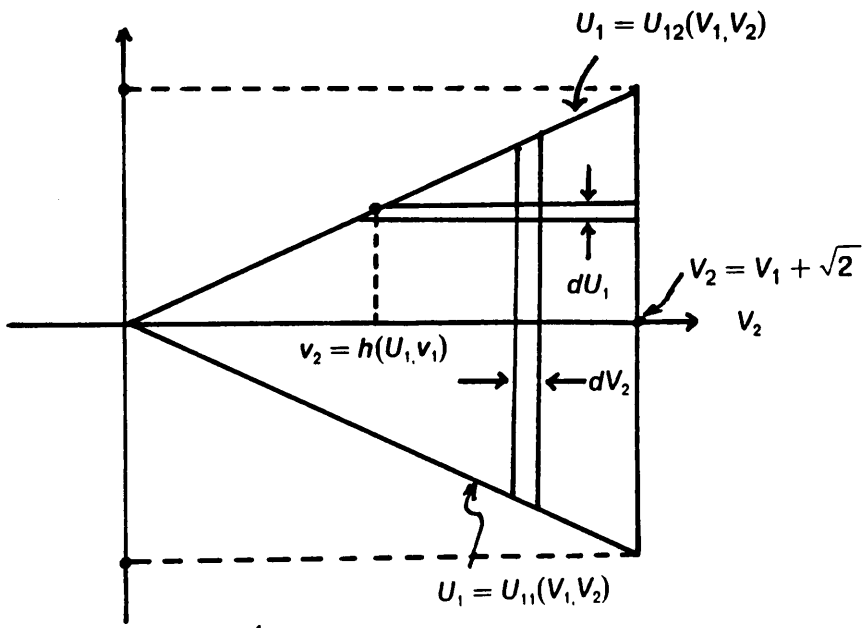

$$U_1 = -\frac{1}{\sqrt{2}}\left[1 - \frac{1}{2}\left\{2v_1 + \sqrt{2}\right\}^2\right]^{\frac{1}{2}}$$

Domain of Integration For v_2 and U_1 in (F.14) and (F.15)

Figure F.4

$$- [1 - \frac{1}{2}(V_2 - V_1)^{21/2}\} \tag{F.14b}$$

$$U_{12}(V_1, V_2) = - U_{11}(V_1, B_2) = \frac{1}{\sqrt{2}}\Big\}[1 - \frac{1}{2}(v_1 + v_2)^2]/2 - [1 - \frac{1}{2}(V_2 - V_1)^2]^{1/2}\Big\} \tag{F.14c}$$

$$U_{21}(U_1, V_1, V_2) = U_1 - \sqrt{2}\, f(\eta_1) = U_1 - \sqrt{2}\,[1 - \frac{1}{2}(V_2 - V_1)^2]^{1/2} \tag{F.14d}$$

$$U_{22}(U_1, V_1, V_2) = U_1 + \sqrt{2}\, f(\eta_1) = U_1 + \sqrt{2}\,[1 - \frac{1}{2}(V_2 - V_1)^2]^{1/2} \tag{F.14e}$$

In (F.14), we can exchange orders of integration between U_1 and V_2 to obtain (see Figure F.4)

$$J_{12}(x) = \int_{-\sqrt{2}}^{(up4)} 0 \int_{-gV_1)}^{g(v_1)} H(U_1, V_1) \exp[-2x,(U_1^2 + V_1^2)]dU_1 dV_1 \tag{F.15a}$$

where

$$H(U_1, V_1) = \int_{h(U_1, V_1)(down8)}^{V_1 \_ \sqrt{2}} U_{21,}(U_1, V_1.V_2)U_{22,}(U_1, V_1, V_2)G(U_1, V_1, U_2, V_2)dU_2 dV_2 \tag{F.15b}$$

$$g(V_1) = \frac{1}{\sqrt{2}}[1 - \frac{1}{2}(wV_1 + \sqrt{2^2}\,]^{1/2?} \tag{F.15b}$$

and $h(U_1, V_1)$ is as shown in Figure F.4

We now apply Laplace's method to obtain as the leading asymptotic behavior of $J_{12}(x)$ as $x \to \infty$

$$J_{12}(x) \sim H(O,), \int_{-\infty}^{0} \int_{-\infty}^{\infty} \exp[-2x(U_1^2 + V_1^2)]dU_1 dV_1, \quad x \to \infty \tag{F.16}$$

We note that

$$H(0,0) = \int_{}^{\sqrt{2}} \int_{-\sqrt{2}\, f(V_2/\sqrt{2})}^{\sqrt{2}\, f(V_2/\sqrt{2})} G(0,0,U_2,V_2)\,dU_2\,dV_2 \tag{F.17}$$

Therefore , after evaluating the integral s in (F.16) using the elementary solution

$$\int_0^{\infty} \exp(-a^2y^2)\,dy = \frac{1}{2a}\sqrt{\pi} \tag{F.18}$$

we obtain

$$J_{12}(x) \sim \frac{\pi}{4x} \int_0^{\sqrt{2}} \int_{-\sqrt{2}\, f(V_2/\sqrt{2})}^{\sqrt{2}\, f(V_2/\sqrt{2})} G(0,0,U_2,Vsu2)\,dU_2,\,dV_2,\; x \to \infty \tag{F.19}$$

Using a similar procedure we find that

$$J_{22}(x) \sim \frac{\pi}{4x} \int_{-\sqrt{2}}^{o} \int_{-\sqrt{2}\, f(V_2/\sqrt{2})}^{\sqrt{2}\, f(V_2/\sqrt{2})} G(0,0,U_2,V_2)\,dU_2 dV_2\,,\; xrarror\infty \tag{F.20a}$$

$$32(x) \sim \frac{\pi}{4x} \int_{down8)}^{-\sqrt{2}\sqrt{2}} \int_{-\sqrt{2}\, f(V_2/\sqrt{2}\sqrt{2}\sqrt{2}\, f(V_2/\sqrt{2})}^{} G(0,0,U_2,V_2)\,dU_2 dV_2\,,\; xrarror\infty \tag{F.20b}$$

$$k_{42} \sim \frac{\pi}{4x} \int_{(downo\sqrt{2}}^{} \int_{-\sqrt{2}\, f(V_1/\sqrt{2}\sqrt{2}\, f(V_2/\sqrt{2}} G(0,0,U_2,V_2)\,dU_2 dV_2\,,\; xrarror\infty \tag{F.20c}$$

$$J_{ij}(x) = 0(x^{-3/2} \quad ; \quad i = 1, 2; j = 1 \text{ or } 3 \tag{F.21a}$$

$$k_{ij}(x) = 0(X^{-3/2/} \quad ; \quad i = 3, 4, ; \; j + 1 \text{ or } 3 \tag{F.21b}$$

where $0(x^{-3/2})$ indicates that $J_{ij}(x)$ *or* $k_{ij}(x)$ is on the order of $x^{-3/2}$ as $xrarror\infty$. We will neglect these contributions since

$$x^{-3/2} << x^{-1} \quad , \quad xrarror\infty \tag{F.22}$$

Doing so and substituting (F.19) and (F.20) into (F.11) yields

$$I_2 \sim \frac{\pi}{2x} \int_{-\sqrt{2}}^{\sqrt{2})} \int - \sqrt{2}\, f(V_2/\sqrt{2})\sqrt{2}\, f(V_2/\sqrt{2}\, G(0, 0, U_2, V_2) dU_2 dV_2 \quad , \quad xrarror\infty \tag{F.23}$$

Using (F.8) and (F.12) we see that

$$G(0, 0, U_2, V_2) = |\psi_a(R_a U_2/\sqrt{2}\,, R_a V_2/\sqrt{2}\,)|^2 \tag{F.24}$$

Thus, if we make the variable substitutions

$$si = \ell_a U_2/\sqrt{2} \tag{F.25a}$$

$$\eta = R_a Y_2/\sqrt{2} \tag{F.25b}$$

(F.23) can be recast as

$$I_2(x) \sim \frac{\pi}{x} R_a^2 \int_{(down8)} S_a) \int |\psi_a(\xi_1 \eta)|^2 d\xi d\eta \quad , \quad x \to \infty \tag{F.26}$$

Substituting now (F.3) into (F.26) and the result of doing so into (F.5), we find that for large apertures

$$I_1(z') \simeq -4\pi \frac{Q_r(z')(L-z')^2}{|Q(z')|^2} \iint_{S_a} |\psi_a(\xi,\eta)|^2 d\xi d\eta \tag{F.27}$$

(F.27) can be further reduced by noting that based upon the definition of $\psi_a(\xi,\eta)$ put forth in Chapter 4 (see (4.2)) and the definition of an antenna's directivity [53]

$$\iint_{S_a} |\psi_a(\xi,\eta)|^2 d\xi d\eta = \frac{4\pi}{\lambda^2} \tag{F.28}$$

Substituting (F.28) into (F.27) gives

$$I_1(z') \simeq -\frac{16\pi^2}{\lambda^2} \frac{Q_r(z')(L-z')^2}{|} Q(z')|^2 \tag{F.29}$$

Appendix G. Program for Computing the Ratio of the Coherent to Incoherent Power

This Appendix contains the program used to obtain the plots of IC/IF vs. slablength provided in Chapter 4, Section 4.4.

G.1 Program Flow Chart and Program Listing

The program flow chart is in Figure G.1. SUBROUTINE SPARAM computes forward scattering amplitudes and scattering cross sections for spherical raindrops and SUBROUTINE PLOTT plots the data. The spherical Bessel fundtion subprograms are SBESJ, SBESST, CBESJ, CBESST and SBESY.

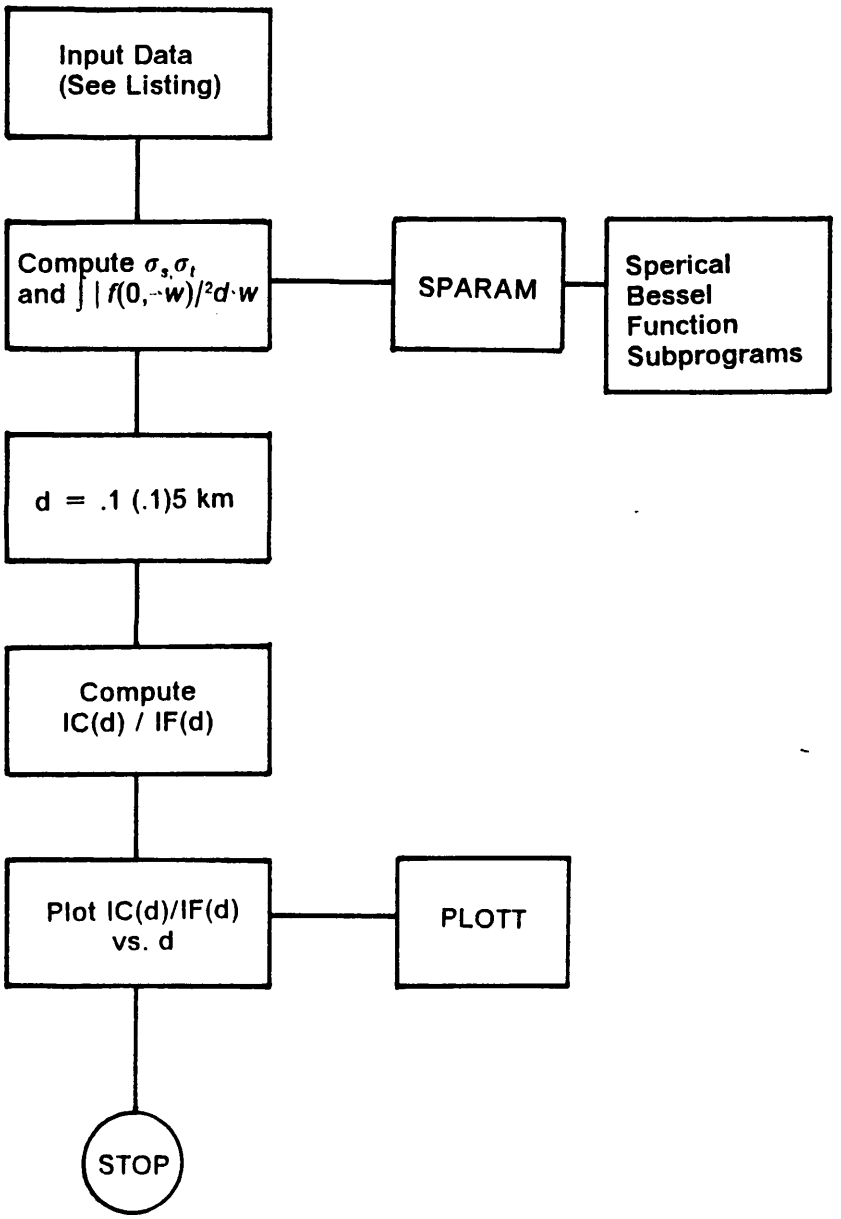

Flow Chart of Program for IC(d)/IF(d)

Figure G.1

```
C****** RATIO OF COHERENT TO INCOHERENT POWER **********************
C                                                                  *
C    THIS PROGAM COMPUTES AND PLOTS THE RATIO OF THE COHERENT TO   *
C  THE INCOHERENT POWER AT THE OUTPUT OF A RECEIVER DURING A RAIN  *
C  EVENT. CALCULATIONS ARE MADE FOR RAIN RATES OF 2.5,12.5,50 AND  *
C  150 MM/HR.  USER INPUTS ARE:                                    *
C                                                                  *
C            FREQ= FREQUENCY OF OPERATION IN GHZ.                  *
C                                                                  *
C            RIRE(RIIM)= REAL (IMAG) PART OF THE REFRACTIVE        *
C                        INDEX OF WATER AT THE FREQUENCY OF        *
C                        OPERATION.                                *
C                                                                  *
C            ANTGN= RECEIVER GAIN IN DB.                           *
C                                                                  *
C            PO= FRACTION OF THE TOTAL NUMBER OF DROPS             *
C                IN THE RAINCELL WHICH ARE SPHERICAL.              *
C                                                                  *
C            FSAMPO= ARRAY CONTAINING THE FORWARD SCATTER-         *
C                    ING AMPLITUDES (IN METERS) FOR OBLATE         *
C                    SPHEROIDAL RAINDROPS AT THE FREQUENCY         *
C                    AND POLARIZATION OF INTEREST. VALUES          *
C                    INPUT FOR DROP EQUIVOLUMETRIC RADII OF        *
C                    .25(.25)3.5 MM.                               *
C                                                                  *
C            CS= ARRAY CONTAINING THE SCATTERING CROSS SEC-        *
C                TIONS (IN METERS SQ.) FOR OBLATE SPHEROIDAL       *
C                RAINDROPS AT THE FREQUENCY AND POLARIZATION       *
C                OF INTEREST AND EQUIVOLUMETRIC RADII .25(.25)     *
C                3.5 MM.                                           *
C******************************************************************

      COMPLEX RI,FSAMPO(14)
      REAL KO,S(3),PARAM(3,14),DKM(52),SNR(202)
      REAL CS(14),RRATE(4),CI(350),NSR
      COMMON /BLOC1/ DKM,SNR
      COMMON /BLOC2/ KO,PI,RI,PARAM
      COMMON /BLOC3/ FSAMPO,CS,PO

C  INPUT DATA.

      DATA RRATE/2.5,12.5,50.,150./
      PI=3.1415927
      NO=16000
      READ(5,*)FREQ,RIRE,RIIM,ANTGN,PO
      WRITE(6,100)FREQ,ANTGN,PO
      DO 33 I=1,14
      READ(5,*)FR,FI,CS(I)
   33 FSAMPO(I)=CMPLX(FR,FI)
      RI=CMPLX(RIRE,RIIM)
      KO=20.*PI*FREQ/3.
      ALFAR=10.**(ANTGN/10.)/4.

C  COMPUTE SIGMAS, SIGMAT AND THE MAGNITUDE OF F(O,A) SQUARED
C  INTEGRATED OVER THE DROP SIZE DISTRIBUTION.
```

```
      CALL SPARAM
      IMIN=1
      IMAX=50
      DO 603 II=1,4
      BETA=8.2*RRATE(II)**(-.21)
      DO 1 I=1,3
      S(I)=4.*PARAM(I,1)*EXP(-.25*BETA)+PARAM(I,14)*EXP(-3.5*BETA)
      DO 1 J=1,6
    1 S(I)=S(I)+2.*PARAM(I,2*J)*EXP(-.5*BETA*J)
     &          +4.*PARAM(I,2*J+1)*EXP(-(.5*J+.25)*BETA)
      SIGMAT=N0*S(1)/12.
      SIGMAS=N0*S(2)/12.
      F2=N0*S(3)/12.

C     OBTAIN THE RATIO IC/IF FOR SLAB LENGTHS UP TO 5 KM.

      D=100.
      DO 2 I=IMIN,IMAX
      P=2.*PI*F2/(2.*ALFAR+SIGMAT*D)
      Q=SIGMAT/(2.*ALFAR+SIGMAT*D)
      M0=1
    3 TEST=(Q*D)**M0
      IF(TEST.GT.1.0E-06) THEN
         M0=M0+1
         GO TO 3
      ENDIF
      SUM=0.
      DO 4 M=0,M0
      DO 4 N=0,M
    4 SUM=SUM+(-1.)**(M+N)*FACT(M)*Q**M*D**(M-N)/(FACT(M-N)*SIGMAS**N)
      NSR=P*(EXP(SIGMAS*D)*SUM-1.)/SIGMAS
      SNR(I)=-10.*ALOG10(NSR)
      CI(I)=ANTGN+10.*ALOG10(EXP(-SIGMAT*D))
    2 D=D+100.
      IMIN=IMIN+50
  603 IMAX=IMAX+50

C     OUTPUT DATA.

      DO 60 I=1,50
   60 DKM(I)=.1*I
      JMIN=10
      JMAX=50
      DO 61 I=1,4
      WRITE(6,102)RRATE(I)
      II=10
      DO 62 J=JMIN,JMAX,10
      WRITE(6,101)DKM(II),SNR(J),CI(J)
   62 II=II+10
      JMIN=JMIN+50
      JMAX=JMAX+50
   61 WRITE(6,104)

      CALL PLOTT
```

```
100 FORMAT(1X,'FREQUENCY:',F5.1,' GHZ',/,1X,'ANTENNA GAIN:',
   &F5.1,' DB',/,1X,'FRACTION SPHERICAL DROPS:',F5.2,/)
101 FORMAT(7X,F3.1,4X,F7.2,3X,F7.2)
102 FORMAT(1X,'RAIN RATE:',F6.1,' MM/HR',//,6X,'D(KM)',3X,
   &'SNR(DB)',4X,'CI(DB)')
104 FORMAT(//)
    STOP
    END


    SUBROUTINE PLOTT
    REAL DKM(52),SNR(202),SNR1(52)
    COMMON /BLOC1/ DKM,SNR
    CALL PLOTS(0,0,50)
    CALL SCALE(DKM,5.,50,1)
    CALL SCALE(SNR,6.,200,1)
    CALL PLOT(2.,2.,-3)
    CALL AXIS(0.,0.,'SLAB LENGTH(KM)',-15,5.,0.,DKM(51),DKM(52))
    CALL AXIS(0.,0.,'IC/IF(DB)',9,6.,90.,SNR(201),SNR(202))
    DO 1 I=1,50
  1 SNR1(I)=SNR(I)
    SNR1(51)=SNR(201)
    SNR1(52)=SNR(202)
    CALL LINE(DKM,SNR1,50,1,0,0)
    DO 2 J=1,3
    CALL PLOT(0.,0.,-3)
    DO 3 I=1,50
  3 SNR1(I)=SNR(50*J+I)
  2 CALL LINE(DKM,SNR1,50,1,0,0)
    CALL PLOT(0.,0.,999)
    RETURN
    END


    SUBROUTINE SPARAM
    COMPLEX IMAG,RI,SUM1,SUM0,Y,FSAMPO(14),CBESJ
    COMPLEX Q1,Q2,Q3,Q4,AL,BL,FSAMPS,JY,GY
    REAL K0,JX,PARAM(3,14),CS(14)
    COMMON /BLOC2/ K0,PI,RI,PARAM
    COMMON /BLOC3/ FSAMPO,CS,P0
    P1=1.-P0
    IMAG=(0.,1.)
    RAD=.25
    DO 1 I=1,14
    X=K0*RAD/1000.
    Y=X*RI
    SUM0=(0.,0.)
    SUM1=(0.,0.)
    SUM2=0.
    L=1
 70 TLP1=2*L+1
    JX=SBESJ(X,L)
```

```
      JY=CBESJ(Y,L)
      GX=((L+1)*SBESJ(X,L-1)-L*SBESJ(X,L+1))/TLP1
      GY=((L+1)*CBESJ(Y,L-1)-L*CBESJ(Y,L+1))/TLP1
      Q1=JX*GY
      Q2=GX*JY
      Q3=JY*CMPLX(GX,-((L+1)*SBESY(X,L-1)-L*SBESY(X,L+1))/TLP1)
      Q4=GY*CMPLX(JX,-1.*SBESY(X,L))
      AL=(RI*Q1-Q2)/(Q3-RI*Q4)
      BL=(RI*Q2-Q1)/(Q4-RI*Q3)
      SUM1=SUM1+TLP1*(AL+BL)
      SUM2=SUM2+TLP1*(CABS(AL)**2+CABS(BL)**2)
      IF(CABS((SUM1-SUM0)/SUM1).GT.1.0E-06) THEN
         L=L+1
         SUM0=SUM1
         GO TO 70
      ENDIF
      FSAMPS=IMAG*SUM1/(2.*K0)
      PARAM(1,I)=-4.*PI*(P0*AIMAG(FSAMPS)+P1*AIMAG(FSAMPO(I)))/K0
      PARAM(2,I)=2.*P0*PI*SUM2/K0**2 +P1*CS(I)
      PARAM(3,I)=P0*CABS(FSAMPS)**2+P1*CABS(FSAMPO(I))**2
    1 RAD=RAD+.25
      RETURN
      END



      FUNCTION SBESJ(X,N)
      Z=SIN(X)/X
      IF(N.EQ.0) THEN
         SBESJ=Z
         RETURN
      ENDIF
      IF(ABS(.5*X*X/FLOAT(2*N+3)).LT.1.0) THEN
         SBESJ=SBESST(X,N)
         RETURN
      ENDIF
      M=X+10.
      IF(M.LE.N) M=N+5
      Q2=SBESST(X,M+1)
      Q1=SBESST(X,M)
      MM=M
      DO 1 I=1,M
      IF(MM.EQ.N) QN=Q0
      Q0=(2*MM+1)*Q1/X-Q2
      Q2=Q1
      Q1=Q0
    1 MM=MM-1
      SBESJ=Z*QN/Q0
      RETURN
      END
```

```
      FUNCTION SBESST(X,N)
      F=1.
      DO 1 I=1,N
    1 F=F*X/FLOAT(2*I+1)
      K1=1
      K2=2*N+3
      Z=-.5*X*X
      Q1=1.
      Q2=Z/FLOAT(K2)
    2 Q1=Q1+Q2
      IF(ABS(Q2).GT.1.0E-09) THEN
         K1=K1+1
         K2=K2+2
         Q2=Q2*Z/FLOAT(K1*K2)
         GO TO 2
      ENDIF
      SBESST=F*Q1
      RETURN
      END



      COMPLEX FUNCTION CBESJ(Y,N)
      COMPLEX Y,Z,Q0,Q1,Q2,QN,CBESST
      Z=CSIN(Y)/Y
      IF(N.EQ.0) THEN
         CBESJ=Z
         RETURN
      ENDIF
      IF(CABS(.5*Y*Y/FLOAT(2*N+3)).LT.1.0) THEN
         CBESJ=CBESST(Y,N)
         RETURN
      ENDIF
      M=CABS(Y)+10.
      IF(M.LE.N) M=N+5
      Q2=CBESST(Y,M+1)
      Q1=CBESST(Y,M)
      MM=M
      DO 1 I=1,M
      IF(MM.EQ.N) QN=Q0
      Q0=(2*MM+1)*Q1/Y-Q2
      Q2=Q1
      Q1=Q0
    1 MM=MM-1
      CBESJ=Z*QN/Q0
      RETURN
      END



      COMPLEX FUNCTION CBESST(Y,N)
      COMPLEX Y,Z,F,Q1,Q2
      F=(1.,0.)
```

```
      DO 1 I=1,N
    1 F=F*Y/FLOAT(2*I+1)
      K1=1
      K2=2*N+3
      Z=-.5*Y*Y
      Q1=(1.,0.)
      Q2=Z/FLOAT(K2)
    2 Q1=Q1+Q2
      IF(CABS(Q2).GT.1.0E-09) THEN
         K1=K1+1
         K2=K2+2
         Q2=Q2*Z/FLOAT(K1*K2)
         GO TO 2
      ENDIF
      CBESST=F*Q1
      RETURN
      END



      FUNCTION SBESY(X,N)
      Z0=-1.*COS(X)/X
      IF(N.EQ.0) THEN
         SBESY=Z0
         RETURN
      ENDIF
      Z1=Z0/X-SIN(X)/X
      IF(N.EQ.1) THEN
         SBESY=Z1
         RETURN
      ENDIF
      DO 1 I=2,N
      NN=I-1
      SBESY=(2*NN+1)*Z1/X-Z0
      Z0=Z1
    1 Z1=SBESY
      RETURN
      END



      FUNCTION FACT(N)
      FACT=1.
      IF(N.EQ.0.OR.N.EQ.1) RETURN
      DO 1 I=2,N
    1 FACT=I*FACT
      RETURN
      END
```

The vita has been removed from the scanned document